1977

Igneous And Metamorphic Petrology Of The Mafic Units Of The Betts Cove And Blow-me-down Ophiolites, Newfoundland

Raymond Alpheaus Coish

NOTICE

The quality of this microfiche is heavily dependent upon the quality of the original thesis submitted for microfilming. Every effort has been made to ensure the highest quality of reproduction possible

If pages are missing, contact the university which granted the degree.

Some pages may have indistinct print especially if the original pages were typed with a poor typewriter ribbon or if the university sent us a poor photocopy.

Previously copyrighted materials (journal articles, published tests, etc.) are not filmed.

Reproduction in full or in part of this film is governed by the Canadian Copyright Act, R.S.C. 1970, c C-30. Please read the authorization forms which accompany this thesis.

THIS DISSERTATION
HAS BEEN MICROFILMED
EXACTLY AS RECEIVED

AVIS

La qualité de cette microfiche dépend grandement de la qualité de la thèse soumise au microfilmage. Nous avons tout fait pour assurer une qualité supérieure de reproduction.

S'il manque des pages, veuillez communiquer avec l'université qui a conféré le grade.

La qualité d'impression de certaines pages peut laisser à désirer, surtout si les pages originales ont été dactylographiées à l'aide d'un ruban usé ou si l'université nous a fait parvenir une photocopie de mauvaise qualité.

Les documents qui font déjà l'objet d'un droit d'auteur (articles de revue, examens publiés, etc.) ne sont pas microfilmés.

La reproduction, même partielle, de ce microfilm est soumise à la Loi canadienne sur le droit d'auteur, SRC 1970, c. C-30. Veuillez prendre connaissance des formules d'autorisation qui accompagnent cette thèse.

LA THÈSE A ÉTÉ
MICROFILMÉE TELLE QUE
NOUS L'AVONS REÇUE

ACKNOWLEDGEMENTS

The author would like to express sincere thanks to Dr. W. R. Church for close and invaluable supervision of the project from the initial field investigations to final writing, and to Dr. W. S. Fyfe for supervision of metamorphic aspects of the thesis.

Thanks also go to staff and students of the Geology Department at the University of Western Ontario especially A. J. Andrews for ideas concerning ocean floor metamorphic processes, G. A. Jenner for rare earth element analyses, R. L. Barnett for assistance with microprobe analyses, Dr. H. W. Hunter for advice on X-Ray Fluorescence Spectrometry and T. E. La Tour for many stimulating discussions.

I would also like to thank B. A. Merz for editing portions of the thesis and for providing encouragement throughout the course of the study.

Financial support for the project was made possible through a National Research Council of Canada postgraduate scholarship to the author and NRC grant N21 to W. R. Church.

ABSTRACT

The Betts Cove and Blow-Me-Down ophiolites of Newfoundland represent obducted segments of Cambrian oceanic crust. The Betts Cove ophiolite has unusual stratigraphic and chemical characteristics whereas the Blow-Me-Down complex is similar in all aspects to modern oceanic crust. Both ophiolites have undergone low grade metamorphism of the mafic zone.

The mafic rocks of the Betts Cove ophiolite are extremely low in TiO_2, P_2O_5, Zr, Y, and FeO^t/MgO and high in Ni and Cr compared with those of the Blow-Me-Down ophiolite and modern oceanic tholeiite. Clinopyroxenes of the Betts Cove mafic rocks are low in TiO_2, Al_2O_3 and FeO/MgO. Chromites, in comparison to those from ocean floor basalts, are extremely rich in Cr_2O_3 and depleted in Al_2O_3.

Computer modelling using trace element data, in addition to features of the mineral compositions, indicate that the primary liquid of the Betts Cove basalts could have been derived by 30-35% partial melting of a severely depleted lherzolite (approaching harzburgite). Furthermore, variations in the chemical composition of the whole rocks can be accounted for by simple fractional crystallization models involving olivine, orthopyroxene, clinopyroxene, spinel and plagioclase. However, initial liquids for the Blow-Me-Down basalts were probably derived

from a source similar to that postulated for modern oceanic tholeiite.

Metamorphism of the Betts Cove ophiolite probably involved vigorous hydrothermal circulation of seawater near a mid-ocean ridge as indicated by: 1) the increase in degree of metamorphism with depth of burial, 2) the apparent high geothermal gradient (300°C/km), 3) massive metasomatism of the mafic rocks: SiO_2, MgO, FeO, CaO, Na_2O, K_2O, Ba, Rb and Sr being mobile and TiO_2, P_2O_5, Zr, Y, Ni, Cr and possibly FeO^t/MgO stable during metamorphism, 4) the occurrence of hematite and calcite in the upper portions of the ophiolite and their decrease in abundance downwards, 5) the presence of rodingitic gabbro similar to hydrothermal gabbro alteration observed near modern ocean ridges, 6) the occurrence of massive sulphide bodies. Metamorphism in the Blow-Me-Down ophiolite, however, may have involved less vigorous hydrothermal circulation as suggested by the absence of pervasive fractures and faults and the decrease in metasomatic activity.

Regional variations in the Newfoundland ophiolites may be related to changing processes at mid-ocean ridges. The Blow-Me-Down ophiolite may have formed at a slow spreading centre where the source available for melting was slightly depleted lherzolite. On the other hand, it appears that the Betts Cove ophiolite formed at a fast spreading ridge and severely depleted lherzolite was being melted.

ACKNOWLEDGEMENTS

The author would like to express sincere thanks to Dr. W. R. Church for close and invaluable supervision of the project from the initial field investigations to final writing, and to Dr. W. S. Fyfe for supervision of metamorphic aspects of the thesis.

Thanks also go to staff and students of the Geology Department at the University of Western Ontario especially A. J. Andrews for ideas concerning ocean floor metamorphic processes, G. A. Jenner for rare earth element analyses, R. L. Barnett for assistance with microprobe analyses, Dr. H. W. Hunter for advice on X-Ray Fluorescence Spectrometry and T. E. La Tour for many stimulating discussions.

I would also like to thank B. A. Merz for editing portions of the thesis and for providing encouragement throughout the course of the study.

Financial support for the project was made possible through a National Research Council of Canada postgraduate scholarship to the author and NRC grant N21 to W. R. Church.

TABLE OF CONTENTS

and perknite material is absent. Furthermore, up to 50% of dykes in the Blow-Me-Down complex are thoroughly brecciated (Williams and Malpas, 1972). The principal igneous minerals are plagioclase, which occurs both as phenocrysts and as euhedral laths, and clinopyroxene, which is invariably interstitial to the plagioclase forming sub-ophitic to ophitic texture. Rare olivine pseudomorphs occur in the picritic dykes cutting the gabbro member.

The gabbro member in the Blow-Me-Down ophiolite comprises an upper massive and a lower layered unit (Figure 3) (Riccio, 1976). The massive gabbro comprises plagioclase, clinopyroxene, and hornblende, with minor magnetite. Layered gabbros include olivine gabbros, norites, anorthosites, and ilmenite gabbros (Riccio, 1976). The order of crystallization of minerals in the mafic and ultramafic cumulates is olivine (chromite)- plagioclase-clinopyroxene- (orthopyroxene?) (Riccio, 1976; Church and Riccio, 1977). The precipitation order is consistent with mineralogical observations in the sheeted dykes and pillow lavas and contrasts markedly with the crystallization order at Betts Cove (Church and Riccio, 1977).

LIST OF PHOTOGRAPHIC PLATES

LIST OF TABLES

LIST OF FIGURES

LIST OF FIGURES

LIST OF FIGURES

LIST OF APPENDICES

CHAPTER 1

BACKGROUND INFORMATION

A. Introduction and Purpose

Ophiolites of the western part of the Newfoundland Appalachians occur within two contrasting geologic environments, the one represented by the Western Platform (Zone A, Williams et al., 1972) and the other by the Fleurs-de-Lys orthotectonic zone (Church, 1969) or Zones C & D (Figure 1). The Blow-Me-Down and Betts Cove ophiolites are located in Zones A and D, respectively. Both ophiolites probably represent allochthonous fragments of a Cambrian proto-Atlantic ocean situated somewhere to the east of the present position of the boundary between Zones C and D (Figure 1). Although superficially similar, the two ophiolites exhibit differences in terms of internal stratigraphy, crystallization sequences and geochemistry of the intrusive and extrusive basaltic rocks. The Betts Cove ophiolite is unusual chemically and stratigraphically compared to modern ocean crust, whereas the Blow-Me-Down ophiolite has all the characteristics of 'normal' oceanic crust.

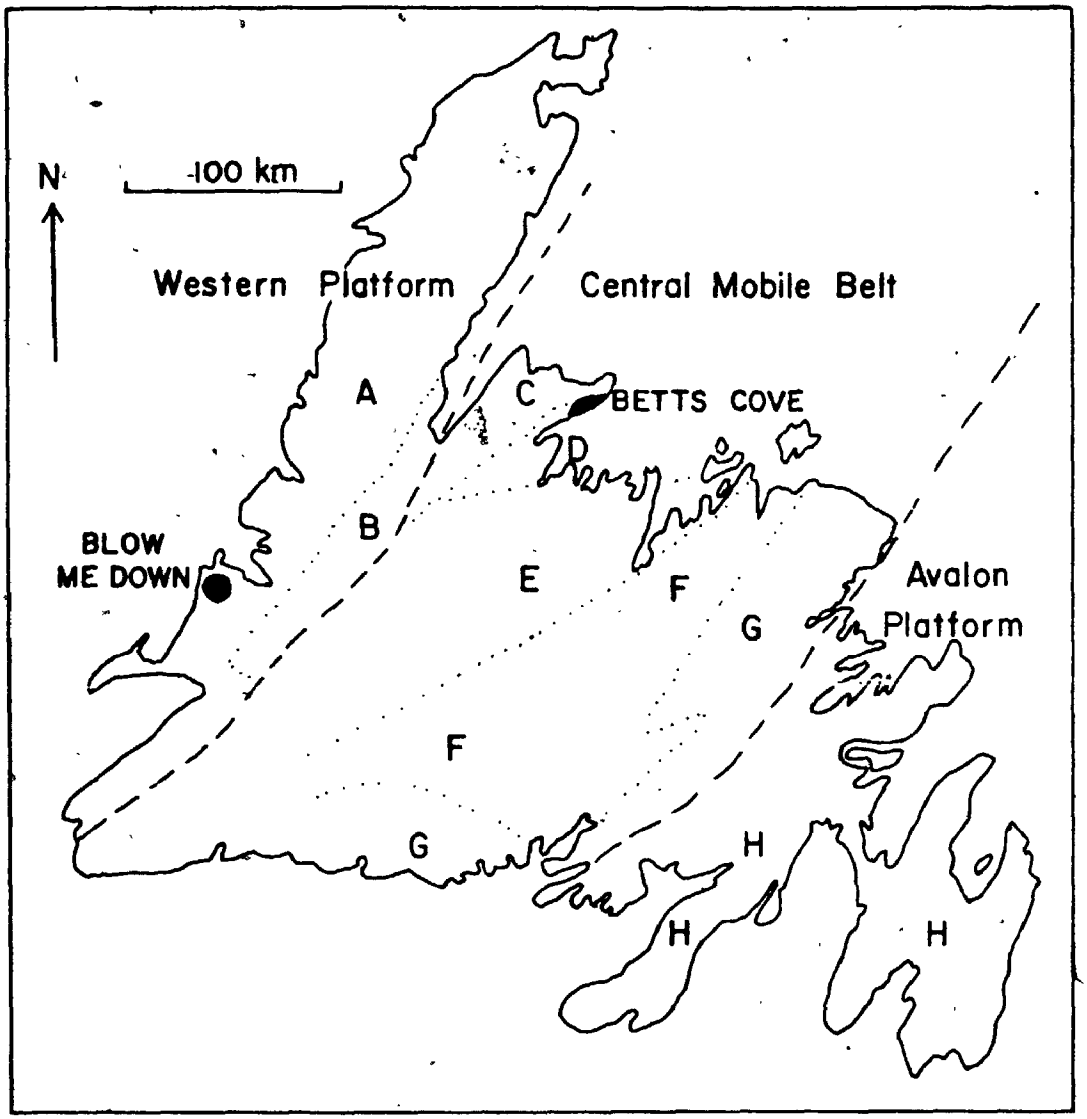

FIGURE 1. MAP OF THE ISLAND OF NEWFOUNDLAND SHOWING THE TECTONO-STRATIGRAPHIC SUBDIVISIONS (AFTER WILLIAMS ET. AL.,1972).

The purpose of this study is to describe and explain the unusual chemical, and metamorphic features of the Betts Cove ophiolite, and to compare these characteristics to those of the Blow-Me-Down ophiolite.

Some specific questions which this thesis proposes to answer are:

1) Is the metamorphism which both ophiolites have undergone related to ocean floor metamorphism involving hydrothermal circulation of seawater (Spooner and Fyfe, 1973)?

2) Which elements are mobile during low grade metamorphism and which are stable, and therefore of use in unravelling igneous processes?

3) What significance does the difference in chemistry of the internal zone (Betts Cove) and the external zone (Blow-Me-Down) (Church, 1977) ophiolites of the Newfoundland Appalachians hold in terms of their origin?

4) To what extent can whole rock chemistry be used to determine the tectonic setting of a suite of metamorphosed volcanic rocks?

In order to answer some of these questions, detailed sampling in both the Betts Cove and Blow-Me-Down ophiolites was carried out over a period of three field seasons. Samples were collected so as not to bias a particular compositional variety of the mafic zone, and care was taken to note the position of the sample with respect to the centres of dykes and pillows. Over 200 thin sections were examined for metamorphic as well as relict igneous

features. Bulk major and trace element analyses were carried out on approximately 100 selected samples. Relict clinopyroxenes and chromites as well as epidotes were analyzed by electron microprobe.

B. Regional Geological Settings

The Betts Cove ophiolite (lat. 49°50'N, long. 55°50'W) occurs within zone D of the Central Mobile Belt of the Newfoundland Appalachians (Figure 1). The ophiolite represents the basal unit of the Snooks Arm Group (Figure 2), the upper formations of which consist of volcaniclastic sediments and basaltic pillow lavas. The Snooks Arm Group has been interpreted as oceanic crust (Betts Cove ophiolite) overlain by an island arc. However, the validity of the interpretation of the upper Snooks Arm Group as of island arc origin is now in doubt in light of results of recent geochemical studies on the volcanics (Jenner, 1977).

The relationships of the Snooks Arm Group (and therefore the Betts Cove ophiolite) to the surrounding rocks are controversial (see Bursnall and DeWit, 1975; Kennedy, 1975; Neale et al., 1975; Church, 1976; DeGrace et al., 1976; Williams et al., 1977 for summaries). Only two points can be made with certainty. The base of the ophiolite is intruded by the Burton's Pond Porphyry (possibly part of the Cape Brule Porphyry (Riccio, 1972) and the Snooks Arm Group is overlain unconformably by the Cape

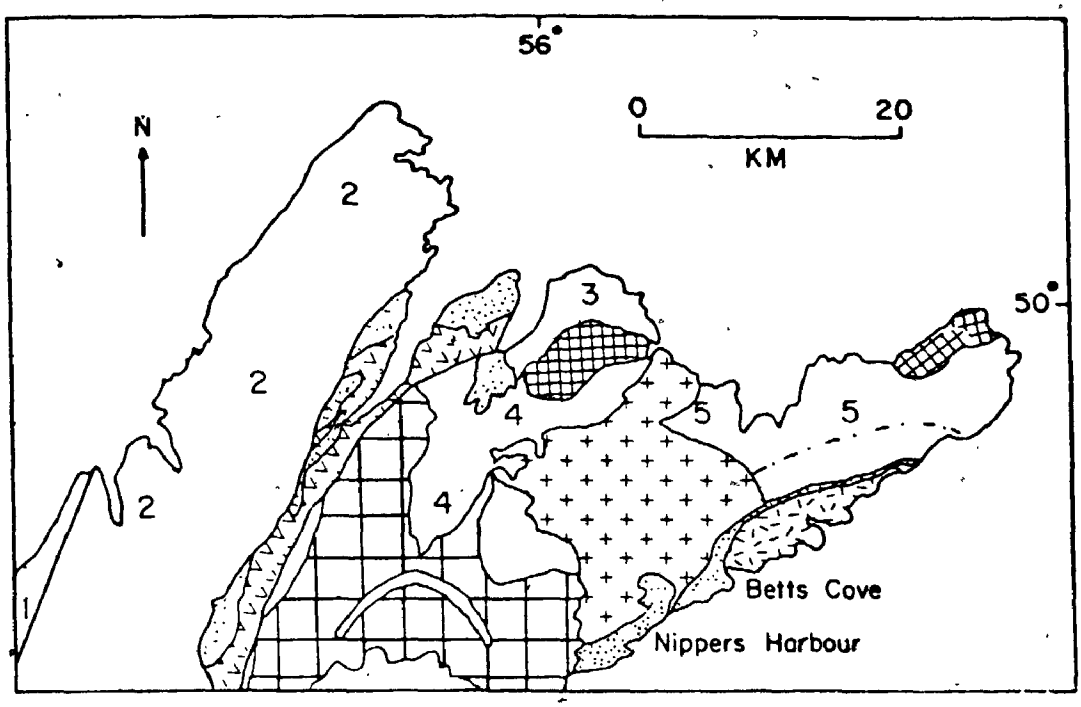

Cape St. John Group

Baie Verte Group

Snooks Arm Group

Ophiolites

Burlington granodiorite

Gabbroic intrusions

Fleur de lys Supergroup

Eastern Sequence

Cape Brule Porphry

5 Grand Cove Group

4 Pacquet Harbour Group

3 Mings Bight Group

Western Sequence

2 Rattling Brook Group

1 White Bay Group

FIGURE 2. GEOLOGICAL SKETCH MAP OF THE BURLINGTON PENINSULA SHOWING THE PRINCIPAL STUDY AREA OF BETTS COVE (AFTER RICCIO, 1972).

St. John Group (Figure 2) (Neale et al., 1975) and the Rogues Harbour Formation (Schroeter, 1971). The Snooks Arm Group is therefore certainly pre-Siluro-Devonian.

The Betts Cove ophiolite is also pre-Middle Arenigian since Middle Arenig graptolites occur in the upper parts of the Snooks Arm Group (Snelgrove, 1931) and the ophiolite is transected by trondhjemitic rocks with a minimum absolute age of 463 m.y. (Mattinson, 1975; Church, 1976).

The Blow-Me-Down ophiolite (lat. 49°3.25'N, long. 58°16'W) is located within the exogeosynclinal sequence of the Appalachian Western Platform (Figure 1). It is the highest structural slice of a series of sedimentary and igneous allochthonous units which were emplaced from the east onto a subsiding carbonate shelf sequence in late-early to early-middle Ordovician times (Stevens, 1970, 1976; Dallmeyer and Williams, 1975). The ophiolite has been interpreted to represent oceanic crust and the underlying units sediments laid down as a continental rise-prism between the carbonate shelf and the open ocean (Stevens, 1970). The ophiolite, as the highest structural slice, is thought to have originated farthest to the east.

The age of the Blow-Me-Down ophiolite is 508 m.y., as determined on zircons from a trondhjemitic phase of the gabbro member (Mattinson, 1976).

C. Ophiolite Stratigraphy

The term ophiolite is taken to mean a section of

oceanic crust and mantle as defined by Dewey and Bird (1971), Church and Stevens (1971), Moores and Vine (1971) and Church (1972). A composite section of the western Newfoundland ophiolites (Figure 3) shows that an ideal ophiolite comprises an ultramafic (tectonite and cumulate). unit overlain by layered and massive gabbro, sheeted dykes, pillow lavas and chemical sediments. Not all ophiolites are complete and the ultramafic tectonite, layered gabbro and chemical sediment units are commonly lacking. Seismic studies of modern ocean crust indicate that the structure of the crust can be matched with the stratigraphy of some ophiolites (Christensen and Salisbury, 1975).

The stratigraphy of the Betts Cove ophiolite (Figure 4) has been deciphered by Riccio (1972) and Upadhyay (1973). Differences in interpretations are, however, apparent. Riccio (1972) divided the Betts Cove ophiolite into an ultramafic and a mafic zone (Figure 4). The ultramafic zone comprises rhythmically layered peridotite, dunite and pyroxenite within which repetition of layering is common. The lower part of the ultramafic zone consists of dunite-harzburgite, the middle portion dunite, ortho-pyroxenite, and websterite, and the upper section dunite, wehrlite, olivine-clinopyroxenite and clinopyroxenite. All the ultramafic rocks are interpreted to be cumulates derived from a mafic liquid (Riccio, 1972). This interpretation contradicts the opinion of Upadhyay et al. (1971) who state that "the dunites, harzburgites and

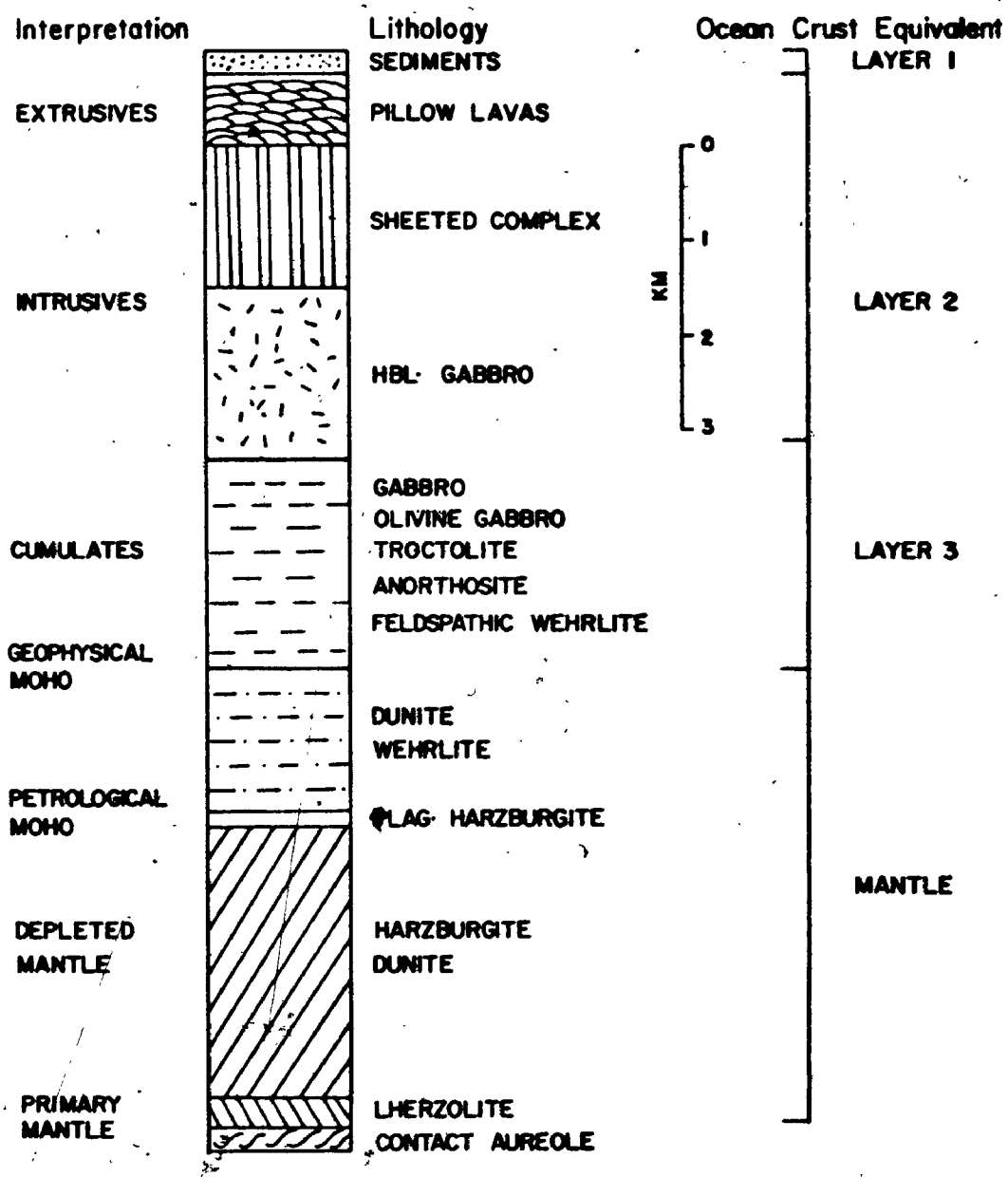

FIGURE 3. COMPOSITE STRATIGRAPHIC SECTION OF THE WESTERN NEWFOUNDLAND OPHIOLITES COMPARED WITH MODERN OCEAN CRUST STRUCTURE (MODIFIED AFTER WILLIAMS AND STEVENS, 1974 AND RICCIO, 1976).

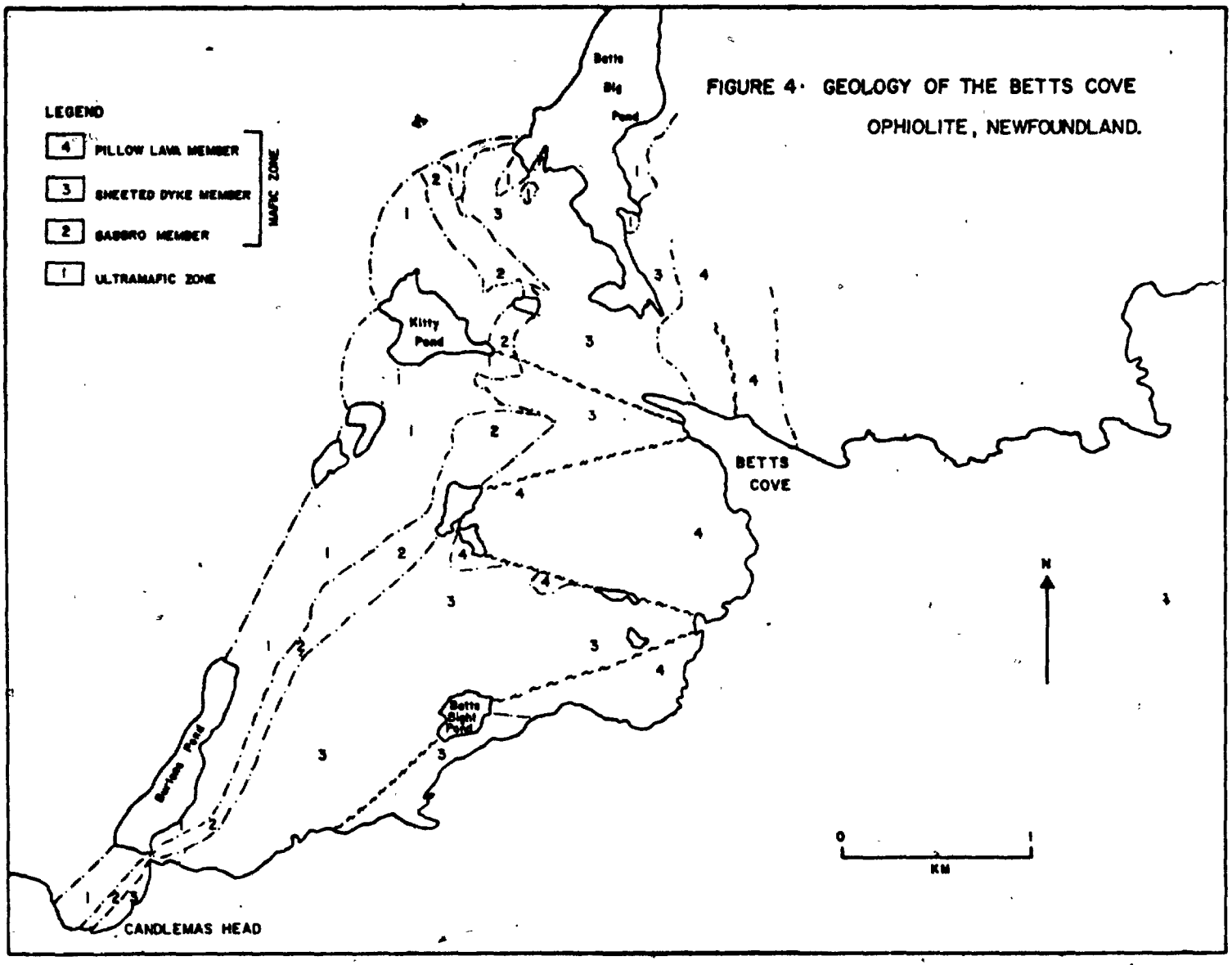

FIGURE 4· GEOLOGY OF THE BETTS COVE OPHIOLITE, NEWFOUNDLAND.

pyroxenites represent the depleted upper mantle". The presence of cumulate textures, the chemistry of the pyroxenes, the absence of tectonite fabrics (Jackson et al., 1975) as well as of a basal contact aureole indicate that the ultramafics are not depleted upper mantle (Church and Riccio, 1974). If Riccio's interpretation is accepted, it must be assumed that the depleted mantle portion of the Betts Cove ophiolite has been structurally removed, presumably during the emplacement process.

The mafic zone at Betts Cove has been divided into three members (Figure 4):

1) lower member of clinopyroxenite and leucogabbro.
2) middle member of sheeted dykes.
3) upper member of basaltic pillow flows.

The lower member of the mafic zone is in contact with the ultramafic zone east of Kitty Pond (Plate 1A). Upadhyay et al. (1971) recognize the contact as transitional from ultramafic through intercalcated pyroxenite and gabbro into gabbro, whereas Church and Riccio (1974) state that there is a major discontinuity between the ultramafic and mafic zones. The following points support the latter suggestion: 1) clinopyroxenite of the lower member of the mafic zone injects the ultramafic zone (Plate 1A). 2) xenoliths of ultramafic cumulate material occur within the lower member (Plate 1B). 3) the compositions of clinopyroxenes in the ultramafic cumulates and

the massive gabbro are different (Riccio, 1972). The gabbro unit is very thin (0.5 km.), massive and rarely layered. It appears to grade into the basal clinopyroxenite unit. The limited thickness of the gabbro unit contrasts with that of gabbro of the Bay of Islands, Troodos, Vourinos and Papuan ophiolites where cumulate gabbros up to 1.5 km. thick are developed. The above peculiar feature of the Betts Cove ophiolite appears also in the Thetford ophiolites of southeastern Quebec and is one of the criteria in the recognition of the duality of Appalachian ophiolites (Church, 1977; Church and Riccio, 1977).

The middle member of the mafic zone is represented by a sheeted dyke complex. Included in the complex are parallel, straight, massive as well as brecciated, dykes of varying composition, texture and grain size. In places, outcrops are occupied by 100% dykes whereas gabbro screens and plugs are common in other parts of the complex.

The upper member of the mafic zone comprises variolitic pillow lavas layered at right angles to the strike of the underlying dykes. The lavas are cut by fine grained dykes.

The internal stratigraphy of the Blow-Me-Down ophiolite is similar to the composite ophiolite section (Figure 3) and varies significantly from that of the Betts Cove ophiolite. The total thickness of the Blow-Me-Down ophiolite is 10 km. - 5 km. of ultramafic and 5 km. of mafic rocks (Riccio, 1976). The ophiolite is underlain

by a pyroxene-amphibolitic contact aureole, which was imprinted during emplacement of the ophiolite. The aureole is succeeded by a unit of depleted upper mantle ultramafic material, ultramafic cumulates, mafic cumulates, massive hornblende gabbro, sheeted dykes and pillow lavas.

The Blow-Me-Down ophiolitic stratigraphy contrasts with that of the Betts Cove ophiolite in the following features: 1) the Blow-Me-Down ophiolite is much thicker (10 vs 5 km.), 2) it has a residual mantle zone, 3) there is no major clinopyroxenite/gabbro unit at the contact between the ultramafic and mafic zones at Blow-Me-Down, 4) it has more than 2 kms. of cumulate gabbro versus less than 0.25 km. at Betts Cove, 5) sheeted dykes at Blow-Me-Down consist of up to 50% brecciated dykes (Williams and Malpas, 1972) whereas the Betts Cove ophiolite has less than 5% brecciated dykes.

D. Physiography and Accessibility

Relief in the Betts Cove area is generally uniform at about 180 metres above sea level. Occasional steep fault scarp valleys interrupt the uniformity of the nearly vegetation-free plateau. Most of the major lakes (Betts Big Pond, Kitty Pond and Burtons Pond) lie in depressions of glacial origin. Exposures are excellent along-shore between Nippers Harbour and Betts Cove and the stratigraphy of the ophiolite is well represented in the coastal section between these locations. Total rock exposure is

approximately 90% of the surface area of the ophiolite.

Access to the area is by boat from either Nippers Harbour or Tilt Cove or overland via a narrow trail from Nippers Harbour to Betts Cove.

The Blow-Me-Down ophiolite is exposed as a 2500 feet high flat-topped mountain. The ophiolite is tilted on edge so that an easy traverse along the top of the mountain reveals well exposed (85% rock outcrop) ultramafic, gabbro and sheeted dyke members as well as the pillow lava member.

Access to the Blow-Me-Down ophiolite is by a two-lane gravel road as far as Lark Harbour and then by narrow trails to the top of the mountain.

CHAPTER 2

PETROGRAPHY OF THE MAFIC ZONE OF THE NEWFOUNDLAND OPHIOLITES

A. Betts Cove Ophiolite

A.1. Introduction

Stratigraphically downwards the Betts Cove mafic zone comprises an upper and lower pillow lava member, a sheeted dyke member and a thin gabbro member (Figure 4). The upper boundary of the pillow lava members appears to be a fault above which pillow lavas and sediments of the Snooks Arm Group (Jenner, 1977) occur. The contact of the pillow lava members with the sheeted dykes is also faulted in many places and is frequently marked by the presence of brecciated rocks. Dykes cut the pillow lavas, especially in the lower parts of the lower lava member. However, in passing from the sheeted dyke member to the lower pillow lava member, the frequency of dyke occurrence does not decrease gradually; rather the frequency drops abruptly from 95-100% to 10-20% across the sheeted dyke/pillow lava contact. The dykes also cut massive gabbro underlying the sheeted dyke complex, as well as several small isolated

leucocratic bodies within the sheeted member (Plate 1F).

A.2. Pillow lava members

The pillow lava sequence at Betts Cove is divisible into an upper and a lower member on the basis of texture and mineralogy. The upper pillow lava member comprises nonvariolitic, vesicular pillows averaging 0.75 m by 0.25 m in size. Phenocryst phases include clinopyroxene and plagioclase, but not olivine. Plagioclase and clinopyroxene also occur as laths in the groundmass where they are partially or totally replaced by albite and actinolite/chlorite, respectively. Often plagioclase and clinopyroxene form spherulitic fan or bow-tie structures (Lofgren, 1974). Magnetite, usually replaced by hematite, and sphene are accessory minerals. Altered interstitial mud and chert occur between pillows (Plate 1C).

The lower pillow lava member (Plate 1D) has pillows which are variolitic and only occasionally vesicular. Very little interstitial material occurs. Clinopyroxene is found as a phenocryst phase, as laths in the groundmass of the cores of pillows (Plate 1E) and commonly as radiating spherulitic crystals. Olivine, pseudomorphed by chlorite, and commonly containing minute chromite inclusions, is usually present as a phenocryst phase. Plagioclase, invariably replaced by albite, is always interstitial to clinopyroxene laths. Pyrite is the only opaque mineral recognized.

PLATE 1

A. Clinopyroxenite rock cutting across layered ultramafic (layering perpendicular to hammer handle). Southwest of Kitty Pond.

B. Clinopyroxenite (coarse-grained) with inclusion of ultramafic rock (dark fine-grained). Candlemas Head.

C. Upper pillow lavas with epidote and calcite (lighter colours) between pillows. East side of Betts Cove.

D. Lower pillow lavas showing concentrations of varioles (white) toward the centre of the pillow.

E. Photomicrograph of the centre of lower pillow lava, BC-74-101, with elongate clinopyroxene crystal (left side of photo) in a matrix of albite and quartz (white) and stubby clinopyroxene crystals.

F. Diabase dykes (dark) cutting leucogabbro (light colour) along coastline south of Betts Bight Pond.

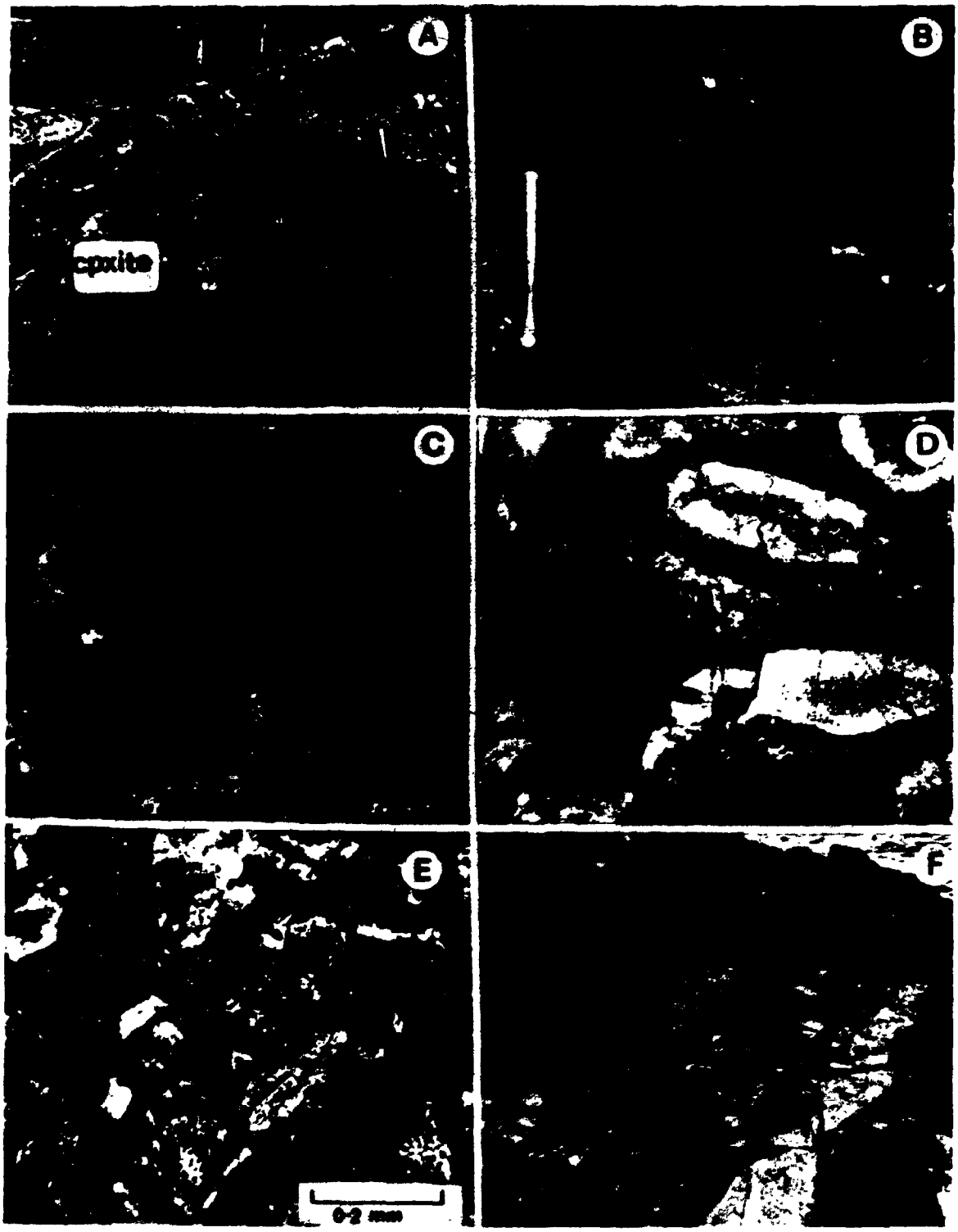
A
epxite
B
C
D
E
F

A.3. Sheeted Dyke Member

Sheeted dykes are described as parallel or sub-parallel sheets of intrusive material which occupy up to 100% of rock exposure. The dykes at Betts Cove strike N60°E in the south, east-west in the central part and N30°W in the north. Chilling on one or both sides of fine grained dykes occurs against coarse dykes (Plate 2A, B, C).

Three compositional rock types are present in the Betts Cove sheeted dyke member: 1) Diabase Dykes, 2) Picritic Dykes, 3) Perknite material.

A.3a. Diabase Dykes

Diabase dykes are the most common, and the latest, set of intrusions in the sheeted dyke member. They cut all other types of dykes and often branch and vein older dykes and gabbro in random directions (Plate 1F). The diabase dykes are usually fine to medium grained and exhibit considerable grain size change from the chilled margins to their centres (Plate 2A). They range from 15 cm to 0.5 m in width, and in general, appear to outcrop more frequently in the upper portions of the sheeted dyke complex than in the lower parts.

The diabase dykes comprise nearly equal proportions of clinopyroxene/actinolite and albite. The clinopyroxene shows all degrees of uralitization and it always has a lath-like crystal form whereas plagioclase is anhedral and interstitial to the clinopyroxene. Orienta-

PLATE 2

A. Fine grained dyke cutting coarser grained porphyritic dyke. Note the chilling (lighter colours) on both sides of the fine grained dyke. Southwest of Betts Bight Pond.

B. Chilling of medium grained dyke against perknite rock. Along coast west of Betts Bight Pond.

C. Photomicrograph showing typical contact zone between a fine and medium grained dyke in sheeted complex.

D. Chlorite pseudomorph (dark) after olivine? in a matrix of altered pyroxene and albite in picritic dyke in Betts Cove sheeted complex (crossed nicols).

E. Euhedral chromite grains in a very fine grained chlorite-actinolite alteration of large phenocryst in picritic dyke, Betts Cove (plane light).

F. Typical perknite rock with interlocking actinolite grains and irregular patches of chlorite (dark areas). (crossed nicols).

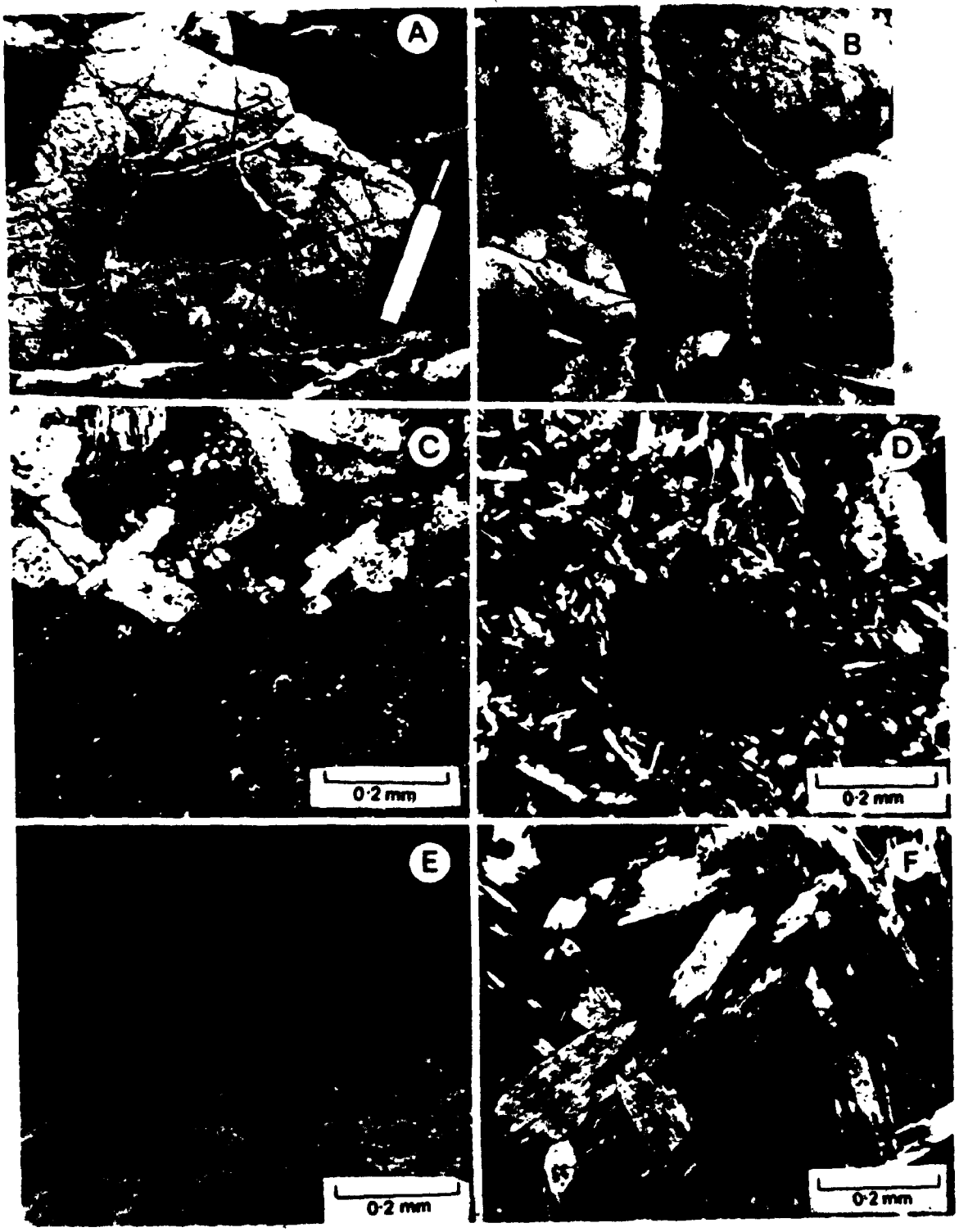
A
B
C
0·2 mm
D
0·2 mm
E
0·2 mm
F
0·2 mm

tion of the clinopyroxene/actinolite laths is observed only adjacent to local faults. Otherwise, original igneous texture is preserved. Where diabase dykes cut pillow lavas, they often have similar quench textures to those of the surrounding lavas. Clinopyroxene in these cases crystallizes as feathery, inclusion-filled skeletal crystals usually arranged in a fan-shaped pattern (Lofgren, 1974), indicating that the stratigraphically higher dykes cooled more rapidly than their lower counterparts.

A.3b. Porphyritic Picritic Dykes

Porphyritic dykes, which weather to a rusty red colour, occur predominantly in the lower parts of the sheeted dyke member and often cut the gabbro member. However, they are found less frequently within the higher levels of the complex. They are wider than the diabase dykes, usually averaging 1 to 1.5 meters. Chilled margins are common where the dykes abut very coarse grained dykes or gabbro. In some, the Bernoulli effect (Bhattacharjii, 1967) results in the concentration of phenocrysts at the centre of these dykes.

Two phenocryst phases, which may occupy up to 50% by volume of some specimens, are present in the porphyritic dykes: 1) Clinopyroxene, partially replaced by actinolite, either alone or in clusters with individual crystals up to 1 mm. long; 2) Chlorite-serpentine patches with a typical olivine crystal form (Plate 2D). The latter

pseudomorphs contain chromite inclusions (Plate 2E) and the rocks in which they occur are relatively enriched in nickel. Thus, it is strongly suggested that olivine was the phenocryst phase although orthopyroxene cannot be ruled out entirely as a possible alternative in some cases.

The groundmass of the porphyritic picritic dykes comprises alteration products of plagioclase and clinopyroxene. The clinopyroxene is usually subhedral to euhedral and the plagioclase interstitial.

A.3c. Perknite Material

Perknite rocks (Peterson, 1961), are very coarse grained (Plate 2F) and consist of actinolite, chlorite and clinopyroxene with less than 5% felsic minerals. At Betts Cove, the green-grey weathering perknite rocks are usually found near the base of the sheeted dyke member. In some instances, the 'dykes' may be discontinuous along their strike whereas, in other cases, they may be traced, and retain a uniform width, over considerable distances. This irregularity in outcrop pattern and the lack of chilled margins make it difficult in the field to determine whether the perknite material is intrusive like the other dykes or represents country rock which has been thoroughly invaded by diabase and picritic dykes.

Actinolite and chlorite are the principal minerals present. Clinopyroxene occurs as unreplaced relicts as

well as cores to actinolite crystals. The amount of clinopyroxene originally present, in some specimens, may have been as high as 80%. Patches of chlorite without crystal form are probably after olivine as is suggested by the occurrence of euhedral chromite in the patches and the high concentration of nickel in these rocks (Chapter 3). Albite occurs in minor quantities interstitial to the mafic minerals. Texturally, all grains interlock and there is little variation in grain size within a single thin section.

The perknites are similar in mineralogy to the coarse, grey clinopyroxenite at the base of the complex gabbroic transition zone located between the ultramafic and mafic zones of the Betts Cove ophiolite (Riccio, 1972; Church, 1977).

A.3d. Brecciated Dykes

Dykes which have been brecciated are relatively uncommon except near the contact between the pillow lava and sheeted dyke members. Fragments consist of angular to sub-rounded diabase dyke material. Apparently other compositional dyke types have escaped this brecciation. The matrix in the brecciated dykes is now a metamorphic mineral assemblage of epidote, calcite, chlorite and quartz. It has been suggested, for the Betts Cove (Riccio, 1972) and the Bay of Islands (Williams and Malpas, 1972) ophiolites, that the brecciation is a result

of gas release. Brecciation by pressurized gas is probably a reasonable explanation for the fragmentation of isolated dykes in the complex, but the brecciation which occurs along the pillow lava/sheeted dyke contact may be better explained by the flow of hot seawater during hydrothermal metamorphism in an ocean-floor circulatory system (see Chapter 4).

A.4. Gabbro Member

The gabbro member, which consists primarily of leucogabbro, outcrops as a thin (0.5 km) stratigraphic unit below the sheeted dyke member (Figure 4), as isolated bodies within the sheeted complex, and as small screens between the sheeted dykes. The basal part of the gabbro is composed of a coarse to medium grained unit of clinopyroxenite which grades upwards into gabbro. Grain size variations occur on a cm. scale and pegmatitic patches of gabbro within normal grain size gabbro are frequent. Normal and melanocratic gabbro also occur (Riccio, 1972). The occurrence of ultramafic blocks in the gabbro and the observation that diabase as well as picritic dykes cut the gabbro indicate that its formation post-dates the ultramafic material and predates the sheeted dyke complex.

Plagioclase and clinopyroxene, the two principal minerals in the gabbro member, are partially altered by metamorphism. However, sub-ophitic to ophitic features are preserved in the leucogabbro. On the other hand, in

some screens of melanocratic metagabbro, plagioclase is anhedral and interstitial to euhedral clinopyroxene and actinolite pseudomorphs after clinopyroxene. The presence of patches of chlorite with included grains of red chromite, possibly representing olivine crystals, suggests that the melanocratic metagabbros may have been olivine gabbros. Such rocks may form an important constituent of the ophiolite.

There is difficulty in distinguishing fine grained gabbro screens from coarse grained diabase dykes. The best criterion is probably the morphology of the outcrop. If the material terminates along strike within a few metres, it is likely to be a gabbro screen; in contrast, dykes would be expected to continue for tens of metres.

B. Blow-Me-Down Ophiolite

The pillow lavas in the Blow-Me-Down ophiolite can be divided into an upper and lower member mainly on the basis of field observations. The upper lavas are reddish and highly vesicular whereas the lower lavas are black and less vesicular. Plagioclase is a major phenocryst and lath phase, clinopyroxene being interstitial - in contrast to the situation described for the Betts Cove ophiolite. Olivine pseudomorphs appear to be absent.

The sheeted dykes at Blow-Me-Down are principally fine grained diabase dykes. Picritic dykes are restricted to a few outcrops which cut the gabbro member

and perknite material is absent. Furthermore, up to 50% of dykes in the Blow-Me-Down complex are thoroughly brecciated (Williams and Malpas, 1972). The principal igneous minerals are plagioclase, which occurs both as phenocrysts and as euhedral laths, and clinopyroxene, which is invariably interstitial to the plagioclase forming sub-ophitic to ophitic texture. Rare olivine pseudomorphs occur in the picritic dykes cutting the gabbro member.

The gabbro member in the Blow-Me-Down ophiolite comprises an upper massive and a lower layered unit (Figure 3) (Riccio, 1976). The massive gabbro comprises plagioclase, clinopyroxene, and hornblende, with minor magnetite. Layered gabbros include olivine gabbros, norites, anorthosites, and ilmenite gabbros (Riccio, 1976). The order of crystallization of minerals in the mafic and ultramafic cumulates is olivine (chromite)- plagioclase-clinopyroxene- (orthopyroxene?) (Riccio, 1976; Church and Riccio, 1977). The precipitation order is consistent with mineralogical observations in the sheeted dykes and pillow lavas and contrasts markedly with the crystallization order at Betts Cove (Church and Riccio, 1977).

CHAPTER 3

GEOCHEMISTRY OF THE MAFIC ZONE OF NEWFOUNDLAND OPHIOLITES

A. Betts Cove Ophiolite

A.1. Whole Rock Chemistry

A.1a. Introduction

Because metamorphism has remobilized many elements in the Betts Cove ophiolitic mafic rocks, only certain immobile elements can be used to interpret the igneous evolution of these rocks. As shown in Chapter 4 and Table 5, TiO_2, P_2O_5, FeO^t/MgO, Ni, Cr, Zr and Y appear to have remained stable during low grade metamorphism of the ophiolite. Other oxides, such as MgO and Al_2O_3, appear to have been mobile; nevertheless, they may still be used to distinguish between igneous groups with significant primary chemical differences. However, because of the metasomatic movement of most major elements, normative compositions of the metamorphosed mafic rocks at Betts Cove cannot be used to classify them.

In this section, therefore, the abundances of the immobile elements listed above will be examined in an

attempt to unravel the igneous trends of the lavas, dykes and gabbros of the Betts Cove ophiolite.

A.1b. Variation of Nickel Against FeO^t/MgO Ratio

Crystal field theory (Burns and Fyfe, 1966, 1967; Burns, 1970; Fyfe, 1974a) predicts that Ni^{2+} has a great affinity for octahedral mineral sites. During cooling of a mafic liquid, nickel will preferentially enter the crystallizing olivine solid phase. This presumably is because the solid phase has more octahedral sites than the liquid and therefore the element Ni gains considerable stabilization energy by entering the solid phase. Furthermore, due to crystal field effects, it is difficult to remove nickel from these sites during low grade metamorphism. Consequently, even in metamorphosed mafic rocks, the nickel content can indicate the amount of olivine originally present and can reveal fractionation trends. Another chemical parameter which varies significantly with igneous fractionation is the FeO^t/MgO ratio. Because most of the early crystallizing phases from a mafic liquid are magnesium rich, it is expected that the FeO^t/MgO ratio of the basaltic liquids will increase during the early stages of fractionation.

Figure 5 shows the variation of Ni against FeO^t/MgO ratio for the Betts Cove pillow lava and sheeted dyke members. The curve reveals an initially large decrease in

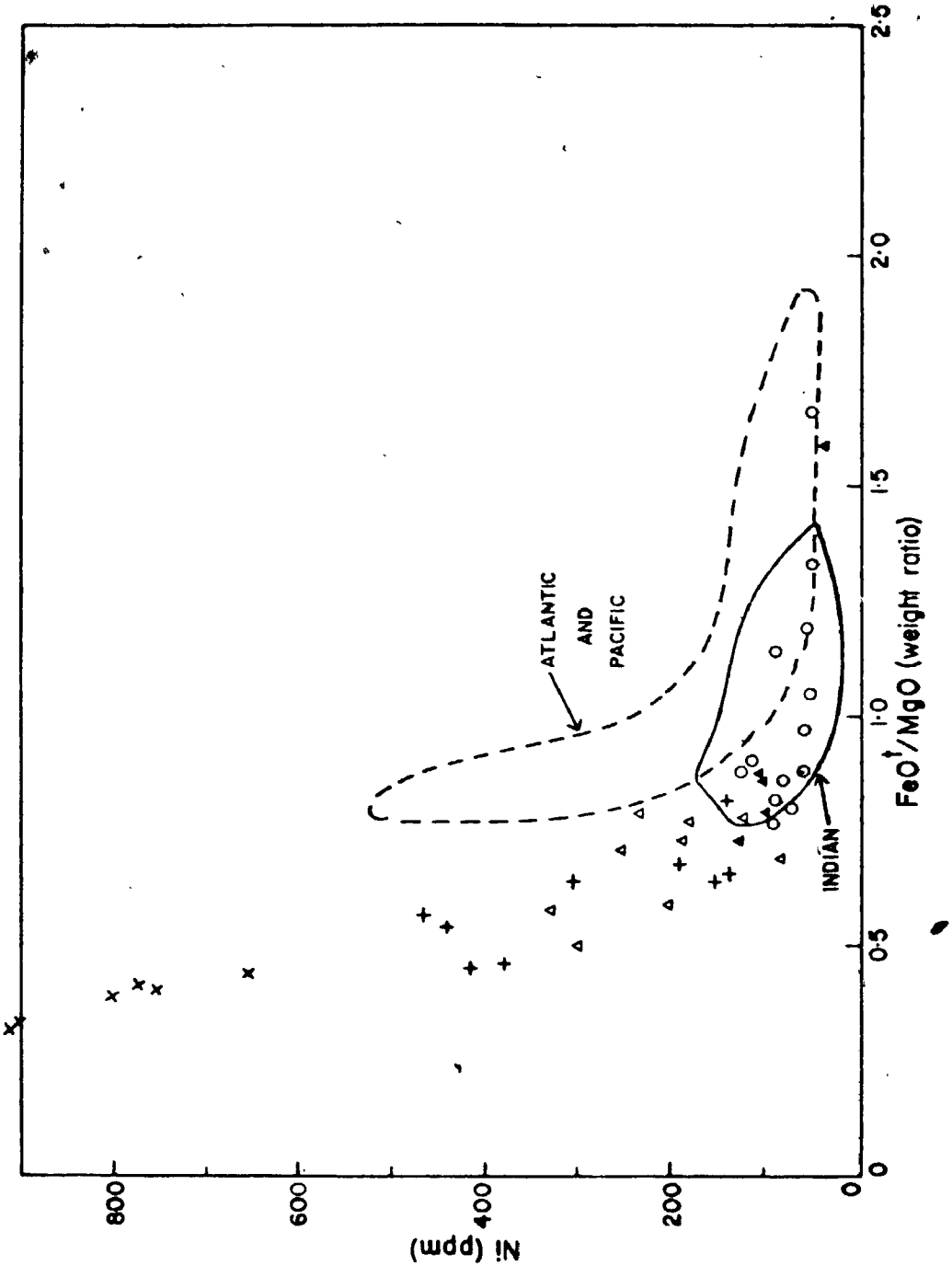

FIGURE 5. VARIATION OF Ni AGAINST FeO^T/MgO RATIO FOR THE BETTS COVE PERKNITE MATERIAL (×), PICRITIC DYKES (+), DIABASE DYKES (○), LOWER PILLOW LAVAS (△) AND UPPER PILLOW LAVAS (▲) COMPARED TO MODERN OCEAN FLOOR BASALTS.

the nickel contents of the mafic rocks with a small increase in the FeO^t/MgO ratio followed by a very small decrease in Ni with further increase in FeO^t/MgO. Perknite material has the highest Ni and lowest FeO^t/MgO values; the diabase dykes and some of the pillow lavas have the lowest Ni and highest FeO^t/MgO whereas the porphyritic dykes and lower pillows have intermediate values. The high Ni content (600-900 ppm) of the perknite material is far above nickel values for even the most picritic basalts (300-375 ppm) from the ocean floor (Frey et al., 1974) and also exceeds the maximum solubility of nickel in a basaltic liquid. The high nickel and low FeO^t/MgO of the perknite material may then be due to the accumulation of olivine. Further evidence will be presented in succeeding sections to indicate that the perknite rocks are cumulates.

The porphyritic dykes and lower pillow lavas have nickel values similar to those of picrites and high magnesium olivine basalts. There is evidence to suggest that some of the analyses of the picritic porphyritic dykes which have higher nickel values than the lower lavas (Figure 5) may represent rocks which have accumulated olivine due to flow within the dykes. Analysis of one porphyritic dyke reveals that the whole rock chemistry varies considerably from the margin to the centre (Table 1). The significant point is that the centre of the dyke has lower FeO^t/MgO and higher Ni and Cr than the margin. This is consistent with the flow differentiation of olivine

TABLE 1

Whole rock analyses of specimens from different portions of a single picritic dyke. (Oxides in wt.%, traces in ppm).

Sample #	BC7417 Margin	BC7418 Medial Zone	BC7419 Centre
SiO_2	55.44	47.11	49.29
TiO_2	.08	.06	.06
Al_2O_3	12.30	9.48	8.47
Fe_2O_3	.78	1.68	1.57
FeO	5.97	8.42	7.54
MnO	.16	.19	.18
MgO	11.60	19.31	18.60
CaO	4.88	6.47	6.88
Na_2O	4.35	.87	.95
K_2O	n.d.	n.d.	n.d.
P_2O_5	.01	n.d.	.02
L.O.I.	3.34	5.96	4.97
Total	98.91	99.55	98.55
FeO^t/MgO	.57	.51	.48
Ni	112	397	526
Cr	521	1452	1589
Zr	7		4
Y	7	4	7
Sr	90	27	26
Rb	nd	nd	1
Ba	15	19	17

n.d. - not detectable
FeO^t - Total iron as FeO

toward central portions of the dyke as found by the experiments of Bhattacharjii (1967). Other elemental variations such as the changes in Ti and Zr contents can be accounted for by dilution due to the addition of Ti-Zr free phases. Thus, some of the very primitive dyke analyses of the Betts Cove ophiolite probably do not represent true liquid compositions. However, the lower pillows, which were liquids, are more magnesian than any modern ocean floor rocks.

The diabase dykes, upper pillow lavas and some of the lower pillows have Ni concentrations similar to oceanic tholeiite. However, at a given Ni content, the FeO^t/MgO ratio in the Betts Cove mafic rocks is lower than averages from the Atlantic and Pacific basalts (Figure 5). There is some overlap between Indian ocean basaltic values and some of the more differentiated Betts Cove material.

In qualitative terms, the exponential drop in nickel with increasing FeO^t/MgO observed for the Betts Cove mafic rocks is typical of fractionation of olivine from a very mafic liquid. Rapid loss of olivine in the initial stages of fractionation severely depletes the Ni content of the liquid while later more limited fractionation of olivine as well as other mafic minerals extracts less nickel.

A.1c. Nickel versus Chromium Variations

The Betts Cove mafic rocks show a sympathetic relationship between the concentrations of nickel and

chromium (Figure 6). Again the perknite material has the highest Ni and Cr values with the lower green lavas, picritic dykes, diabase dykes and upper pillow lavas plotting at successively lower values of Ni and Cr. Values of Cr as high as 2000 ppm in the perknite material, for the same reasons given above for nickel, support a cumulate origin for these rocks. The diagram also shows that the picritic dykes and most of the lower lavas are more mafic than the diabase dykes and upper pillow lavas.

The reason for the close relationship between Ni and Cr is that early crystallizing olivine (the principal source of nickel) usually contains small inclusions of chromite (the major site for Cr). With increasing time and lower temperatures, the amount of olivine and included chromite precipitating decreases, thereby giving lower values of Ni and Cr. Also, the Cr content of the chromites will decrease with increasing fractionation due to the increase in the iron content of the liquid (Irvine, 1974; Hill and Roeder, 1974).

The range of Ni and Cr values from the Betts Cove dykes and lavas falls within the range of concentrations of these elements reported from basaltic rocks from the ocean floor (Blanchard et al., 1976). However, there appears to be a significantly larger number of rocks with very high Ni and Cr contents at Betts Cove than found to date on the ocean floor. Less than 10% of dredged oceanic rocks are picritic or very high magnesium whereas at Betts

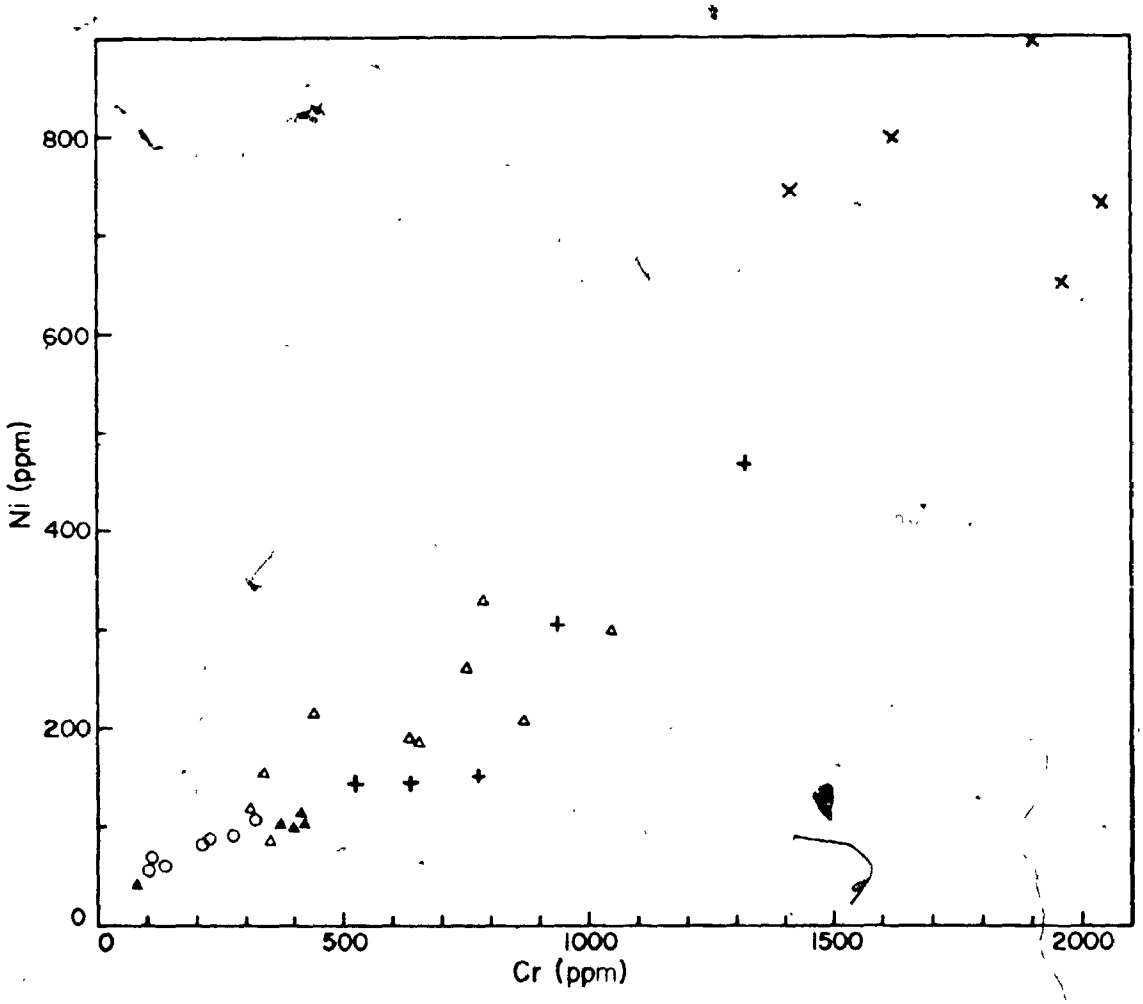

FIGURE 6. VARIATION OF NI AGAINST CR FOR THE BETTS COVE OPHIOLITIC MAFIC ROCKS. SYMBOLS AS IN FIGURE 5.

Cove the porphyritic dykes and high Ni-Cr lower lavas constitute more than 50% of the basaltic effusive and intrusive material present. Assuming statistical sampling for both the Betts Cove ophiolite and ocean floors, it is implied that Betts Cove has a disproportionate amount of high temperature magnesian basaltic liquid.

A.1d. Titanium, Zirconium and Ytrium Variations

The Betts Cove dykes and pillow lavas are different in terms of the contents of Ti, Zr and Y from most basalts. (Figures 7 and 8). On a Ti vs. Zr plot (Figure 7) the Betts Cove mafic rocks have extremely low values of Ti and Zr compared to the concentrations of these elements in basalts from island arc, ocean floor, and within-plate tectonic environments. The picritic dykes, perknite rocks and lower pillow lavas have the lowest Ti and Zr values plotting even below the field of island arc tholeiites. The diabase dykes and upper pillow lavas have higher Ti and Zr values. Nevertheless, most analyses of the rocks plot outside the fields of tholeiitic basalt; only a few occurring within the field of low-K island arc tholeiite (Figure 7). Similarly, the Ti-Zr-Y diagram of Pearce and Cann (1971, 1973) (Figure 8) fails to classify the Betts Cove mafic rocks since all analyses except the four upper pillow lavas fall outside all proposed basaltic environment fields.

If the Betts Cove mafic rocks were not basalts, they

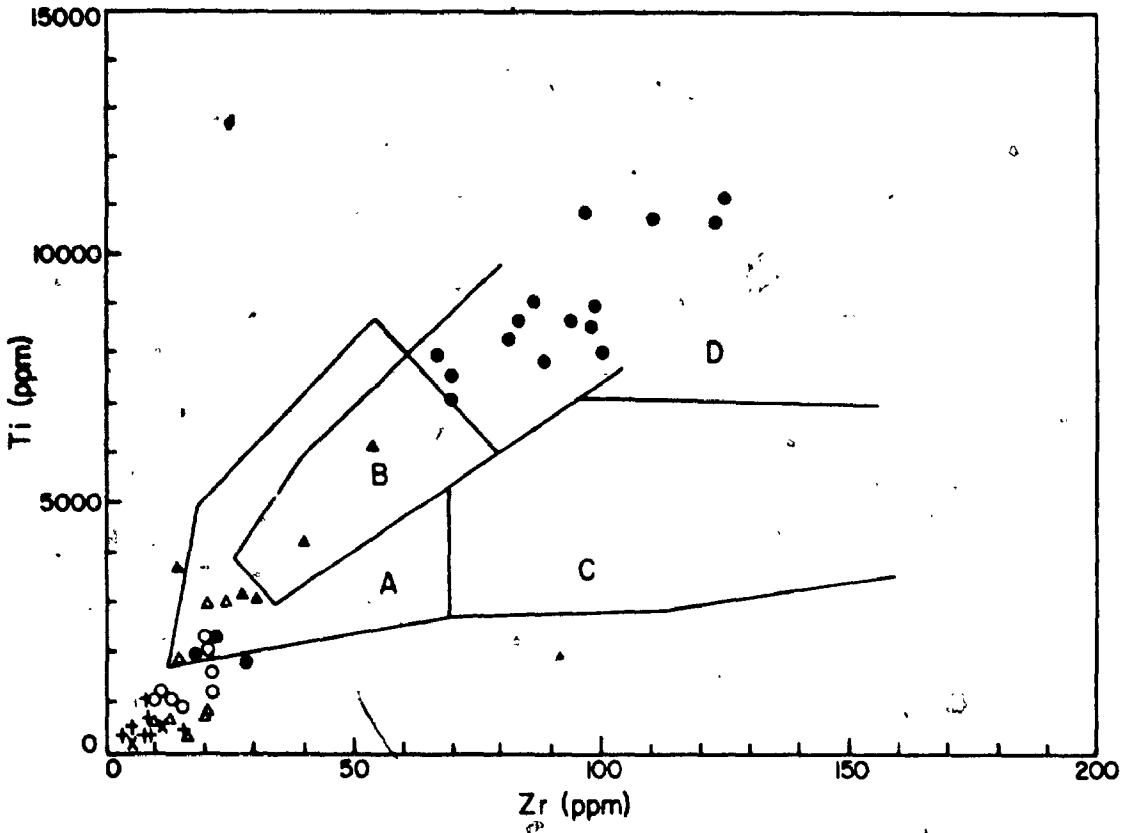

FIGURE 7. VARIATION OF TI WITH ZR OF THE BETTS COVE MAFIC ROCKS COMPARED WITH THE BLOW-ME-DOWN LAVAS AND DYKES (●). LOW K THOLEIITES PLOT IN FIELDS A AND B, CALC-ALKALINE ROCKS IN C AND B AND OCEAN FLOOR BASALTS IN B AND D (PEARCE AND CANN, 1971). OTHER SYMBOLS AS IN FIGURE 5.

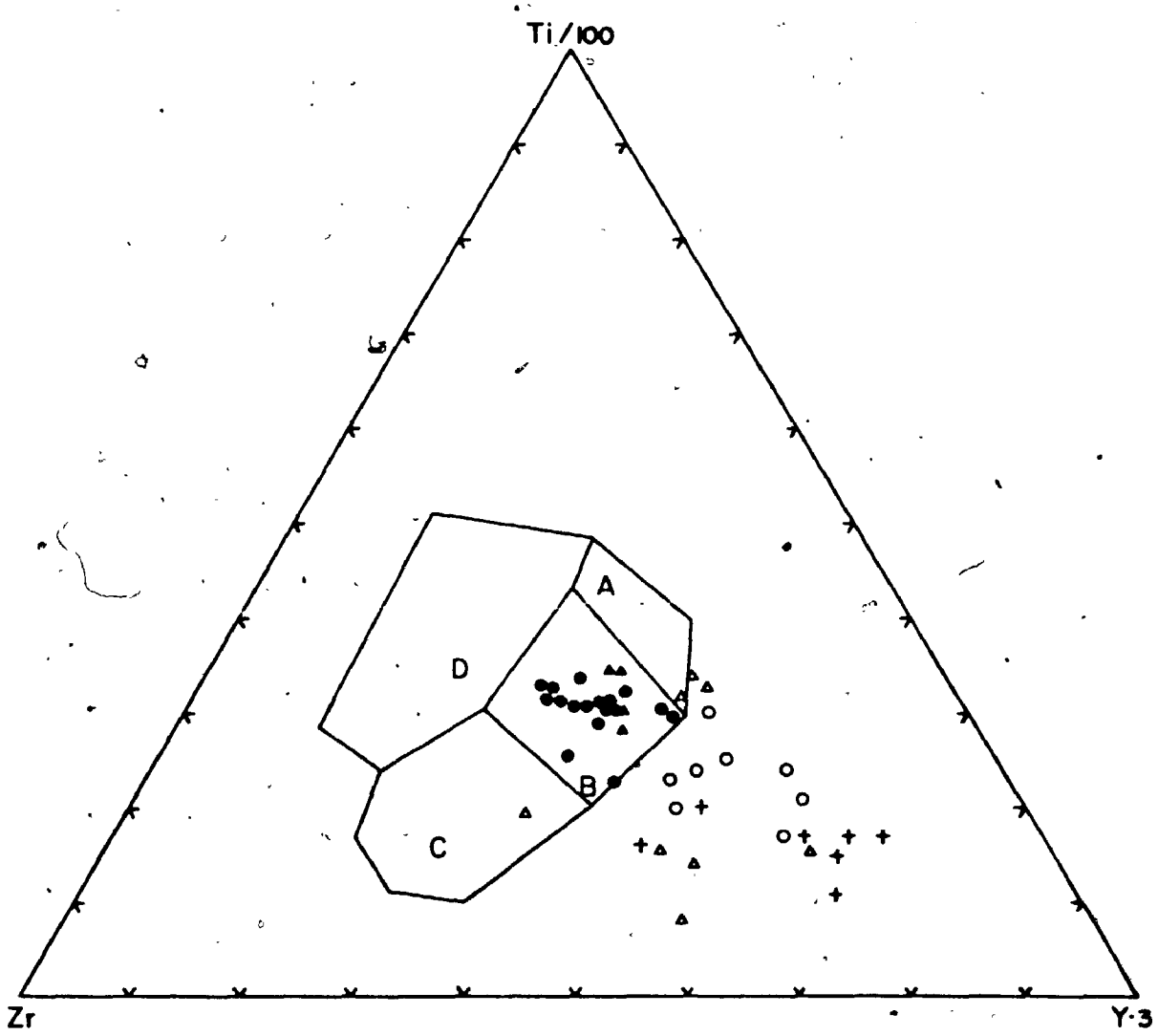

FIGURE 8. TI-ZR-Y RELATIONSHIPS FOR THE BETTS COVE AND BLOW-ME-DOWN MAFIC ROCKS. SYMBOLS AS IN FIGURE 7. OCEAN FLOOR BASALTS PLOT IN FIELD B, ISLAND ARC BASALTS IN FIELDS A AND B, CALC-ALKALI BASALTS IN FIELDS B AND C AND WITHIN PLATE BASALTS IN FIELD D (PEARCE, 1975).

would not be expected to plot in any of the basaltic environment fields. However, the Ni, Cr and FeO^t/MgO ratio values clearly indicate that the Betts Cove rocks are indeed basalts, although high magnesian. Therefore, the low Ti and Zr characteristics of the dykes and pillows are a reflection of variables other than tectonic environment.

The variation of TiO_2 against FeO^t/MgO weight ratio has been used to distinguish tholeiitic from calc-alkaline trends in basaltic rocks (Miyashiro, 1973, 1974, 1975a; Miyashiro and Shido, 1975). In a tholeiitic rock series, TiO_2 initially increases with increasing FeO^t/MgO until titanomagnetite crystallizes, at which point TiO_2 decreases with further increase in the FeO^t/MgO ratio. On the other hand, rocks of the calc-alkaline series tend to show a monotonic decrease in TiO_2 with increasing FeO^t/MgO weight ratio (Miyashiro and Shido, 1975).

Figure 9 is a plot of the variation of TiO_2 against FeO^t/MgO ratio for the Betts Cove pillow lavas and sheeted dykes compared with trends from recent ocean-floor rocks and the Troodos ophiolitic basalts. The plot shows that 1) the Betts Cove rocks exhibit a slight increase in TiO_2 with increasing FeO^t/MgO ratio; in this respect, therefore the rock series is tholeiitic. 2) the concentration of TiO_2, at a given FeO^t/MgO, in the Betts Cove material is much lower than in either the Troodos ophiolitic basalts or in modern ocean floor mafic rocks, suggesting that the

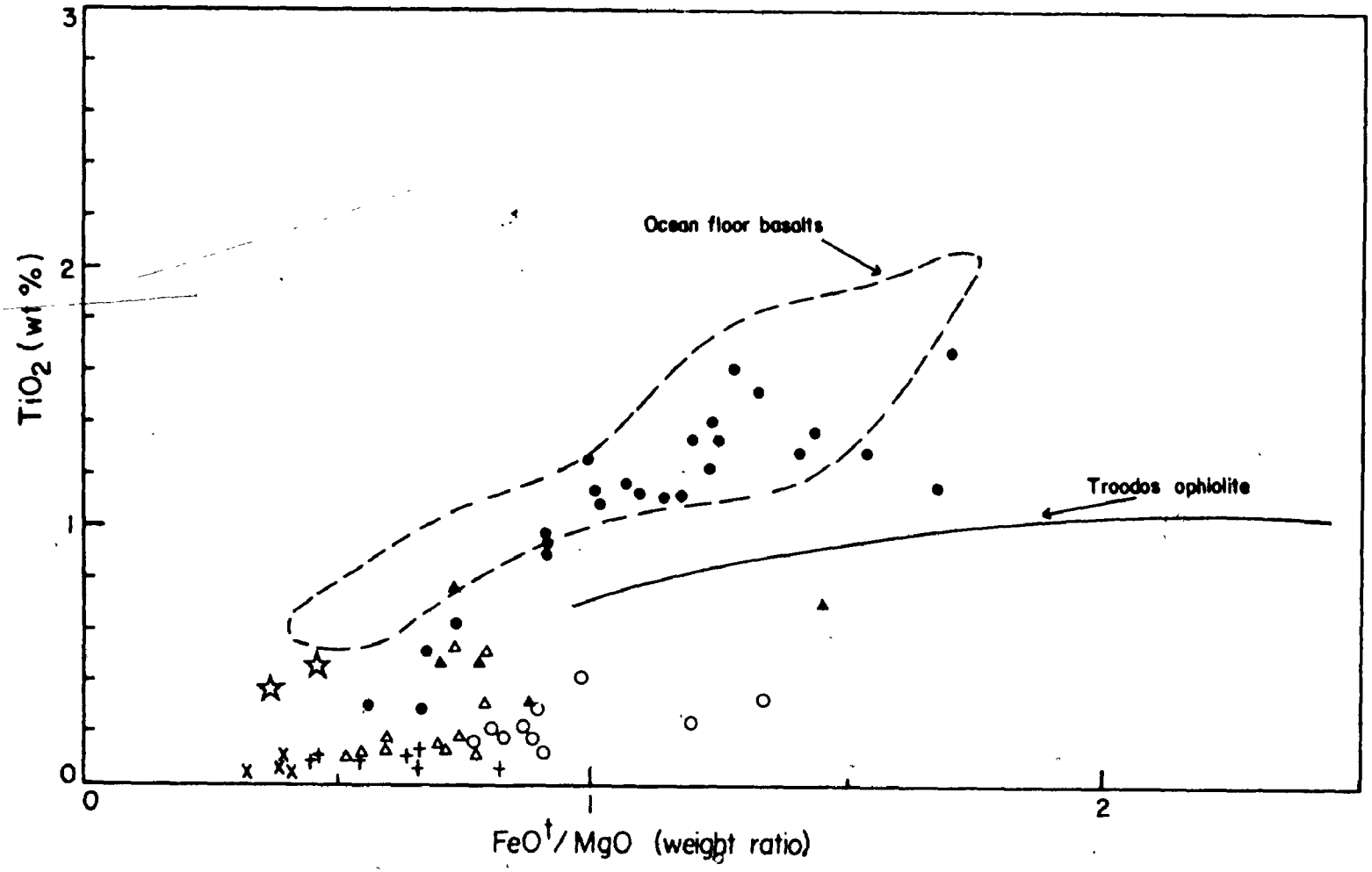

FIGURE 9. VARIATION OF TiO_2 AGAINST FeO^T/MgO FOR THE BETTS COVE AND BLOW-ME-DOWN LAVAS AND DYKES COMPARED TO MODERN OCEANIC THOLEIITE AND THE TROODOS OPHIOLITIC BASALTS. ☆ REPRESENTS PICRITIC BASALTS FROM THE OCEAN FLOOR. OTHER SYMBOLS AS IN FIGURE 7.

low content of TiO_2 in the Betts Cove rocks is not because these rocks are less fractionated than either the ocean floor rocks or the Troodos basalts. Rather, it appears that the parental magmas from these separate regions had different TiO_2 contents.

A.1e. Phosphorus Variations

P_2O_5 appears to be stable during low grade metamorphism. It also has very low distribution coefficients (P_2O_5 in mineral/P_2O_5 in liquid) so that it is strongly fractionated into residual liquids (Clague and Bunch, 1976). Because of these two properties, phosphorus has been used in combination with other elements as an indicator of magma type and tectonic setting (Floyd and Winchester, 1975; Winchester and Floyd, 1976) and as a measure of the degree of fractionation of basaltic rocks (Clague and Bunch, 1976).

Winchester and Floyd (1976) use a P_2O_5 versus Zr plot to distinguish alkalic from tholeiitic basalts. They admit, however, that these parameters cannot be used to differentiate different tectonic environments. The Betts Cove ophiolitic rocks on this basis are tholeiitic in nature and are depleted in Zr and P_2O_5 compared to most oceanic tholeiites and other ophiolitic basalts (Figure 10).

It is also noted that there is a spread in Zr and P_2O_5 values with the upper pillows being higher in both Zr

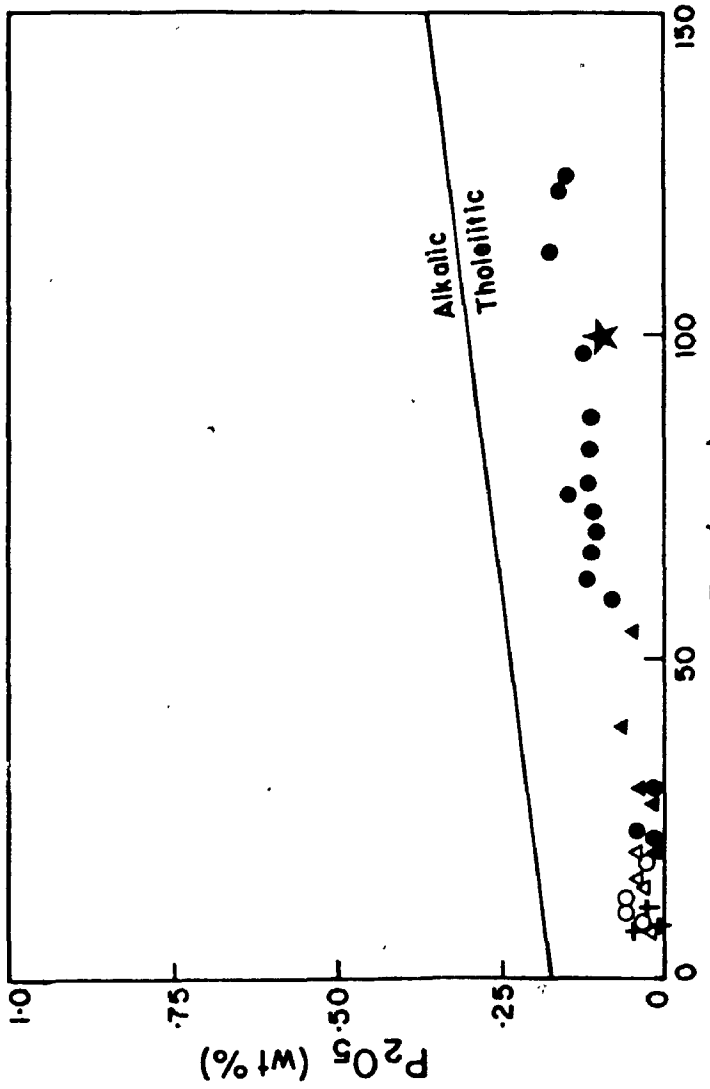

FIGURE 10. P_2O_5 - ZR RELATIONSHIPS FOR THE BETTS COVE AND BLOW-ME-DOWN MAFIC ROCKS. (★) REPRESENTS MODERN OCEANIC THOLEIITE. SYMBOLS AS IN FIGURE 7.

and P_2O_5 than other ophiolite members. This variation is what would be expected during fractionation of a basaltic rock series. If it is assumed that these two elements are not strongly partitioned into any fractionating mineral phase, then approximately 50% of the original liquid has to have been removed to account for the observed variations at Betts Cove. Further analysis of fractionation processes is presented in Chapter 5.

A.1f. Al_2O_3 and MgO as Igneous Discriminants

Although magnesium migrates during low grade metamorphism and Al_2O_3 may be mobile in at least the upper portions of the Betts Cove ophiolite (Chapter 4), it is apparent that the mobilization of these oxides does not obliterate all original igneous differences between the various rock types. Figure 11 shows that, generally, diabase dykes and upper pillow lavas can be distinguished from picritic dykes and lower pillow lavas, and from perknite (cumulate) rocks. In fact, the distribution pattern on the Al_2O_3 - MgO diagram is similar to that exhibited by the immobile parameters - Ni and FeO^t/MgO (Figure 11). The low Al_2O_3 and high MgO contents of the perknite rocks support their cumulate origin and further suggest that the cumulate minerals were mainly ferromagnesian with little plagioclase. The higher Al_2O_3 and lower MgO of the diabase dykes and upper pillow lavas suggests that they are more differentiated than the pic-

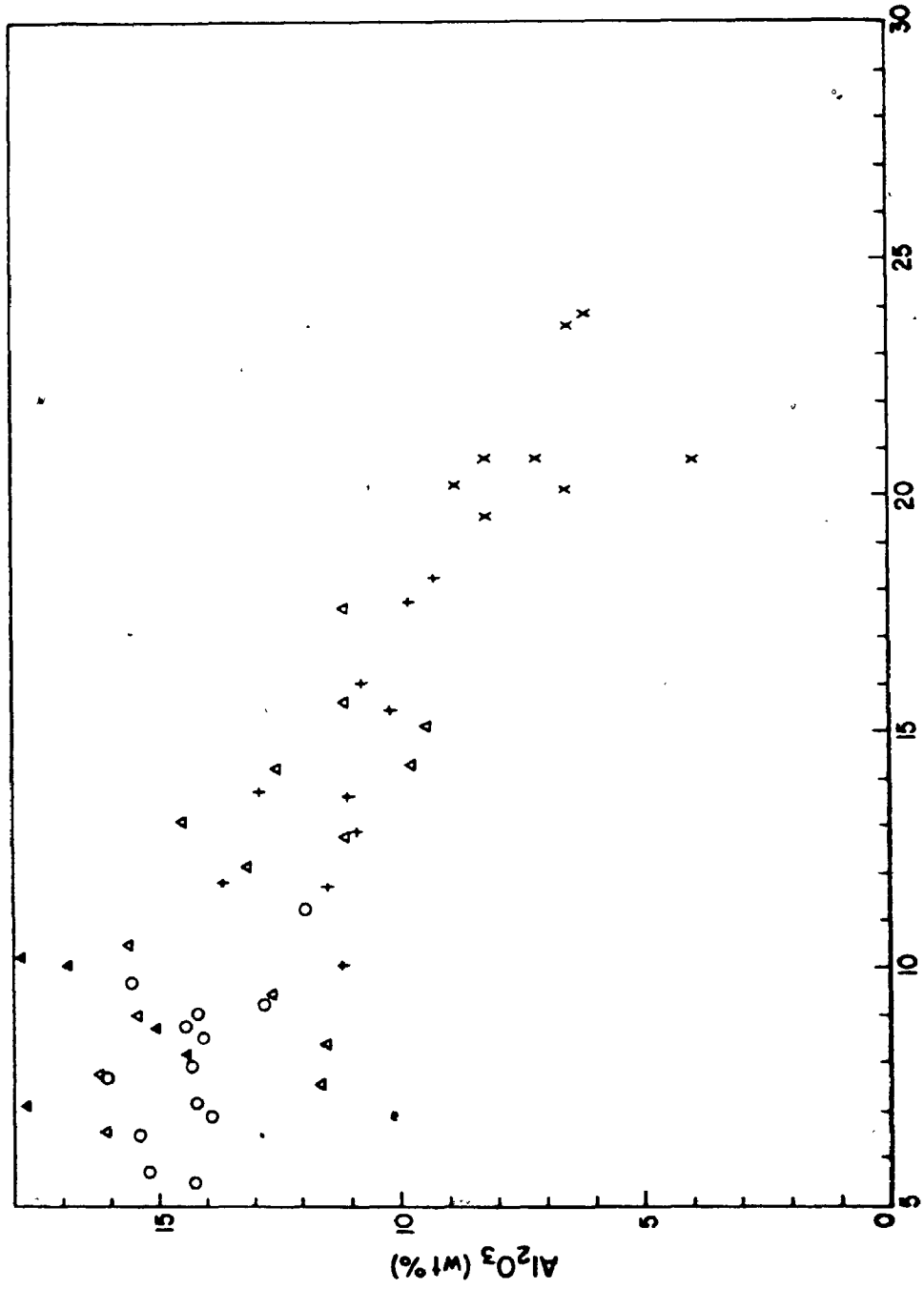

FIGURE 11. VARIATION OF Al_2O_3 AGAINST MgO FOR THE BETTS COVE MAFIC ROCKS. SYMBOLS AS IN FIGURE 5.

ritic dykes and some of the lower pillow lavas. The scatter of MgO values within each rock group (presumably due to metasomatism), however, negates the use of these two parameters to quantitatively discuss fractionation processes.

A.1g. Rare Earth Element Distribution

The effects of alteration on the concentrations of the rare earth elements (REE) in basalts are still little known. Frey et al. (1974) concluded that low temperature alteration of glassy rocks from the ocean floor resulted in a decrease in the overall abundances of REE but that the alteration of crystalline material caused an increase in light REE relative to heavy REE. Systematic studies of the mobility of REE in greenschist and higher grade metamorphic facies rocks are lacking. Nevertheless, the rare earth element patterns in greenschist facies oceanic rocks have been used to delineate igneous trends (Philpotts et al., 1969; Kay et al., 1970; Montigny et al., 1973; Kay and Senechal, 1976; Smewing and Potts, 1976) under the assumption of the immobility of the rare earth elements. This assumption appears to be valid simply because igneous patterns similar to trends from fresh oceanic rocks are present in the metamorphosed oceanic material. Furthermore, by careful examination of REE patterns and comparison with other trace element concentrations, it is possible to distinguish patterns caused

by metasomatic movement of the elements from those of primary igneous origin.

The rare earth element patterns of the Betts Cove dykes and lavas show a slight depletion in LREE, a negative Eu anomaly and a flat HREE distribution (Figure 12). The absolute abundances can be correlated with the TiO_2 content of the rock. For example, sample BC-74-101 has the lowest REE abundance and a TiO_2 content of 0.14 wt. % whereas samples BC-75-3, BC-74-58b and BC-73-236 have higher REE values with TiO_2 contents between 0.3 and 0.5 wt. %. Thus, the rare earth elements and TiO_2 behave similarly in igneous processes (Smewing and Potts, 1976). At a given TiO_2 content, there is no difference in the rare earth element distribution pattern of the lower pillow lavas and the sheeted dykes (Figure 12). This is consistent with a simple fractionation relationship between the above members of the ophiolite.

The light rare earth element depleted pattern of the Betts Cove mafic rocks is typical of patterns exhibited by modern oceanic tholeiite (Kay et al., 1970; Bryan et al., 1976) but, as Figure 12 reveals, the absolute abundances of the REE in the Betts Cove rocks are lower than values for oceanic tholeiites. There is limited overlap in values between the most enriched Betts Cove basalts and the most depleted oceanic tholeiite.

The rare earth element patterns for the Troodos ophiolite of Cyprus (Kay and Senechal, 1976; Smewing and

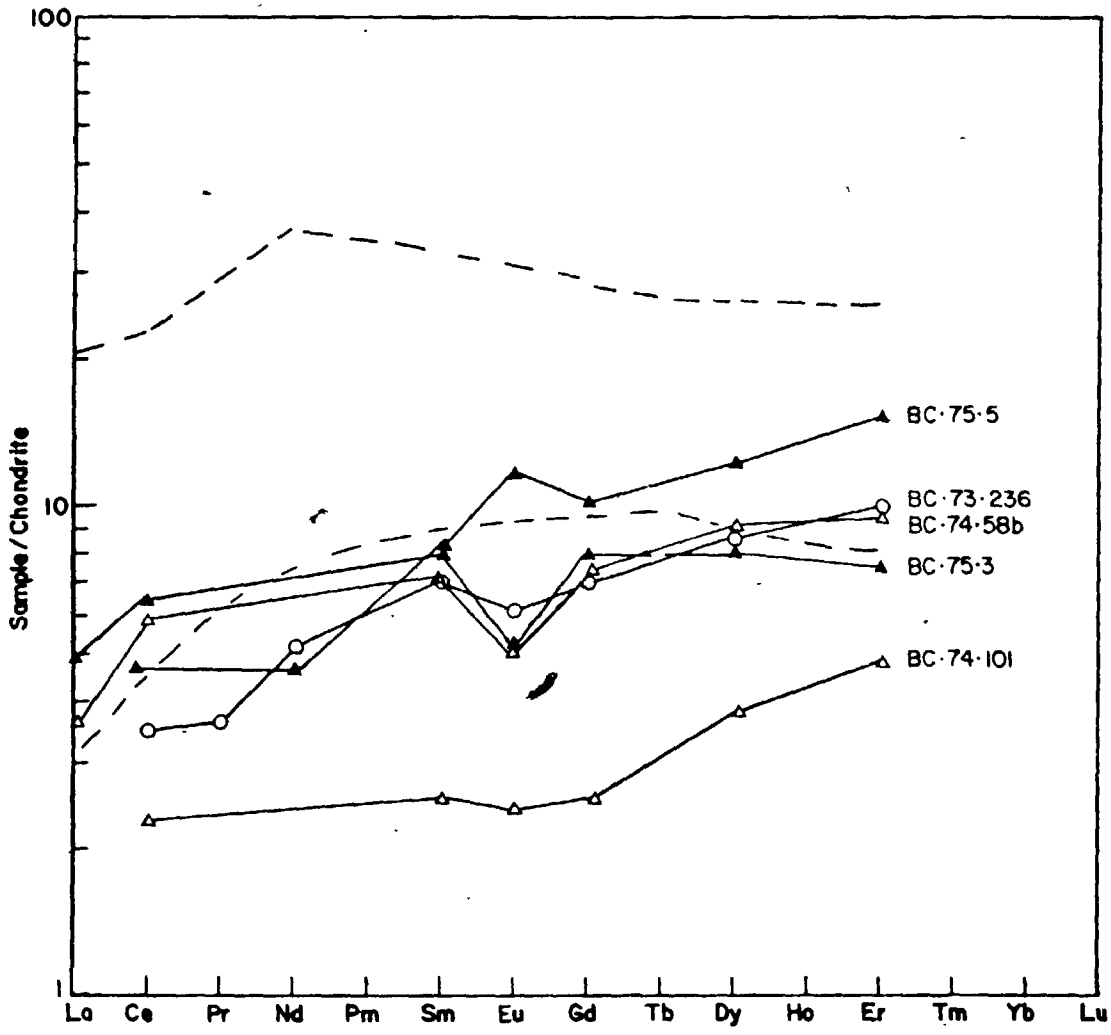

FIGURE 12. CHONDRITE NORMALIZED (HASKIN ET AL., 1968) RARE EARTH ELEMENT PATTERNS FOR THE BETTS COVE LAVAS AND DYKES. SYMBOLS AS IN FIGURE 5. DASHED LINES REPRESENT THE UPPER AND LOWER LIMITS FOR LOW K OCEANIC THOLEIITE (BRYAN ET AL., 1976).

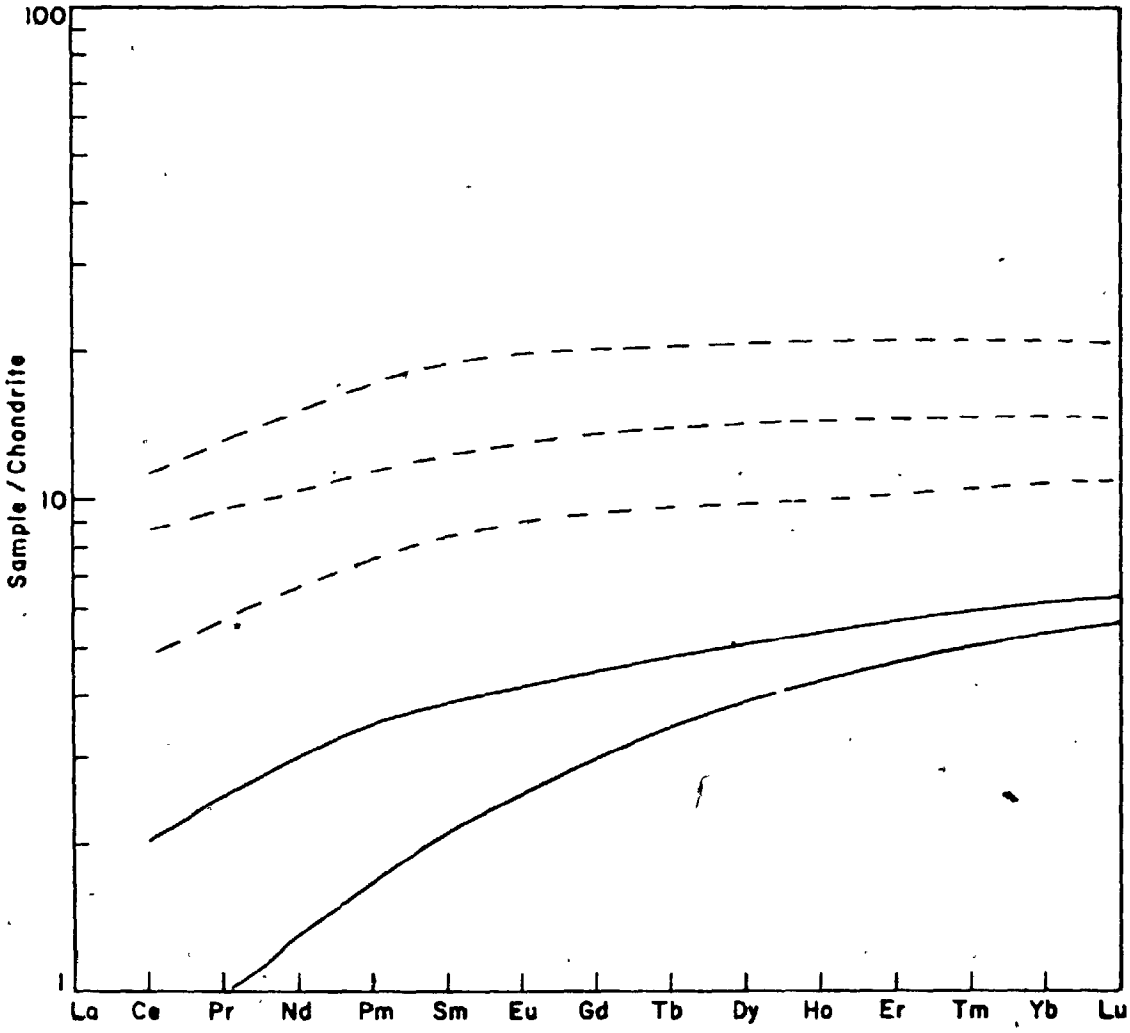

FIGURE 13. RARE EARTH ELEMENT PATTERNS OF THE TROODOS OPHIOLITIC LOWER PILLOW LAVAS (---) AND UPPER PILLOW LAVAS (——) (AFTER SMEWING AND POTTS, 1976).

Potts, 1976) (Figure 13) can be compared with those of the Betts Cove basalts. The Troodos basalts are LREE depleted and are divided into two groups: the first group (lower lava and dykes) has REE abundances between 7 to 10 times chondrite with only a slight LREE depletion; the second group (upper lavas) has much lower REE abundances and a greater depletion in the LREE. Smewing and Potts (1976) concluded that because of the greater depletion in the LREE in the low REE abundance upper lavas, these rocks could not be fractionated to give the REE patterns of the lower lavas. Rather, they invoked different episodes of partial melting of changing source composition to explain the REE patterns. At Betts Cove, the low REE rocks are from the lower lavas and are less depleted in LREE than the rocks (including upper lavas, dykes and lower lavas) with higher REE values. Therefore, the arguement against fractionation used for the Troodos basalts is not valid in the case of the mafic members of the Betts Cove ophiolite.

A.2. Clinopyroxene Chemistry

A.2a. General Comments

Clinopyroxenes occur as phenocrysts, microphenocrysts, laths and skeletal feathery crystals in the mafic members of the Betts Cove ophiolite. All forms are present in the pillow lava members whereas the sheeted dyke and gabbro members usually contain only phenocrysts and microphenocrysts. Microprobe analyses (Appendix III,

types in Hawaii may therefore not be universally applicable, since the clinopyroxenes from Betts Cove cannot be unequivocally assigned to one magma type.

A clearer indication that the Betts Cove clinopyroxenes are tholeiitic is shown on an SiO_2 versus Al_2O_3 diagram (Figure 16) from Lebas (1962). The high silica and low Al_2O_3 contents of the Betts Cove clinopyroxenes are characteristic of non-alkaline lava types.

The tholeiitic nature of the pyroxenes is also revealed in plots of Si and Ti versus Al cations (Figure 17). Ti/Al ratios are much less than 0.2 which according to Kushiro (1960) is characteristic of clinopyroxenes fractionating from a tholeiitic magma. The trend of decreasing Si with increasing Al indicates substitution of Al for Si in tetrahedral sites. Al must also be in octahedral sites since all the clinopyroxenes plot well above the Si + Al = 2 line.

An indication of the behaviour of the clinopyroxenes at Betts Cove during fractionation is shown by the variation of Al, Ti, Si and Cr_2O_3 against Fe/Mg (atomic ratio) (Figures 18 and 19). The degree of fractionation increases with increasing Fe/Mg atomic ratio. The variation of Al with fractionation seems to reveal a typical alkalic magma trend. Although there is a scatter of data points on the Al-Fe/Mg diagram (Figure 18), it is apparent that there is a general increase in Al with Fe/Mg, especially in the pillow lava specimens. Following Lebas (1962), this trend

intrusions.

The SiO_2, CaO, Al_2O_3 and TiO_2 contents of clinopyroxenes have been utilized to distinguish magma type. At any given level of fractionation, tholeiitic clinopyroxenes generally have lower contents of CaO, Al_2O_3, and TiO_2 and higher values of SiO_2 than clinopyroxenes from alkaline magmas (Kushiro, 1960). Using a similar approach, Fodor et al. (1975) report that the calcium content of the Ca-rich pyroxenes differentiates alkalic, tholeiitic and nephelinic rock suites: high Ca pyroxenes in tholeiitic rocks have wollastonite contents of between 30 and 40; those of alkalic magmas have Wo 38-48; those of nephelinic rocks have Wo 47-51. It has also been suggested that Ti/Al ratios of less than 0.2 (if Al is greater than 0.15 cations per 6 oxygen) characterize tholeiitic clinopyroxenes whereas alkalic magmas crystallize clinopyroxenes with Ti/Al ratios greater than 0.2 (Kushiro, 1960). Finally, it is claimed that with advancing fractionation the Al_2O_3 content of Ca-rich pyroxenes in tholeiitic magmas decreases whereas Al_2O_3 increases with fractionation in clinopyroxenes of alkaline magmas (Lebas, 1962).

A.2c. Chemical Variations in Clinopyroxenes from the Betts Cove Basaltic Members

The Betts Cove mafic rocks contain clinopyroxenes which exhibit a range of compositions extending from the endiopside field into the augite field of the pyroxene quadri-

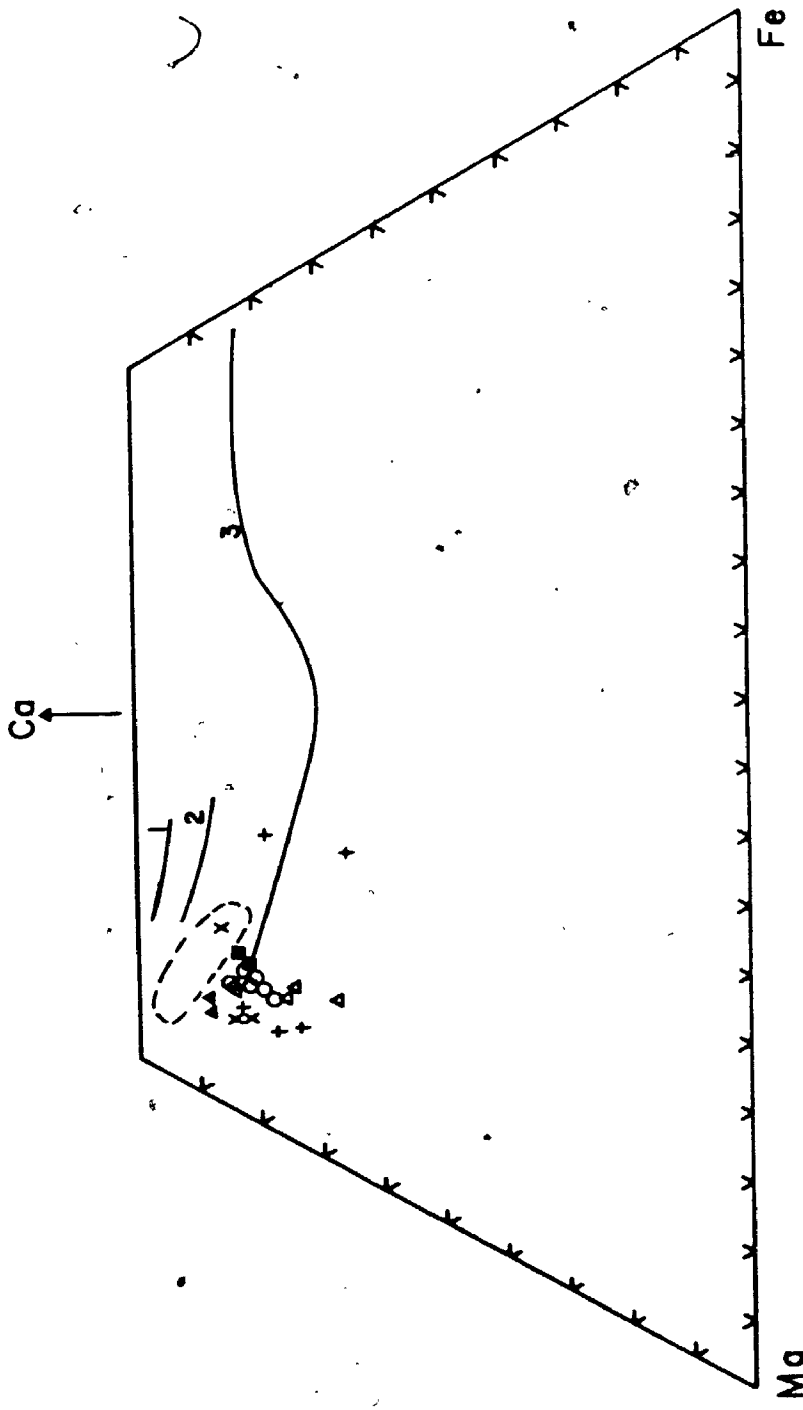

FIGURE 14. CA-MG-FE PLOT OF CLINOPYROXENES FROM THE BETTS COVE GABBROS (■), PERKNITE ROCKS (X), PICRITIC DYKES (+), DIABASE DYKES (O), LOWER LAVAS (△), UPPER LAVAS (▲) COMPARED TO TRENDS FROM BLOW-ME-DOWN (---) (RICCIO, 1976), 1-BLACK JACK SILL (WILKINSON, 1956), 2-GARBH EILEAN SILL (MURRAY, 1954), 3- SKAERGAARD (WAGER AND BROWN, 1968).

lateral (Figure 14). The trend exhibits slight calcium depletion with limited iron enrichment. The analyses plot close to the early fractionated clinopyroxenes from known tholeiitic intrusions but have lower wollastonite contents than early clinopyroxenes from both the Black Jack alkalic intrusion and the Bay of Islands ophiolitic rocks. The trends for the transitional Bay of Islands clinopyroxenes and the Betts Cove clinopyroxenes probably merge at high Fe contents (Riccio, 1976).

Fodor et al. (1975) analyzed clinopyroxenes from the volcanoes of Hawaii and separated tholeiitic, alkalic and nephelenic magma types on the basis of the variation of elements against mole percent wollastonite. In Figure 15, clinopyroxene compositions of the Betts Cove ophiolitic mafic rocks are plotted using the parameters of Fodor et al. (1975). The variations of Al_2O_3, Na_2O and MnO against Wo content follow the trend of tholeiitic basalts from Hawaii but it is clear that many points fall outside the tholeiitic limits set by Fodor et al., and some overlap with alkalic basalts. The TiO_2 contents of clinopyroxenes from the Betts Cove rocks are very low and fall far below the TiO_2 contents of clinopyroxenes from all magma types at Hawaii. Thus, it is apparent that the Betts Cove mafic liquid from which the clinopyroxenes crystallized was unusually low in titanium and the low TiO_2 values of the whole rock specimens are due to igneous processes and not later metamorphism. The parameters used by Fodor et al. (1975) to distinguish magma

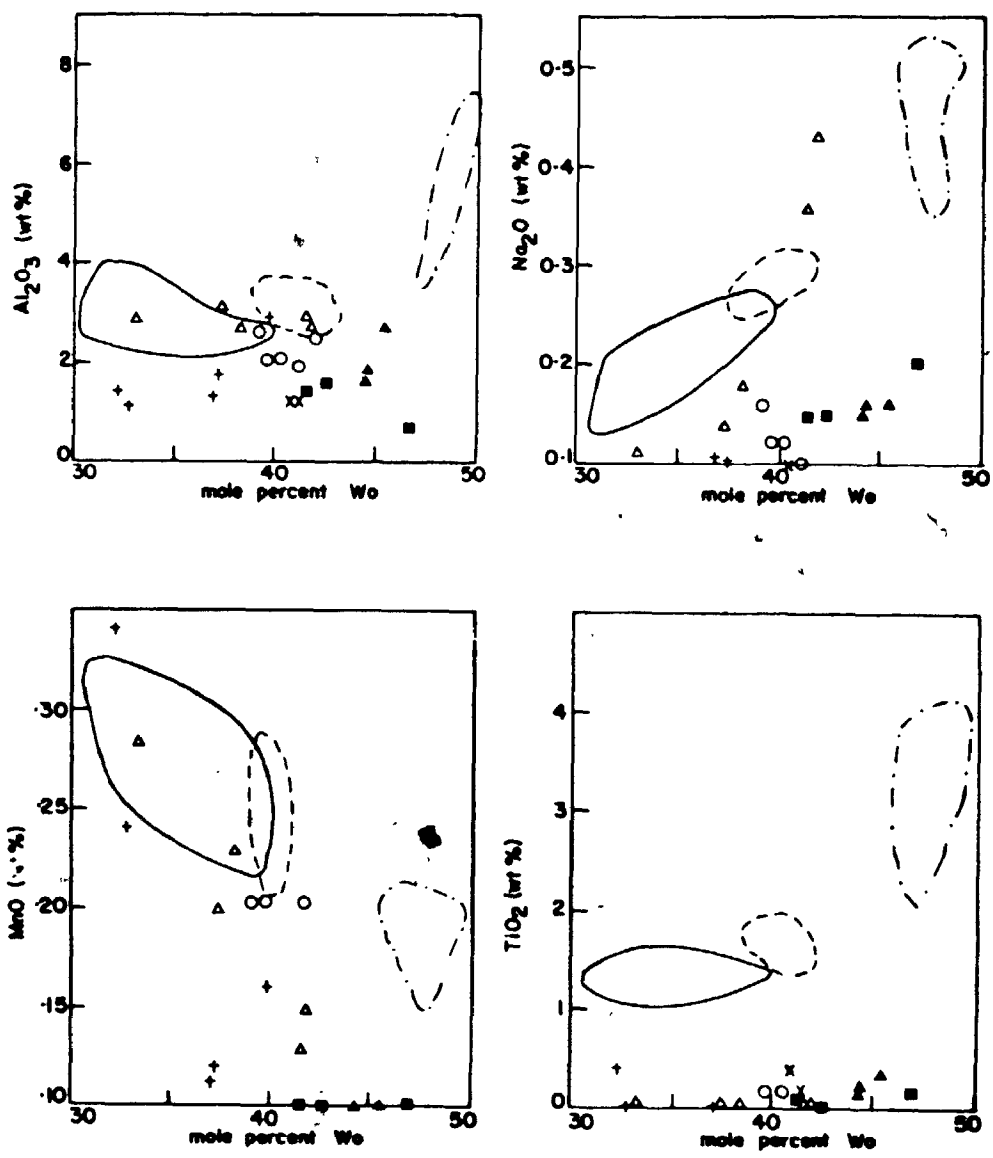

FIGURE 15. WEIGHT PERCENT OXIDE VARIATION IN CLINOPYROXENES OF THE BETTS COVE MAFIC ROCKS AGAINST MOLE PERCENT WOLLASTONITE COMPARED TO TRENDS FROM HAWAIIAN THOLEIITIC BASALTS (——), ALKALI BASALTS (- - -) AND NEPHELENITES (- -) (FODOR ET AL., 1975). SYMBOLS AS IN FIGURE 14.

types in Hawaii may therefore not be universally applicable, since the clinopyroxenes from Betts Cove cannot be unequivocally assigned to one magma type.

A clearer indication that the Betts Cove clinopyroxenes are tholeiitic is shown on an SiO_2 versus Al_2O_3 diagram (Figure 16) from Lebas (1962). The high silica and low Al_2O_3 contents of the Betts Cove clinopyroxenes are characteristic of non-alkaline lava types.

The tholeiitic nature of the pyroxenes is also revealed in plots of Si and Ti versus Al cations (Figure 17). Ti/Al ratios are much less than 0.2 which according to Kushiro (1960) is characteristic of clinopyroxenes fractionating from a tholeiitic magma. The trend of decreasing Si with increasing Al indicates substitution of Al for Si in tetrahedral sites. Al must also be in octahedral sites since all the clinopyroxenes plot well above the Si + Al = 2 line.

An indication of the behaviour of the clinopyroxenes at Betts Cove during fractionation is shown by the variation of Al, Ti, Si and Cr_2O_3 against Fe/Mg (atomic ratio) (Figures 18 and 19). The degree of fractionation increases with increasing Fe/Mg atomic ratio. The variation of Al with fractionation seems to reveal a typical alkalic magma trend. Although there is a scatter of data points on the Al-Fe/Mg diagram (Figure 18), it is apparent that there is a general increase in Al with Fe/Mg, especially in the pillow lava specimens. Following Lebas (1962), this trend

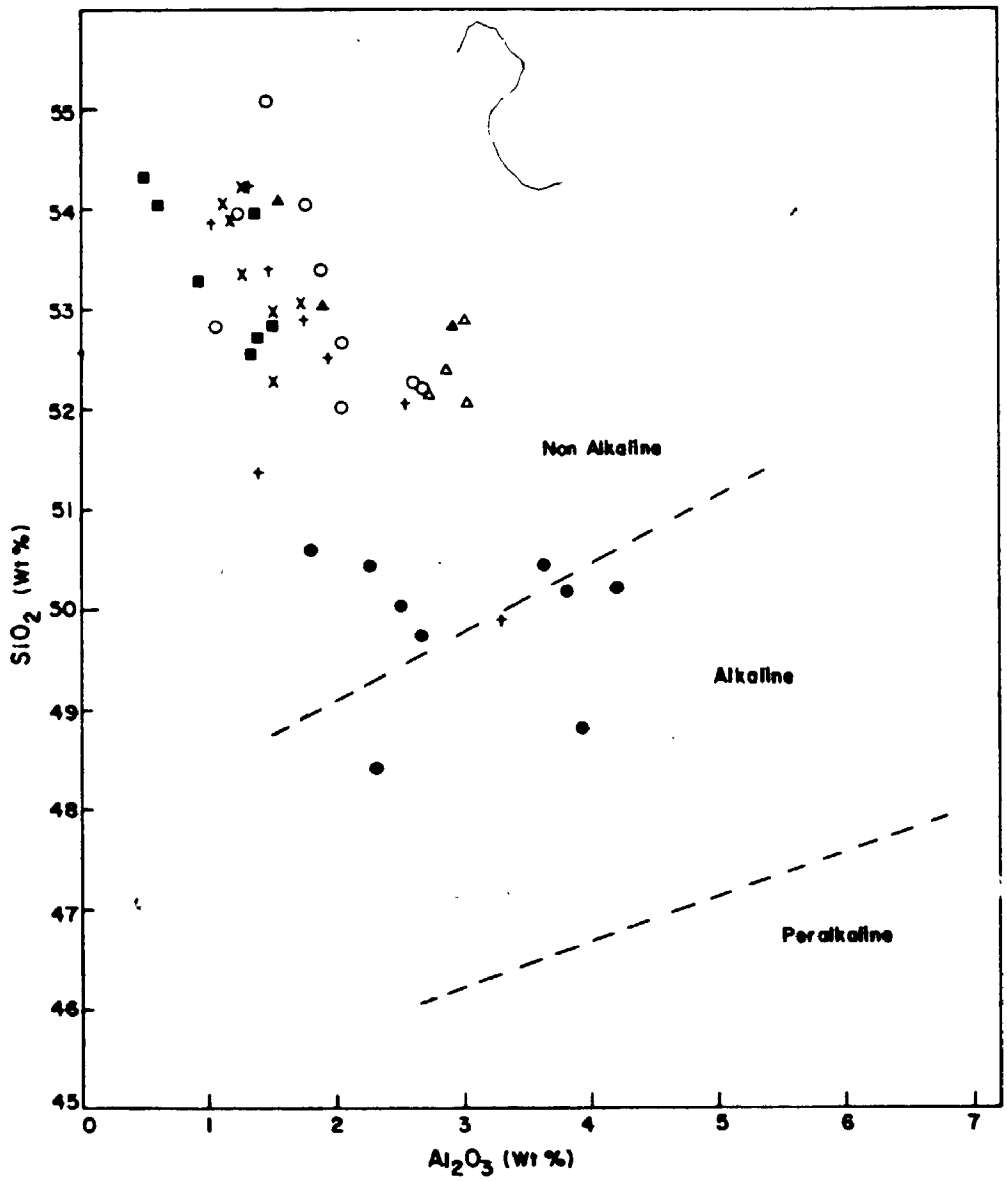

FIGURE 16. VARIATION OF AL_2O_3 AGAINST SiO_2 IN CLINOPYROXENES OF THE BETTS COVE AND BLOW-ME-DOWN MAFIC ROCKS. SYMBOLS AS IN FIGURES 14 AND 7. FIELDS AFTER LEBAS (1962).

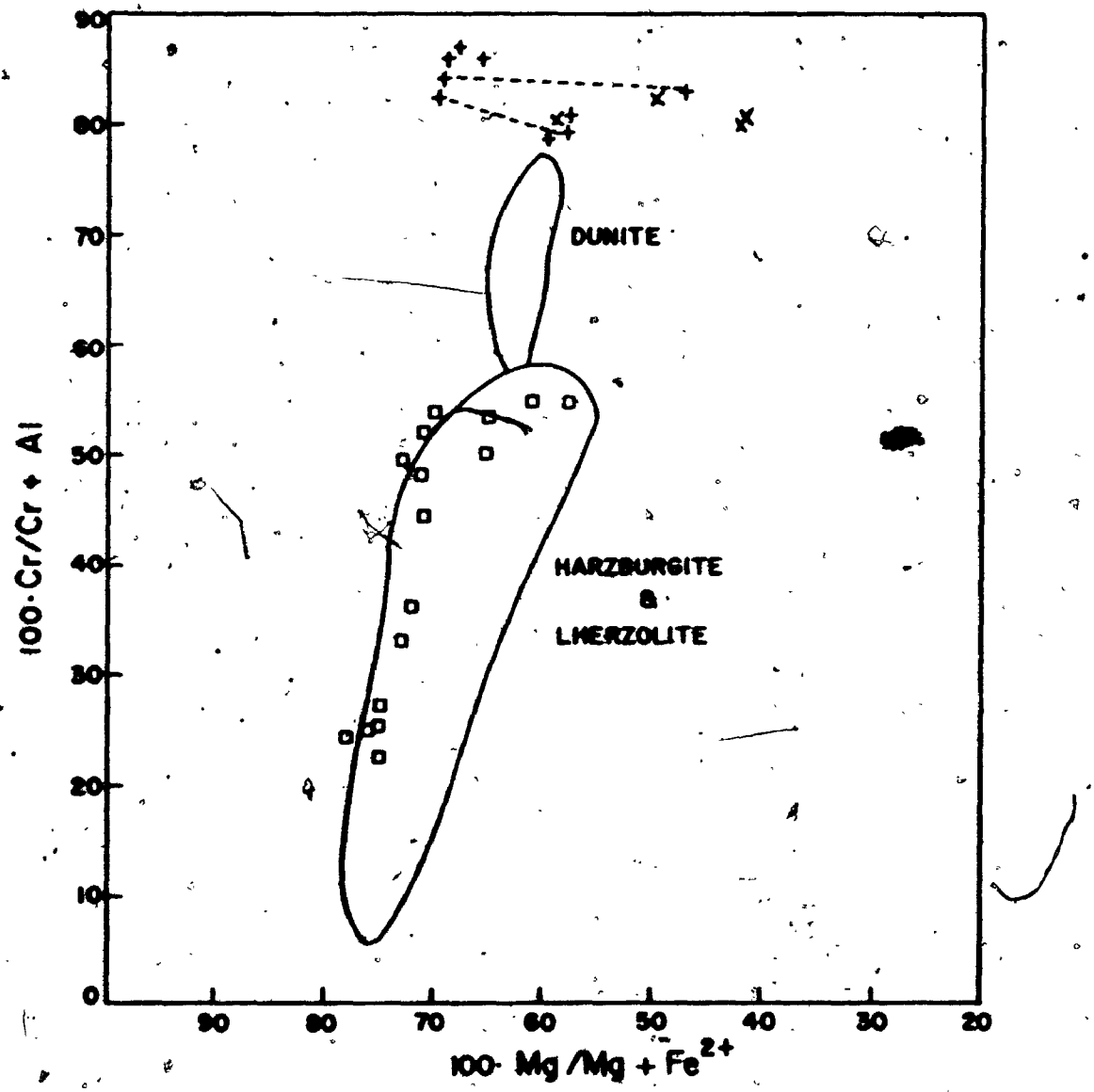

FIGURE 20. COMPOSITION OF SPINELS FROM THE BETTS COVE DYKES (+,X) COMPARED TO SPINEL ANALYSES FROM MODERN OCEAN FLOOR BASALTS (□) (FREY ET AL., 1974; SIGURDSSON AND SCHILLING 1976) AND FROM ULTRAMAFIC ROCKS (SOLID LINES) FROM THE BAY OF ISLANDS OPHIOLITE (RICCIO, 1976). DASHED LINES JOIN MG-RICH CORES TO THEIR CORRESPONDING RIMS.

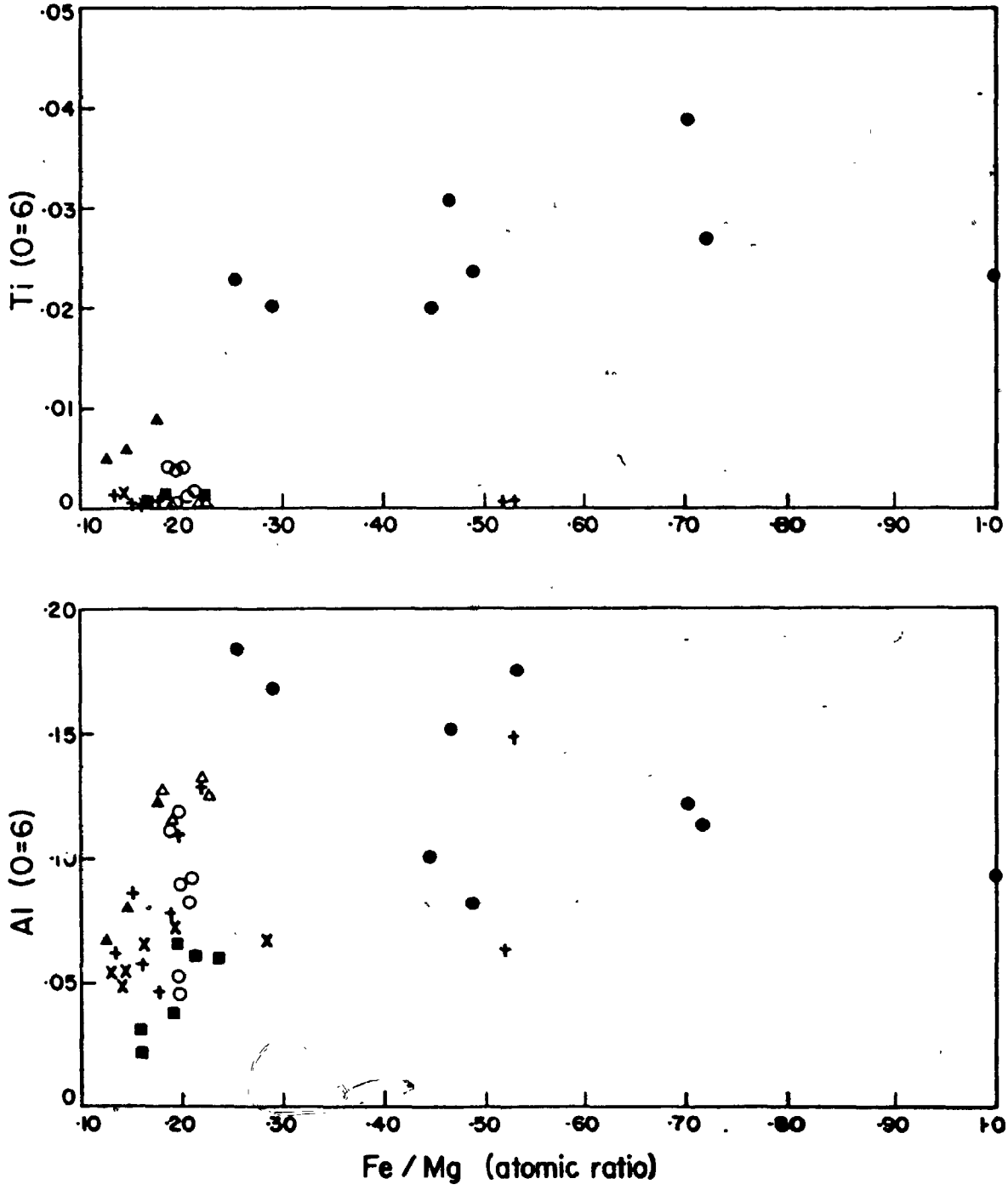

FIGURE 18. AL AND TI VARIATIONS AGAINST FE/MG RATIO FOR CLINOPYROXENES FROM THE BETTS COVE AND BLOW-ME-DOWN MAFIC ROCKS. SYMBOLS AS IN FIGS. 14 AND 7.

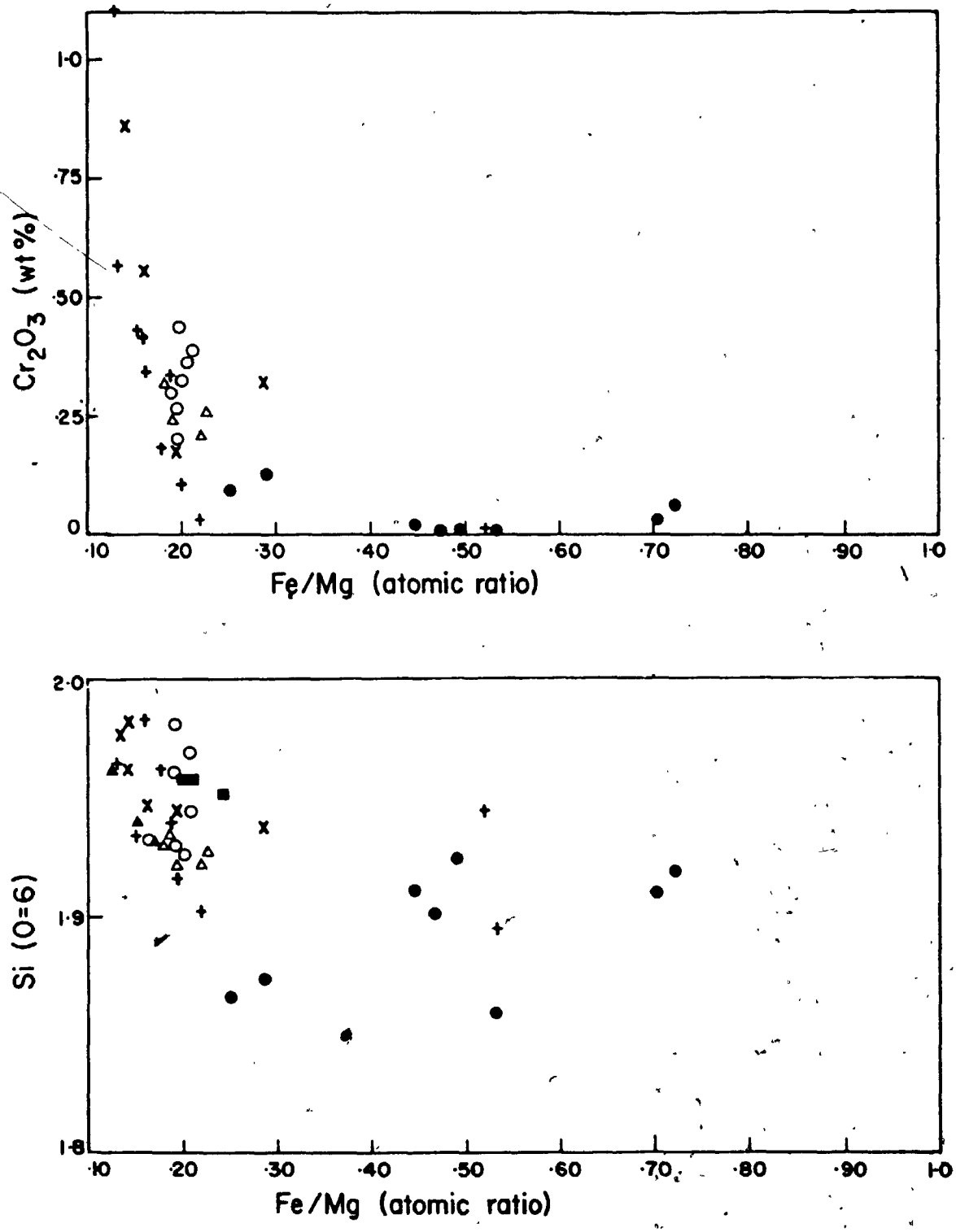

FIGURE 19. Cr_2O_3 AND SI VARIATIONS WITH FE/MG ATOMIC RATIO FOR CLINOPYROXENES FROM THE BETTS COVE AND BLOW-ME-DOWN OPHIOLITES. SYMBOLS AS IN FIGS. 14 AND 7.

is indicative of alkaline magma clinopyroxenes. The reasoning behind using this criterion is that the Al content in clinopyroxenes is inversely proportional to the SiO_2 activity in the magma and presumably, in alkalic magmas SiO_2 activity decreases with fractionation and increases in tholeiitic magmas. However, not only is SiO_2 activity important in determining the Al content of clinopyroxenes, but the Al content of the magma is also a determining factor. This is shown by the following equation:

$$\underset{\text{(Anorthite)}}{CaAl_2Si_2O_8} = \underset{\text{(Ca-Tsch.)}}{CaAl_2SiO_6} + SiO_2$$

The equilibrium constant for this equation is

$$K = \frac{(\text{Ca-Tsch})_a \ (SiO_2)_a}{(\text{Anorthite})_a}$$

Thus, the Ca-tschermak (Al bearing molecule in clinopyroxene) can be changed by varying either the silica activity or the activity of anorthite (Al content) of the magma. Increasing the activity of anorthite in the magma will have the same effect as decreasing the silica activity; therefore, unless the activity of anorthite behaves antipathetically with the SiO_2 activity during fractionation, the Al variations in clinopyroxenes against Fe/Mg are not necessarily indicative of a particular magma type.

Ti contents remain very low with increasing Fe/Mg

ratio and are significantly lower than values from clinopyroxenes from the Blow-Me-Down ophiolite (Figure 18).

The Si content of the clinopyroxenes decreases with increasing fractionation (Figure 19). Since Al substitutes for Si in the clinopyroxene structure, the decrease in Si in the clinopyroxene may be related to increasing Al content of the magma and thus increasing Al content of the clinopyroxene. Alternatively, decreasing SiO_2 activity of the magma with increasing fractionation will result in decreasing Si content of the clinopyroxenes.

The Cr_2O_3 content of the clinopyroxenes drops exponentially with increasing fractionation in the Betts Cove mafic rocks (Figure 19). This is consistent with the decrease in the Cr content of the mafic liquid by early crystallization of chromite (see this chapter, section C.3).

A.2d. Clinopyroxene-Liquid Relationships in the Betts Cove Mafic Rocks

The composition of a liquid coexisting with a crystallizing clinopyroxene can be calculated on the basis of the partitioning of certain elements between the solid and liquid phases (Roeder and Emslie, 1970). In particular, the K_D for FeO/MgO between clinopyroxene and liquid has been determined empirically from experimental data on olivine-liquid partitioning (Riccio, 1976). The distribution constant is:

$$K_D = \frac{(FeO/MgO)\ cpx}{(FeO/MgO)\ liquid} = 0.237$$

Applying this K_D value, the FeO/MgO weight ratios in the clinopyroxenes from the Betts Cove mafic rocks have been used to calculate the FeO/MgO weight ratio of the co-existing liquid (Table 2). The calculated value of the FeO/MgO ratio of the liquid agrees with the measured value for the whole rock in only the upper pillow lava specimen. All other members of the ophiolite have much lower FeO/MgO measured ratios than the calculated values. The discrepancy between the measured and calculated values of the FeO/MgO ratio in the lower pillow lavas, diabase and picritic dykes suggests that the clinopyroxenes are not liquidus phases. The crystallization of other phases, for example olivine and orthopyroxene, before the precipitation of clinopyroxene will alter the FeO/MgO ratio of the initial liquid. Thus, when clinopyroxene does crystallize, it is in equilibrium with a differentiated liquid and its FeO/MgO ratio will therefore not be indicative of the FeO/MgO of the initial liquid. Furthermore, if the perknite and gabbro rocks are cumulates, then their whole rock compositions cannot represent liquid compositions. The FeO/MgO ratio of the cumulates, then, cannot be taken as corresponding to the FeO/MgO weight ratio of the liquid from which they crystallized (cf. Church and Riccio, 1977).

It is concluded from the clinopyroxene-liquid relation-

TABLE 2

Calculated FeO/MgO (weight ratio) of liquids in equilibrium with phenocryst clinopyroxenes of the Betts Cove mafic rocks.

Specimen	FeO/MgO_{cpx}	$FeO/MgO_{liq.}$	FeO/MgO_{rock}
BC-74-90	0.264	1.12	1.19
Upper Pillows	0.313	1.32	
	0.223	0.95	
BC-74-101B	0.322	1.36	0.71
Lower Pillows	0.403	1.70	
	0.347	1.46	
BC-73-260	0.370	1.57	0.83
Diabase Dyke	0.347	1.46	
	0.373	1.58	
BC-73-141	0.239	1.01	0.45
Picritic Dyke	0.269	1.14	
	0.317	1.34	
BC-73-61	0.251	1.06	0.42
Perknite rock	0.226	0.95	
	0.290	1.23	
BC-73-33	0.347	1.47	0.64
Gabbro	0.341	1.44	
	0.420	1.77	

ships in the Betts Cove mafic rocks that clinopyroxene is not a liquidus phase and that olivine and orthopyroxene are likely to have crystallized before clinopyroxene.

Even though the clinopyroxenes are not liquidus phases, it is still apparent that the picritic and perknite rocks crystallized from a liquid with lower FeO/MgO ratio than the lower pillow lava, sheeted dyke and gabbro liquid. The low FeO/MgO ratio of the liquids which produced the picritic dykes indicates that the picritic material represents a less differentiated basalt magma than the diabase dykes and pillow lavas. The primitive nature is supported by the high Ni and Cr and low TiO_2 and Zr values of the picritic dykes.

A.3. Chromite Chemistry

Euhedral chromite grains are common in picritic dykes and perknite rocks where they occur as inclusions in chlorite pseudomorphs presumably after olivine. Chromite is also present in some of the highly magnesian lower pillow lavas. Because the occurrence of chromite is restricted to these 'primitive' rocks, it is suggested that chromite is an early crystallizing phase from the primitive Betts Cove magma.

Appendix III, Table II and Figure 20 summarize the chemical aspects of the chromites in the Betts Cove mafic rocks. The chromites are rich in Cr_2O_3 and impoverished in Al_2O_3. They contain even more Cr than chromite segregations

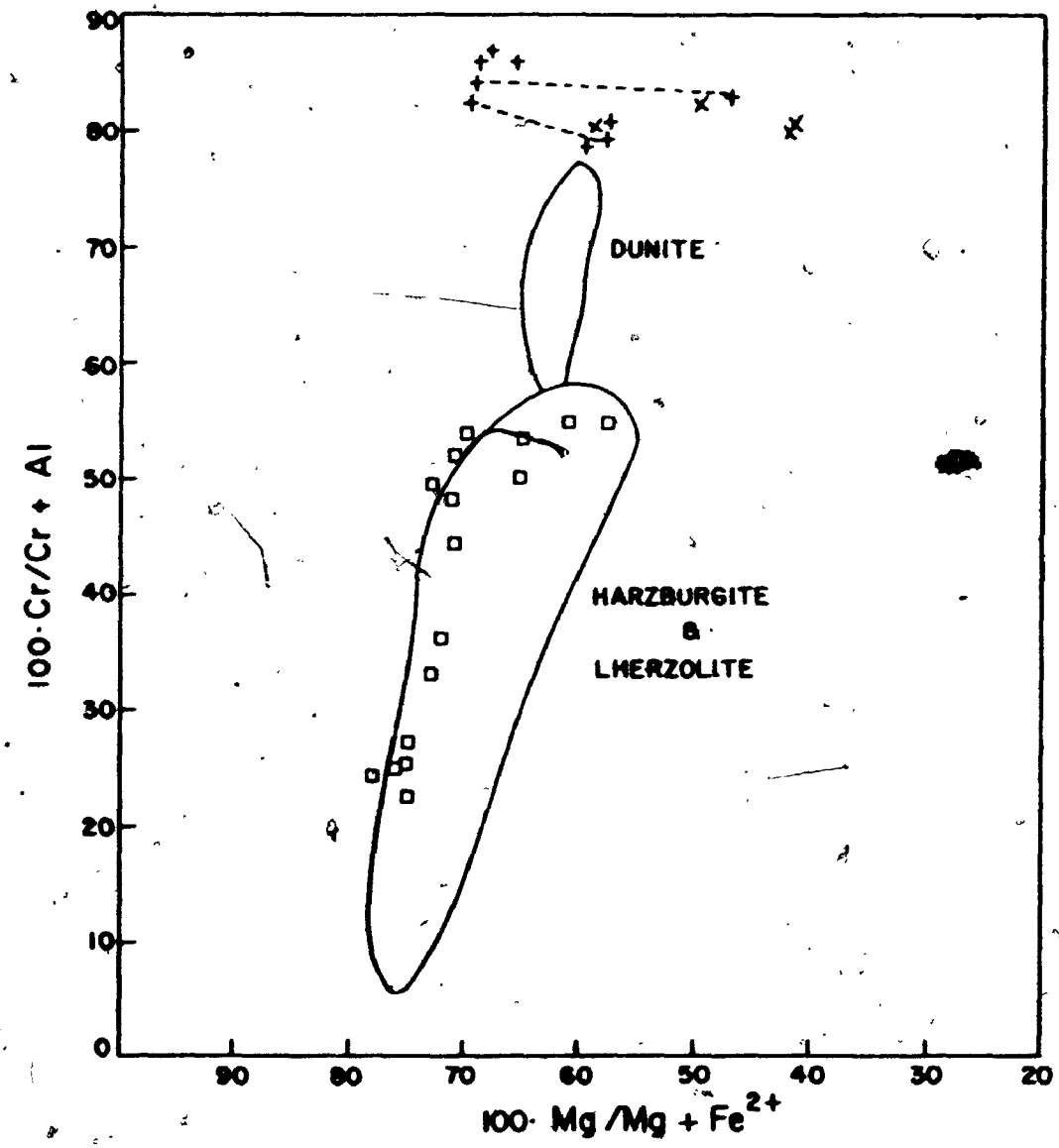

FIGURE 20. COMPOSITION OF SPINELS FROM THE BETTS COVE DYKES (+,X) COMPARED TO SPINEL ANALYSES FROM MODERN OCEAN FLOOR BASALTS (□) (FREY ET AL., 1974; SIGURDSSON AND SCHILLING 1976) AND FROM ULTRAMAFIC ROCKS (SOLID LINES) FROM THE BAY OF ISLANDS OPHIOLITE (RICCIO, 1976). DASHED LINES JOIN MG-RICH CORES TO THEIR CORRESPONDING RIMS.

in equilibrium with dunite and have greater Cr values than chromites from the most primitive oceanic basalts. Mg/Mg + Fe ratios of the Betts Cove chromites span the range for dunite segregations.

Some of the larger chromite grains are chemically zoned (Appendix III, Table II; Figure 20). Between the core and rim of a single chromite grain, Cr_2O_3 and MgO decrease and FeO, Al_2O_3, CaO and SiO_2 increase. These trends are consistent with fractionation processes in the primary liquid.

B. Blow-Me-Down Ophiolite

B.1. Whole Rock Chemistry

In contrast to the Betts Cove ophiolitic mafic rocks, the Blow-Me-Down basalts show chemical features similar to 'normal' recent oceanic tholeiites (Figures 7, 8, 9, 10). Most of the analyzed samples have TiO_2, Zr, Y, P_2O_5, and FeO^t/MgO ratios within the range of values quoted for oceanic basalts. Three samples of picritic dykes from Blow-Me-Down are similar in terms of TiO_2- FeO^t/MgO to picritic basalts dredged from the ocean floor (Figure 9). It is noted that the most primitive Blow-Me-Down basalts show limited overlap in TiO_2, Zr and P_2O_5 values with the most fractionated Betts Cove basalts. Also, it is significant that at a given FeO^t/MgO ratio, the TiO_2 content in the Blow-Me-Down mafic rocks is higher than in the Betts Cove basaltic material. In fact, there are separate trends

of TiO_2 enrichment with increasing FeO^t/MgO ratio: the Blow-Me-Down and Betts Cove mafic rocks define a high and a low Ti trend, respectively, whereas the Troodos basalts occupy an intermediate position (Figure 9). Since FeO^t/MgO is a good indicator of fractionation (Miyashiro, 1975a), it would seem that the Blow-Me-Down and Betts Cove mafic rocks are not fractionation products one of the other.

As at Betts Cove, chemical differences exist between the upper lavas and lower lavas at Blow-Me-Down; however, the element variation trends are opposite to those of the Betts Cove rocks. In the Blow-Me-Down ophiolite, the lower lavas are enriched in TiO_2, Zr, Y, P_2O_5 and FeO^t/MgO and depleted in Ni and Cr relative to the upper lavas - a trend opposite to that found in the Betts Cove pillow lava members (Figures 5 to 10). The compositional variations between the upper and lower lavas at Blow-Me-Down are analogous to those observed between the upper and lower lavas in the Troodos ophiolite, Cyprus (Pearce, 1975; Smewing et al., 1975). However, the upper pillows at Blow-Me-Down are not as severely depleted in TiO_2, Zr, Y and FeO^t/MgO as the upper lavas in the Troodos ophiolite.

B.2. Clinopyroxene Chemistry

Riccio (1976) concluded that clinopyroxenes from the ultramafic and mafic cumulates in the Blow-Me-Down ophiolite were transitional to slightly alkalic in character and significantly different from the Betts Cove cumulate

clinopyroxenes. The same differences in clinopyroxene chemistry occur between the pillow lava/sheeted dyke members of the two ophiolites. The clinopyroxenes in the Blow-Me-Down pillow lava member are richer in Al_2O_3, TiO_2, Na_2O, MnO and FeO/MgO ratios and are depleted in SiO_2 and Cr_2O_3 relative to the Betts Cove mafic clinopyroxenes (Appendix III, Table I; Figures 16, 18, 19). The variation of SiO_2 against Al_2O_3 shows that most of the clinopyroxenes at Blow-Me-Down lie within the alkaline field or plot close to the boundary between the nonalkaline and alkaline fields (Figure 16). The only Betts Cove clinopyroxene to plot close to the alkaline field is the rim of a microphenocryst. Presumably, this analysis is representative of a clinopyroxene which crystallized from a late stage Betts Cove liquid.

It is unlikely that the clinopyroxenes in the Blow-Me-Down lavas crystallized from a more differentiated magma of the same parentage as the Betts Cove liquid. Although Fe/Mg ratios in the Blow-Me-Down clinopyroxenes are higher than in Betts Cove clinopyroxenes, and SiO_2 and Cr_2O_3 variations are as would be expected in fractionation sequences, Al and Ti variations do not support a fractionation hypothesis. Ti in clinopyroxenes from the Betts Cove dykes and lavas remains extremely low at high Fe/Mg ratios whereas Ti in clinopyroxenes from the Blow-Me-Down lavas is higher at all Fe/Mg ratios than the Betts Cove clinopyroxenes (Figure 18). Also, Al in the Betts Cove clinopyroxenes shows a general

increase with increasing Fe/Mg ratio whereas Al in the Blow-Me-Down clinopyroxenes is high at low Fe/Mg ratios and decreases sporadically with increasing Fe/Mg ratio (Figure 18). Furthermore, on a Ti-Al diagram (Figure 17), the Blow-Me-Down clinopyroxenes, at a given Al content, have higher contents of Ti than the Betts Cove clinopyroxenes. They also plot close to the line where Ti/Al = 0.2 (a line sometimes used as a boundary to separate clinopyroxenes with alkaline affinities from those which have crystallized from a tholeiitic magma).

CHAPTER 4

METAMORPHISM IN NEWFOUNDLAND OPHIOLITES

A. Betts Cove Ophiolite

A.1. Introduction

It is now recognized that weathering, cold hydration and hydrothermal metamorphism caused by circulating heated seawater are the three principal processes involved in the alteration of modern oceanic crust (Lister, 1972; Hart, 1973; Spooner and Fyfe, 1973; Keen, 1975; Andrews and Fyfe, 1976; Wolery and Sleep, 1976). The effects of cold hydration and hydrothermal alteration have also been seen in the ophiolites of Cyprus (Gass and Smewing, 1973; Spooner, 1977) and the E. Ligurian Alps (Spooner and Fyfe, 1973).

The Betts Cove ophiolite is metamorphosed to the greenschist facies and in the following discussions, an attempt will be made to relate the metamorphism in the ophiolite to hydrothermal metamorphism observed in modern oceanic crust.

A.2. Macroscopic and Microscopic Observations

A.2a. Introduction

The rocks of the Betts Cove ophiolite have been metamorphosed to the greenschist facies without significant modification of their original igneous textures. The degree of metamorphism increases downward and the metamorphic zonation is described in descending stratigraphic order in the following sections.

A.2b. Upper Pillow Lava Member

Clinopyroxene and plagioclase phenocrysts are only partially replaced by actinolite/chlorite and albite/muscovite. Chlorite is the dominant mafic metamorphic mineral in the groundmass. Calcite, epidote and quartz occupy vesicles and numerous discrete fracture zones criss-crossing the upper part of the ophiolite. Hematite fills fractures and also occurs along grain boundaries, thus imparting a distinct red colour to the pillows. Nevertheless, since alteration products are concentrated in fractures and narrow margins around igneous minerals, a significant percentage of the pillows remains unaltered.

A.2c. Lower Pillow Lava Member

In contrast to the upper lavas, the lower lavas are green, are essentially non-vesicular and have little interstitial sedimentary altered material. Brecciated zones are frequent (Plate 3A) and in fact most of the lower

PLATE 3

A. Brecciated lower pillow lavas with epidote-quartz-calcite filling veins.

B. Vesicle in lower pillow lava filled by chlorite (dark), quartz (white) and calcite (speckled protruding into the chlorite). (crossed nicols).

C. Vesicle in lower pillow lavas, Betts Cove, filled by chlorite. Chlorite is radial and anomalous blue on the outside of the vesicle (lighter colour), green in a narrow intermediate zone and grey (black area) in the central area. (crossed nicols).

D. Altered phenocryst in a picritic dyke, Betts Cove. The alteration comprises fine needles of actinolite and chlorite. Note euhedral chromites (black) surrounded by coarse actinolite. (crossed nicols).

E. Alteration of gabbro, Betts Cove. The plagioclase is altered to sericite (white central portion of photo) whereas clinopyroxenes (darker cleaved grains) on either side are unaltered. (crossed nicols).

F. Rodingitic alteration of gabbro, Betts Cove. Dark patches are epidote-chlorite (paragarnet) alterations of plagioclase. Partially uralitized clinopyroxenes are also present. (crossed nicols).

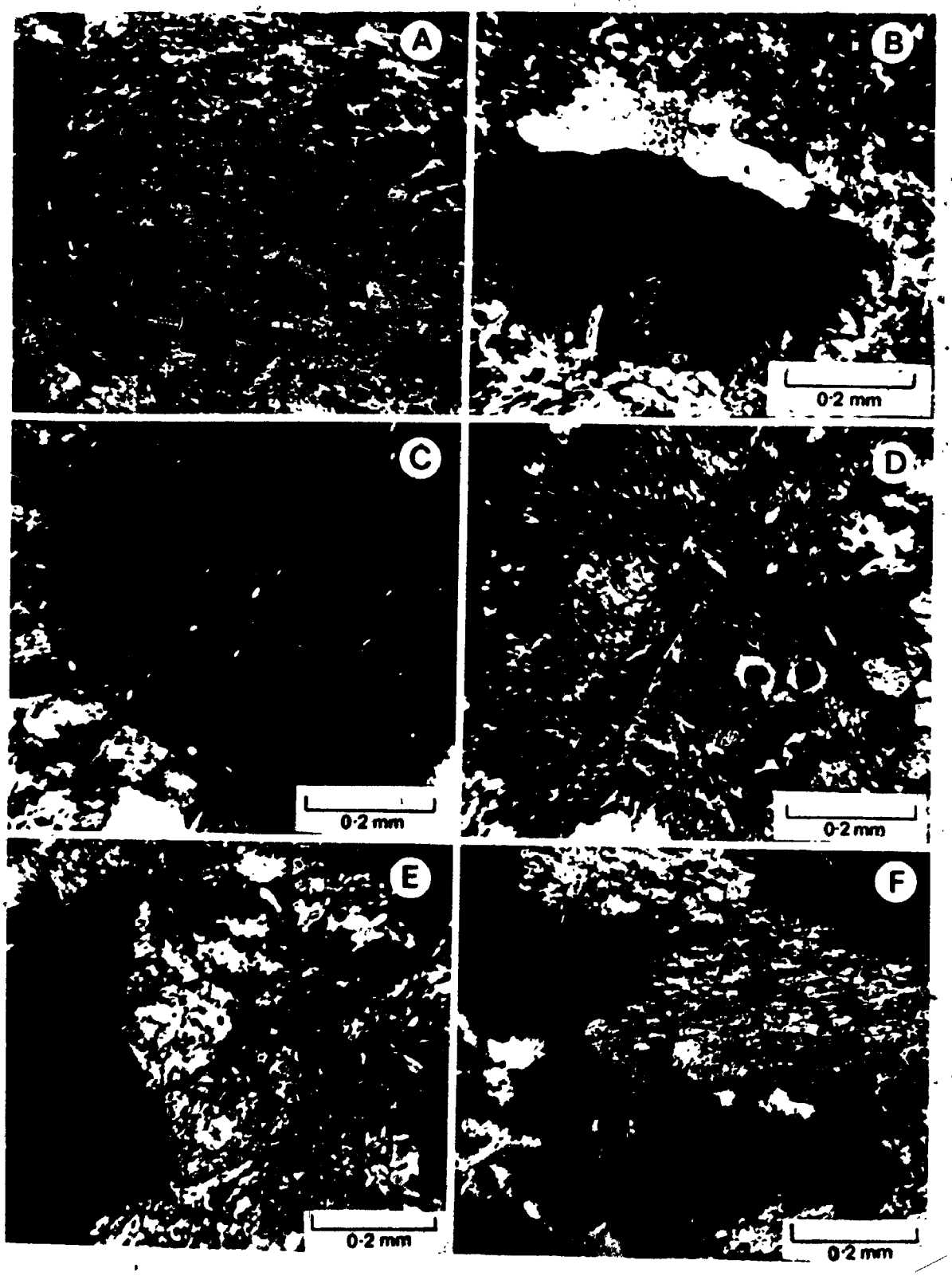
A
B
0·2 mm
C
0·2 mm
D
0·2 mm
E
0·2 mm
F
0·2 mm

contact of this unit with the sheeted dyke member is a breccia zone comprising epidote, calcite, chlorite and quartz.

The metamorphic mineralogy and degree of reconstitution of igneous minerals varies within individual pillow specimens. The pillow rims usually comprise chlorite, actinolite, epidote and calcite with minor albite (10%) and quartz. On the other hand, the cores consist of albite (40%), clinopyroxene partially replaced by actinolite (40%), chlorite pseudomorphs after olivine, and minor epidote, calcite and quartz. The main by-product of the transformation of plagioclase to albite is an epidote mineral and trivial amounts of muscovite.

The few vesicles present are commonly filled by quartz, chlorite, calcite, epidote, sericite and pyrite. Zonation in vesicles from rim to core include chlorite-calcite, chlorite-epidote, chlorite-epidote-calcite, calcite-quartz, and quartz-chlorite-calcite assemblages (Plate 3B, C). Commonly, chlorites near the rim of a vesicle have anomalous brown or blue interference colours whereas low birefringent chlorite is found at the center. Pyrite cubes in vesicles are sometimes surrounded by thin hematite rims.

In summary, alteration in the lower pillows is controlled by fracture systems and the nature of the material interacting with the metamorphic fluid.

A.2d. Sheeted Dyke Member

Dykes of the sheeted complex reveal spatial variation in the pervasiveness of greenschist facies alteration, reflected in the degree of uralitization of the clinopyroxene. Mineralogically, the dykes range in composition from albite-cpx-chlorite-epidote ± actinolite to albite-actinolite-epidote ± cpx. In general, the former assemblage occurs near the stratigraphic top of the sheeted complex whereas the latter is principally found near the base. In detail, however, the two end members can be found adjacent to one another suggesting that variables other than temperature and depth of burial are involved in the metamorphism. Permeability is probably an important factor.

All primary compositional varieties of the sheeted dyke member show similar mineralogical transformations. Plagioclase alters to albite and clinozoisite with minor carbonate and prehnite. Clinopyroxene is altered to actinolite which ranges in abundance from 10% to 80% of the rock depending upon the original amount of clinopyroxene and the degree of alteration of the clinopyroxene. Chlorite occurs as an interstitial alteration product. There is an antipathetic relationship between the occurrence of actinolite and chlorite. Chlorite is most abundant when the greatest amount of fresh clinopyroxene is preserved. As clinopyroxene is increasingly altered to actinolite, interstitial chlorite decreases in abundance.

In the picritic dykes, pseudomorphs after olivine

comprise anomalous blue chlorite and quartz. Small criss-crossing actinolite needles occur as overgrowths on the chlorite. Chromite crystals in these pseudomorphs are often surrounded by coarse actinolite crystals (Plate 3D). Also the margins of the chromites are sometimes altered to a chromian (2 wt. % Cr_2O_3) chlorite.

Fractures in the sheeted dyke member are smaller and less numerous than in the overlying pillow lavas. Fracture filling minerals include quartz, clinozoisite, prehnite, and chlorite with minor carbonate and pyrite.

A.2e. Gabbro Member

The thin gabbro member of the Betts Cove ophiolite comprises two distinct metamorphic mineral assemblages:
1) a greenschist facies assemblage of albite, actinolite, clinozoisite, prehnite and quartz with muscovite as a prominent by-product of the alteration of plagioclase to albite (Plate 3E); uralitization of clinopyroxene varies from only 10% in some specimens to 100% in others; thin (0.5 mm), sporadic veins contain prehnite, clinozoisite and quartz;
2) an incipient rodingitic assemblage in which clinopyroxene alters to actinolite and chlorite, and plagioclase is altered to either monomineralic clinozoisite or prehnite or a dark brown, high relief aggregate (Plate 3F), known as paragarnet (Honnerez and Kirst, 1975); (paragarnet probably represents an intermediate stage in the

alteration of plagioclase to clinozoisite/prehnite and its alteration to hydrogarnet. X-ray diffraction patterns and microprobe analyses indicate that paragarnet is a mixture of clinozoisite, prehnite and chlorite). This assemblage is similar to that of rodingitic gabbro from the mid-Atlantic ridge (Honnerez and Kirst, 1975).

Rodingite is usually associated with serpentinized ultramafic and therefore it has been suggested that rodingtization is a complementary process to the alteration of olivine and orthopyroxene to serpentine (Coleman, 1967; Riccio, 1972). Silica lost during the alteration of plagioclase to hydrogarnet is used in the formation of serpentine while calcium removed from the alteration of pyroxenes in the ultramafic is used up in hydrogarnet. Presumably, there is an external source of fluid. In the case of ocean floor rodingites and those at Betts Cove, there is another possible theory of formation. Honnerez and Kirst (1975) suggest that rodingites on the ocean floor form at temperatures of between 400°C and 500°C. It has also been noted that the rodingites are associated with faults, which are probably the locii for the escape of hot fluids to the ocean above. The hot fluids may have been involved in lower temperature greenschist alteration during downward penetration and consequently are saturated with calcium, the element most needed in the formation of rodingite. Thus, in this theory, the external fluid, possibly altered seawater, contains the necessary elements

to form rodingite.

A.2f. Ultramafic Zone

Ultramafic rocks at Betts Cove are intensely altered to both high and low temperature minerals. Serpentine is the main mineral and forms at temperatures of less than 500°C whereas small amounts of talc form at higher temperatures. Riccio (1972) suggested that enstatite was converted to talc and olivine at high temperatures, then to talc and serpentine and at the lowest temperatures to serpentine alone.

A.2g. Summary

The salient features of the metamorphism at Betts Cove are: 1) alteration changes from being fracture controlled at the top of the ophiolite to more evenly dispersed throughout the gabbroic rocks; 2) actinolite occurs as part of the metamorphic mineral assemblage at high levels in the ophiolite (allowing for some erosion at the top of the ophiolite, actinolite probably formed less than 1 km. below the ocean floor). The abundance of actinolite increases downwards at the expense of chlorite; 3) calcite and hematite are concentrated in the pillow lavas; 4) epidote decreases in abundance with depth of burial and changes in composition from pistacite to clinozoisite; 5) quartz is a common vein and vesicle filling mineral throughout the stratigraphic column; 6) pyrite occurs as a

2

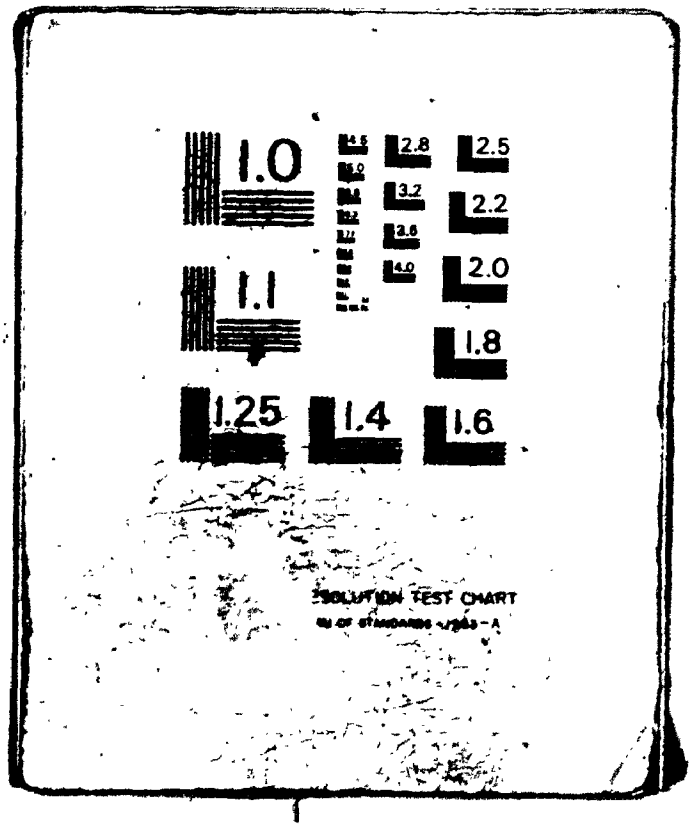

secondary mineral phase below the hematite rich zone; 7) incipient development of rodingite takes place near the base of the gabbro member.

A.3. Geochemical Changes During Metamorphism

A.3a. Introduction

During low grade greenschist metamorphism involving the interaction of fresh basalt with large volumes of water, metasomatic changes in the composition of the basalt are likely to occur. It is important to decipher which elements have moved and to what extent in order 1) to distinguish the type of metamorphism involved and 2) to be able to use whole rock chemistry in unravelling the igneous evolution of the ophiolite.

A.3b. Variation of Elemental Concentration Against a Known Immobile Element

Zirconium has been shown to be relatively immobile during greenschist facies metamorphism (Cann, 1970; Pearce and Cann, 1971; R. A. Hart, 1973; Pearce, 1975). It also varies systematically and significantly with igneous processes such as fractionation and partial melting. Thus, any rock suite whose chemistry has not been altered by post-igneous processes will exhibit regular trends (straight or exponential curves) of changing element concentration against changing Zr content. On the other hand, any element expected to covary with Zr during fractiona-

tion, but which varies erratically may be suspected of having been mobilized by later alteration (Wood et al., 1976).

Figure 21 shows the variations in Zr content with changes in major and some trace element values of the Betts Cove pillow lava members. There are no obvious systematic trends for SiO_2, CaO, $Fe_2O_3^t$, MgO, Na_2O, K_2O, Ba, Rb, and Sr. These elements have thus been mobilized by metamorphic events. TiO_2, P_2O_5 and Y increase with increasing Zr content. This trend is expected through fractionation or partial melting and consequently the concentration of these elements has not been detectably changed since the formation of the pillows. Ni and Cr values decrease exponentially with increasing Zr concentration. This is consistent with early fractionation of olivine and chromite from a mafic liquid.

The above data indicate which elements have been mobilized during metamorphism but provide no information as to the extent or the direction of the movement.

A.3c. Element Mobility as a Function of Volatile Content

R. A. Hart (1973) plotted major element concentrations of metamorphosed ocean floor basalts against their water contents to determine the direction of movement of elements during greenschist metamorphism. He reasoned that during low grade metamorphism water was introduced through the

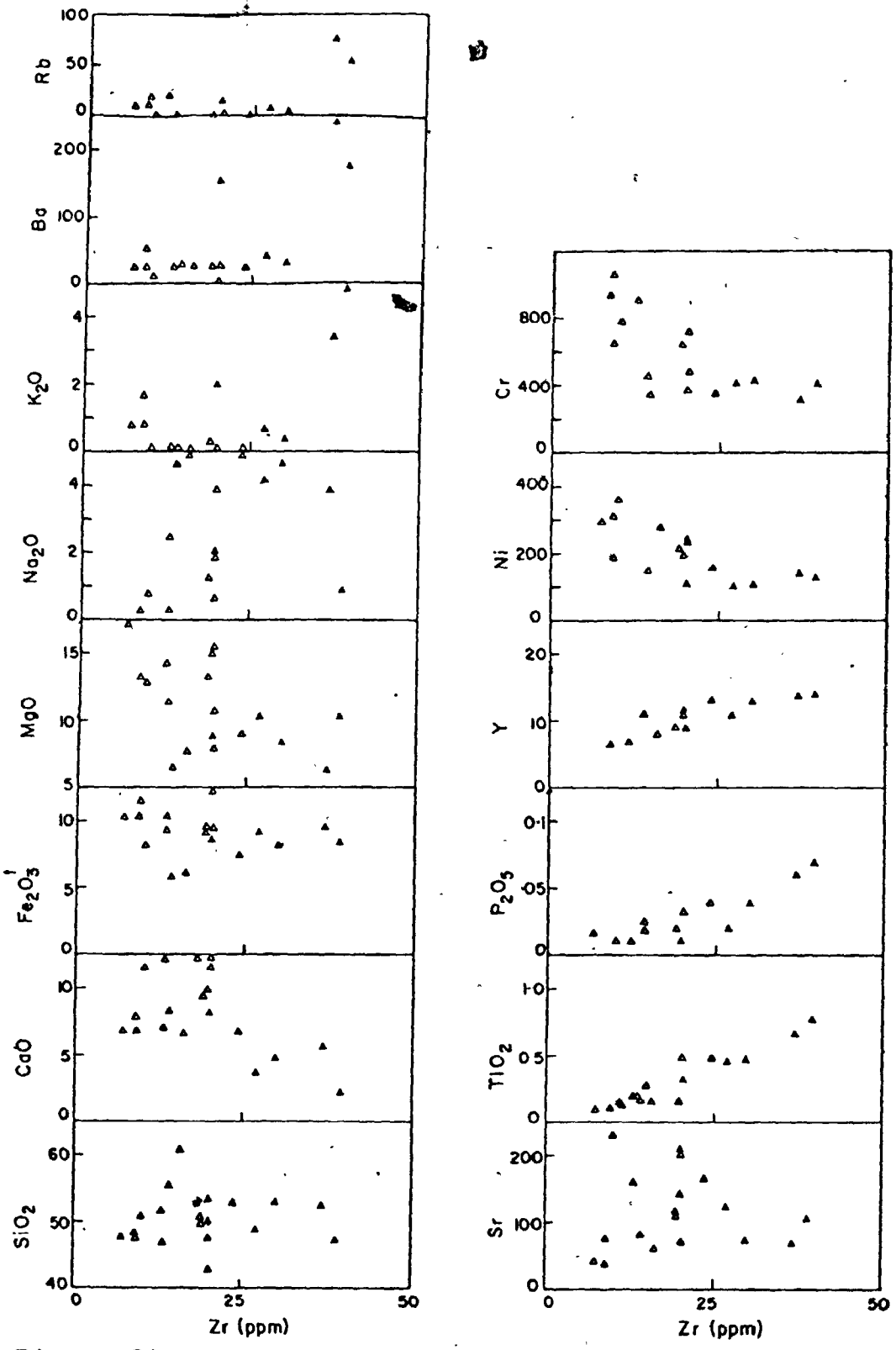

Figure 21. Variation of Zr against selected elements for the Betts Cove upper lava (▲) and lower lava (△) members. Majors in wt. % oxide, traces in ppm.

formation of hydrous minerals. On this basis, the concentration of elements (calculated water-free) introduced or removed at the time of formation of the hydrous minerals should vary systematically with water content. If, however, only local redistribution of the elements has occurred, then the concentration of the elements should be independent of the water content.

There are differences in element variation against volatile content between the lower pillow lava and the sheeted dyke members. The lower pillow lavas (Figure 22a) exhibit drastic increases in MgO, Fe_2O_3, total iron and CaO, and decreases in SiO_2 and Na_2O. In the sheeted dyke member (Figure 22b), MgO and FeO increase, and Fe_2O_3, CaO and Na_2O decrease. TiO_2, P_2O_5, K_2O, Ba, Rb, Sr, Ni, Cr, and Y show no marked systematic variation with volatile content.

The above chemical changes are reflected in mineralogical changes in the ophiolite. Magnesium is added to the basalts to form chlorite and actinolite in both stratigraphic members. Total iron and Fe_2O_3 increase in the pillow lavas due to crystallization of actinolite-chlorite-epidote assemblages in the pillow rims. Fe_2O_3 decreases with volatile content in the sheeted dykes probably reflecting the decline in amount of epidote as a major volatile-bearing phase. Silica decreases with volatile content in the lower pillow lavas because of its leaching from pillow rims concomitant with the formation of hydrous

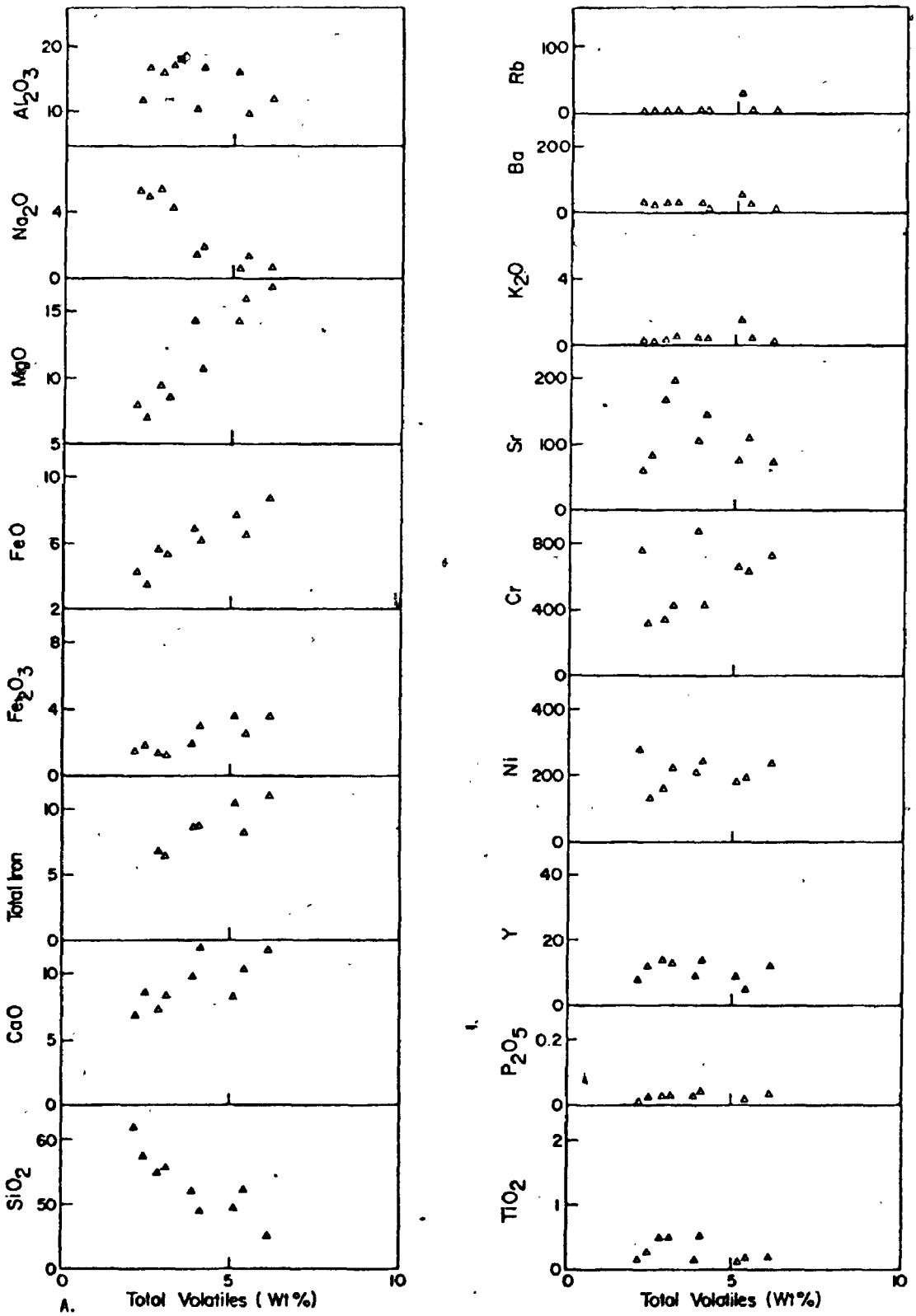

Figure 22. Variation of total volatiles against selected elements for the Betts Cove lower pillow lava (A) and sheeted dyke (B) members.

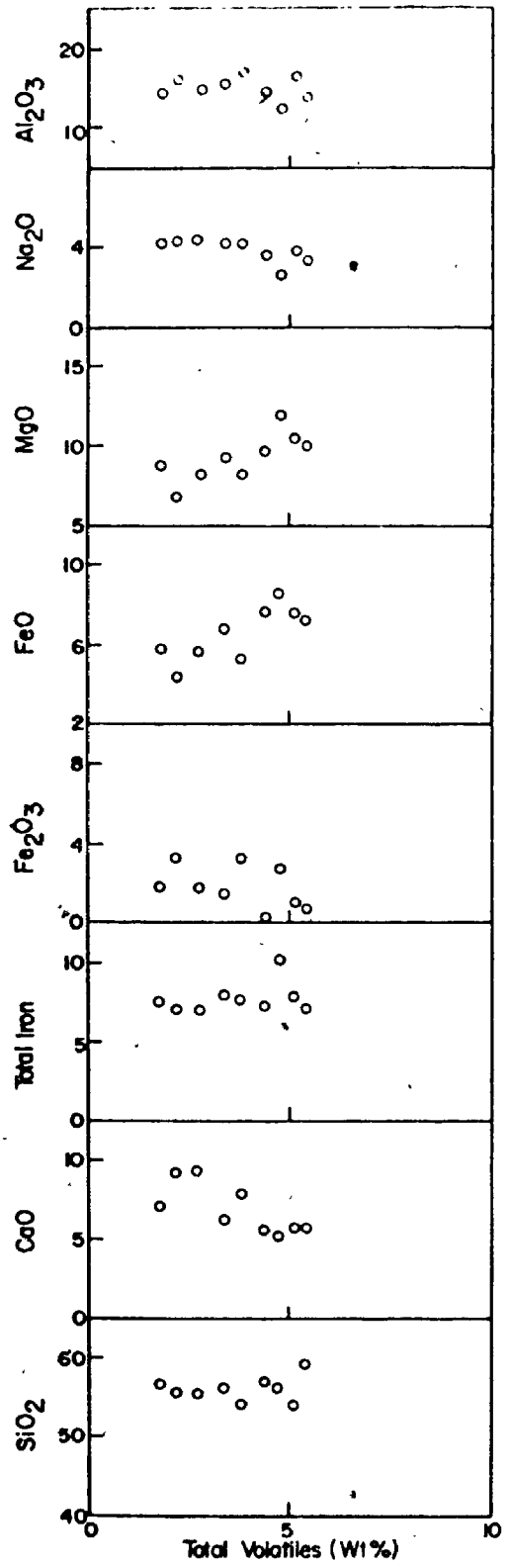
Al_2O_3
Na_2O
MgO
FeO
Fe_2O_3
Total Iron
CaO
SiO_2
Total Volatiles (Wt %)

B.

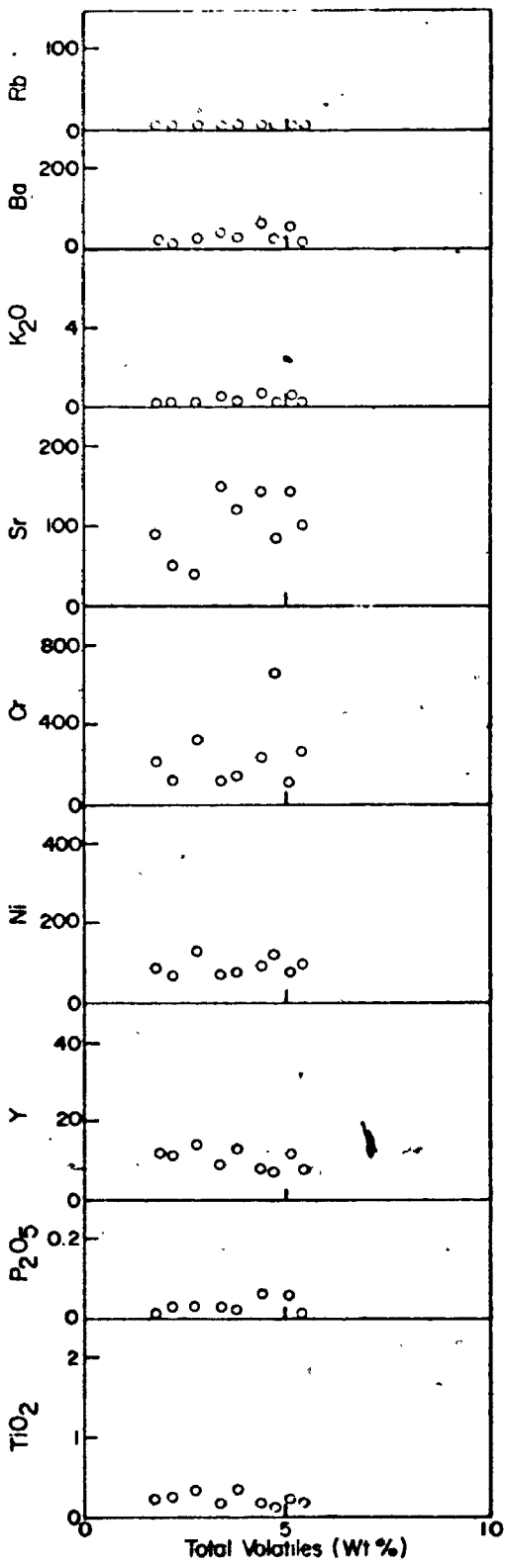
Rb
Ba
K_2O
Sr
Cr
Ni
Y
P_2O_5
TiO_2
Total Volatiles (Wt %)

phases; it shows no variation in the sheeted dyke complex because SiO_2 is added as free quartz. Calcium increases with volatiles in the pillows because of the introduction of calcite and epidote to pillow rims; it is, however, leached from the sheeted dykes. Overall sodium abundances in all crystalline parts of the ophiolite are enhanced over fresh basalts - the Na_2O is introduced in albite. However, there is a slight decrease in sodium with volatile content in the dykes; this is probably a dilution effect of the introduction of large amounts of sodium-free hydrous phases. On the other hand, the large decreases in sodium content in the lower lavas can only be explained by leaching of sodium from glassy rims of pillows (see following section).

It is apparent from the above discussion that caution must be exercised in interpreting element variation with volatile content and a thorough knowledge of the mineralogical changes is necessary before any conclusions concerning the movement of elements can be made.

A.3d. Chemical Variations Within Individual Pillows

Table 3 lists five pillow rim and core analyses from the lower pillow lava member of the Betts Cove ophiolite. With the exception of specimen #BC-74-37, the pillow rims are consistently depleted in SiO_2, Na_2O and Ba and enriched in Fe_2O_3, total iron, MgO, CaO and total volatiles

TABLE 3

Rim and Core analyses of the Betts Cove lower pillow lavas.*

	BC-74-101		BC-74-58		BC-74-61		BC-74-45			BC-74-37	
	Rim	Core	Rim	Core	Rim	Core	Rim	Int.	Core	Rim	Core
SiO_2	45.70	61.74	49.14	55.14	48.59	52.71	53.51	61.10	57.98	50.54	50.68
TiO_2	0.15	0.12	0.55	0.53	0.20	0.18	0.18	0.13	0.15	0.11	0.11
Al_2O_3	11.76	11.94	16.35	16.80	13.18	11.67	13.89	11.77	13.00	11.65	10.89
Fe_2O_3	3.56	1.47	2.89	1.18	3.07	1.07	1.78	1.32	1.11	2.38	2.31
FeO	8.58	4.25	6.23	5.49	5.77	6.60	6.93	5.04	5.67	6.99	7.02
MnO	0.20	0.15	0.17	0.16	0.16	0.14	0.20	0.16	0.17	0.19	0.18
MgO	16.58	7.77	11.07	8.17	14.97	13.34	11.96	8.68	9.80	18.77	18.98
CaO	12.42	6.86	12.56	8.38	13.71	12.26	7.58	7.35	7.06	7.72	8.13
Na_2O	0.55	5.14	1.96	4.05	0.18	0.74	2.55	2.61	3.96	0.00	0.00
K_2O	0.01	0.01	0.05	0.16	0.04	0.08	0.13	0.11	0.07	0.83	0.89
P_2O_5	0.04	0.01	0.04	0.03	0.01	0.01	0.01	0.02	0.02	0.02	0.02
L.O.I.	6.09	2.19	4.08	3.22	3.97	3.27	3.80	2.58	2.87	5.83	5.43
FeO^t/MgO	.71	.71	.79	.79	.59	.58	.74	.73	.70	.51	.50
Ni	231	268	244	224	387	335	98	94	88	298	301
Cr	730	756	432	436	918	787	407	330	350	958	1050
Zr	20	16	20	20	13	10	13	11	14	6	9
Y	11	8	14	13	3	1	5	2	6	-	-
Sr	74	60	146	202	160	237	62	87	77	39	33
Rb	1	-	2	2	nd	2	nd	1	nd	16	16
Ba	12	28	8	28	5	11	25	32	31	32	35
Cu	133	113	54	79	-	-	-	-	-	-	-

* - Major elements in weight percent oxide, traces in ppm.
nd - Not detected.
L.O.I. - Loss on Ignition.
FeO^t - Total iron as FeO.
Int. - Intermediate zone between pillow rim and core.

relative to the pillow cores. TiO_2, Al_2O_3, K_2O, Zr, Y, Rb, Sr, Ni and Cr contents either vary inconsistently or show no change between the rims and cores. Specimen #BC-74-37 has the same major and trace element content throughout the pillow. This is presumably due to the fact that the pillow is intensely sheared because of its proximity to a fault. The shearing has facilitated the homogenization of both texture and chemistry.

The observed chemical differences between the rims and cores of the pillows are unlikely to have been the result of igneous processes. If the large differences in SiO_2, total iron and MgO were due to igneous differentiation or liquid immiscibility, then large differences in the values of trace elements such as Zr, Ni and Cr would be expected. However, as Table 3 reveals, Zr, Ni and Cr contents vary very little from the rims to the cores of the analyzed pillows.

Chemical changes within individual pillows may also be due to metasomatism. Many authors have suggested that pillow rims tend to be more altered than their cores because of the greater accessibility of fluids to the rims (for example, S. R. Hart, 1969; S. R. Hart et al., 1974; Shido et al., 1974; Aumento et al., 1976). This idea is applicable to weathered basalts but in the case of the Betts Cove pillows and other greenschists, the cores as well as the rims are intensely altered. A more likely cause of the observed chemical and mineralogical variations

may be related to the differences in original texture between a glassy rim and a crystalline core. In a glassy rim, minerals with low nucleation energies will form during metamorphism. Chlorite, actinolite and epidote appear to form preferentially to plagioclase (Cann, 1969). On the other hand, pillow cores already contain plagioclase and clinopyroxene crystals which provide sites for the growth of albite and actinolite/chlorite. Thus, during alteration, the rims will transform to mafic hydrous minerals while losing their siliceous components whereas the chemistry of the cores will be determined to some extent by the pre-existing mineralogy.

In summary, it is concluded that: 1) SiO_2, Na_2O and Ba are depleted whereas Fe_2O_3, FeO, MgO, CaO and H_2O are enriched in glassy material. 2) CaO is leached whereas SiO_2, Na_2O, Fe_2O_3 and H_2O are added to crystalline cores. Although FeO and MgO values in the crystalline cores are slightly lower than contents of fresh oceanic basalts, this decrease can be accounted for by the large increases in silica and sodium and consequent summing to 100%. 3) TiO_2, P_2O_5, Zr, Y, Cr, Ni and FeO^t/MgO are immobile regardless of starting material.

A.3e. Other Changes

A.3ei. Fe_2O_3/FeO Ratios

In section A.3c, it is apparent that the amount of ferric iron (and thus oxidation) in the Betts Cove ophio-

litic rocks is dependent on stratigraphic position. Fe_2O_3/FeO ratios provide a clear indication of oxidation and Table 4 shows that the ophiolitic rocks at Betts Cove have been intensely oxidized relative to fresh basalt and the degree of oxidation decreases with depth of burial. Not only does the weight ratio of Fe_2O_3/FeO decrease because of the disappearance of hematite and a decrease in the abundance of epidote downwards but also because of a change in the composition of the epidotes with depth. Microprobe data (Figure 23) indicate that the epidotes become less iron rich and more aluminous with depth of burial. The decrease in the Fe3+ component in the epidotes is a reflection of a decrease in the oxygen fugacity and an increase in the temperature of the metamorphosing fluid (Liou, 1973; Raith, 1976).

A.3eii. Na_2O/K_2O Ratios

The mobilities of sodium and potassium during metamorphism of the Betts Cove ophiolite also vary with stratigraphic position but not in the simple manner seen for the oxidation ratio. This is evident in the plots of Na_2O/K_2O versus $Na_2O + K_2O$ (Miyashiro, 1975a) (Figure 24). Clearly, two trends of alkali mobility are present:
1) The nearly vertical trend extending to very low values of Na_2O/K_2O for the upper pillow lava and gabbro members (Figure 24b) is only explicable in terms of significant potassium addition with possible small increases in Na_2O.

TABLE 4

Fe_2O_3/FeO and Na_2O/K_2O weight ratios for the mafic members of the Betts Cove ophiolite compared with ratios from average fresh oceanic tholeiite (Melson and Thompson, 1971).

	Fe_2O_3/FeO	Na_2O/K_2O
Upper lava member	1.36	13
Lower lava member	0.47	85
Sheeted dykes	0.33	61
Gabbro member	0.34	3
Fresh basalt	0.25	12

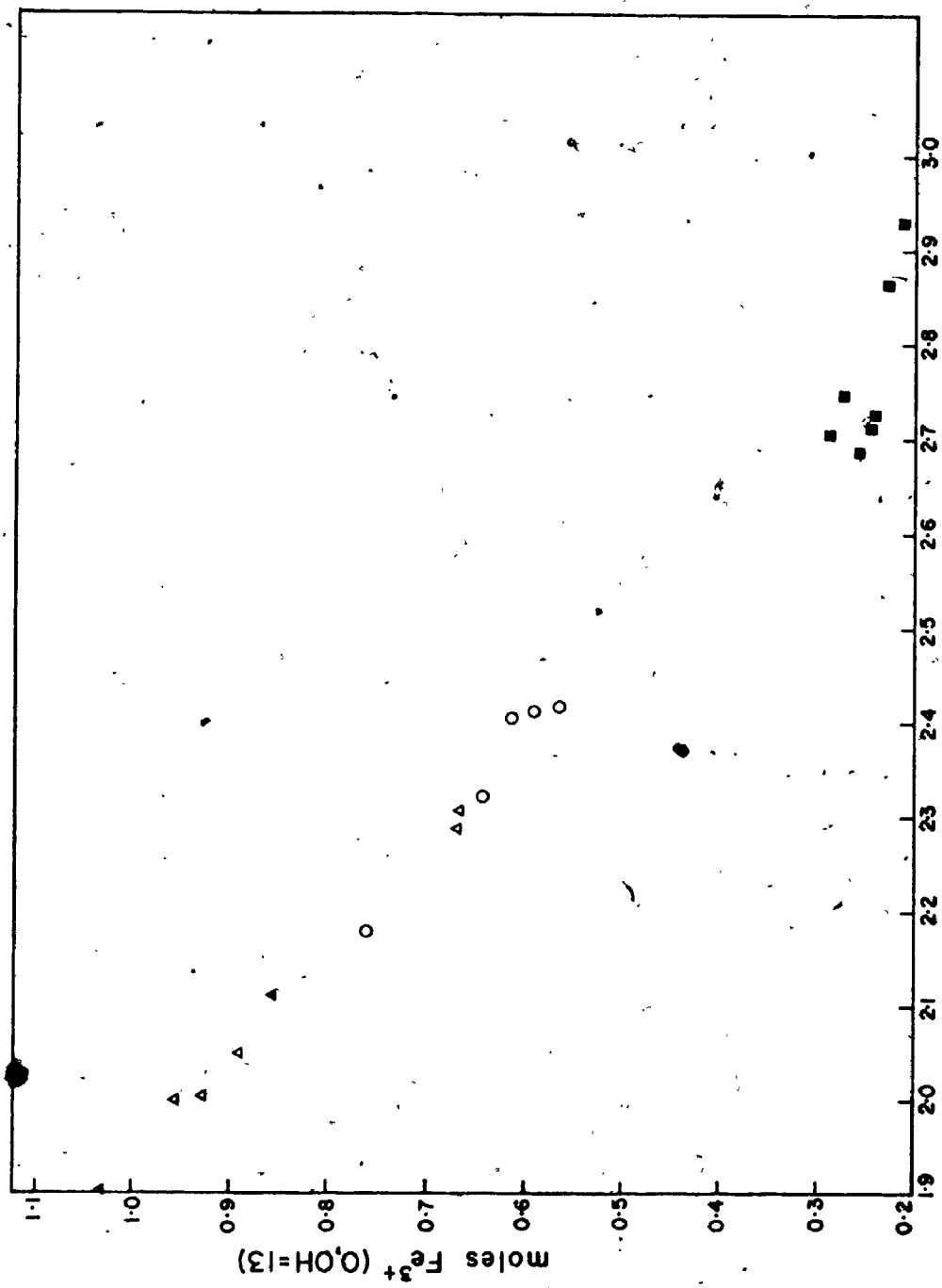

FIGURE 23. VARIATION OF Fe^{3+} AGAINST Al^{3+} IN EPIDOTES FROM THE UPPER PILLOW LAVAS (▲), LOWER PILLOW LAVAS (△), SHEETED DYKES (○), AND GABBROS (■) OF THE BETTS COVE OPHIOLITE.

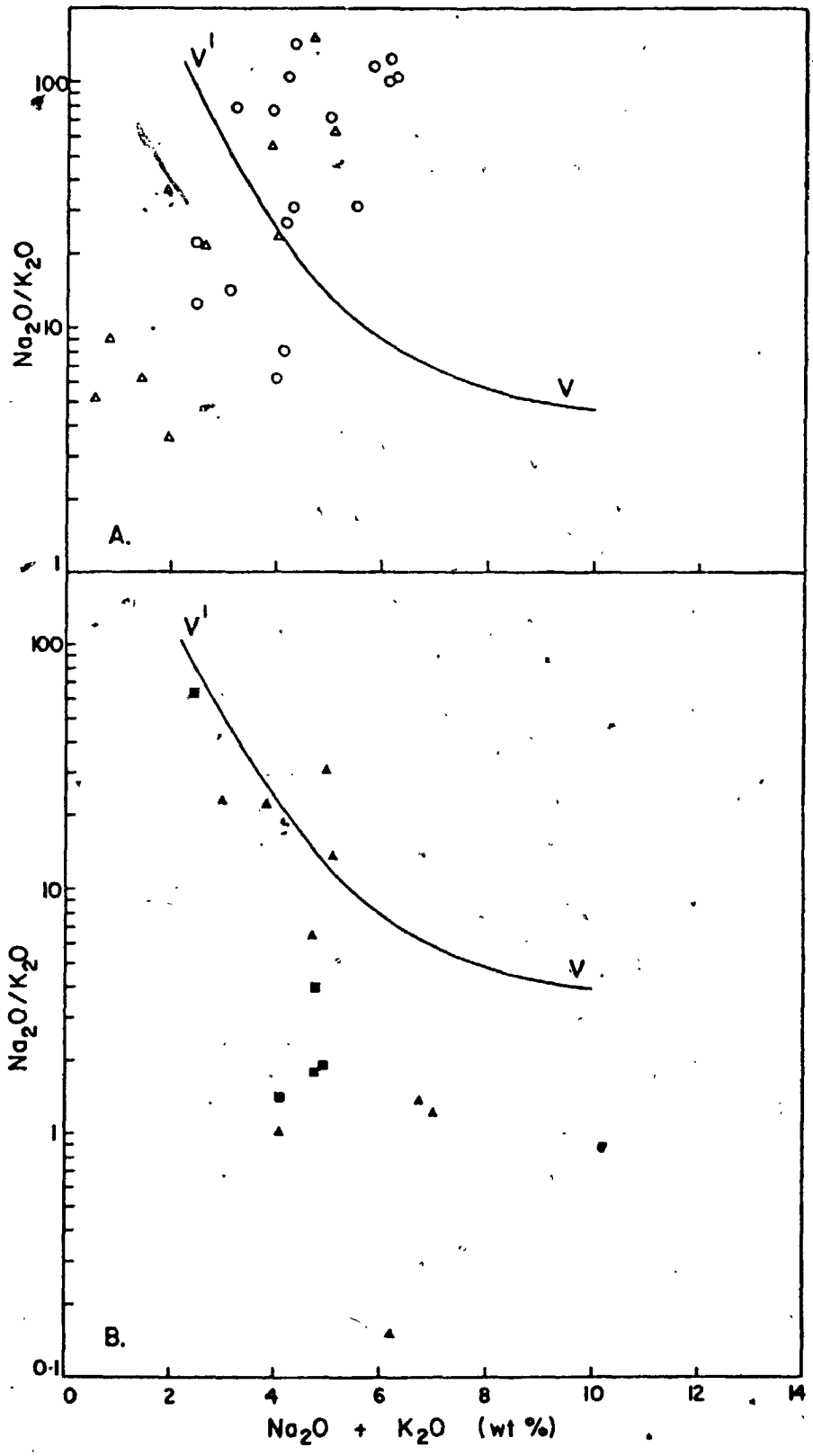

FIGURE 24. VARIATION OF Na_2O/K_2O WITH $Na_2O + K_2O$ FOR THE BETTS COVE LOWER LAVAS (▲) AND SHEETED DYKES (○) (A), AND UPPER LAVAS (▲) AND GABBROS (■) (B). ALL FRESH CENOZOIC BASALTS PLOT BELOW THE CURVE V' - V (MIYASHIRO, 1975).

2) The trend of increasing Na_2O/K_2O with $Na_2O + K_2O$ in the lower pillow lava and sheeted dyke members (Figure 24a) indicates sodium enrichment with no change or a slight decrease in potassium content for these rocks.

Mineralogically, the potassium enrichment in the upper pillow lavas and the gabbros is accommodated by the alteration of plagioclase to phengitic muscovite. In the lower pillows and sheeted dykes, muscovite is rare whereas albite is abundant.

A.4. Ocean Floor Metamorphism in the Betts Cove Ophiolite

A.4a. Model for Modern Ocean Floor Metamorphism

Metamorphism of modern ocean crust involves weathering, cold hydration and hydrothermal activity due to convective circulation of seawater (Lister, 1972; Spooner and Fyfe, 1973; Williams et al., 1974; Keen, 1975; Andrews and Fyfe, 1976; Wolery and Sleep, 1976). Weathering and cold hydration involve reaction of the upper 600 meters of oceanic crust with cold (~5°C) seawater. These processes begin at the oceanic ridge and increase in intensity with distance from the spreading center (Hart, 1973; Keen, 1975). Hydrothermal circulation of heated seawater, however, is restricted to a few kilometers on either side of the ridge axis but is responsible for high temperature alteration to depths of 4 or 5 kilometers below the ocean floor.

The hypothesis that convective circulation of seawater occurs at mid-ocean ridges is based on: 1) the interpretation of observed heat flow profiles across ocean ridges (Williams et al., 1974), 2) the study of alteration products in dredged metamorphosed oceanic rocks (Hart, 1973; Bonatti et al., 1975; Honnerez and Kirst, 1975), 3) the oxygen isotope geochemistry of dredged oceanic greenstones (Muehlenbachs and Clayton, 1972, 1975) and on-land ophiolites (Spooner et al., 1974; Magaritz and Taylor, 1976), 4) experimental investigations of element mobility and alteration during seawater-basalt interactions under simulated ocean crust conditions (Hajash, 1974, 1975; Mottl et al., 1974; Bischoff and Dickson, 1975) and 5) theoretical predictions of the movement of water through a permeable medium in the vicinity of a heat source (Elder, 1967; Lister, 1972, 1974; Lowell, 1975).

The model of hydrothermal metamorphism within the oceanic crust as developed by Spooner and Fyfe (1973), Andrews and Fyfe (1976) and Wolery and Sleep (1976) is shown in Figure 25. Seawater enters the oceanic crust via numerous fractures in dispersed recharge zones, penetrates to at least 1 km. (Wolery and Sleep, 1976) or even farther to 4 or 5 km. (Andrews and Fyfe, 1976) and returns to the ocean in a modified state along concentrated fault zones. Because large heat sources exist at mid-ocean ridges, the temperature of the seawater will increase as it penetrates

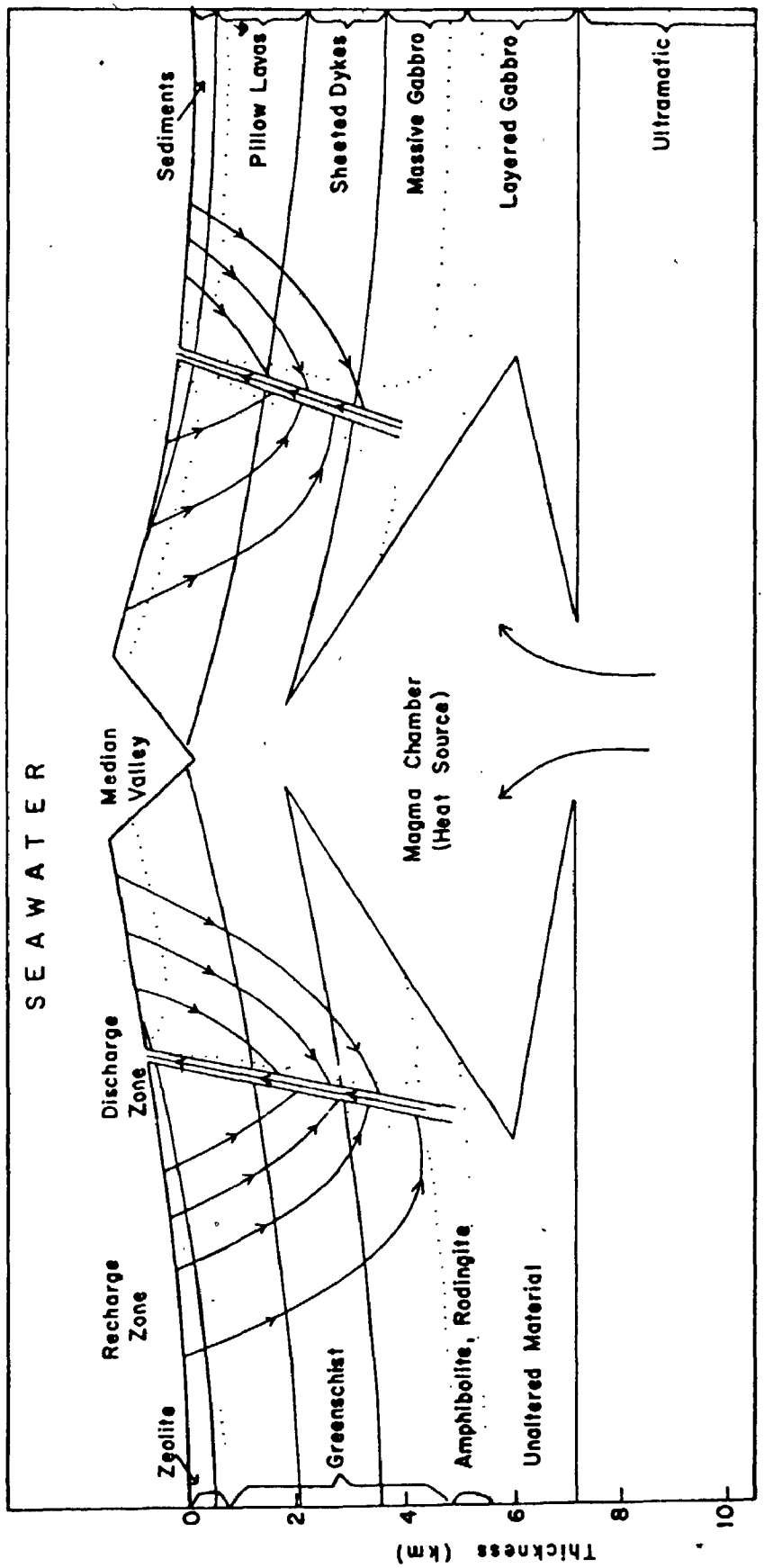

FIGURE 25. GENERALIZED MODEL FOR OCEAN FLOOR METAMORPHISM NEAR A MID-OCEAN RIDGE (MODIFIED AFTER SPOONER AND FYFE, 1973; ANDREWS AND FYFE, 1976). SOLID LINES REPRESENT LITHOLOGIC BOUNDARIES; DOTTED LINES ARE METAMORPHIC BOUNDARIES.

the crust. Heated seawater in contact with fresh basalt will result in the development of zeolite, greenschist and even amphibolite facies oceanic rocks in the crust. Accompanying the metamorphism of the oceanic crust are large scale metasomatic changes in its composition. The movement of elements during ocean floor metamorphism has far reaching effects concerning 1) the deposition of massive sulphides in the ocean crust (Andrews and Fyfe, 1976), 2) the geochemical balance in the composition of the oceans (R. A. Hart, 1973; Wolery and Sleep, 1976), 3) the composition of chemical sediments deposited on the ocean floor (Sayles et al., 1975; Bonatti et al., 1976; Cronan, 1976) and 4) the nature of geochemical reactions occurring during subduction of oceanic crust (Fyfe and McBirney, 1975; Fyfe, 1976).

A.4b. Interpretation of the Metamorphism at Betts Cove

It is proposed that hydrothermal circulation of heated seawater near a mid-ocean ridge resulted in the metamorphic effects observed in the mafic members of the Betts Cove ophiolite. This conclusion is based on the following criteria:

1) the alteration in the ophiolite is sporadic, indicating metamorphic fluids followed discrete permeable horizons. Furthermore, the preservation of igneous textures suggests confining pressures were low - a suitable condition for

fracture development.

2) the occurrence of actinolite at high stratigraphic levels in the ophiolite suggests a geothermal gradient of greater than 300°C/km; geothermal gradients as high as this are associated with mid-ocean ridges and convective transfer of heat by circulating seawater (Williams et al., 1974; Lowell, 1975).

3) the concentration of calcite and hematite in the upper portions of the Betts Cove ophiolite is consistent with the seawater-oceanic crust interaction hypothesis. Seawater is a source of Ca^{2+} and HCO_3^-. Ca^{2+} is also released by the breakdown of plagioclase to albite. Thus, a seawater brine in the ocean crust is saturated with calcium carbonate. Penetration of this brine through the crust will heat the seawater and since the solubility of calcite decreases drastically with increasing temperature, calcite will precipitate rapidly at high levels in the ocean crust.

Because of the abundance of hematite in the upper pillow lavas at Betts Cove, Fe_2O_3/FeO ratios are as high as 1.5 (Table 4). In order to oxidize a basalt to such an extent, a large amount of oxygenated fluid is required. In fact, E.T.C. Spooner (pers. comm.), on this basis, has estimated water to rock ratios of greater than 100 to 1 for similarly oxidized rocks in the Troodos ophiolite of Cyprus. In the oceanic environment, seawater is a convenient and large source of the needed oxygenated fluid. Furthermore, the disappearance of hematite and the decrease

in the iron content of epidotes downward in the ophiolite indicate that the oxygen fugacity of the metamorphosing fluid decreases with depth. This is expected as seawater becomes reduced with depth of penetration due to massive oxidation of upper levels of the crust.

4) The previously described patterns of element migration during metamorphism of the Betts Cove ophiolite are consistent with trends deduced from studies of hydrothermally altered oceanic basalts (Cann, 1969; Miyashiro et al., 1971; Cann, 1971; Bonatti et al., 1971; R. A. Hart, 1973) and from experimental basalt-seawater interactions (Hajash, 1974, 1975; Mottl et al., 1974; Bischoff and Dickson, 1975) (Table 5).

The trends indicated for SiO_2, FeO^t and K_2O in Table 5 are, on superficial perusal, inconsistent and require further explanation. The discrepancy in silica mobilities between experimental results and studies of natural systems may be related to two factors. First, in natural systems, glassy as well as coarse crystalline rocks are altered whereas experiments are usually performed on only glassy or very fine grained material. Secondly, experimental systems only simulate the downward portion of a convective cycle (silica leaching) whereas ascent and cooling of a silica saturated fluid in natural systems can result in silica precipitation.

Total iron is clearly added to some Betts Cove basalts and some oceanic dredged rocks but decreases in

TABLE 5

Comparison of the mobilities of selected elements during greenschist metamorphism as ascertained from experimental basalt/seawater interactions (Hajash,1974;1975;Mottl et al., 1974;Bischoff and Dickson,1975), studies of dredged oceanic material (Cann,1969;Miyashiro et al.,1971;R.A. Hart,1973), and this study. Loss/gain refers to subtraction/addition from/to the altered rock.

	Experimental	Oceanic Basalts	Betts Cove
SiO_2	Loss	Loss or Gain	Loss(glassy) Gain(crystalline)
TiO_2	Immobile	Immobile	Immobile
Al_2O_3	?	Loss?	Immobile?
Fe_2O_3	?	Gain	Gain
FeO^t	Loss	Loss or Gain	Gain(glassy)
MnO	Loss	Loss	?
MgO	Gain	Gain	Gain
CaO	Loss	Loss	Loss
Na_2O	Gain	Gain	Gain(crystalline) Loss(glassy)
K_2O	Gain/Loss	Loss	Erratic
P_2O_5	?	Immobile	Immobile
H_2O	Gain	Gain	Gain
Cu	Loss	Loss	Loss
Ni	Loss?	?	Immobile
Cr	?	Immobile	Immobile
Zr,Y	?	Immobile	Immobile
Ba,Rb,Sr	?	Gain/Loss	Erratic

material which has been experimentally interacted with hot seawater. Again the inconsistency is probably related to position in the convective cycle and whether or not iron is at a saturation level in the hydrothermal fluid. This is supported by the experimental results of Bischoff and Dickson (1975). They found that heated seawater, during interaction with basalt, experienced an initial increase in iron up to a certain saturation concentration after which iron precipitated.

The behaviour of potassium during metamorphism is highly dependent on temperature. At low temperatures (< 200°C), K_2O is added to oceanic basalts whereas above 200°C, it is leached (Bischoff and Dickson, 1975). Most of the greenschists in the ocean crust have low potassium values. However, some high potassium rocks, like the upper lavas and gabbros at Betts Cove, have been described from oceanic areas. Potassium feldspar precipitating from a cooling hydrothermal brine at the Reykjanes geothermal system in Iceland gives rise to K_2O enriched basalts at high levels in the ocean crust (Bjornsson et al., 1972; Tómasson and Kristmannsdóttir, 1972). Also, potassium enriched gabbros have been dredged from the Indian ocean (Cann, 1971).

5) The occurrence of pyrite-chalcopyrite massive sulphide bodies at Betts Cove has been attributed to volcanogenic processes (Upadhyay and Strong, 1973). However, a re-evaluation is warranted on the basis of the recent evolu-

tion in thought concerning ocean floor massive sulphide generation (Bonatti, 1975; Andrews and Fyfe, 1976). The massive sulphide bodies at Betts Cove are restricted in occurrence to a highly permeable breccia zone at the sheeted dyke/pillow lava contact. Also, Cu concentrations in the sheeted dykes decrease significantly (from 75 to 10 ppm) with increasing intensity of metamorphism. In light of these observations, it appears feasible that the deposits could have precipitated by a process involving metal leaching of oceanic crust by heated circulating seawater and concentration during hydrothermal discharge along the sheeted dyke/pillow lava contact.

6) The occurrence of rodingitic gabbro near the base of the Betts Cove mafic zone is to be expected in a circulating seawater system since similar rodingitic gabbros have been described as having been formed by rapid hydrothermal discharge at modern mid-ocean ridges (Honnerez and Kirst, 1975).

B. Blow-Me-Down Ophiolite

The Blow-Me-Down ophiolite is metamorphosed from the zeolite facies at the top to prehnite-pumpellyite through greenschist and into amphibolite facies in the upper parts of the gabbro unit (Einarson, 1975; Williams and Einarson, 1976). Stratigraphically below the amphibolitic gabbro, fresh gabbro with occasional rodingitic patches occurs (Riccio, 1976) suggesting perhaps that the fluid responsible

for the metamorphism penetrated downwards through the ophiolite.

Faults and fractures in the Blow-Me-Down ophiolite are much less common than in the Betts Cove ophiolite. Epidote and quartz, so common at Betts Cove, occur in minor amounts in the Blow-Me-Down sequence. Calcite, however, is very prominent in the upper portions of both ophiolites. Hematite, in large quantities, is restricted to the upper pillows at Blow-Me-Down.

Using Zr versus the elements diagram described above, it appears that the patterns of element mobility during the Blow-Me-Down metamorphic episode are different from those observed for the Betts Cove metamorphism (Figure 26). MgO, FeO^t, Na_2O and possibly CaO and Al_2O_3 in addition to TiO_2, P_2O_5, Ni, Cr, Y and FeO^t/MgO have probably not moved significantly during post-igneous processes. SiO_2, Fe_2O_3, K_2O and Ba, however, have irregular trends against Zr, indicating their mobility.

The oxidation ratio, Fe_2O_3/FeO, of the metamorphosed rocks in the Blow-Me-Down ophiolite behaves similarly to Fe_2O_3/FeO variations in the Betts Cove rocks (Figure 27). The decrease in Fe_2O_3/FeO downwards, again, indicates that the metamorphosing fluid became reduced with depth of burial.

Although it is probable that the metamorphism of the Blow-Me-Down ophiolite took place on the ocean floor (Williams and Einarson, 1976), the lack of pervasive

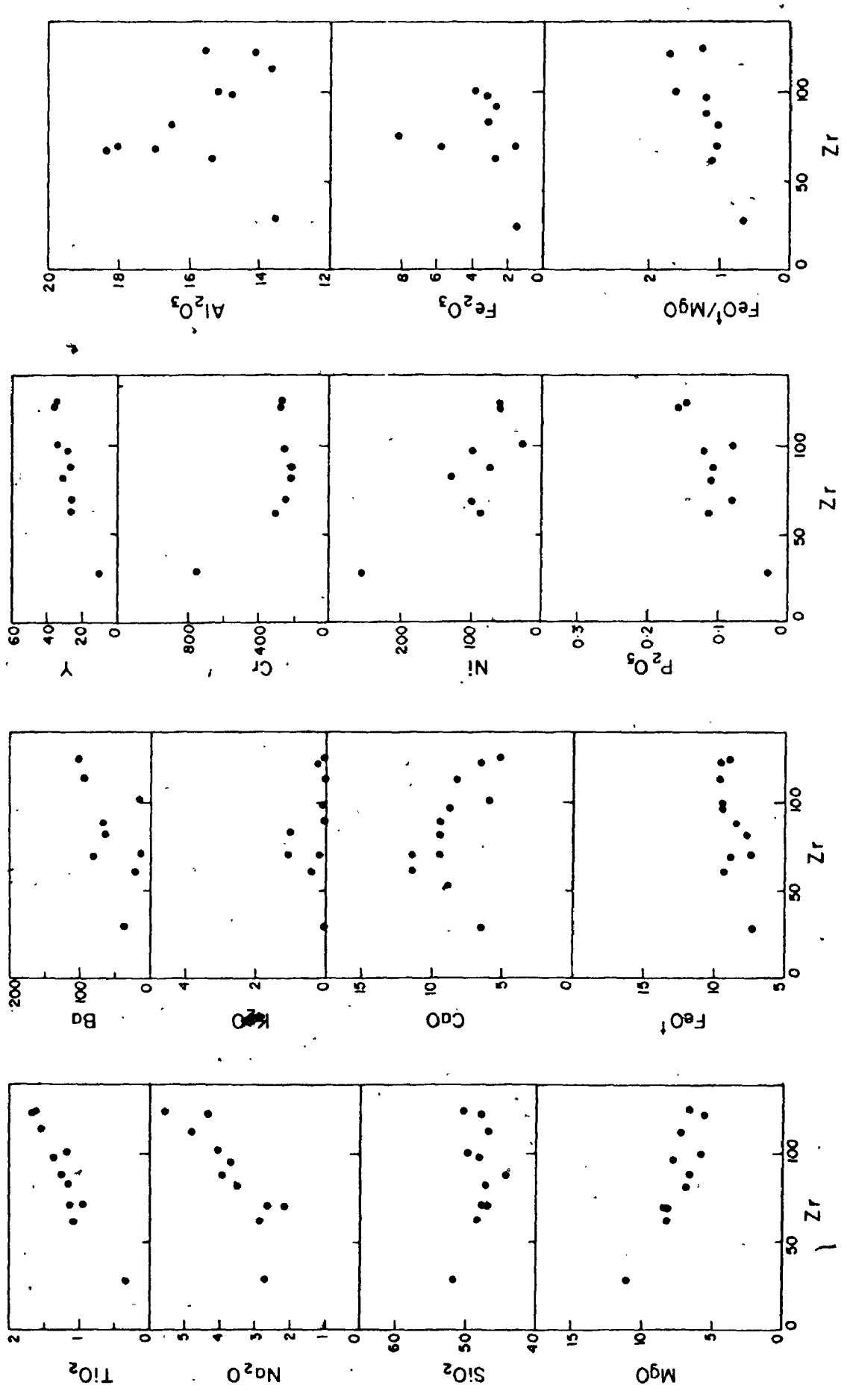

FIGURE 26. VARIATION OF ZR AGAINST SELECTED ELEMENTS IN THE BLOW-ME-DOWN OPHIOLITE PILLOW LAVA AND SHEETED DYKE MEMBERS. MAJOR OXIDES IN WEIGHT PERCENT, TRACES IN PPM.

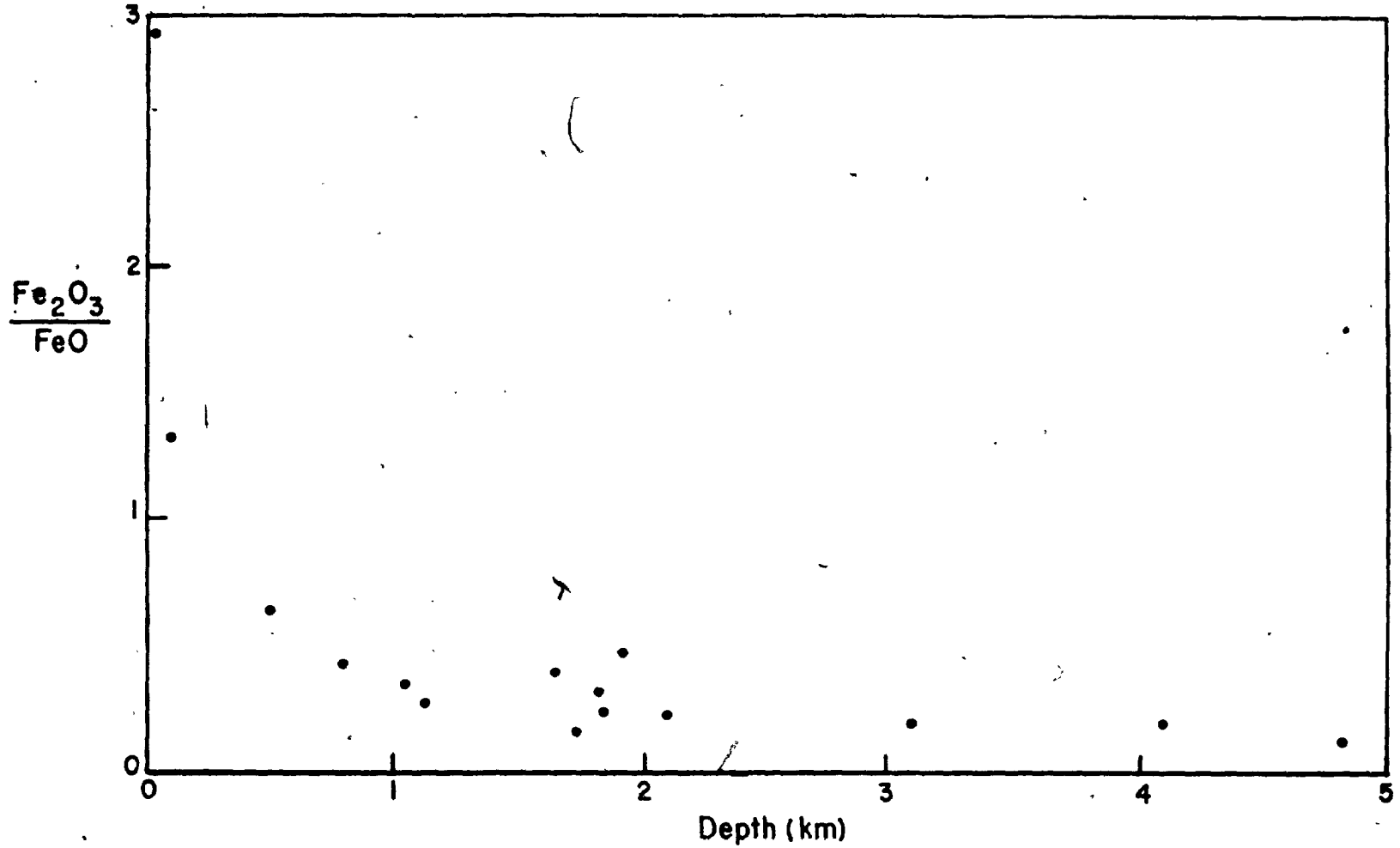

FIGURE 27. VARIATION OF Fe_2O_3/FeO RATIO WITH DEPTH OF BURIAL IN THE BLOW-ME-DOWN OPHIOLITE, WESTERN NEWFOUNDLAND. THE SCATTER OF POINTS NEAR THE 2 KM. LEVEL COINCIDES APPROXIMATELY WITH THE SHEETED DYKE/GABBRO CONTACT.

mineral-filled fractures and the apparent decrease in metasomatic activity suggest that vigorous hydrothermal circulation may not have been as significant in the metamorphism of the Blow-Me-Down ophiolite as at Betts Cove. Rather, it is likely that burial conditions were more closely approached with seawater percolating slowly down through the crust but with limited hydrothermal convection. During slow percolation of seawater, the calcite and hematite distribution and the variation of the oxidation ratio would still behave as observed in the Blow-Me-Down ophiolite.

CHAPTER 5

IGNEOUS PETROGENESIS OF THE BETTS COVE OPHIOLITE AND COMPARISON WITH THE BLOW-ME-DOWN OPHIOLITE

A. Introduction

It has been shown that the mafic rocks of the Betts Cove ophiolite have unusual chemical characteristics when compared with normal modern oceanic tholeiite and most other ophiolite complexes. The Betts Cove rocks are low in TiO_2, Zr, Y, REE and FeO^t/MgO and high in MgO, Ni and Cr relative to recent oceanic tholeiite. The clinopyroxenes and chromites also have low Ti and FeO^t/MgO, and high MgO and Cr contents.

From the FeO^t/MgO versus TiO_2 diagram (Figure 9) and the clinopyroxene chemistry, it has been shown that the Betts Cove basaltic rocks are not less differentiated equivalents of magmas which gave rise to normal modern oceanic tholeiite. Rather the source material of the Betts Cove basalts must be chemically different from that of modern oceanic tholeiites.

In this chapter, a primary (least differentiated) liquid composition of the Betts Cove mafic rocks is used

to calculate a source composition. Then, the range of compositions exhibited by the pillow lavas and dykes are related through simple crystal fractionation of the primary liquid. Also, the chemical, genetic and chronological relationships of the various stratigraphic members are related. Finally, the link between geochemistry and tectonic setting of the Betts Cove and other ophiolites is discussed.

B. Source Composition for the Betts Cove Mafic Rocks

B.1. Summary of Previous Work on Basalt Sources

Basaltic magmas are derived from partial melting of upper mantle material, probably of peridotitic composition rather than eclogite (Green and Ringwood, 1967; Wyllie, 1971; Ringwood, 1975). Pyrolite, a mixture of approximately 3 parts peridotite to 1 part oceanic tholeiite, is the postulated upper mantle composition (Ringwood, 1966, 1975; Green and Ringwood, 1967) (Table 6). Pyrolite occurs as three stable sub-solidus mineral assemblages: plagioclase, spinel or garnet pyrolite depending upon pressure conditions in the upper mantle (Figure 28). According to Green and Ringwood (1967), various degrees of partial melting of the upper mantle coupled with fractionation at differing P-T conditions of the resulting liquid will produce the observed range of major element compositions in basalt magmas. However, Gast (1968), in reviewing trace element contents of oceanic tholeiites and alkaline

TABLE 6

Pyrolite Model Mantle Compositions (after Ringwood, 1975).

	1	2	3	4
SiO_2	45.20	44.90	46.10	45.10
TiO_2	0.70	0.24	0.20	0.20
Al_2O_3	3.50	4.30	4.30	4.60
Fe_2O_3	0.50	-	-	0.30
FeO	8.00	8.20	8.20	7.60
MnO	0.14	0.10	-	0.10
MgO	37.50	38.90	37.60	38.10
CaO	3.10	2.50	3.10	3.10
Na_2O	0.60	0.23	0.40	0.40
K_2O	0.13	0.02	0.03	0.02
P_2O_5	0.06	0.02	-	0.02
Cr_2O_3	0.40	0.40	-	0.30
NiO	0.20	0.20	-	0.20

1 - Pyrolite model composition (Ringwood, 1966).

2 - Pyrolite model composition: 99% Lizard peridotite + 1% nephelenite.

3 - Pyrolite model composition: 83% residual harzburgite + 17% oceanic tholeiite.

4 - Average mantle pyrolite (Ringwood, 1975). Average includes (2), (3), bulk composition of the Vourinos ophiolite and the upper mantle composition from Carter (1970).

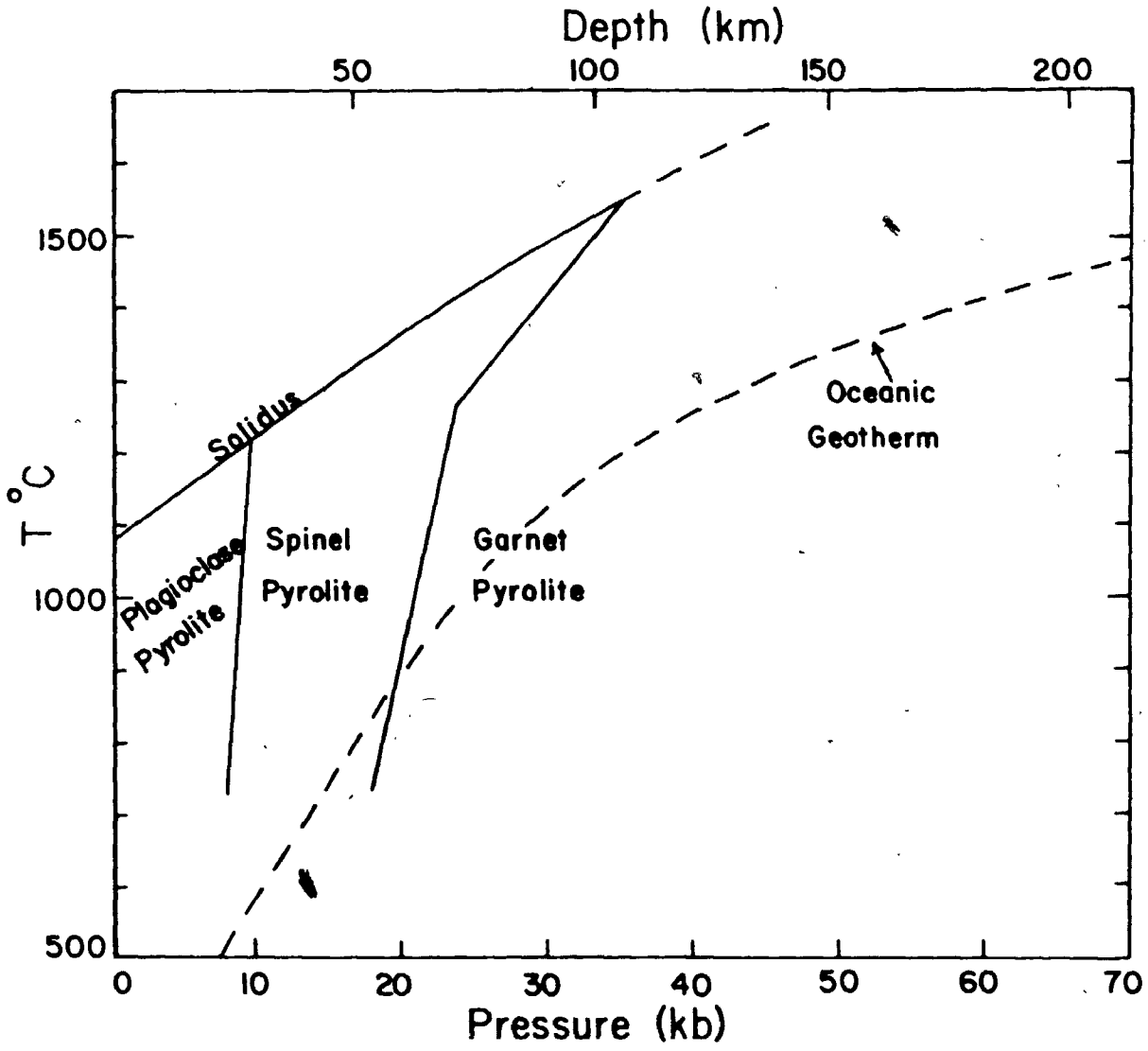

FIGURE 28. STABILITY FIELDS FOR SUB-SOLIDUS MINERAL ASSEMBLAGES OF A PROPOSED MANTLE PYROLITE (RINGWOOD, 1975).

basalts, concluded that both rock series could not have been produced from the same source. He postulated that oceanic tholeiite was derived by 15-30% partial melting of a pyrolite upper mantle which had already been depleted in incompatible elements during prior episodes of incipient partial melting and melt separation. On the other hand, alkaline basalts could form by only 2-5% partial melting of undepleted upper mantle.

Although Gast's scheme can explain the origin of the majority of low-K oceanic tholeiites, the discovery of varying compositional types such as picritic basalts, alkali olivine basalts, andesites and dacites (Bougault and Hekinian, 1975; Byerly et al., 1976; Bryan et al., 1976; Hekinian and Thompson, 1976) in areas of normal oceanic volcanism (i.e. mid-ocean ridges) has rendered the problem more complicated than originally realized. Crystal fractionation can account for some of the observed variance but in many cases, especially with respect to TiO_2 and the incompatible elements, different source compositions of the primary liquids have been advocated (Frey et al., 1974; O'Nions and Pankhurst, 1976), and it has been proposed that the sub-oceanic mantle is laterally heterogeneous as well as being vertically zoned.

B.2. Selection of a Primary Liquid in the Betts Cove Ophiolite

Primary basaltic liquids produced by melting of a peridotitic source will have high concentrations of MgO, Cr, and Ni and low TiO_2, Zr, Y and P_2O_5 compared to more differentiated basalts. At Betts Cove, perknite material contains the highest MgO, Cr, and Ni and the lowest TiO_2, Zr, Y, and P_2O_5 (Appendix II, Table I). However, this rock type is probably of cumulate origin and therefore, is not a candidate for the primary liquid of the Betts Cove basalts. Picritic dykes are also quite primitive chemically since they contain large amounts of olivine. However, because of accumulation of olivine in certain parts of a single dyke, it is not possible to obtain with certainty a composition which represents the liquid of the picritic dykes (see Chapter 3 for discussion of the concentration of olivine phenocrysts in picritic dykes). Nevertheless, slightly fractionated extrusive equivalents of the picritic dykes are probably represented by some lower pillow lavas and consequently, BC-74-101 is taken to represent the closest approximation to the Betts Cove 'primary' liquid. An average analysis of the sample is presented in Table 7 and its rare earth pattern is shown in Figure 12. It has low TiO_2, Zr, Y, P_2O_5 and REE and high Ni and Cr. It should be noted that despite the very primitive nature of the chosen 'primary' liquid, it may still have undergone limited olivine fractionation prior

TABLE 7

Chemical composition* of the Betts Cove primary liquid.

SiO_2	51.65	Ni	250
TiO_2	0.14	Cr	743
Al_2O_3	11.36	Zr	18
Fe_2O_3	2.39	Y	10
FeO	6.11	Sr	67
MnO	.18	Rb	1
MgO	11.58	Ba	20
CaO	9.19	Cu	123
Na_2O	2.78		
K_2O	.01		
P_2O_5	.02		
L.O.I.#	4.14		
Total	99.54		

*Majors in weight percent oxide, traces in ppm.

#Loss on ignition.

to its extrusion. Other major and trace elements are mobile during low grade metamorphism so that their concentrations listed in Table 7 may not be representative of igneous values.

Using the concentrations of the above immobile elements in the chosen 'primary' liquid, a source composition will be calculated.

B.3. Partial Melting Models for the Generation of the Betts Cove Primary Liquid

B.3a. Trace Element Methods

The concentration of a trace element in a magma reflects the value of the distribution coefficient for that element between the magma and the solid phases in the residue. The theoretical basis of trace element partitioning relies on the assumption that trace elements form dilute solid solutions and thus behave according to Henry's Law. Equilibrium conditions are also assumed and thus the chemical potential, u, of element i in phase a (solid) equals the chemical potential of i in phase b (liquid in this case):

$$U_i^{solid} = U_i^{liquid} \qquad (1)$$

In terms of activity, A, and the chemical potential for the standard state, U^o, equation (1) becomes:

$$U_i^{o(solid)} + RT\ln A_i^{(solid)} = U_i^{o(liquid)} + RT\ln A_i^{(liquid)} \quad (2)$$

which can be reduced to:

$$\exp\left[\frac{U_i^{o(solid)} - U_i^{o(liquid)}}{RT}\right] = A_l^{liquid}/A_i^{solid} = K \quad (3)$$

In terms of concentrations rather than activities, equation (3) is

$$Y_i^{(liquid)} \cdot C_i^{(liquid)} = K \cdot Y_i^{(solid)} \cdot C_i^{(solid)} \quad (4)$$

where Y_i = activity coefficient

C_i = concentration of element i

K = distribution coefficient.

But because trace elements are dilute solid solutions, Y approaches 0 to yield:

$$\frac{C_i^{(solid)}}{C_i^{(liquid)}} = K^{solid/liquid} \quad (5)$$

Equation (5) tells us that if the distribution coefficient is experimentally determined, then the natural distribution of elements between a solid and its equilibrated liquid can be determined. This equation is the basis for the prediction of trace element concentrations in liquids after partial melting.

Equations describing trace element fractionation

during partial melting processes have been formulated by Schilling and Winchester (1967), Gast (1968), Shaw (1970) and Hertoogen and Gijbels (1976). The form of the equations vary depending upon the type of melting which is presumed to have occurred. The principal types of partial melting processes are:

1) Batch melting, where the liquid remains in equilibrium with the solid. Modal batch melting implies that the minerals melt in the same proportions as they occur in the source whereas non-modal melting requires different melting proportions.

2) Fractional melting occurs both modally and non-modally. In this case, each small increment of partial melt is removed from equilibrium with the residual solid.

3) Zone melting (Harris, 1957; Shimazu, 1959; Yoder, 1976) involves the movement of a liquid or partially melted layer upward in the mantle by simultaneous melting and mixing of the roof rocks and crystallization and deposition at the floor of the chamber.

4) Disequilibrium melting implies that equilibrium is not attained between the liquid produced and the residual solid. If this were the case in upper mantle melting processes, then obviously, trace element partitioning laws could not be applied. However, there is no evidence to suggest that disequilibrium melting does occur in the mantle (Yoder, 1976).

The melting mechanism invoked for the purposes of

determining a source for the Betts Cove basalts is non-modal batch melting. The equations are from Shaw (1970) with modifications by Hertoogen and Gijbels (1976). The derived equation describing the relationship between the concentration of a trace element in a source and its concentration in a partial melt is:

$$C_l/C_o = 1/(D_o + F(1-P)) \qquad (6)$$

where C_l = concentration of trace element in the partial melt

C_o = original concentration of trace element in source

D_o = Bulk Distribution Coefficient defined as:

$$D_o = X_o^a K_i^{a/l} + X_o^b K_i^{b/l} + ... + X_o^n K_i^{n/l} \qquad (7)$$

where X_o^a is the initial weight fraction of phase a in the source and K is the mineral distribution coefficient of element i between a solid phase and the liquid.

$$P = p^a K^{a/l} + p^b K^{b/l} + ... + p^n K^{n/l} \qquad (8)$$

where p^a, p^b, etc. are the fractions of liquid contributed by phases a, b, etc. during melting.

F = fraction of melting.

In Shaw's equation (6), the factor P remains constant at all degrees of partial melting. However, because some minerals in mantle sources are complex solid solutions, then the proportion of the liquid contributed by each phase will vary with the degree of partial melting. To approximate this change in P, Hertoogen and Gijbels (1976) suggested that the weight fractions in the liquid contributed by each phase be estimated (using experimental data) at some very small degree of melting and also at some high degree of melting (at the disappearance of the first phase). Then, at all degrees of partial melting between these two limits, P can be calculated by assuming linear varying melt proportions. Thus,

$$P(F) = Po + \left(\frac{Pa - Po}{Fa}\right)F \qquad (9)$$

where P(F) - P value at fraction of melting F

Po - P value at very small fraction of melting

Pa - P value at upper limit (disappearance of first phase)

Fa - Fraction of melting at disappearance of first phase.

The point of disappearance of a phase will vary depending upon the system under consideration. If no phases disappear then Fa is 100 and P varies linearly between some very small degree of melting and 100% melting. In this case, Pa is equal to Do in equation (6) since all phases

are in the melt at 100% melting. On the other hand, if a phase or more than one disappears at say 30% melting, then equation (6) is applicable only for degrees of melting less than 30%. More complex equations (see Appendix IV) are needed for higher degrees of melting to account for the loss of a phase from the source material.

The use of the above equations assumes that the distribution coefficients remain constant at all degrees of partial melting. In reality, this is probably not the case but due to the scarcity of experimental data on distribution coefficients, it is futile at the present time to attempt to estimate the change in K with degree of partial melting. Also ignored in the use of the partial melting equations is total pressure.

A short computer program (Appendix IV) has been written to carry out the necessary partial melting calculations. Input to the program includes:

1) proposed source modal composition as weight fraction of minerals.

2) weight proportions of liquid contributed by each phase at a very small degree (2%) of melting and at the degree of melting where a phase disappears. (If eutectic melting is assumed, then the weight proportions of liquid contributed by each phase will be the same at the lower and upper limit of melting considered).

3) assumed original concentrations of elements in the source.

4) distribution coefficients between minerals and liquid. The concentrations of the elements in the liquid at various degrees of partial melting are then calculated. Thus, various models can be tried until there is a match between the calculated trace element concentrations in the liquid and the measured concentrations in the proposed primary liquid.

Ni, Ti and the rare earth elements have been used to model the generation of the Betts Cove primary liquid. It has been shown previously that the Betts Cove primary liquid is depleted in Ti and REE and enriched in Cr and Ni compared to normal oceanic tholeiite. Can these differences be explained if the Betts Cove primary liquid represents higher degrees of partial melting of a source similar to that postulated for modern oceanic tholeiite? Schilling (1975) calculated a mantle source for oceanic tholeiite on the basis of observed rare earth element patterns in ocean floor basalts. Model calculations of Schilling's postulated source show that at the degree of partial melting (20-30%) required to satisfy the Ni concentrations in the Betts Cove primary liquid, the calculated Ti and REE concentrations are much higher than the observed values in the primary liquid (Figure 29). To attain the necessary low REE and Ti abundances of the Betts Cove liquid, greater than 80% melting is required. At this point, Ni would be greater than 500 ppm and it is also doubtful that the major element composition would be basaltic.

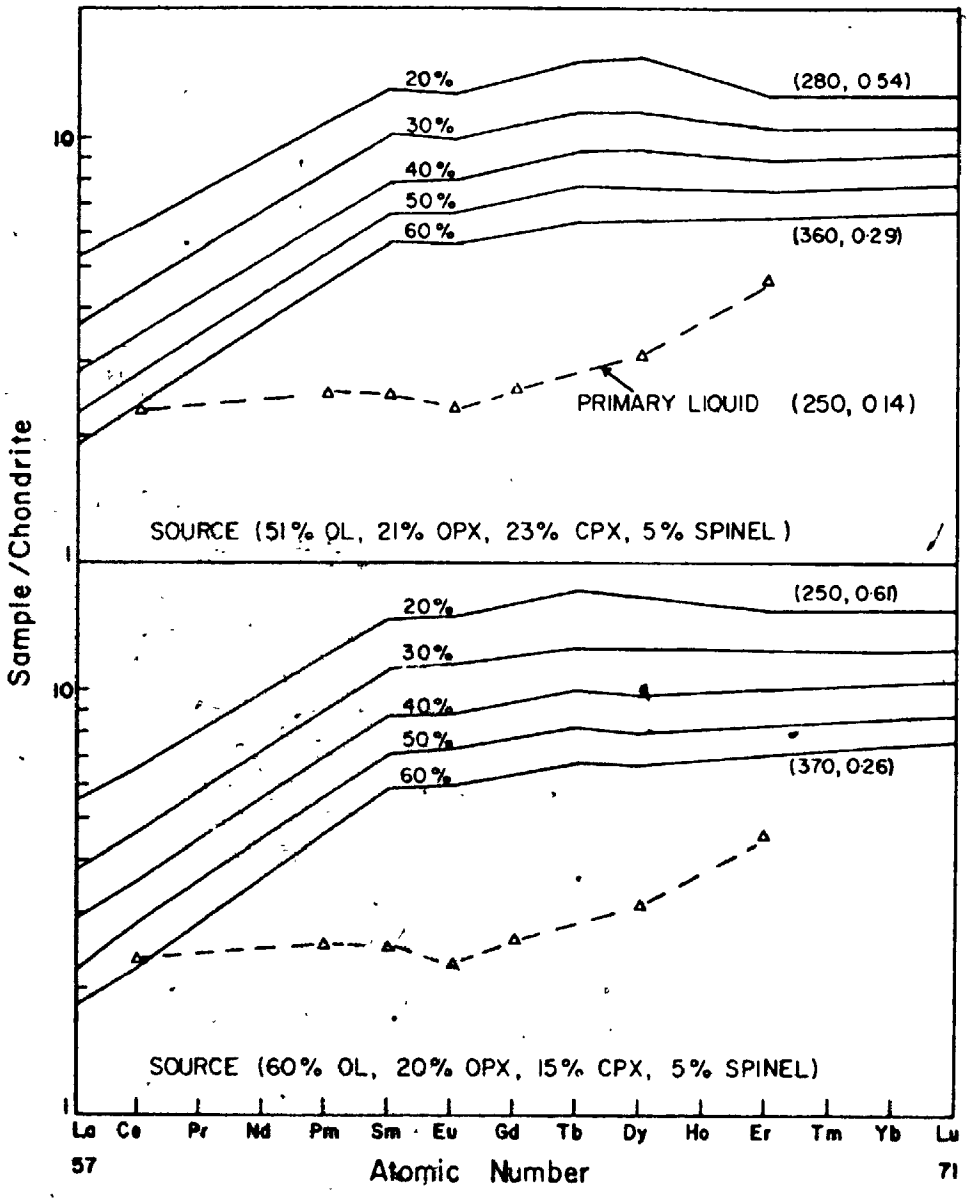

FIGURE 29. REE PARTIAL MELTING MODELS OF TWO PROPOSED MANTLE COMPOSITIONS (SCHILLING, 1975) COMPARED TO OBSERVED REE CONTENTS IN THE BETTS COVE PRIMARY MELT. NUMBERS IN PARENTHESES REFER TO THE CONTENTS OF Ni (PPM) AND TiO_2 (WT. %), RESPECTIVELY. 20 % ETC. REFER TO DEGREES OF PARTIAL MELTING. SEE TEXT FOR FURTHER EXPLANATION.

Thus, it is apparent that the Betts Cove primary liquid cannot be generated by high degrees of partial melting of a Recent oceanic tholeiite source. It is noted that the source postulated for oceanic tholeiites is already depleted in incompatible elements relative to pristine undepleted upper mantle.

An even more depleted source than that for oceanic tholeiite must be the source of the Betts Cove primary liquid. A depleted lherzolite from the Othris ophiolite (Menzies, 1976a) when melted to 30-40% yields Ni concentrations in the liquid similar to contents in the Betts Cove primary liquid. The absolute abundances of the rare earth elements are roughly similar but the pattern is somewhat different (Figure 30a). The TiO_2 contents are between .28 and .36 wt. % - much higher than the 0.14 wt. % in the primary liquid. In fact, because the TiO_2 content of this Othris lherzolite is approx. 0.11 wt. %, greater than 80% partial melting would have to occur before the TiO_2 content of the liquid reaches 0.14 wt. %.

The Betts Cove source material then should have a TiO_2 content less than 0.11 wt. % and be ultramafic in order to produce the low FeO/MgO and high Ni and Cr. Since most of the TiO_2 in ultramafic rocks is in clinopyroxene, the titania content of the whole rock can be reduced by either (1) removing some of the clinopyroxene or (2) decreasing the Ti content of the clinopyroxene. The first alternative implies that the ultramafic rock

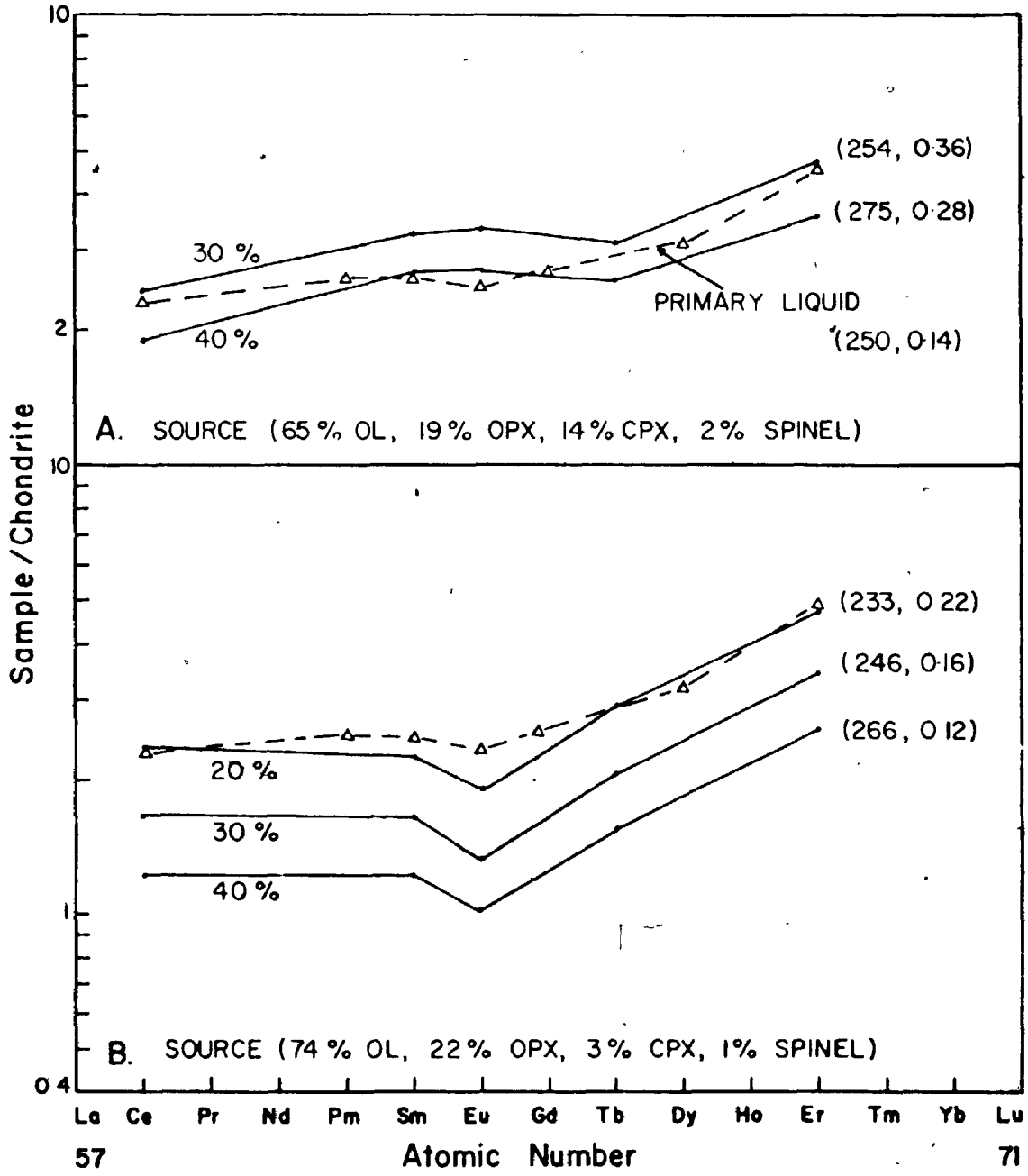

FIGURE 30. CALCULATED REE, NI AND TiO_2 CONTENTS IN LIQUIDS PRODUCED BY PARTIAL MELTING OF LHERZOLITE (A) AND HARZBURGITE (B) FROM THE OTHRIS OPHIOLITE. REE CONTENTS FOR THE TWO SOURCES ARE AVERAGES FROM MENZIES (1976A). DASHED LINE REPRESENTS REE CONTENTS OF THE BETTS COVE PRIMARY LIQUID. OTHER SYMBOLS AS IN FIGURE 29.

approaches harzburgite. Thirty to thirty-five percent partial melting of a typical harzburgitic rock (Ni = 2200 ppm, TiO_2 = .045 wt. %) from the Bay of Islands ophiolite, Newfoundland (Riccio, 1976) does give concentrations of Ti and Ni in the liquid similar to the respective contents in the Betts Cove primary liquid (Figure 30b). Since no rare earth data is available for the Bay of Islands harzburgite, data from harzburgites in the Othris ophiolite (Menzies, 1976a) were used in the partial melting calculations. The calculated rare earth element concentrations in the liquid, at 30 to 35% partial melting of the harzburgite, are lower than the values of REE in the Betts Cove liquid (Figure 30b).

If we assume that the Ni and Ti contents of the Betts Cove material are obtained by 30% partial melting of a harzburgitic rock, then the REE concentrations in this source can be calculated (Figure 31). The calculated concentrations show that the source is depleted in LREE and the absolute abundances lie between measured values for harzburgite and depleted lherzolite.

It is possible that the Ti content of the source rock is low because of a low content of Ti in the clinopyroxenes of a lherzolite. This possibility is, however, remote since to date no pristine lherzolite containing the required low Ti clinopyroxene has been observed anywhere in the world.

In summary, trace element calculations show that the

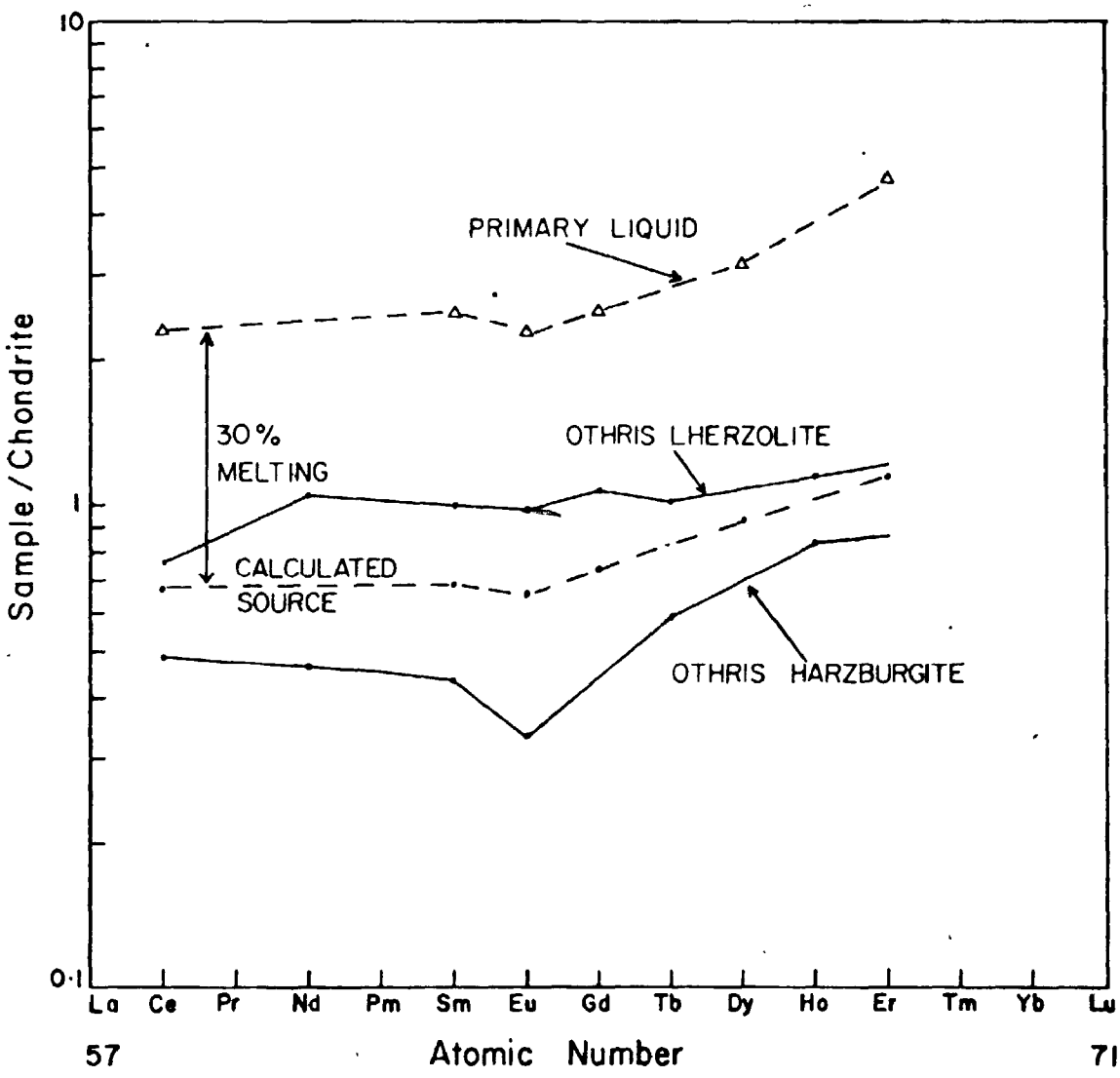

FIGURE 31. CALCULATED REE CONCENTRATIONS IN THE SOURCE WHICH PRODUCED THE BETTS COVE PRIMARY LIQUID COMPARED TO REE CONTENTS IN THE OTHRIS LHERZOLITE AND HARZBURGITE (MENZIES, 1976A).

Betts Cove primary liquid was produced from an upper mantle source more depleted in its incompatible elements than mantle source material postulated for Recent oceanic tholeiite (Schilling, 1975). The Ni and TiO_2 contents of the Betts Cove liquid can be obtained by 30 to 35% partial melting of a harzburgitic rock (Cpx content about 5%). However, the REE contents suggest that the source had REE concentrations similar to depleted lherzolite, rather than harzburgite. Thus, the closest approximation to a source composition which would satisfy Ni, Ti and REE contents in the Betts Cove primary liquid lies between a slightly depleted lherzolite and a harzburgite. It should be noted at this point that there is striking scarcity of REE data for harzburgites and the available data are not of the highest quality. This may account for some of the discrepancy between the Ni and Ti calculations and the REE results for the harzburgite source.

B.3b. Mineral Chemistry and Source Composition

It has been shown in Chapter 3, section A3 that spinels (magnesiochromites) from the most mafic rocks at Betts Cove were unusually high in Cr/Al ratio compared to chromites from very primitive modern ocean floor basalts (Figure 20). Can these differences in Cr/Al ratio be explained if the source of the Betts Cove liquid was harzburgite or severely depleted lherzolite whereas the source for modern ocean floor basalts was relatively un-

depleted lherzolite?

Chromites from ocean floor basalts plot near or within the field of chromites from harzburgites or lherzolites whereas chromites from the Betts Cove mafic rocks plot close to the field of dunitic chromites (Figure 20). Since liquidus chromites from a primary liquid should be in equilibrium with their residue, it is logical to suggest that the residue left after melting of the source for ocean floor basalts was harzburgite whereas the residue was dunitic in the case of the Betts Cove basalts. Mysen and Kushiro (1976) showed that 30% partial melting of a lherzolite will leave a harzburgite residue whereas 25-30% partial melting of harzburgite leaves a dunite residue. Therefore, it is possible that similar degrees of partial melting of a lherzolite and a harzburgitic source, respectively, produced the chemically different chromites in modern ocean floor basalts and the Betts Cove mafic rocks.

The above discussion is valid only if the variations in the Cr/Al ratios in the chromites are principally due to bulk composition and temperature variables of the melt. Other factors which can affect the crystallization of chromite from a mafic liquid are: 1) pressure, 2) oxygen fugacity, 3) the presence or absence of pyroxene as a co-crystallizing phase (Hill and Roeder, 1974; Sigurdsson and Schilling, 1976). The first factor, pressure, apparently does affect the amount of Al entering the

chromite (Sigurdsson and Schilling, 1976); however, the magnitude of the differences in Cr/Al ratio between the Betts Cove and the plotted ocean floor chromites is too great to be solely due to differences in pressure. Furthermore, the major reason for the large observed differences in Cr/Al ratio is the large difference in Cr, and not Al, content of the chromites from the two basalt regions. The effect of oxygen fugacity on chromite crystallization is to vary the total amount of chromite which precipitates but the amount of Cr tied up in the spinel structure may not change (Hill and Roeder, 1974). The third factor is not applicable in the present discussion because in both the Betts Cove basalts and the ocean floor basalts in question, chromites as a probable liquidus phase, crystallized before clinopyroxene. Thus, bulk composition which is intimately related to temperature of melting, is the most important variable causing the high Cr/Al ratios in the Betts Cove chromites.

In summary, the chromite chemistry in the Betts Cove mafic rocks supports the suggestion that these rocks were derived from a severely depleted lherzolite (harzburgitic) source.

C. Fractionation in the Betts Cove Basaltic Rocks

Many specimens of pillow lavas and dykes at Betts Cove exhibit chemical differences from the proposed primary liquid. The variations occur in the contents of

TiO_2, P_2O_5, Zr, Y, Ni, Cr, REE and FeO^t/MgO (Appendix II, Figures 5 to 12). These observed compositional differences may be due to low pressure fractionation. Crystal fractionation in the Betts Cove magma is qualitatively supported by: 1) the occurrence of cumulate ultramafic rocks (Riccio, 1972; Upadhyay, 1973), 2) the occurrence of large phenocryst phases in the lavas and dykes, 3) the observation that the dykes having the highest contents of Ti, FeO^t/MgO, Zr, Y and the lowest Ni and Cr (diabase dykes) cut older more primitive picritic dykes.

To quantitatively test the possibility that the compositional basaltic varieties in the Betts Cove ophiolite can be related by fractional crystallization, equations from Arth (1976) were incorporated into the computer program already utilized for partial melting calculations. There are two commonly used equations which describe the behaviour of trace elements during magma crystallization. The first assumes that equilibrium has been attained between the surface of the crystallizing solid and the liquid (commonly called Rayleigh fractionation) and according to Greenland (1970) may be written as:

$$C_L/C_i = F' \exp(D_s - 1) \qquad (10)$$

where C_L - concentration of trace element in differentiated liquid

C_i - concentration of trace element in primary melt

F' - fraction of the liquid remaining

D_s - Bulk Distribution Coefficient given by

$D_s = W^a K^{a/l} + W^b K^{b/l} + ... + W^n K^{n/l}$ where W^a is the weight fraction of phase a in the precipitating solids and K represents the solid - liquid distribution coefficient for a given trace element.

The second equation describing trace element behaviour during magma crystallization assumes that the total crystallizing solid has equilibrated with the melt. It is expressed as:

$$C_L/C_i = 1/ (F' + D_s(1-F')) \qquad (11)$$

with symbols the same as in equation (10).

A simplifying assumption implicit in both equations is that phases crystallize in constant proportions with constant distribution coefficients. Arth (1976) suggested that the surface equilibrium model (equation (10)) may be appropriate for rapidly cooling, shallowly emplaced magmas whereas the total equilibrium model may better describe slow cooling under plutonic conditions. In the case of the Betts Cove lavas and dykes, surface equilibrium conditions are probably approached.

To model fractionation processes in the Betts Cove mafic material, sample BC-74-101 was chosen as the primary

liquid from which sample BC-73-236, a fine-grained diabase dyke, was derived. Only TiO_2, Ni and the rare earth elements were considered in the calculations. Titanium is treated as a trace element since it occurs only in trace amounts in mineral phases present in the Betts Cove rocks. Cr cannot be considered in the trace element calculations since it occurs as a major component (up to 63 wt. %) in chromite inclusions in olivine. All other elements are either mobile during metamorphic processes or else there is insufficient distribution coefficient data available to allow their use in the calculations.

Various modal proportions of olivine, clinopyroxene, orthopyroxene, spinel, plagioclase and garnet were fractionated from a liquid of BC-74-101 trace element composition. The best fit between calculated trace element abundances and their abundances in BC-73-236 were attained at between 60 and 70% total crystallization with the crystallizing phases in the following proportions: 7-10 wt % olivine, 40-50% orthopyroxene, 15-20 wt % clinopyroxene, 2-3 wt % spinel and 20-30 wt % plagioclase. Figure 32 shows the calculated rare earth concentrations compared with the measured contents of BC-73-236. It is noted that the light rare earth pattern calculated cannot be entirely matched with the observed pattern. This is probably a reflection of the difficulty, already mentioned in partial melting processes, of obtaining accurate estimates of light rare element contents of the primitive

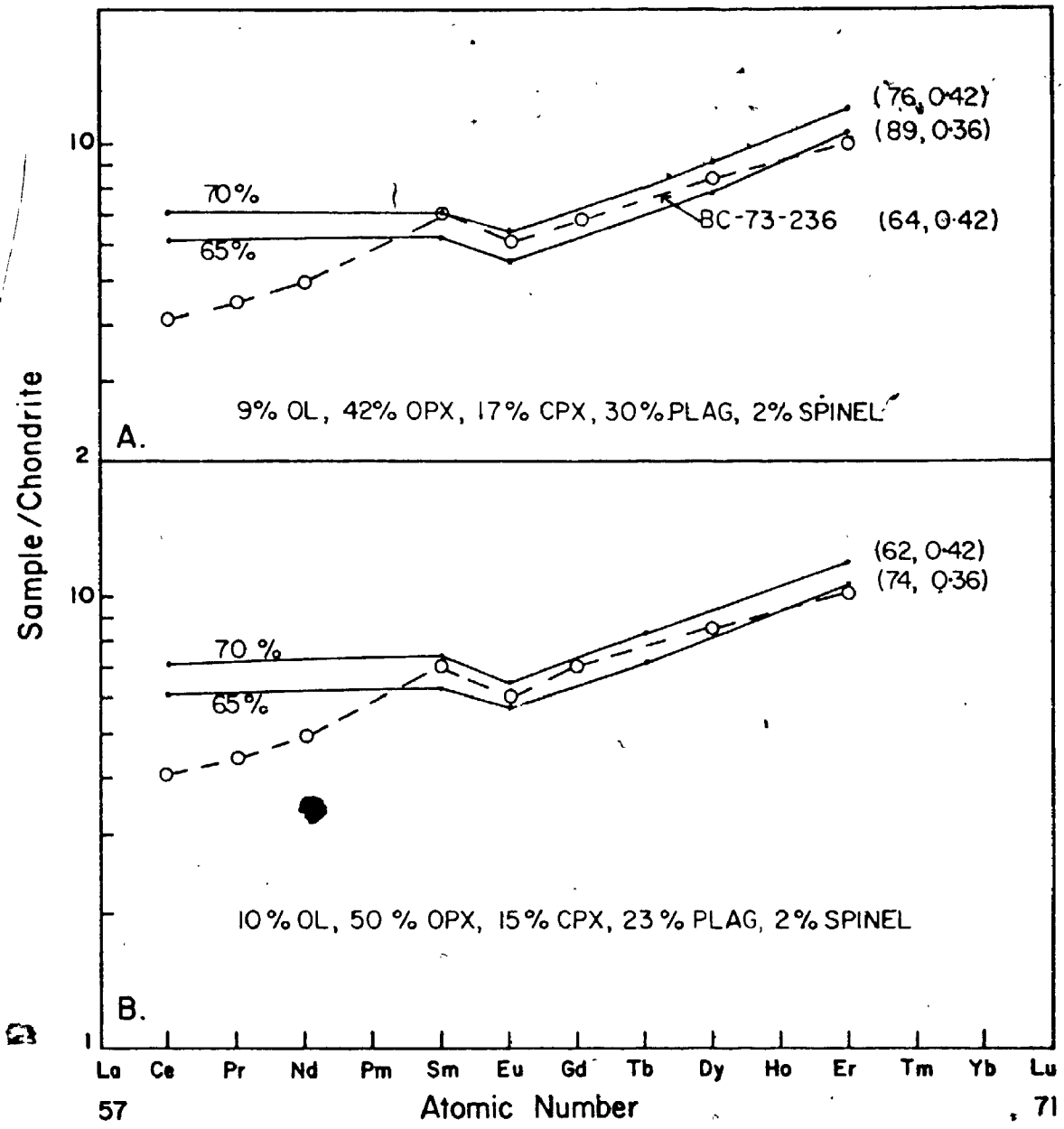

FIGURE 32. TWO MODELS, A AND B, SHOWING CALCULATED (SOLID LINE) REE AND NI, TiO_2 (IN PARENTHESES) CONTENTS OF LIQUIDS FRACTIONATED FROM THE BETTS COVE PRIMARY LIQUID. DASHED-LINE REPRESENTS OBSERVED REE VALUES IN A DIFFERENTIATED BETTS COVE DYKE. % MINERAL REFERS TO % OF THAT MINERAL INVOLVED IN THE TOTAL FRACTIONATION. 65% AND 70% REFER TO THE TOTAL AMOUNT OF CRYSTALLIZATION.

liquid because of the extremely low abundances. Titanium and nickel values in the calculated fractionated liquid correspond approximately to the measured values (Figure 32) and severely limit the amount of clinopyroxene and olivine fractionation.

The above trace element fractionation calculations represent a theoretically possible scheme but are the proposed proportions of minerals fractionated reasonable? If olivine, orthopyroxene, spinel, clinopyroxene and plagioclase are fractionated from the liquid, then cumulates of these minerals should exist. In fact, cumulates of harzburgite, wehrlite, websterite, clinopyroxenite, orthopyroxenite have been described underlying the Betts Cove mafic zone (Riccio, 1972). Also, this work has concluded that some portions of the gabbro and sheeted dyke members are cumulate in origin.

It is surprising that the amount of olivine fractionated is so low since most of the cumulates contain considerable olivine in the ultramafic portion of the ophiolite. The amount of fractionated olivine allowable by the calculations depends upon 1) the concentration of nickel in the primary liquid and in the fractionated liquid and 2) the distribution coefficient of nickel between olivine and liquid. The latter is assumed, for the purpose of simplifying calculations, to remain constant during the total fractional crystallization. However, recent studies (Irvine, 1975; Mysen, 1976) show that this

distribution coefficient can vary with temperature and nickel content of the liquid. A distribution coefficient of 12 was used in the above calculations. A K_D as high as this may have caused an underestimation of the amount of olivine fractionated. Thus, the actual amount of olivine fractionated from the Betts Cove primary liquid may be slightly greater than the calculated amount.

Unfortunately, the trace element fractionation calculations cannot reveal the order in which the above minerals crystallized. Textures, however, suggest that olivine with included chromite crystallized first. These minerals were followed by orthopyroxene, clinopyroxene and finally plagioclase. The late appearance of plagioclase is also suggested by the clinopyroxene and chromite chemistry. In both minerals the Al content increases with fractionation indicators (Figures 18 and 20). This suggests that the Al content of the magma increased during the greater part of the fractionation process and therefore it is unlikely that plagioclase was an early crystallizing phase.

Although the chemical variations in the sheeted dyke and lower pillow lava members can be accounted for by low pressure fractionation, one of the upper pillow lava specimens cannot be related to the primary liquid by fractionation. At the degrees of crystallization (80-85%) required to produce the Ti content of BC-75-5, the calculated REE concentrations are much higher than the observed

values if a starting composition of the Betts Cove primary liquid is used. This statement is supported by the clinopyroxene chemistry (Figure 17). At a given Fe/Mg ratio, the Ti content of the upper lava clinopyroxenes is higher than Ti values in clinopyroxenes from the lower pillows, sheeted dykes and gabbros. It is thus probable that some of the upper pillow lavas represent partial melts of a less depleted source than the underlying members.

D. Petrogenetic Relationships among Stratigraphic Members

It has been proposed that 1) the primary liquid of the Betts Cove basaltic rocks is represented by primitive analyses of the lower pillow lava unit, 2) the picritic dykes of the sheeted dyke unit are equivalent to these lower lavas, 3) the diabase dykes and more fractionated lower lavas can be related to the primary liquid by simple fractionation schemes involving olivine, chromite, orthopyroxene, clinopyroxene and plagioclase in that order of crystallization. Time stratigraphic relationships are consistent with the above interpretations in that the diabase dykes are always later than the picritic dykes and lower lavas. Thus, the sheeted dykes and lower lavas can be related to a single period of magma production from a severely depleted lherzolite source followed by crystal fractionation.

The upper pillows, however, are probably not derived from the same liquid which produced the sheeted dykes and

lower lavas. This is suggested by: 1) the failure, using crystal fractionation calculations, to satisfy the Ni, Ti and REE concentrations of sample BC-75-5, an upper pillow lava, by differentiation of the primary liquid (this chapter, section C), 2) the difference in whole rock chemistry between the upper lavas and lower ophiolitic members as revealed in the Ti-Zr-Y diagram (Figure 8) and more significantly in the FeO^t/MgO versus TiO_2 diagram (Figure 9). In the latter diagram, it is observed that at a given FeO^t/MgO ratio, the TiO_2 content of the upper lavas is slightly higher than Ti contents of the sheeted dykes and lower lavas, 3) the higher Ti content, at a given Fe/Mg ratio (Figure 18), of clinopyroxenes from the upper lavas compared to Ti values in lower member clinopyroxenes. The different chemistry of the upper lava member is probably a reflection of a minor change in the source composition toward a less depleted lherzolite.

The perknites of the sheeted dyke member are cumulates. Presently composed of actinolite-chlorite-clinopyroxene ± albite, they were probably originally made of clinopyroxene and olivine with minor plagioclase (Chapter 2), and as such can be classified as plagioclase-bearing olivine clinopyroxenites. The cumulate origin is indicated by their extremely low TiO_2, Al_2O_3 and FeO^t/MgO and high Ni and Cr and the occurrence of clinopyroxenes with rims rich in FeO/MgO and TiO_2 surrounding homogeneous cores low in Ti, Al, and FeO/MgO (Appendix III, Table I,

analyses 68d, e, f, g). The rims possibly represent adcumulate growth.

The perknite material, although concentrated near the base of the sheeted dyke complex, is also found in lesser amounts at higher structural levels in the ophiolite. Because the dyke-like bodies of perknite material never exhibit chilling and appear to be of cumulate origin, it seems likely that the perknite material represents the country rock into which the picritic and diabase dykes were intruded. The precipitation of this perknite material probably represents the end stage of ultramafic cumulate formation (Riccio, 1972).

As already mentioned in Chapter 1, the sheeted dyke complex (and consequently the perknite rocks) is separated from the main body of ultramafic cumulates by a gabbro/clinopyroxenite member (Figure 4). Also, the gabbro/clinopyroxenite member is intruded by picritic dykes (Plate 1F). Therefore, it is likely that a gabbro magma was injected into the upper portions of the ultramafic cumulates prior to or during the emplacement of dykes in the sheeted complex.

Thus, there is a hiatus between the ultramafic cumulate and gabbro formation, and also between gabbro emplacement and the intrusion of the sheeted dykes and extrusion of the lower pillow lavas. The upper lavas were then extruded without there being any apparent related dyke injection in the sheeted complex.

E. Geochemistry and Tectonic Setting of the Betts Cove Ophiolite

E.1. Introduction

Classification schemes relating the chemistry of volcanic rocks to their tectonic mode of origin (Pearce and Cann, 1971, 1973; Miyashiro, 1973, 1975a, b, c; Miyashiro and Shido, 1975) have been devised using statistical compilations of chemical data from known modern tectonic environments. Application of these classification schemes to ancient volcanic rocks has led to considerable controversy. This is especially true in the attempts which have been made to distinguish oceanic volcanics from those found in island arcs. The Troodos ophiolite of Cyprus, which has long been considered a classic remnant of oceanic crust (Moores and Vine, 1971), has been re-interpreted on the basis of the chemistry of the volcanic effusive and intrusive rocks as having formed in an island arc (Miyashiro, 1973). Likewise, it has recently been suggested that the chemistry of the Betts Cove pillow lava and dyke rocks has "island arc affinity" (Upadhyay and Neale, 1976). However, the indiscriminant use of whole rock chemistry to delineate tectonic environment has been criticized (Hynes, 1975; Moores, 1975; Gass et al., 1975; Church and Coish, 1976). In the following sections, an analysis is presented of the applicability of some of the chemical criteria commonly used.

E.2. SiO_2 versus FeO^t/MgO Diagrams

Miyashiro (1973, 1975a) used the variation of silica against FeO^t/MgO (an indication of the degree of fractionation) to separate tholeiitic from calc-alkaline magmas (Figure 33). On this plot, many analyses of basaltic rocks from both the Betts Cove and Troodos ophiolites lie, at low FeO^t/MgO ratios, within the calc-alkaline field, thus suggesting that the ophiolites originated in an island arc. However, it is apparent that silica has been introduced into the high MgO, Ni and Cr basalts at Betts Cove (Coish, 1977; Chapter 4) and the seeming calc-alkaline affinity (Figure 33) is the result of silica metasomatism. Because of the ease with which silica moves during low grade alteration, the SiO_2-FeO^t/MgO diagram cannot therefore be used to discriminate calc-alkaline from tholeiitic environments.

Furthermore, it is difficult at high silica and FeO^t/MgO ratios to distinguish calc-alkaline from tholeiitic differentiates. This is illustrated by some analyses of gabbros and spatially associated trondhjemites in the Bay of Islands (Blow-Me-Down) ophiolite. Differentiation of the gabbroic magma begins in the tholeiitic field at low SiO_2 and FeO^t/MgO values. With increasing fractionation, silica and FeO^t/MgO values both increase up to a FeO^t/MgO ratio of 6 after which silica continues to increase but FeO^t/MgO decreases. The decrease in FeO^t/MgO is accompanied by decreases in the contents of titanium,

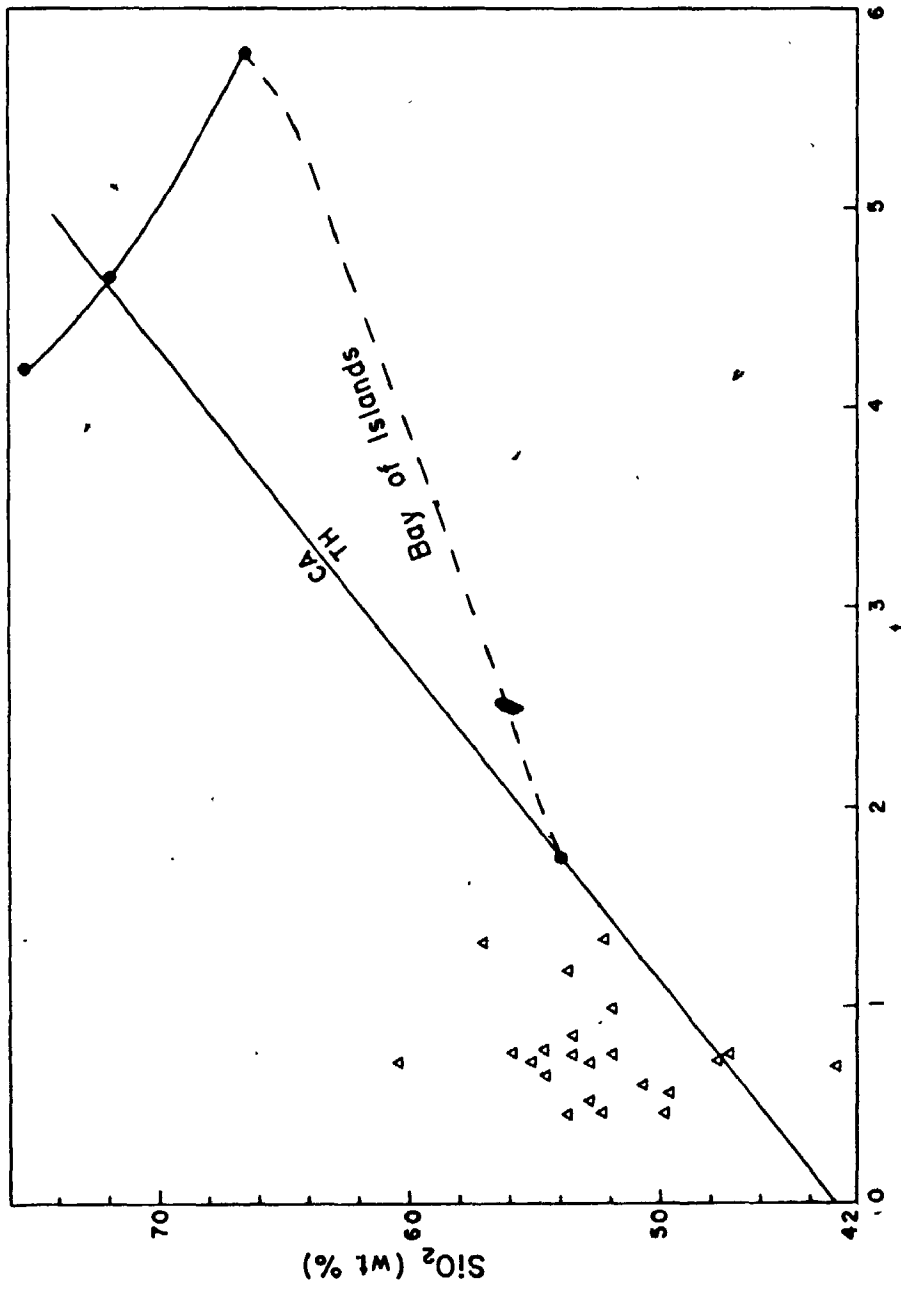

FIGURE 33. SiO_2 - FeO^T/MgO VARIATION DIAGRAM SHOWING FIELDS OF CALC-ALKALINE (CA) AND THOLEIITIC (TH) ROCKS (MIYASHIRO, 1973). ALSO SHOWN ARE THE BETTS COVE BASALTIC ROCKS (Δ) AND THE BAY OF ISLANDS GABBRO-TRONDHJEMITE SUITE (●).

zirconium and the alkali elements due to the fractionation of titaniferous magnetite, zircon and alkali feldspar (Church and Coish, 1976). Because of the decrease in FeO^t/MgO at the late stages of fractionation, the differentiation line moves from the tholeiitic field into the calc-alkaline field on the SiO_2 versus FeO^t/MgO diagram (Figure 33). The arbitrary line separating calc-alkaline from tholeiitic lineages is thereby invalidated.

E.3. Titanium Variation Diagrams

Titanium has been extensively used in combination with other immobile elements (Ti-Zr, Ti-Zr-Y, Ti-Zr-Sr, Ti-Cr, and TiO_2-FeO^t/MgO) to distinguish tectonic environments of basalts (Pearce and Cann, 1971, 1973; Miyashiro and Shido, 1975; Pearce, 1975). Oceanic tholeiite, island arc tholeiite, calc-alkaline basalts and within-plate basalts are differentiated using the above parameters (Figures 7, 8, 9).

On the Ti-Zr and Ti-Zr-Y diagrams (Figures 7 and 8), most of the Betts Cove basalts plot outside all tectonic fields but lie close to the field of low-K island arc tholeiites. The Troodos ophiolitic rocks also plot in the low-K tholeiite field (Pearce, 1975). On this basis, it has been suggested that these ophiolites are of island arc origin (Miyashiro, 1973, 1975a, b, c). However, the low TiO_2 characteristics of the Betts Cove and Troodos ophiolites are not necessarily diagnostic of an island

arc environment. Typically, island arc tholeiites have lower TiO_2 contents than oceanic tholeiites but there are notable exceptions to this generalization. Low TiO_2, FeO^t/MgO basalts have recently been recovered from drilling of the ocean floor and analyses of clinopyroxenes from some of the drill core reveals that titanium contents are sometimes lower than contents from clinopyroxenes found in island arc basalts (Church and Coish, 1976). Thus, the low Ti contents of the Betts Cove and Troodos ophiolites do not preclude their origin at a mid-ocean ridge. In fact, it is now apparent that, in both modern ocean crust and ophiolitic complexes, the titanium content of the basaltic rocks varies considerably (Church and Coish, 1976; Menzies, 1976b). This variation can be explained by variable degrees of partial melting of the same source material or by melting of different source compositions in the same tectonic environment (Chapter 5, Section C).

The titanium variation diagrams are therefore not effective discriminants with regard to tectonic environment because the behaviour of elements used in their construction (Ti, Zr, Y and Cr) may be related to variations in the composition of sub-oceanic mantle sources as much as to processes involved in the development of island arcs.

A.4. Internal Stratigraphy of Ophiolites

The typical section of an ophiolite - depleted upper mantle overlain by ultramafic cumulates, mafic cumulates,

massive gabbro, sheeted dykes and pillow lavas - has been matched with the stratigraphy of modern ocean crust both by detailed geophysical surveys (Christensen and Salisbury, 1975; Riccio, 1976) and by dredge sampling of ocean crust exposed in fracture zones (Engel and Fisher, 1975). There is therefore general agreement that ophiolites have a similar stratigraphy to the structure of modern ocean crust. However, the sub-surface structure of island arcs is little known, and, therefore, some authors have conjectured that sub-volcanic island arc structure may also be similar to ophiolite stratigraphy (Miyashiro, 1973, 1975a; Brock, 1974).

There are two aspects of ophiolite stratigraphy, however, which are difficult to explain in an island arc setting:

1) beneath the pillow lava unit, sheeted dykes consisting of up to 100% dykes occur over lateral distances of several kilometers. Their existence implies that considerable lateral spreading has taken place, a feature consistent with ophiolite formation at oceanic ridges where hundreds of kilometers of lateral movement are accommodated. Miyashiro (1973, 1975a) argued that beneath island arc volcanoes, sheeted complexes might also occur. These dykes, however, are limited in lateral extent to the widths of individual volcanoes and often have radial areal distribution patterns. Thus, dyke complexes beneath island arc volcanoes should be readily distinguishable

from sheeted complexes formed at mid-ocean ridges where continuous spreading results in uniform orientation of dykes;

2) the lowermost unit in some ophiolites has been interpreted as mantle tectonites representing the depleted residue after partial melting to produce the basaltic portion of the ophiolite (Moores and Jackson, 1974; Riccio, 1976; Church and Riccio, 1977). Mantle rocks directly overlain by cumulate rocks followed by dyke and pillow lava members are difficult to explain if the ophiolite formed in an island arc environment. Volcanic arcs are built on oceanic crust or on continental crust. Thus, if ophiolites represent island arc tectonic processes, the magmatic part will be underlain by oceanic or continental crust. However, mantle rocks usually underlie cumulates in ophiolites and short of evoking the existence of an erosional unconformity between the mantle and overlying cumulates, an 'oceanic type' ophiolitic sequence of rocks is unlikely to form in an island arc.

In summary, although the chemistry of some ophiolites is similar to the chemistry of island arc tholeiites, the internal stratigraphy of ophiolites is only compatible with an origin at oceanic spreading centres.

F. Comparison with the Blow-Me-Down Ophiolite and Significance of Regional Variations in the Newfoundland Ophiolites

Variations in the internal stratigraphy and chemistry of ophiolites throughout the world have been ascribed to differing tectonic environments of origin (Miyashiro, 1973, 1975; Christensen and Salisbury, 1975), to different degrees of partial melting of similar source compositions (Menzies, 1976b) and to different spreading rates at mid-ocean ridges (Christensen and Salisbury, 1975; Church and Riccio, 1977). With respect to the Betts Cove and Blow-Me-Down ophiolites, however, differences in their internal stratigraphy and geochemical characteristics can be explained perhaps best in terms of varying degree of partial melting of different source compositions combined with changes in spreading rate. It is suggested that the above variations are related to the timing of formation of oceanic crust in the opening of the proto-Atlantic ocean.

The geographical position of the Blow-Me-Down ophiolite in relation to that of Betts Cove suggests that the western Newfoundland ophiolites may have originated early in the development of the proto-Atlantic with the Betts Cove ophiolite having been produced at a slightly later time. If the two ophiolites were originally part of the same sheet of ocean crust, the most westerly portion of the oceanic crust would be nearest the North American continent and thus would have been produced in the early

stages of splitting of the continent. The more easterly portions of the oceanic crust (at least the portions west of the mid-ocean ridge) would have been formed as spreading continued and the proto-Atlantic widened. It is proposed that the different stages (i.e. early versus late) in the opening of the proto-Atlantic resulted in variations of spreading rate and differences in the composition of the available source material for melting. These factors in turn resulted in the stratigraphic and geochemical differences between the Blow-Me-Down and Betts Cove ophiolites.

The spreading rate at the time of initiation of formation of the proto-Atlantic may have been slow due to the reluctance of the continental mass to split. The slow spreading rate would encourage slow cooling of magma chambers and any cumulate minerals would have ample time for adcumulate growth, thereby using up interstitial liquid. On the other hand, once ocean crust formation has begun, an increase in spreading rate is possible because gravitational forces in addition to thermal forces move the oceanic plate. Fast spreading would inhibit the formation of thick upper oceanic crust (Lister, 1977). Also, fast cooling is associated with fast spreading since any small magma chambers are removed quickly from the central heat source. Fast cooling would prevent significant adcumulate growth but instead interstitial liquid would be frozen between the cumulus minerals. The latter

situation of fast spreading can be applied to the Betts Cove ophiolite whereas the former slow spreading process can explain some physical features of the Blow-Me-Down ophiolite (Church and Riccio, 1977).

Differing rates of spreading cannot account for the differences in order of crystallization of cumulus minerals or differences in the chemistry of the intrusive and extrusive rocks between the Blow-Me-Down and Betts Cove ophiolites. Rather, it is proposed that different source compositions will upon melting yield the observed mineralogical and chemical differences in the Newfoundland ophiolites.

It has already been shown that the high Ni, Cr and low Ti, Zr, Y and FeO^t/MgO Betts Cove primary basalts were derived from a severely depleted lherzolite. The Blow-Me-Down basalts, however, are more enriched in Ti, Zr, Y and FeO^t/MgO and more depleted in Ni and Cr and by analogy with modern oceanic basalt, its source was probably slightly depleted lherzolite (Schilling, 1975). If, as suggested above, the Blow-Me-Down ophiolite formed early in ocean basin development, then the source for the ophiolitic magma is liable to be lherzolitic mantle material depleted in incompatible elements as a result of small degrees (5%) of partial melting. Extraction of basaltic liquid from such material will leave a residue approaching harzburgite in composition. This residue, initially formed in the low velocity zone, is probably convected to

the base of the ocean crust in a manner described by Church and Riccio (1974). If the path of the convecting residue takes it into the zone of intense magma collection beneath the mid-ocean ridge, the solidus temperature of the residue may be exceeded and it may undergo partial melting. This melting episode would naturally be later than the time of initiation of rifting and could give rise to magmas of the type found in the Betts Cove ophiolite. This does not mean that all partial melts in these later stages of ocean crust development will be from a harzburgitic source since in addition to harzburgite, lherzolite in the low velocity zone is still available for melting.

Can the different order of crystallization of cumulus minerals between the two ophiolites also be related to the proposed different sources? To answer this question it is necessary to consider the effect of initial bulk composition on crystallization sequences. Firstly, it is expected that partial melts from a lherzolite (Blow-Me-Down) will be enriched in CaO and Al_2O_3 relative to partial melts from a severely depleted lherzolite source (Betts Cove). This is because undepleted lherzolite contains more clinopyroxene and Al-spinel. In terms of mineral phases, a lherzolite partial melt will be enriched in plagioclase relative to a melt from a source approaching harzburgite in composition.

In Figures 34 and 35, two bulk compositions with different plagioclase contents are crystallized in the

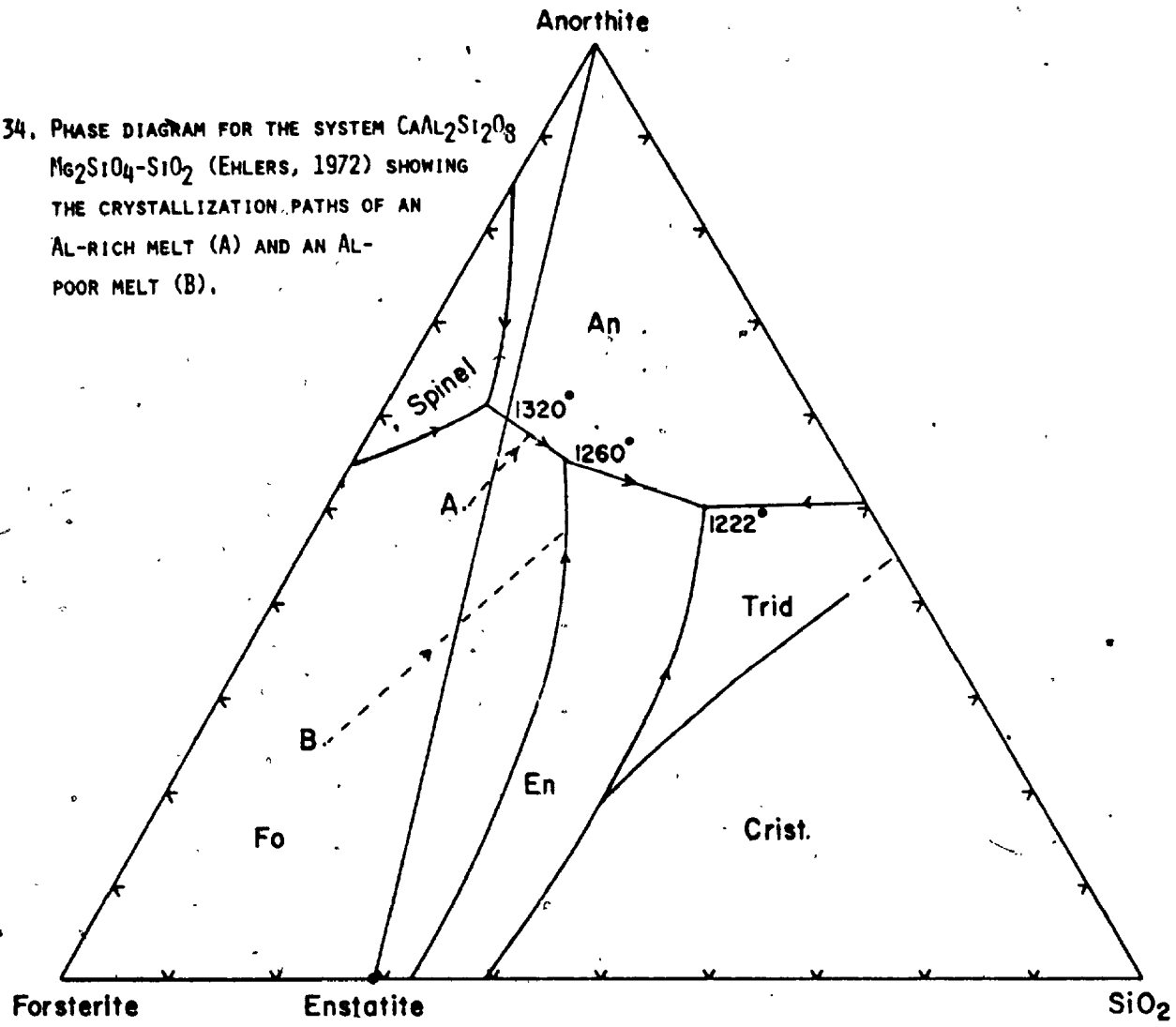

FIGURE 34. PHASE DIAGRAM FOR THE SYSTEM $CaAl_2Si_2O_8$ Mg_2SiO_4-SiO_2 (EHLERS, 1972) SHOWING THE CRYSTALLIZATION PATHS OF AN AL-RICH MELT (A) AND AN AL-POOR MELT (B).

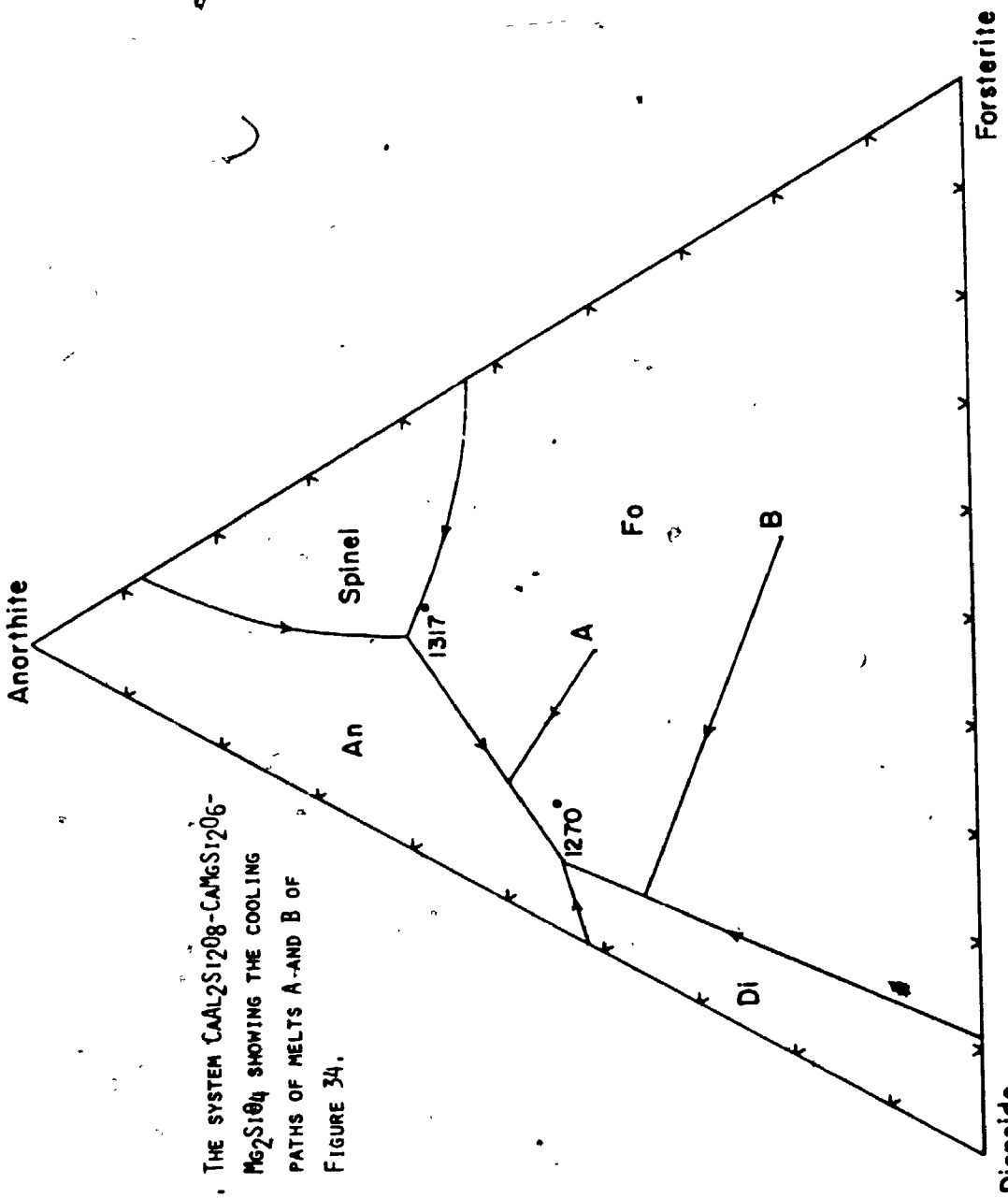

FIGURE 35. THE SYSTEM $CaAl_2Si_2O_8$-$CaMgSi_2O_6$-Mg_2SiO_4 SHOWING THE COOLING PATHS OF MELTS A AND B OF FIGURE 34.

system anorthite, diopside, silica, forsterite. In the case of bulk composition A - rich in anorthite component - crystallization begins with the precipitation of olivine driving the liquid composition away from the forsterite end member. The path of the liquid leads to the olivine-plagioclase cotectic where plagioclase also crystallizes. Olivine and plagioclase are joined by clinopyroxene at 1270°C (Figure 35) and shortly after by orthopyroxene at 1260°C (Figure 34). The order of crystallization is then olivine-plagioclase-clinopyroxene-orthopyroxene - similar to that observed in the Blow-Me-Down cumulates (Church and Riccio, 1977). For a liquid of composition B (low in anorthite component), olivine is again the first mineral to precipitate. The liquid then proceeds to the reaction boundary (Figures 34 and 35) with orthopyroxene and the cotectic with clinopyroxene before it precipitates plagioclase. Thus, a crystallization sequence olivine-orthopyroxene-clinopyroxene-plagioclase can be produced. This is the Betts Cove crystallization order (Church and Riccio, 1977). A point in support of the Blow-Me-Down being a more An rich composition than the Betts Cove liquid is the average higher Al_2O_3 content of the Blow-Me-Down lower lavas, dykes and gabbros (Table 8).

In summary, the igneous differences of internal stratigraphy, bulk composition and crystallization order between the Blow-Me-Down and Betts Cove ophiolites can be

TABLE 8

Average compositions for the Betts Cove and Blow-Me-Down ophiolites, Newfoundland.

	BETTS COVE				BLOW-ME-DOWN			
Wt. %	1	2	3	4	1	2	3	4*
SiO_2	50.53	51.78	53.69	51.19	41.02	47.93	48.40	47.34
TiO_2	0.54	0.26	0.24	0.08	1.21	1.48	1.19	0.46
Al_2O_3	15.91	13.92	14.26	17.05	14.86	14.56	15.84	18.82
Fe_2O_3	4.22	1.99	1.79	1.82	7.03	3.25	2.71	1.53
FeO	4.12	5.91	6.24	4.27	3.61	6.58	6.68	4.64
MnO	0.16	0.17	-	0.16	0.23	0.19	0.21	0.16
MgO	8.74	11.21	8.84	9.37	7.96	6.81	7.45	7.91
CaO	4.95	9.07	6.61	7.15	10.52	7.62	9.24	13.35
Na_2O	3.18	2.68	3.67	3.11	2.94	4.45	3.16	2.38
K_2O	2.48	0.20	.18	1.55	0.82	0.06	0.56	0.08
P_2O_5	0.04	0.02	0.03	0.02	0.09	0.14	0.11	0.01
L.O.I.	4.71	3.70	3.57	3.85	9.70	6.34	4.14	3.38
FeO^t/MgO	1.06	.69	.89	.63	1.24	1.40	1.22	.76
ppm								
Ni	94	202	80	128	460	75	77	117
Cr	282	540	243	251	806	267	286	402
Zr	29	15	16	5	73	108	79	5
Y	12	8	11	8	26	32	30	10
Sr	118	117	102	180	333	206	300	212
Rb	33	2	4	12	13	2	5	1
Ba	92	28	33	94	539	212	39	10

1 - Upper Pillow lavas, 2 - Lower Pillow lavas, 3 - Diabase Dykes, 4 - Gabbro.

L.O.I. - Loss on Ignition.

FeO^t - Total iron as FeO.

* - Average excludes ilmenite gabbro.

explained if the Blow-Me-Down ophiolite formed at an early stage in ocean crust development where spreading was slow and the source material was lherzolite and the Betts Cove ophiolite formed later when spreading was faster and at least some of the source available for partial melting was severely depleted lherzolite.

The more intense metasomatic activity which has occurred at Betts Cove as compared to Blow-Me-Down, if associated with vigorous hydrothermal activity, may also be related to differing rates of spreading. Fast spreading produces a thin crust overlying a hot magma chamber as opposed to slow spreading where a thicker crust overlies a smaller, cooler magma chamber (Lister, 1977). The thin crust is more susceptible to small scale fracturing than the thick crust. Secondly, higher heat flow at fast spreading ridges provides a greater heat supply to drive the convective system and thirdly, magma chambers at fast spreading ridges are probably of greater lateral extent than at slow spreading ridges. The heat source, at fast spreading ridges, is therefore more extensive, and hydrothermal circulation is active at greater distances from the ridge axis than is the case under conditions of slow spreading when magma chambers may be of limited lateral width.

APPENDIX I

LIST OF ANALYZED SPECIMENS AND THEIR LOCALITIES

A list of analyzed specimens from both the Betts Cove and Blow-Me-Down ophiolites is presented in Appendix I. Analysis number corresponds to the numbering system adopted in following appendices for whole rock analyses (Appendix II) and mineral analyses (Appendix III). In the field number, the locality (BC - Betts Cove, BMD - Blow-Me-Down), the year (73, 74, 75) and the specimen number are listed. Also the position of the analyzed sample in the ophiolite is given under the heading 'Stratigraphic Member'. The exact location of the samples can be obtained from the accompanying locality maps for each ophiolite. Thin section and probe section numbers refer to numbers which appear on the appropriate section. The numbers in parentheses after the probe section number refer to the minerals probed in that specimen according to the following code: 1 - Clinopyroxene, 2 - Chromite, 3 - Epidote, 4 - Actinolite, 5 - Chlorite, 6 - Plagioclase, 7 - Sericite, 8 - Rodingitic alteration. For example, in analysis number 10 (Field number BC-74-101B, Probe Section # 6822), clinopyroxene and epidote minerals were probed.

APPENDIX I, TABLE I

LIST OF ANALYZED SAMPLES FROM BETTS COVE AND BLOW-ME-DOWN OPHIOLITES

Analysis #	Field #	Thin Section #	Stratigraphic Member	Probe Section #
1	BC-74-90	5286	Upper Pillow Lava	5299 (1, 3, 4)
2	BC-75-5	6831	"	
3	BC-75-4	6830	"	
4	BC-75-3		"	
5	BC-75-2	6829	"	
6	BC-75-1		"	
7	BC-73-58		Lower Pillow Lava	4185 (3, 6)
8	BC-73-238	4153	"	
9	BC-74-101A	5260	" (Rim)	6821
10	BC-74-101B	5261	" (Core)	6822 (1, 3)
11	BC-74-55	5262	"	6823
12	BC-74-57	5264	"	6824
13	BC-74-58A	5265	" (Rim)	
14	BC-74-58B	5266	" (Core)	
15	BC-74-60	5267	"	
16	BC-74-37A	5283	" (Rim)	
17	BC-74-37B	5284	" (Core)	
18	BC-74-61A		" (Rim)	
19	BC-74-61B		" (Core)	

APPENDIX I, TABLE I (Cont'd)

Analysis #	Field #	Thin Section #	Stratigraphic Member	Probe Section #
20	BC-74-45	5253	Lower Pillow (Rim)	
21	BC-74-46		" (Intermediate)	
22	BC-74-47	5254	" (Core)	
23	BC-74-29	5280	"	5289 (1)
24	BC-73-242	4143	Diabase Dyke	
25	BC-73-59	4167	"	
26	BC-73-57	4162	"	5287 (1, 5, 6)
27	BC-73-84	3979	"	
28	BC-73-236	4124	"	
29	BC-73-239	4137	"	
30	BC-73-254		"	4102
31	BC-73-256		"	4103 (1)
32	BC-73-257		"	4104
33	BC-73-258		"	4105
34	BC-73-259		"	4106
35	BC-73-260		"	4107 (1)
36	BC-73-261		"	4108
37	BC-74-23	5293	" (Margin)	
38	BC-74-24	5294	" (Centre)	
39	BC-73-163	4141	"	
40	BC-73-72	3977	"	

APPENDIX I, TABLE I (Cont'd)

Analysis #	Field #	Thin Section #	Stratigraphic Member	Probe Section #
41	BC-73-97	4118	Diabase Dyke	
42	BC-73-38	4171	"	4171
43	BC-73-73	3986	"	
44	BC-73-131	4127	"	
45	BC-73-230	4122	"	
46	BC-74-28	5279	Picritic Dyke	5288 (1)
47	BC-73-141	4148	"	5275 (1, 2, 5)
48	BC-73-67	3975	"	
49	BC-73-88	3982	"	
50	BC-73-47	7347	"	
51	BC-73-143	4128	"	
52	BC-73-149	4145	"	
53	BC-73-185	4152	"	
54	BC-73-207	4121	"	
55	BC-74-17	5290	" (Margin)	5290
56	BC-74-18	5291	" (Int.)	5291
57	BC-74-19	5292	" (Centre)	
58	BC-75-12		"	
59	BC-73-178	4130	Perknite Rock	
60	BC-73-46	7346	"	

APPENDIX I, TABLE I (Cont'd)

Analysis #	Field #	Thin Section #	Stratigraphic Member	Probe Section #
61	BC-73-21	4164	Perknite Rock	
62	BC-73-22	4163	"	
63	BC-73-161	4146	"	
64	BC-73-167	4151	"	4151 (3)
65	BC-73-169	4125	"	
66	BC-73-174	4142	"	
67	BC-73-191	4135	"	
68	BC-73-61	4858	"	5274 (1)
69	BC-73-17	4198	Gabbro	4198 (3, 7)
70	BC-73-33	4179	"	4179 (1)
71	BC-73-5	4196	"	
72	BC-73-90	4188	"	4188
73	BC-73-64	3978	"(Rodingitic)	4861 (1)
74	BC-73-216	4150	Rodingitic Dyke	
75	BC-73-234	4149	Post-ophiolite Dyke	6828
76	BMD-73-16	4417	Upper Pillow Lava	6826
77	BMD-75-25		"	
78	BMD-75-30		Lower Pillow Lava	
79	BMD-75-31		"	
80	BMD-75-32		"	

APPENDIX I, TABLE I (Cont'd)

Analysis #	Field #	Thin Section #	Stratigraphic Member	Probe Section #
81	BMD-75-33		Lower Pillow Lava	
82	BMD-73-2	5269	Diabase Dyke	
83	BMD-73-6	4425	"	
84	BMD-73-8	5270	"	
85	BMD-73-10	4422	"	
86	BMD-73-11	4421	"	
87	BMD-73-13	4419	"	
88	BMD-73-28	5271	"	
89	BMD-73-32	5272	"	
90	BMD-73-33	5273	"	6827 (1)
91	BMD-75-28		"	
92	BMD-75-36		"	
93	BMD-73-23		"	
94	BMD-75-35		"	
95	BMD-75-15		"	
96	BMD-75-16		"	
97	BMD-75-19		"	
98	BMD-73-20	4875	" (Cuts Gabbro)	
99	BMD-75-1		" "	
100	BMD-75-39		" "	

APPENDIX I, TABLE I (Cont'd)

Analysis #	Field #	Thin Section #	Stratigraphic Member	Probe Section #
101	BMD-75-6		Diabase Dyke (Cuts Gabbro)	
102	BMD-75-40		Gabbro (Foliated)	
103	BMD-75-4		" (Massive)	
104	BMD-75-7		" (Layered)	
105	BMD-75-34		" (Massive)	
106	BMD-75-22		Ilmenite Gabbro	

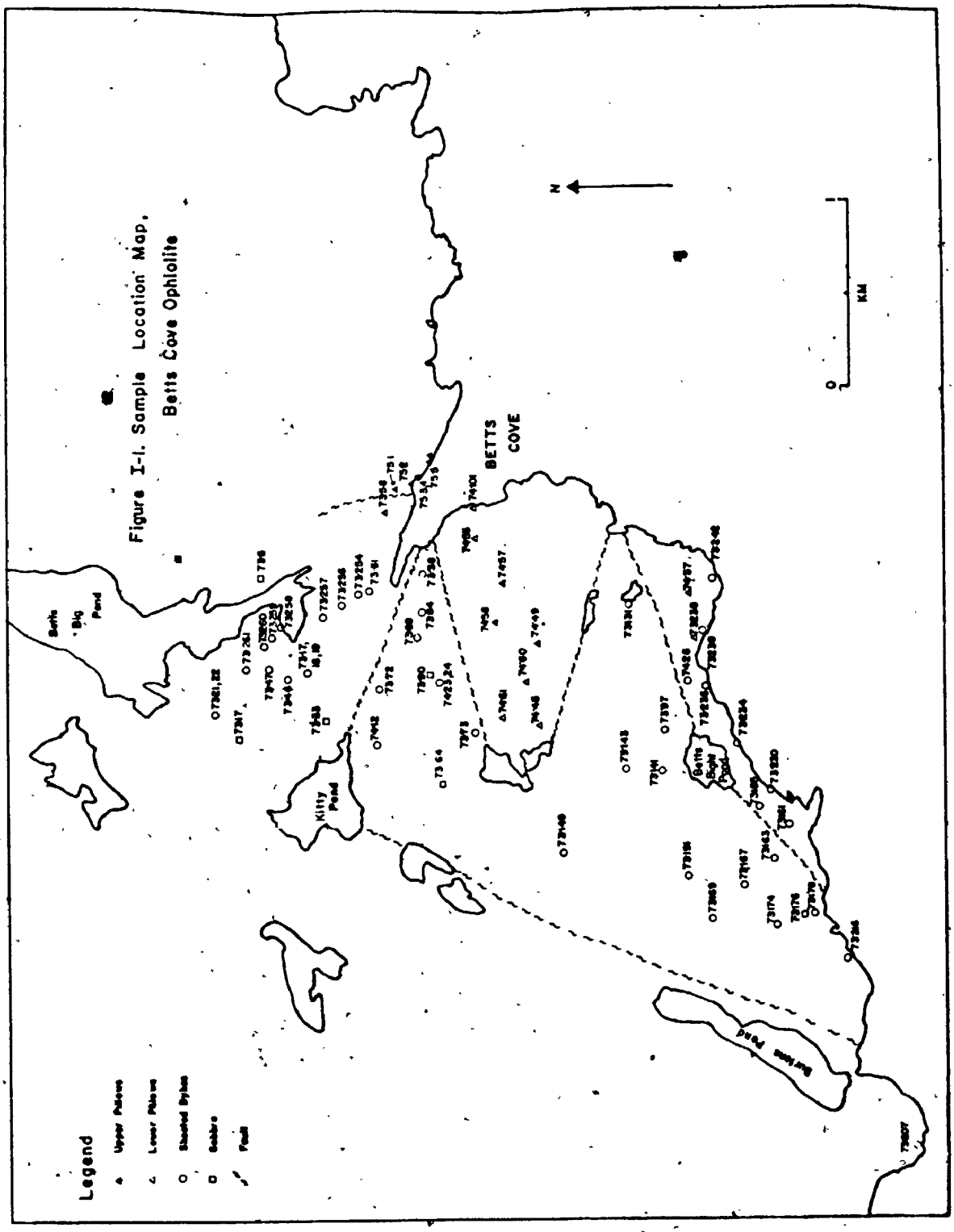
Figure I-1. Sample Location Map,
Betts Cove Ophiolite
BETTS
COVE
Kitty
Pond
Big
Pond
N
KM
0
Legend
Upper Pillows
Lower Pillows
Sheeted Dykes
Gabbro
Fault

APPENDIX II. TABLE I (Cont'd)

	24$	25	26	27	28	29	30	31	32	33	34
SiO_2	57.15	55.79	54.54	51.75	51.76	53.57	50.98	50.87	54.40	56.02	52.47
TiO_2	.34	.16	.19	.21	.42	.35	.14	.14	.14	.10	.10
Al_2O_3	15.28	12.85	14.11	15.52	16.10	14.35	13.25	12.64	13.42	13.76	14.49
Fe_2O_3	9.20*	.73	.02	1.03	2.91	1.82	8.53*	8.56*	1.29	1.54	1.80
FeO	–	6.62	7.38	7.22	5.04	5.50	–	–	6.44	6.80	6.62
MnO	.22	.14	.14	.16	.15	.14	.18	–	.18	.17	.17
MgO	6.03	9.31	9.15	9.82	7.84	8.04	12.60	13.40	10.04	9.36	12.17
CaO	5.93	5.27	5.30	5.39	7.57	9.07	6.71	6.11	4.60	3.39	4.02
Na_2O	5.78	3.16	3.44	3.53	3.95	4.27	3.01	1.63	3.13	2.87	3.55
K_2O	.05	.04	.57	.44	.15	.03	.01	.36	.06	.14	nd
P_2O_5	.04	nd	.06	.06	.02	.03	.01	.01	.01	nd	nd
L.O.I.	–	5.37	4.59	5.06	3.82	2.75	4.29	6.26	5.50	5.05	4.96
Total	100.01	99.44	99.49	100.19	99.73	99.92	99.70	99.98	99.21	99.20	100.35
FeO^t/MgO	1.33	.77	.82	.80	.97	.88	.61	.58	.75	.87	.67
Ni	58	95	93	71	64	128	239	238	115	113	75
Cr	–	274	229	107	139	323	727	670	340	260	140
Zr	–	15	13	11	19	20	11	13	12	8	8
Y	–	8	8	12	13	14	9	9	7	7	7
Sr	–	102	141	142	122	41	67	71	110	124	38
Rb	–	5	5	6	4	nd	nd	4	2	2	nd
Ba	–	16	62	60	34	25	11	30	18	24	14
Cu	20	42	60	94	85	73	86	19	6	183	160
S	3099	300	-	-	-	350	–	–	70	340	–

* - Total iron expressed as Fe_2O_3.

$ - This analysis is recalculated water free. Analyst- B. Gunn , Université de Montréal.

APPENDIX II

WHOLE ROCK ANALYSES

Tables I, II and III list major and trace element whole rock analyses of the Betts Cove and Blow-Me-Down ophiolitic mafic rocks. Analyses numbers correspond to those of Appendix I.

Major and trace element analyses were obtained on a Phillips 1450 automated X-ray Fluorescence Spectrometer. Major elements, excluding sodium, were determined on fused discs after the method of Norrish and Hutton (1969). .3733 grams of -200 mesh rock power were mixed with 2 gms. of Spectroflux (which comprises lanthanum oxide, lithium tetraborate and lithium carbonate) and .0267 gms. of $NaNO_3$. The mixture was fused in a platinum crucible at 1000°C and the liquid poured onto an aluminium plate and pressed into a glass disc. The glass discs were analyzed with a Cr tube at 60 KV and 45 MA.

Sodium determinations were made on pressed powder pellets, which consist of 2 gms. of finely powdered sample mixed thoroughly with 0.2 gms. of Somar binding agent and backed by boric acid all pressed under a hydraulic press at 50 tons/inch^2. The pressed pellets were run on the XRF under major element conditions above for sodium results.

Manganese was determined on fused discs using a W tube at 40 KV and 30 MA.

Ferrous iron was determined by a titration method using ammonium metavanadate as an oxidizing agent. The rocks are dissolved in cold HF in the presence of a known amount of ammonium metavanadate. The ferrous iron in the samples is oxidized quantitatively and the excess pentavalent vanadium is titrated against standardized ferrous ammonium sulphate. The amount of metavanadate consumed during the oxidation is proportional to the amount of ferrous iron present.

Trace elements, except the REE, were analysed on pressed powder pellets with a W tube at 60KV 40MA on the Phillips 1450 XRFS. Reduction of trace element raw data was done using calibration curves of international standards incorporated into the trace element computer program TRATIO.

Rare earth element analyses were done by G. Jenner of the University of Western Ontario. The REEs were separated by ion-exchange chromatography and exchanged onto Reeve Angel SA-2 ion exchange papers. Thulium was added as an internal yield standard. The ion exchange papers were analysed on the 1450 X-ray Fluorescence unit with a W tube.

Analytical error for major elements, except sodium, is less than 2%; for sodium it is 5 to 7%. Trace elements are within 10% of quoted values on international standards except for Tb, which is within 20% of accepted values.

APPENDIX II, TABLE I

WHOLE ROCK ANALYSES OF THE BETTS COVE OPHIOLITIC MAFIC ROCKS.#

	1[a]	2	3	4	5	6	7	8	9	10	11
SiO_2	52.93	47.17	50.16	49.34	53.08	52.05	47.41	55.30	42.92	60.39	49.49
TiO_2	.65	.78	.31	.48	.49	.11	.11	.31	.14	.12	.13
Al_2O_3	15.28	17.83	15.06	16.96	14.42	14.79	14.49	16.14	11.04	11.68	9.42
Fe_2O_3	7.04	3.42	3.64	2.96	4.02	5.30	3.42	1.74	3.34	1.44	2.50
FeO	2.41	4.46	4.46	5.54	3.73	3.38	7.34	3.60	8.06	4.16	6.02
MnO	.15	.18	.16	.16	.17	.16	.17	.12	.20	.15	.18
MgO	6.04	10.24	8.84	10.28	8.30	5.92	13.42	6.56	15.57	7.60	15.08
CaO	5.34	2.29	8.22	3.95	4.94	9.69	7.67	8.38	11.67	6.71	9.49
Na_2O	3.88	.97	2.13	4.16	4.74	1.24	.29	4.63	.52	5.03	1.26
K_2O	3.23	6.13	2.00	.67	.35	1.98	1.69	.03	.01	.01	.19
P_2O_5	.06	.07	.01	.02	.04	.01	nd	.03	.03	nd	.02
L.O.I.	2.98	6.67	4.34	4.80	4.78	5.42	5.03	2.52	6.09	2.19	5.39
Total	99.99	100.21	99.43	99.32	99.06	100.05	101.04	99.36	99.59	99.48	99.17
FeO^t/MgO	1.44	.73	.87	.79	.88	1.33	.77	.78	.71	.71	.54
Ni	145	136	106	100	110	74	185	128	231	268	191
Cr	304	415	376	404	423	81	650	301	730	756	642
Zr	37	39	20	27	30	12	9	14	20	16	19
Y	14	14	9	11	13	7	7	12	11	8	5
Sr	70	107	213	125	77	141	75	81	74	60	113
Rb	74	57	19	10	4	23	27	2	1	nd	3
Ba	262	173	156	41	32	43	54	27	12	28	26
Cu	11	286	329	30	19	10	161	38	133	113	113
S	-	-	-	-	150	-	-	90	-	-	1000

\# Major elements expressed as weight percent oxides, traces in ppm

a Numbers correspond to the analyses numbers of Appendix I

L.O.I. Loss on Ignition

nd Not detected

FeO^t Total iron as FeO

\- Analysis not done

APPENDIX II, TABLE I (Cont'd)

	12	13	14	15	16	17	18	19	20	21	22
SiO_2	52.93	47.14	53.37	50.63	47.65	47.93	46.66	50.99	51.48	59.52	56.32
TiO_2	.50	.53	.51	.13	.10	.10	.19	.17	.17	.13	.15
Al_2O_3	15.47	15.69	16.26	9.85	10.99	10.30	12.66	11.29	13.36	11.47	12.63
Fe_2O_3	1.36	2.77	1.14	1.86	2.38	2.31	3.07	1.07	1.78	1.32	1.11
FeO	5.49	5.98	5.31	6.79	6.99	7.02	5.77	6.60	6.93	5.04	5.67
MnO	.16	.17	.16	.18	.19	.18	.16	.14	.20	.16	.17
MgO	9.08	10.62	7.91	14.33	17.70	17.95	14.36	12.89	11.51	8.46	9.52
CaO	6.80	12.05	8.11	9.78	7.28	7.69	13.17	11.86	7.29	7.16	6.86
Na_2O	4.94	1.88	3.92	1.32	nd	nd	.17	.72	2.45	3.54	3.85
K_2O	.08	.05	.15	.22	.78	.84	.04	.08	.12	.11	.07
P_2O_5	.03	.04	.03	.03	.02	.02	.01	.01	.01	.02	.02
L.O.I.	2.91	4.08	3.22	3.90	5.82	5.43	3.97	3.27	3.80	2.58	2.87
Total	99.76	101.00	100.09	99.72	99.90	99.77	100.23	99.09	99.10	99.51	99.24
FeO^t/MgO	.73	.79	.79	.57	.52	.51	.59	.59	.74	.74	.70
Ni	156	244	224	209	298	301	387	335	98	94	88
Cr	339	432	436	873	958	1050	918	787	407	330	350
Zr	24	20	20	19	7	9	13	10	13	11	14
Y	14	14	13	9	nd	nd	1	1	3	2	3
Sr	169	146	202	105	39	33	160	237	62	87	77
Rb	1	2	2	3	16	16	0	2	0	1	0
Ba	25	8	28	29	32	25	5	11	25	32	31
Cu	81	54	79	120	-	-	-	-	-	-	-
S	-	-	1000	-	-	-	-	-	-	-	-

APPENDIX II, TABLE I (Cont'd)

	24$	25	26	27	28	29	30	31	32	33	34
SiO_2	57.15	55.79	54.54	51.75	51.76	53.57	50.98	50.87	54.40	56.02	52.47
TiO_2	.34	.16	.19	.21	.42	.35	.14	.14	.14	.10	.10
Al_2O_3	15.28	12.85	14.11	15.52	16.10	14.35	13.25	12.64	13.42	13.76	14.49
Fe_2O_3	9.20*	.73	.02	1.03	2.91	1.82	8.53*	8.56*	1.29	1.54	1.80
FeO	–	6.62	7.38	7.22	5.04	5.50	–	–	6.44	6.80	6.62
MnO	.22	.14	.14	.16	.15	.14	.18	–	.18	.17	.17
MgO	6.03	9.31	9.15	9.82	7.84	8.04	12.60	13.40	10.04	9.36	12.17
CaO	5.93	5.27	5.30	5.39	7.57	9.07	6.71	6.11	4.60	3.39	4.02
Na_2O	5.78	3.16	3.44	3.53	3.95	4.27	3.01	1.63	3.13	2.87	3.55
K_2O	.05	.04	.57	.44	.15	.03	.01	.36	.06	.14	nd
P_2O_5	.04	nd	.06	.06	.02	.03	.01	.01	.01	nd	nd
L.O.I.	–	5.37	4.59	5.06	3.82	2.75	4.29	6.26	5.50	5.05	4.96
Total	100.01	99.44	99.49	100.19	99.73	99.92	99.70	99.98	99.21	99.20	100.35
FeO^t/MgO	1.33	.77	.82	.80	.97	.88	.61	.58	.75	.87	.67
Ni	58	95	93	71	64	128	239	238	115	113	75
Cr	–	274	229	107	139	323	727	670	340	260	140
Zr	–	15	13	11	19	20	11	13	12	8	8
Y	–	8	8	12	13	14	9	9	7	7	7
Sr	–	102	141	142	122	41	67	71	110	124	38
Rb	–	5	5	6	4	nd	nd	4	2	2	nd
Ba	–	16	62	60	34	25	11	30	18	24	14
Cu	20	42	60	94	85	73	86	19	6	183	160
S	3099	300	–	–	–	350	–	–	70	340	–

* - Total iron expressed as Fe_2O_3.

$ - This analysis is recalculated water free. Analyst- B. Gunn , Université de Montréal.

APPENDIX II, TABLE I (Cont'd)

	35	36	37	38	39$	40$	41$	42	43	44	45
SiO_2	56.14	52.86	54.32	55.83	55.81	56.42	54.64	53.21	53.42	55.37	53.54
TiO_2	.10	.07	.11	.12	.12	.18	.30	.10	.19	.24	.27
Al_2O_3	14.59	12.19	13.26	12.72	13.96	14.29	14.23	11.89	14.39	14.01	15.44
Fe_2O_3	1.65	9.55	.89	1.41	3.72	8.43	4.35	2.64	1.52	1.90	3.13
FeO	6.41	–	6.44	6.49	4.62	–	5.27	7.86	6.57	5.82	4.23
MnO	.17	–	.16	.16	.13	.13	.15	.21	.15	.15	.13
MgO	7.71	12.15	8.46	9.27	6.97	7.23	5.50	11.29	8.92	8.63	6.53
CaO	3.37	7.70	6.57	6.61	8.14	7.04	8.88	4.96	5.83	7.01	9.01
Na_2O	4.21	3.83	5.43	4.93	6.00	6.15	6.05	2.44	3.86	4.23	4.14
K_2O	.02	.02	.17	.07	.06	.06	.05	.11	.27	.14	.04
P_2O_5	nd	nd	.01	.01	.02	.03	.04	nd	.03	.01	.03
L.O.I.	5.10	3.46	2.60	2.10	–	–	–	4.73	3.41	1.80	2.23
Total	99.47	101.83	98.32	99.72	99.55	99.99	99.46	99.44	98.56	99.71	98.72
FeO^t/MgO	1.02	.71	.86	.84	1.14	1.05	1.66	.90	.88	.87	1.19
Ni	59	125	105	114	94	69	58	119	63	85	61
Cr	83	425	222	259	–	–	–	649	109	218	107
Zr	11	nd	11	11	–	–	–	8	9	21	21
Y	7	3	5	7	–	–	–	7	9	12	11
Sr	104	41	93	58	–	–	–	82	152	88	52
Rb	nd	nd	4	nd	–	–	–	3	5	3	nd
Ba	15	9	31	24	–	–	–	23	43	26	11
Cu	141	18	10	11	6	9	22	8	9	7	9
S	160	nd	–	–	421	420	–	–	–	–	400

APPENDIX II TABLE I (Cont'd)

	46	47$	48$	49$	50	51	52	53	54	55	56
SiO_2	54.78	53.89	52.31	53.63	54.78	55.95	53.29	52.82	48.54	55.44	47.11
TiO_2	.10	.08	.16	.14	.08	.06	.11	.08	.13	.08	.06
Al_2O_3	10.77	9.20	10.81	13.58	10.75	11.09	11.38	10.11	12.95	12.30	9.48
Fe_2O_3	1.76	9.14*	9.12*	9.79*	2.10	.80	2.91	1.89	2.92	.78	1.68
FeO	6.53	–	–	–	6.72	7.70	4.96	6.76	6.31	5.97	8.42
MnO	.17	.16	.14	.21	.14	–	.17	–	.17	.16	.19
MgO	12.52	18.33	16.03	11.95	12.95	10.16	11.82	15.53	13.79	11.60	19.31
CaO	7.89	8.60	8.29	6.59	5.75	7.82	8.74	7.35	8.09	4.88	6.47
Na_2O	2.34	.13	2.90	3.14	1.68	3.41	2.52	1.20	2.25	4.35	.87
K_2O	.19	.46	.21	.94	.05	.17	.12	.26	.09	nd	nd
P_2O_5	.01	.02	.03	.02	nd	nd	.02	.01	.02	.01	nd
L.O.I.	3.75	–	–	–	4.81	1.98	3.06	4.89	4.07	3.34	5.96
Total	100.58	100.01	100.01	99.99	99.81	99.88	99.61	100.90	99.33	98.91	99.55
FeO^t/MgO	.65	.45	.47	.68	.66	.82	.64	.54	.64	.58	.51
Ni	190	418	382	190	142	147	155	445	309	112	397
Cr	911	–	–	–	643	532	778	–	939	521	1452
Zr	8	–	–	–	9	3	8	11	8	7	nd
Y	5	–	–	–	10	5	8	5	10	7	4
Sr	74	–	–	–	76	103	196	38	152	90	27
Rb	2	–	–	–	nd	1	4	5	5	nd	nd
Ba	22	–	–	–	27	28	66	–	35	15	19
Cu	–	80	6	172	10	8	20	75	2	42	4
S	–	304	436	514	nd	nd	nd	nd	220	–	–

APPENDIX II TABLE I (Cont'd)

	57	58	59	60$	61	62	63	64	65	66	67
SiO_2	49.29	52.13	49.74	52.50	51.09	49.34	49.17	49.61	47.63	48.68	49.23
TiO_2	.06	.08	.10	.05	.05	.05	.08	.10	.06	.05	.05
Al_2O_3	8.47	10.97	9.74	3.98	6.49	7.12	8.25	8.82	6.45	6.15	8.24
Fe_2O_3	1.57	1.35	2.44	1.58	2.32	2.26	1.79	1.80	1.87	1.46	.99
FeO	7.54	7.45	6.13	7.87	6.92	6.80	6.80	6.71	6.01	6.71	8.72
MnO	.18	.17	.17	.20	.22	.21	.20	.17	.16	.17	.22
MgO	18.60	13.71	17.78	20.81	20.19	20.80	20.89	20.25	23.65	23.95	19.56
CaO	6.88	6.12	8.44	11.94	7.88	7.62	7.67	6.89	7.64	6.67	8.13
Na_2O	.95	3.01	.96	.24	.22	.31	.77	.23	.03	.06	.77
K_2O	nd	.16	.53	.03	.02	nd	.07	.08	nd	nd	.03
P_2O_5	.02	.01	.01	.02	.01	nd	nd	nd	nd	nd	nd
L.O.I.	4.99	3.88	3.76	-	4.84	4.58	3.98	5.84	6.31	5.79	4.27
Total	98.55	99.04	99.80	99.22	100.25	99.10	99.67	100.50	99.81	99.69	100.21
FeO^t/MgO	.48	.63	.47	.41	.44	.42	.40	.41	.32	.33	.49
Ni	526	279	471	323	657	777	805	751	937	915	512
Cr	1589	867	1324	-	1966	2044	1625	1404	1876	1990	-
Zr	4	5	8	-	7	5	11	16	8	7	6
Y	7	5	9	-	9	5	6	10	7	11	6
Sr	26	121	35	-	5	3	21	8	7	76	9
Rb	1	1	9	-	nd	1	2	2	nd	nd	1
Ba	17	85	89	-	11	18	13	26	17	15	
Cu	3	-	6	14	6	25	-	82	58	10	4
S	-	nd	496	nd	110	nd	nd	nd	nd	nd	nd

APPENDIX II TABLE I (Cont'd)

	68	69	70	71	72	73	74$	75
SiO_2	52.07	51.95	51.37	50.92	50.50	47.51	54.22	49.08
TiO_2	.02	.08	.06	.06	.13	.05	.19	.94
Al_2O_3	5.30	17.32	15.89	17.57	17.42	18.97	15.73	12.87
Fe_2O_3	8.99*	1.97	1.29	1.68	2.32	1.11	2.30	2.66
FeO		6.16	5.08	1.70	4.17	3.58	.61	6.26
MnO	.21	.17	.16	.15	–	.09	.05	.16
MgO	19.35	8.82	9.84	9.72	9.09	10.14	6.58	8.56
CaO	10.64	3.86	7.97	9.22	7.56	13.80	16.36	10.29
Na_2O		3.85	2.42	3.06	3.16	1.29	3.82	3.99
K_2O	nd	.97	1.74	1.72	1.75	.42	.05	.42
P_2O_5	nd	.02	.01	nd	.02	nd	.03	.26
L.O.I.		4.12	3.52	3.25	4.49	2.83	–	4.68
Total		99.29	99.35	99.05	100.61	99.68	99.94	100.15
FeO^t/MgO	.42	.90	.63	.33	.69	.45	.41	1.00
Ni	–	89	106	181	134	181	82	76
Cr	–	116	44	615	230	210	–	–
Zr	5	6	6	nd	3	nd	–	–
Y	2	5	14	5	8	nd	–	–
Sr	2	253	149	147	170	179	–	–
Rb	1	10	2	15	21	5	–	–
Ba	2	46	92	88	151	44	–	–
Cu	–	65	2	8	7	–	7	82
S	–	–	120	–	–	–	55	1776

APPENDIX II, TABLE II

WHOLE ROCK ANALYSES OF BLOW-ME-DOWN OPHIOLITIC MAFIC ROCKS.#

	76	77	78	79	80	81	82	83	84	85	86
SiO_2	40.67	41.38	44.76	48.43	50.10	48.43	47.20	48.64	49.88	47.77	49.60
TiO_2	1.17	1.29	1.24	1.68	1.64	1.35	1.18	1.31	1.37	1.15	1.42
Al_2O_3	12.47	17.25	13.83	14.07	15.51	14.83	16.50	14.79	14.37	17.09	13.86
Fe_2O_3	5.85	8.20	9.12*	10.64*	9.46*	3.25	3.04	2.97	2.66	1.53	10.75*
FeO	4.39	2.82	–	–	–	6.58	4.78	6.99	7.81	7.61	–
MnO	.25	.20	.20	.20	.17	–	.22	.24	.24	.22	–
MgO	9.40	6.51	6.70	5.55	6.78	7.90	7.04	6.91	7.15	8.25	7.87
CaO	12.00	9.03	9.59	6.82	5.15	8.94	9.35	10.06	8.45	9.71	8.37
Na_2O	2.41	3.46	3.92	4.33	5.85	3.73	3.54	2.76	3.34	2.11	3.51
K_2O	.42	1.21	.03	.17	.01	.04	1.05	.16	.07	1.09	.30
P_2O_5	.08	.10	.11	.16	.15	.12	.11	.13	.12	.08	.13
L.O.I.	10.82	8.57	9.78	4.73	5.15	5.70	6.72	4.12	3.34	3.44	3.88
Total	99.93	100.02	99.80	98.58	100.27	100.87	100.73	99.38	99.80	100.05	99.95
FeO^t/MgO	1.02	1.56	1.23	1.73	1.26	1.19	1.07	1.40	1.43	1.09	1.23
Ni	645	275	74	60	64	101	127	46	30	98	56
Cr	776	836	211	292	287	278	216	235	124	252	256
Zr	70	76	88	122	124	97	82	81	86	69	96
Y	25	27	27	36	35	28	31	31	33	27	32
Sr	470	195	138	222	126	340	535	116	184	527	292
Rb	8	17	nd	3	nd	1	13	3	2	10	6
Ba	517	560	68	411	108	262	69	28	24	84	25
Cu	99	50	38	31	111	108	11	6	4	18	59
S	nd	nd	7290	17550	4740	nd	nd	1690	nd	nd	nd

Major elements in weight percent oxides, traces in ppm. All symbols same as in Table I of Appendix II.

APPENDIX II, TABLE II (Cont'd)

	87	88	89	90	91	92	93	94	95	96	97
SiO_2	49.91	47.38	48.79	47.66	48.30	47.33	47.59	46.83	47.58	47.73	48.08
TiO_2	1.16	1.12	1.12	1.13	1.54	.96	1.37	.62	.89	1.28	.94
Al_2O_3	15.39	17.28	15.39	15.91	13.53	18.54	15.79	18.58	19.50	14.71	14.91
Fe_2O_3	3.96	2.06	2.74	2.79	10.75*	1.77	2.46	1.03	1.46	2.44	1.45
FeO	5.92	6.82	6.89	6.65	–	5.93	7.59	6.14	5.83	7.91	7.73
MnO	.19	.19	.19	.17	.19	.16	.18	.16	.16	.18	.18
MgO	5.66	8.55	8.19	7.81	7.35	8.18	7.83	10.49	7.76	10.01	9.85
CaO	6.00	9.98	11.32	9.06	8.42	11.35	9.62	11.07	9.56	9.48	10.10
Na_2O	4.18	2.42	2.94	3.98	4.88	2.57	2.84	1.74	2.52	2.62	2.00
K_2O	.03	.88	.40	.25	.02	.29	.77	.18	1.47	.32	.13
P_2O_5	.08	.11	.12	.10	.18	.11	.17	.05	.09	.13	.10
L.O.I.	5.73	3.56	2.05	4.17	4.95	2.21	3.41	2.92	3.50	3.51	3.76
Total	99.63	100.35	100.14	99.68	100.11	99.39	99.62	99.81	100.32	100.31	99.23
FeO^t/MgO	1.67	1.01	1.14	1.17	1.32	.91	1.24	.74	.91	1.00	.91
Ni	24	140	87	88	43	143	82	341	151	165	230
Cr	68	252	293	182	86	267	221	495	271	278	510
Zr	100	66	62	69	113	69	89	–	21	46	10
Y	35	27	27	29	35	23	29	–	–	–	–
Sr	137	445	271	191	117	297	529	248	374	218	180
Rb	nd	4	4	6	1	3	4	nd	10	1	1
Ba	16	54	24	25	99	13	56	17	141	29	25
Cu	15	23	113	71	–	–	–	152	159	174	78
S	5620	nd	50	720	–	–	–	nd	nd	nd	30

APPENDIX II, TABLE II (Cont'd)

o	98	99	100	101	102	103	104	105	106
SiO_2	51.90	51.56	50.72	48.02	47.25	44.16	49.05	48.90	42.66
TiO_2	.30	.39	.32	.35	.17	.16	.32	1.20	3.45
Al_2O_3	13.55	16.90	13.87	16.39	19.22	23.96	16.14	15.96	10.88
Fe_2O_3	8.26*	1.48	.72	1.48	.81	1.14	1.53	2.62	21.03*
FeO	–	7.18	6.34	5.27	3.99	4.45	4.64	5.47	–
MnO	–	.17	.17	.17	.15	.16	.15	–	.21
MgO	11.04	7.40	12.45	9.95	8.38	5.83	10.77	6.66	8.45
CaO	6.65	10.32	10.30	13.01	14.82	11.99	14.68	11.91	6.57
Na_2O	2.74	2.74	1.69	1.90	1.43	2.46	1.41	4.22	3.58
K_2O	.11	.22	.05	.02	.01	.08	nd	.16	.10
P_2O_5	.03	.03	.03	.01	.01	.01	nd	.01	.05
L.O.I.	3.91	1.90	2.35	2.26	3.16	5.86	1.31	3.20	1.86
Total	98.51	100.29	99.01	98.83	99.40	100.26	99.98	100.31	100.56
FeO^t/MgO	.67	1.27	.56	3	.56	.94	.56	1.18	2.27
Ni	264	24	327	143	161	138	137	33	5
Cr	764	38	831	481	388	nd	703	117	61
Zr	28	21	18	4	nd	nd	4	17	nd
Y	11	11	10	10	8	3	10	17	nd
Sr	342	158	127	104	248	231	114	260	142
Rb	2	2	nd	nd	nd	2	nd	1	2
Ba	38	25	13	9	10	6	7	17	99
Cu	7	–	–	–	–	–	–	–	127
S	60	–	–	–	–	–	–	–	–

APPENDIX II, TABLE III

Rare earth element concentrations in selected Betts Cove mafic rocks.

	2	4	10	12	14	28
La	1.18	1.56	-	1.37	.99	1.26
Ce	4.27	6.25	2.03	3.08	5.54	3.65
Pr	.51	.59	-	.36	-	.42
Nd	2.64	4.57	1.81	3.10	4.08	2.76
Sm	1.47	1.46	.42	1.52	1.27	1.06
Eu	.87	.28	-	.54	.26	.42
Gd	2.47	2.01	.59	2.02	2.10	1.46
Dy	3.83	2.49	1.17	2.65	2.91	2.22
Er	3.09	1.49	.95	2.05	1.87	1.60
$(La/Sm)_{EF}$	.44	.58	-	.49	.43	1.19
$(La/Er)_{EF}$	.23	.64	-	.41	.32	.79

EF - Enrichment Factor (Schilling, 1975). Calculated by division of chondrite normalized values.

APPENDIX III

MINERAL ANALYSES

All mineral compositions were determined on an M.A.C. 400 electron microprobe with a Krisel Control automation system. Clinopyroxenes, chromites, plagioclases, epidotes, actinolites, chlorites and sericites were analyzed using an excitation voltage of 15 KV and a sample current of 0.025 and 0.500 milliamps with a beam size of approximately 3 microns. The analyzing crystals used were KAP (for Si, Al, Mg, Na), PET (for Ca, Ti, Cr, K) and LIF (for NI, Fe, Mn).

Tables I to IV of this appendix lists the mineral compositions along with structural formulae based on an appropriate number of oxygen. The analyses numbers correspond to the numbers in appendix I. The letters following the numbers refer to different grains in the same sample.

The accuracy of the analyses is within 3 percent of the amount present. The detection limit is approximately 0.05 percent.

order. In other words, these numbers define the interval limit. For the case above, 30, 50, 100 would appear on this card. Format (10I3). Note that the number of numbers on this card must equal np.

CARDS 18 & 19: same as in the case in which no phases disappear except that these two cards must be repeated as many times as there are melting intervals. For example in the case above, cards 18 & 19 are repeated 3 times; the first two containing the liquid modal composition at low degree and the highest degree (30) in interval I, the second two define the changing liquid composition in interval II. Note that the liquid composition in interval II should be estimated from the new source at 30% melting (a source with only ol and opx). In interval III, only olivine is in the source at 50% so that the liquid modal composition at some small degree of melting in interval III will be 100% olivine as will be the liquid composition at the highest degree of melting in the interval. Note that when separate melting intervals are considered, the liquids derived at the beginning and end of each interval (cards 18 and 19) are estimated as if a completely new source is being melted.

As in the case where no phases disappear, cards 15 through 19 can be repeated as many times as desired.

7/8/9 card
6/7/8/9 card

APPENDIX III, TABLE I

Clinopyroxene Analyses

	1a	1b	1c	23a	23b	10a	10b	10c	10d	10e
SiO_2	53.25	52.85	54.22	56.68	53.83	52.78	52.82	52.05	52.11	52.42
TiO_2	0.22	0.32	0.17	0.00	0.00	0.00	0.00	0.03	0.00	0.01
Al_2O_3	1.89	2.88	1.57	1.31	1.28	2.95	2.92	3.05	2.73	2.83
FeO^t	4.65	5.12	4.01	5.13	4.38	5.64	7.78	7.10	6.35	5.78
MnO	0.04	0.04	0.04	0.09	0.06	0.13	0.28	0.20	0.23	0.15
MgO	17.63	16.34	17.97	17.15	18.26	17.46	19.29	18.06	18.29	17.06
CaO	22.58	22.36	22.19	18.66	18.83	20.39	16.61	18.32	18.86	20.29
Na_2O	0.16	0.16	0.14	0.07	0.09	0.36	0.11	0.14	0.18	0.42
Cr_2O_3	-	-	-	0.73	0.79	0.32	0.26	0.21	0.24	0.14
Total	100.44	100.09	100.32	99.83	99.32	100.05	100.11	99.20	99.01	99.11
					Structural Formulae (O=6)					
Si	1.940	1.933	1.965	2.042	2.015	1.930	1.926	1.922	1.922	1.934
Ti	.006	.009	.005	.000	.000	.000	.000	.000	.000	.000
Al^{iv}	.060	.067	.035	-	-	.070	.074	.078	.078	.066
Al^{vi}	.021	.057	.032	.098	.070	.059	.051	.055	.039	.059
Fe	.142	.157	.122	.155	.133	.172	.238	.219	.195	.180
Mg	.957	.891	.971	.921	.986	.949	1.047	.992	1.008	.938
Mn	.001	.001	.002	.003	.002	.004	.008	.008	.008	.004
Ca	.881	.876	.862	.720	.731	.797	.648	.723	.746	.801
Na	.011	.011	.010	.005	.006	.027	.008	.012	.012	.031
Cr				.021	.023	.008	.008	.008	.008	.004
Mg/Mg + Fe	.871	.850	.889	.856	.881	.847	.814	.819	.838	.716
Fe/Mg	.148	.176	.126	.168	.134	.181	.227	.220	.193	.191
Ca	44.5	45.5	44.1	40.1	39.5	41.5	33.5	37.4	38.3	41.7
Mg	48.3	46.3	49.6	51.2	53.3	49.5	54.2	51.3	51.7	48.9
Fe	7.2	8.2	6.3	8.8	7.3	9.0	12.3	11.3	10.0	9.4

APPENDIX III, TABLE I (Cont'd)

	26a	26b	31a	31b	31c	35a	35b	35c	35d	46a	46b
SiO_2	55.11	54.06	52.22	52.31	52.00	53.42	52.64	53.97	52.75	52.78	54.06
TiO_2	0.03	0.06	0.10	0.09	0.10	0.02	0.04	0.02	0.01	0.00	0.00
Al_2O_3	1.33	1.79	2.68	2.59	2.02	1.88	2.11	1.22	1.05	1.76	1.35
FeO^t	5.26	5.14	6.15	5.70	6.41	6.33	6.58	6.15	6.28	6.48	5.52
MnO	-	-	.21	.21	.21	.06	.01	.01	.03	.12	.11
MgO	16.49	16.38	18.21	17.13	18.17	17.13	17.66	17.70	17.97	19.08	19.13
CaO	19.58	20.14	19.14	20.78	19.79	20.11	19.94	20.32	20.50	18.79	18.23
Na_2O	0.09	0.15	0.16	0.08	0.12	0.10	0.12	0.07	0.12	0.06	0.10
Cr_2O_3	0.39	0.60	0.26	0.30	0.44	0.37	0.39	0.20	0.33	0.34	0.34
Total	98.26	98.31	99.12	99.20	99.27	99.41	99.49	99.65	99.06	99.41	98.99
					Structural Formulae (O=6)						
Si	2.027	1.996	1.926	1.930	1.922	1.970	1.945	1.981	1.960	1.940	1.983
Ti	.001	.002	.004	.004	.004	.001	.001	.001	.000	.000	.000
Al^{iv}		.004	.074	.070	.078	.030	.055	.019	.040	.060	.017
Al^{vi}	.085	.074	.043	.043	.012	.052	.037	.033	.006	.016	.041
Fe	.162	.159	.191	.176	.199	.195	.203	.189	.195	.199	.169
Mg	.904	.901	1.000	.941	1.000	.941	.972	.968	.995	1.045	1.043
Mn	-	-	.008	.008	.008	.002	.000	.000	.001	.004	.003
Ca	.771	.797	.754	.820	.785	.795	.789	.799	.816	.740	.714
Na	.006	.011	.012	.008	.008	.007	.009	.005	.009	.004	.007
Cr	.011	.017	.008	.008	.012	.010	.011	.005	.010	.010	.010
Mg/Mg + Fe	.848	.850	.840	.842	.834	.828	.827	.837	.836	.840	.861
Fe/Mg	.179	.176	.191	.187	.199	.207	.209	.195	.196	.190	.162
Ca	42.0	42.9	38.8	42.3	39.6	41.1	40.2	40.8	40.7	37.2	37.0
Mg	49.2	48.5	51.4	48.6	50.4	48.7	49.5	49.5	49.6	52.0	54.0
Fe	8.8	8.6	9.8	9.1	10.0	10.2	10.3	9.7	9.8	10.2	9.0

APPENDIX III, TABLE I (Cont'd)

	47a	47b	Core 47c	Rim 47d	47e	Core 47f	Rim 47g	47h	68a	68b	68c
SiO_2	53.58	52.03	52.47	53.84	51.32	50.98	49.83	53.34	54.23	53.89	54.07
TiO_2	0.02	0.00	0.00	0.00	0.02	0 00	0.06	0.00	0.02	0.01	0.00
Al_2O_3	1.44	2.54	1.95	1.11	1.40	2.92	3.27	1.47	1.25	1.19	1.17
FeO^{t3}	4.67	6.51	4.92	6.63	14.71	6.91	13.13	5.63	4.70	4.55	4.61
MnO	0.07	0.13	0.18	0.24	0.34	0.16	0.34	0.17	0.00	0.04	0.61
MgO	19.56	18.32	18.29	20.93	15.82	17.71	13.84	20.24	18.71	18.66	18.88
CaO	19.27	19.97	20.89	16.83	15.96	19.73	19.03	18.65	20.34	20.67	20.73
Na_2O	0.11	-	-	-	-	-	-	-	0.04	0.00	0.03
Cr_2O_3	0.56	0.11	0.43	0.18	0.00	0.03	0.02	0.42	0.52	0.57	0.86
Total	99.32	99.61	99.15	99.77	99.55	98.45	99.52	99.94	99.61	99.58	100.95
					Structural Formulae (O=6)						
Si	1.965	1.914	1.934	1.961	1.945	1.902	1.895	1.941	1.980	1.975	1.961
Ti	.001	.000	.000	.000	.000	.000	.000	.000	.001	.000	.000
Al^{iv}	.035	.086	.066	.039	.055	.098	.105	.059	.020	.025	.039
Al^{vi}	.027	.023	.020	.008	.008	.031	.043	.004	.034	.027	.011
Fe	.143	.199	.152	.203	.465	.215	.418	.172	.144	.139	.140
Mg	1.068	1.004	1.004	1.137	.895	.984	.785	1.098	1.018	1.019	1.020
Mn	.002	.004	.004	.008	.012	.004	.012	.004	.000	.001	.025
Ca	.758	.789	.824	.656	.648	.789	.773	.727	.796	.812	.806
Na	.008	-	-	-	-	-	-	-	.003	.000	.002
Cr	.018	.004	.012	.004	.000	.000	.000	.012	.017	.018	.025
Mg/Mg + Fe	.882	.835	.867	.849	.658	.821	.653	.865	.876	.880	.879
Fe/Mg	.134	.198	.151	.178	.520	.219	.532	.157	.141	.136	.137
Ca	38.4	39.6	41.6	32.9	32.3	39.7	39.1	36.4	40.7	41.2	41.0
Mg	54.2	50.4	50.7	57.0	44.6	49.5	39.7	55.0	52.0	51.7	51.9
Fe	7.4	10.0	7.7	10.1	23.1	10.8	21.2	8.6	7.3	7.1	7.1

APPENDIX III, TABLE I (Cont'd)

	Core	Rim	Core	Rim							
	68d	68e	68f	68g	70a	70b	70c	70d	73a	73b	73c
SiO_2	53.30	53.04	52.92	52.25	52.80	52.68	53.91	52.54	54.05	53.26	54.30
TiO_2	0.00	0.00	0.02	0.07	0.00	0.03	0.01	0.01	0.02	0.03	0.01
Al_2O_3	1.26	1.73	1.50	1.50	1.53	1.38	1.38	1.36	0.60	0.89	0.52
FeO^t	4.23	6.18	5.02	8.13	5.96	7.18	6.15	6.43	4.83	5.50	4.75
MnO	0.22	0.53	0.58	0.11	0.04	0.06	0.07	0.08	0.04	0.01	0.08
MgO	18.70	17.98	17.29	16.17	17.16	17.09	18.00	17.18	17.19	16.34	16.81
CaO	21.13	20.91	22.36	21.45	21.19	20.84	20.68	20.83	24.03	23.64	23.45
Na_2O	0.45	0.02	0.26	0.16	0.15	0.15	0.12	0.14	0.05	0.27	0.25
Cr_2O_3	1.68	0.18	0.56	0.32	0.03	0.04	0.07	0.08	0.03	0.02	0.01
Total	100.75	100.56	100.52	100.25	98.86	99.45	100.34	98.62	100.83	99.97	100.19
					Structural Formulae (O=6)						
Si	1.939	1.943	1.944	1.938	1.959	1.953	1.964	1.958	1.969	1.965	1.984
Ti	.000	.000	.001	.002	.000	.001	.000	.000	.000	.000	.000
Al^{iv}	.054	.057	.056	.062	.041	.047	.036	.042	.031	.035	.016
Al^{vi}		.018	.009	.004	.025	.013	.024	.018	-	.004	.007
Fe	.129	.189	.154	.255	.185	.223	.187	.200	.148	.168	.145
Mg	1.014	.982	.946	.894	.949	.944	.978	.954	.934	.898	.918
Mn	.007	.016	.018	.003	.001	.002	.002	.003	.000	.000	.004
Ca	.824	.821	.880	.853	.842	.828	.807	.832	.938	.934	.918
Na	.001	.001	.019	.012	.011	.011	.008	.010	.004	.020	.020
Cr	.048	.005	.016	.012	.000	.000	.002	.000	.000	.000	.000
Mg/Mg + Fe	.887	.838	.860	.778	.837	.809	.839	.826	.863	.842	.864
Fe/Mg	.127	.192	.162	.285	.195	.236	.191	.210	.158	.187	.158
Ca	41.9	41.2	44.4	42.6	42.6	41.5	40.9	41.8	46.4	46.7	46.3
Mg	51.6	49.3	47.8	44.7	48.0	47.3	49.5	48.0	46.3	44.9	46.3
Fe	6.5	9.5	7.8	12.7	9.4	11.2	9.6	10.2	7.3	8.4	7.4

APPENDIX III, TABLE I (Cont'd)

	90a	90b	90c	90d	90e	90f	90g	90h	90i
SiO_2	50.43	49.83	50.58	50.08	48.83	48.46	50.20	50.47	50.13
TiO_2	1.07	1.30	0.75	0.90	1.43	0.82	0.84	0.71	0.74
Al_2O_3	3.43	2.70	1.80	2.46	3.90	1.91	4.18	2.26	3.79
FeO^t	10.78	14.13	12.47	15.56	12.14	18.10	7.01	11.68	7.98
MnO	0.25	0.37	0.34	0.45	0.27	0.59	0.11	0.29	0.25
MgO	12.98	11.30	14.32	12.12	12.87	9.90	15.58	14.68	15.66
CaO	19.72	19.07	18.18	17.21	19.36	18.71	20.87	18.41	20.18
Na_2O	0.57	0.80	0.55	0.62	0.67	0.65	0.48	0.80	0.25
Cr_2O_3	0.00	0.04	0.00	0.07	0.00	0.02	0.09	0.00	0.13
Total	99.25	99.57	99.02	99.50	99.49	99.20	99.37	99.31	99.10
				Structural Formulae (O=6)					
Si	1.906	1.910	1.926	1.922	1.859	1.906	1.867	1.910	1.875
Ti	.031	.039	.023	.02	.043	.023	.023	.020	.020
Al^{iv}	.094	.090	.074	.078	.141	.094	.133	.090	.125
Al^{vi}	.058	.031	.008	.035	.035	-	.051	.012	.043
Fe	.340	.453	.398	.500	.387	.594	.219	.371	.250
Mg	.730	.645	.813	.691	.730	.578	.863	.828	.875
Mn	.008	.012	.012	.016	.008	.020	.004	.008	.008
Ca	.797	.781	.742	.707	.789	.789	.832	.746	.809
Na	.043	.059	.039	.047	.051	.051	.035	.059	.020
Cr	.000	.000	.000	.004	.000	.000	.004	.000	.004
Mg/Mg + Fe	.682	.587	.671	.580	.654	.493	.798	.691	.778
Fe/Mg	.466	.702	.489	.724	.530	1.020	.253	.448	.286
Ca	42.7	41.6	38.0	37.3	41.4	40.2	43.5	38.4	41.8
Mg	39.1	34.3	41.6	36.4	38.3	29.5	45.1	42.6	45.3
Fe	18.2	24.1	20.4	26.3	20.3	30.3	11.4	19.0	12.9

APPENDIX III, TABLE II

Chromite Analyses*

	Core 47a	Rim 47b	Core 47c	Rim 47d	47e	47f	47g	46a	46b	73201
SiO_2	0.16	0.18	0.12	0.20	0.11	0.16	0.15	0.13	0.13	0.16
Al_2O_3	7.33	7.71	8.33	9.70	7.15	6.51	7.32	10.05	9.20	8.30
Cr_2O_3	61.87	57.53	60.59	56.18	63.91	64.36	65.21	55.88	55.90	56.85
TiO_2	0.00	0.04	0.04	0.01	0.01	0.03	0.02	0.51	0.43	0.02
Fe_2O_3	4.67	5.07	4.71	4.77	2.77	2.71	2.13	5.43	6.37	5.24
FeO	11.39	18.69	11.31	15.10	11.56	11.74	12.85	14.94	15.54	17.63
MnO	1.20	0.98	1.19	1.36	-	-	-	0.79	1.34	0.91
MgO	14.12	9.25	14.27	11.57	14.00	13.77	13.54	12.30	11.79	9.81
Total	100.48	99.60	100.61	99.00	99.53	99.34	101.19	100.03	100.70	98.92
					Structural Formulae (O=32)					
Al	2.26	2.48	2.56	3.07	2.21	2.03	2.23	3.11	2.87	2.67
Cr	12.81	12.42	12.49	11.93	13.24	13.43	13.34	11.61	11.69	12.25
Ti	0.00	0.02	0.02	0.00	0.00	0.01	0.00	0.10	0.09	0.00
Fe^{3+}	0.92	1.04	0.92	0.96	0.55	0.54	0.41	1.07	1.27	1.08
Fe^{2+}	2.49	4.27	2.47	3.39	2.53	2.59	2.78	3.28	3.44	4.02
Mg	5.51	3.76	5.55	4.63	5.47	5.41	5.22	4.82	4.65	3.98
$\frac{100 \times Mg}{Mg + Fe^{2+}}$	68.85	46.86	69.22	57.73	68.33	67.63	65.26	59.47	57.49	49.78
$\frac{100 \times Cr}{Cr + Al}$	84.99	83.34	82.99	79.52	85.70	85.89	85.66	78.85	80.29	82.12
$\frac{100 \times Fe^{3+}}{Cr+Al+Fe^{3+}}$	5.76	6.53	5.78	6.04	3.42	3.36	2.59	6.80	8.02	6.72
$MgAl_2O_4$	15.0	16.7	17.0	20.5	14.3	13.1	14.3	21.1	19.7	17.9
$MgCr_2O_4$	58.1	33.9	56.7	41.3	56.5	57.0	52.7	44.3	44.1	35.5
$FeCr_2O_4$	26.9	49.5	26.3	38.2	29.2	29.9	33.0	34.6	36.2	46.6

* - Majors expressed in weight percent oxide

APPENDIX III, TABLE II (Cont'd)

	73201b	73199a	73199b	73199c	73199d	73199e	73199f
SiO_2	0.15	0.20	0.71	0.18	0.20	0.24	0.35
Al_2O_3	9.79	9.33	8.93	9.30	8.68	7.88	7.04
Cr_2O_3	52.71	56.02	54.75	56.84	55.48	54.00	52.07
TiO_2	0.11	0.07	0.09	0.05	0.09	0.02	0.09
Fe_2O_3	4.92	5.39	5.40	4.33	3.86	4.49	7.90
FeO	26.92	14.68	20.47	20.83	24.44	28.55	30.69
MnO	0.89	0.92	0.88	0.94	0.91	1.06	1.29
MgO	4.10	11.67	8.02	8.21	5.50	2.57	1.46
Total	99.59	98.02	99.25	100.68	99.16	98.81	100.89
			Structural Formulae (O=32)				
Al	3.24	2.97	2.90	2.96	2.87	2.68	2.39
Cr	11.68	11.94	11.94	12.14	12.28	12.33	11.86
Ti	0.02	0.03	0.02	0.01	0.02	0.00	0.02
Fe^{3+}	1.04	1.09	1.12	0.88	0.81	0.98	1.71
Fe^{2+}	6.31	3.31	4.72	4.71	5.72	6.90	7.39
Mg	1.71	4.69	3.30	3.31	2.30	1.11	0.63
$\frac{100 \times Mg}{Mg + Fe^{2+}}$	21.35	58.62	41.11	41.26	28.63	13.82	7.82
$\frac{100 \times Cr}{Cr + Al}$	78.31	80.10	80.44	80.39	81.08	82.13	83.22
$\frac{100 \times Fe^{3+}}{Cr+Al+Fe^{3+}}$	6.50	6.83	7.02	5.51	5.10	6.10	10.73
$MgAl_2O_4$	21.7	19.9	19.6	19.6	18.9	14.7	8.8
$MgCr_2O_4$	1.3	43.0	24.9	24.2	11.4		
$FeCr_2O_4$	77.0	37.1	55.5	56.2	69.7	82.1	83.2
$FeAl_2O_4$						3.2	8.0

APPENDIX III, TABLE III

Epidote Analyses

	1a	1b	7a	7b	10a	10b	10c	64a	64b	64c
SiO_2	37.51	37.57	36.95	37.30	37.22	37.58	36.62	37.75	38.42	38.23
Al_2O_3	20.18	22.13	24.17	24.51	21.30	21.27	21.63	23.00	24.74	25.89
Fe_2O_3*	17.24	14.26	11.14	10.98	15.21	15.95	14.53	12.65	10.70	9.51
MgO	0.05	0.03	0.04	0.02	0.14	0.25	0.61	0.02	0.00	0.06
CaO	22.80	22.72	23.78	23.66	23.19	23.30	22.80	23.35	22.79	23.08
Na_2O	0.08	-	0.01	-	0.00	0.28	0.45	-	-	-
MnO	0.13	-	-	-	0.09	0.10	0.08	0.10	0.08	0.06
Total	98.20	97.71	96.73	96.09	96.49	97.15	98.51	96.72	96.86	96.74
					Structural Formula (O,OH)=13					
Si	3.069	3.035	2.984	2.994	3.013	3.002	2.978	3.033	3.056	3.028
Al^{iv}_{vi}	0.000	0.000	0.016	0.006	0.000	0.000	0.022	0.000	0.000	0.000
Al	1.895	2.106	2.285	2.313	2.032	2.002	2.050	2.178	2.319	2.416
Fe^{3+}	1.034	.867	.677	.663	.927	.959	.889	.765	.640	.567
Mg	.006	.004	.005	.002	.017	.030	.074	.002	.000	.007
Ca	1.947	1.966	2.058	2.035	2.011	1.994	1.986	2.010	1.942	1.959
Na	.012	.000	.000	.000	.000	.043	.071	.000	.000	.000
Mn	.009	-	-	-	.006	.007	.006	.007	.005	.003
Mole percent AlFe epidote¢	100	89	70	68	97	99	95	81	67	58

* - Fe_2O_3 calculated as 1.11 times FeO.
¢ - percent of $Ca_2Al_2FeSi_3O_{12}(OH)$.

APPENDIX III, TABLE III (Cont'd)

	64d	64e	170a$	170b	170c	170d	70a	70b	70c
SiO_2	37.72	38.51	38.83	39.30	39.23	39.39	38.53	37.01	38.23
Al_2O_3	25.73	26.02	29.39	29.74	29.60	29.52	33.71	31.92	33.00
Fe_2O_3	10.55	9.74	4.66	4.09	4.00	4.35	3.82	4.65	3.95
MgO	0.04	0.05	0.03	0.11	0.03	0.83	0.20	3.10	0.20
CaO	22.88	23.20	23.30	23.36	23.86	22.84	22.15	20.50	23.18
Na_2O	-	-	-	-	-	-	0.03	0.00	0.00
MnO	0.07	0.03	0.05	0.13	0.08	0.07	0.02	0.00	0.00
Total	97.12	97.71	96.02	96.71	96.79	97.02	98.46	97.18	98.56
				Structural Formula (O,OH)=13					
Si	2.994	3.028	3.035	3.049	3.046	3.046	2.918	2.851	2.907
Al^{iv}	.006	.000	.000	.000	.000	.000	.082	.149	.093
Al^{vi}	2.401	2.411	2.707	2.719	2.708	2.690	2.926	2.748	2.863
Fe^{3+}	.630	.576	.274	.239	.234	.253	.218	.270	.226
Mg	.005	.006	.003	.013	.003	.096	.023	.356	.023
Ca	1.946	1.954	1.951	1.942	1.985	1.892	1.797	1.692	1.888
Na	-	-	-	-	-	-	.004	.000	.000
Mn	.005	.002	.003	.009	.005	.005	.001	.000	.000
Mole percent AlFe epidote	61	58	28	25	25	27	19	27	21

$ - Specimen BC-73-170.

APPENDIX III, TABLE IV

Plagioclase, amphibole, chlorite and sericite analyses.*

	Plagioclase				Amphibole			Chlorite		Sericite	
	1a	1b	1c	93	73a	73b	1	26	47	69a	69b
SiO_2	52.29	67.22	68.72	50.71	52.47	51.93	56.97	35.83	27.97	50.75	47.98
TiO_2	.12	.03	-	-	.13	.11	.01	-	-	-	-
Al_2O_3	29.58	20.81	19.92	29.80	4.13	3.77	1.03	15.20	17.40	35.14	35.32
FeO	.82	.59	.08	.58	10.37	10.88	8.18	17.61	12.23	1.14	1.18
MgO	.27	.15	.05	.21	18.86	17.85	18.88	17.55	25.40	.89	1.28
CaO	13.44	1.15	.61	13.85	11.01	10.93	12.75	3.17	.01	.39	.00
Na_2O	3.05	8.92	10.91	3.14	.82	.66	.19	.18	-	.16	.19
K_2O	.14	.23	.23	.09	-	-	-	-	-	9.25	9.07
MnO	-	-	-	-	.29	.23	.30	-	-	.15	.01
Cr_2O_3	-	-	-	-	-	-	-	-	2.18	-	-
Total	99.71	99.10	100.52	98.43	98.17	96.37	98.31	89.56	85.18	97.88	95.02
					Structural Formulae						
		O=32				(O,OH)=24			(O,OH)=36		(O,OH)=24
Si	9.539	11.820	11.940	9.388	7.447	7.515	7.948	7.016	5.700	6.472	6.310
Al^{iv}	6.359	4.312	4.078	6.501	.553	.485	.052	.984	2.300	1.528	1.690
Al^{vi}					.137	.158	.118	2.523	1.879	3.752	3.783
Fe	.125	.087	.012	.090	1.231	1.317	.954	2.884	2.084	.122	.130
Mg	.073	.039	.013	.058	3.990	3.850	3.926	5.122	7.716	.169	.251
Ca	2.627	.217	.114	2.747	1.674	1.695	1.906	.665	.003	.053	.000
Na	1.079	3.041	3.675	1.127	.226	.185	.051	-	-	.040	.048
K	.033	.039	.051	.021	-	-	-	-	-	1.505	1.521
Mn	-	-	-	-	.035	.028	.035	-	-	.016	.001
Cr	-	-	-	-	-	-	-	-	.351	-	-
Ab	28.9	91.9	95.7	28.9							
An	70.3	6.6	3.0	70.5							
Or	0.8	1.5	1.3	0.5							

* - Analyses expressed as weight percent oxides.

APPENDIX IV

Fortran IV Computer Program PMELT

A. Introduction

PMELT was written by the author to facilitate calculation of trace element fractionation models during both partial melting and fractional crystallization processes. For both processes, the following input is required: 1) the number of elements used, 2) the names of the elements, 3) the number of minerals, 4) the names of the minerals, 5) the mineral/liquid distribution coefficients, 6) trace element contents in the source material or parent liquid. In fractional crystallization calculations, the weight proportions of the minerals to be fractionated should also be input. In partial melting calculations, the source modal proportions, the weight proportions of liquid contributed by each phase at some small degree of melting and the weight proportion of the liquid contributed by each phase at the highest degree of melting in the particular melting interval considered are required. These parameters can be estimated from experimental data. The program then calculates trace element values in the liquid at various degrees of partial melting or fractional crystallization. Equations for the partial melting calculations are based on non-modal batch melting in which the liquid can either be eutectic or can vary in composition between set limits. Both surface and total

equilibrium fractional crystallization equations are included. The program can be used to model partial melting by inputting various values for source composition and liquid composition until a satisfactory agreement between observed and calculated trace element values of the liquid is attained. The validity of fractionating one rock from another can also be tested.

B. Procedure for the use of PMELT

Since both partial melting and fractional crystallization calculations can be done, general information necessary for both sets of calculations is input first. The data cards are numbered in the order in which they should occur in the data deck and a Fortran format is indicated for each card. The layout for running PMELT is as follows:

Control cards

7/8/9 card

PMELT program

7/8/9 card

Data deck:

CARD 1: n, m, Kopt (in this order), where n is the number of elements considered, m is the number of minerals and Kopt is the option utilized: either fractional crystallization (0) or partial melting (1). Note that Kopt can only be 0 or 1.

Format (3I4).

CARD 2: contains a list of element names (up to 4 letters for each name). Format (12A4).

CARD 3: contains a list of mineral names (up to 8 letters long). Format (10A8).

CARDS 4 to 13 (max. number of cards = 10): contains mineral/liquid distribution coefficients. Format (12F6.2). N.B. It is important that a specific order be followed in listing the distribution coefficients. The order depends upon the order in which the element and mineral names were listed above. The distribution coefficients should appear as follows:

KD for element(1)mineral(1), element(1)mineral(2), ..., element(1)mineral(m),..., element(2)mineral(1), ..., element(2)mineral(m),..., element(n)mineral(1), ..., element(n)mineral(m).

The succeeding cards will be numbered assuming that the maximum number of cards was used to list the distribution coefficients although this is unusual in most applications.

CARD 14: contains the trace element concentrations (ppm) in the source composition (for partial melting when Kopt=1) or in the initial unfractionated liquid (for fractional crystallization; Kopt=0). Format (10F7.2).

CARD 15: For partial melting (Kopt=1), this card contains modal weight proportions of minerals in the source being melted. For fractional crystallization (Kopt=0),

this card contains the modal weight fraction of minerals fractionated. The order of listing of weight fractions on the card must correspond to the order of listing of mineral names in card 3. A blank field can occur if a particular mineral listed in card 3 is not used in the calculations. Format (10F5.3).

N.B. For fractional crystallization calculations, this is all the information necessary. Card 15 can be repeated as many times as desired to involve any number of fractionating groups of minerals in the calculations. The following cards are only required for partial melting processes. Two possible situations during partial melting are considered 1) only 1 melting interval is involved, i.e. no phases disappear in the melting interval considered, 2) more than one melting interval occurs, i.e. phases disappear completely from the source at some degree of melting within the range of partial melting considered.

1) No phases disappear <u>within</u> the melting interval.

CARD 16: contains the number 1. Format (I2).

CARD 17: contains the upper limit of % melting considered. maximum(100). Format (I3).

CARD 18: contains weight fractions of the liquid contributed by each phase in the source at some very small degree of melting. Order of weight fractions should be the same as the order of mineral names listed in card 3. Format (10F5.3).

CARD 19: contains weight fractions of liquid, at the

upper limit of melting in the melting interval, contributed by each phase. Order of listing as in card 18. Format (10F5.3).

Note: Cards 18 & 19 will be identical if eutectic melting is considered to have taken place over the entire melting interval.

Cards 15 to 19 can be repeated as many times as desired to model various source modal and liquid modal compositions.

2) Phases disappear from source during melting. In this case separate melting intervals have to be considered, the separation of the intervals being determined by the point at which a phase disappears. For example, consider a source with olivine, orthopyroxene and clinopyroxene which is melted so that cpx disappears from the residue at 30% melting and orthopyroxene disappears at 50% melting. Then the calculations have to be done separately for interval I (from 0-30%), interval II (from 30-50%) and interval III (from 50-100%). In a case such as this, the cards following card 15 are:

CARD 16: contains variable np, which is the total number of phases to disappear (excluding the phases lost at the upper limit of melting) plus 1. For the above example, np= 2 + 1=3. Format (I2).

CARD 17: percent melting at which phases disappear and the upper limit of melting in ascending numerical

order. In other words, these numbers define the interval limit. For the case above, 30, 50, 100 would appear on this card. Format (10I3). Note that the number of numbers on this card must equal np.

CARDS 18 & 19: same as in the case in which no phases disappear except that these two cards must be repeated as many times as there are melting intervals. For example in the case above, cards 18 & 19 are repeated 3 times; the first two containing the liquid modal composition at low degree and the highest degree (30) in interval I, the second two define the changing liquid composition in interval II. Note that the liquid composition in interval II should be estimated from the new source at 30% melting (a source with only ol and opx). In interval III, only olivine is in the source at 50% so that the liquid modal composition at some small degree of melting in interval III will be 100% olivine as will be the liquid composition at the highest degree of melting in the interval. Note that when separate melting intervals are considered, the liquids derived at the beginning and end of each interval (cards 18 and 19) are estimated as if a completely new source is being melted.

As in the case where no phases disappear, cards 15 through 19 can be repeated as many times as desired.

7/8/9 card
6/7/8/9 card

C. Listing of Program PMELT.

```
PROGRAM PMELT      73/73   OPT=1                FTN 4.6+433        30/04/77  14.01.57      PAGE     1

      1               PROGRAM PMELT(INPUT,OUTPUT,TAPE5=INPUT,TAPE6=OUTPUT)
                    C     PROGRAM PMELT R.A. COISH JANUARY 1977
                    C     THE PROGRAM PMELT CAN BE UTILIZED TO EITHER 1) CALCULATE TRACE ELE
                    C     MENT CONCENTRATIONS IN A LIQUID AFTER VARIOUS DEGREES OF PARTIAL
      5             C     MELTING OF A SOURCE COMPOSITION OR 2) CALCULATE THE TRACE ELEMENT
                    C     CONTENT OF A LIQUID FRACTIONATED FROM A PARENT LIQUID
                    C     EQUATIONS ARE FROM ARTH(1976),J.RES.U.S.G.S.,4,P.41 AND FROM
                    C     HERTOGEN AND GIJBELS(1976),GEOCHIM.COSMO.ACTA,40,P.313.
                          DIMENSION NAM(12),MN(10),CK(12,10),X(10,20),Y(10,20),Z(10,20),CO(5
     10                  $0),C(50),P(150),CT(50),P2(150),CA(150,20),MGA(20)
                          READ(5,10) N,M,KOPT
                       10 FORMAT(3I4)
                    C     N IS THE NUMBER OF ELEMENTS, M IS THE NUMBER OF MINERALS, KOPT IS
                    C     0 FOR FRACTIONAL CRYSTALLIZATION OR 1 FOR PARTIAL MELTING .
     15                   READ(5,11) (NAM(I),I=1,N)
                       11 FORMAT(12A4)
                    C     NAM IS AN ARRAY CONTAINING ELEMENT NAMES.
                          READ(5,12)(MN(I),I=1,M)
                       12 FORMAT(10A8)
     20             C     MN IS AN ARRAY OF MINERAL NAMES.
                          READ(5,13)((CK(I,J),J=1,M),I=1,N)
                       13 FORMAT(12F6.2)
                    C     CK IS A TWO DIMENSIONAL ARRAY OF MINERAL/LIQUID DISTRIBUTION
                    C     COEFFICIENTS.
     25                   WRITE(6,59)
                       59 FORMAT(1H1,*VALUES OF DISTRIBUTION COEFFICIENTS*//)
                          WRITE(6,58) ((NAM(I),MN(J),CK(I,J),J=1,M),I=1,N)
                       58 FORMAT(1H ,   4(A4,*(*,A8,*/LIQUID)=*,F6.2,3X),/,1X)
                          READ(5,16) (CO(I),I=1,N)
     30                16 FORMAT(10F7.2)
                    C     CO IS ARRAY OF TRACE ELEMENT CONTENTS IN THE SOURCE ROCK FOR
                    C     EITHER PARTIAL MELTING OR FRACTIONAL CRYSTALLIZATION.
                       30 READ(5,14) (X(1,J),J=1,M)
                       14 FORMAT(10F5.3)
     35             C     X CONTAINS WEIGHT PROPORTIONS OF MINERALS IN SOURCE FOR PARTIAL
                    C     MELTING OR WEIGHT FRACTIONS OF MINERALS CRYSTALLIZED.
                          IF(EOF(5)) 6000,40
                       40 IF (KOPT.EQ.0) GO  TO 2000
                          READ(5,91) NP
     40                91 FORMAT(I2)
                          READ(5,92) (MGA(I),I=1,NP)
                       92 FORMAT(10I3)
                          DO 3000 L=1,NP
                          READ(5,14) (Y(L,J),J=1,M)
     45             C     Y CONTAINS WEIGHT FRACTIONS OF MINERALS IN LIQUID AT SMALL DEGREE
                    C     OF PARTIAL MELTING IN A GIVEN MELTING INTERVAL.
                          READ(5,14) (Z(L,J),J=1,M)
                    C     Z IS AN ARRAY CONTAINING WEIGHT FRACTION OF LIQUID CONTRIBUTED
                    C     BY SOURCE MINERALS AT HIGHEST DEGREE OF MELTING IN MELTING INTERVAL.
     50             3000 CONTINUE
                          WRITE(6,50)
                       50 FORMAT(1H1,////,28X,*CALCULATION OF TRACE ELEMENT PARTIAL MELTING
                         $MODELS*)
                          WRITE(6,51)
     55                51 FORMAT(1H0,//  ,1X,*SOURCE MODAL COMPOSITION*)
                          WRITE(6,52) (X(1,J),MN(J),J=1,M)
                       52 FORMAT(1H ,10(F5.3,A8))
```

D. Sample Calculations

VALUES OF DISTRIBUTION COEFFICIENTS

CR(OLIVINE/LIQUID)= .20	CR(ORTHOPX/LIQUID)= 2.00	CR(CLINOPX/LIQUID)= 10.00	CR(SPINEL /LIQUID)= 10.00
CR(GARNET /LIQUID)= 2.00	CR(PLAG /LIQUID)= .01	CR(AMPHIB /LIQUID)= 12.00	NI(OLIVINE/LIQUID)= 12.00
NI(ORTHOPX/LIQUID)= 1.10	NI(CLINOPX/LIQUID)= 2.00	NI(SPINEL /LIQUID)= 5.00	NI(GARNET /LIQUID)= .40
NI(PLAG /LIQUID)= .01	NI(AMPHIB /LIQUID)= 3.00	TI(OLIVINE/LIQUID)= .01	TI(ORTHOPX/LIQUID)= .06
TI(CLINOPX/LIQUID)= .30	TI(SPINEL /LIQUID)= .40	TI(GARNET /LIQUID)= 0.00	TI(PLAG /LIQUID)= .01
TI(AMPHIB /LIQUID)= 0.00	LA(OLIVINE/LIQUID)= .01	LA(ORTHOPX/LIQUID)= .02	LA(CLINOPX/LIQUID)= .12
LA(SPINEL /LIQUID)= .10	LA(GARNET /LIQUID)= .01	LA(PLAG /LIQUID)= .14	LA(AMPHIB /LIQUID)= .16
CE(OLIVINE/LIQUID)= .01	CE(ORTHOPX/LIQUID)= .03	CE(CLINOPX/LIQUID)= .15	CE(SPINEL /LIQUID)= .08
CE(GARNET /LIQUID)= .03	CE(PLAG /LIQUID)= .10	CE(AMPHIB /LIQUID)= .20	SM(OLIVINE/LIQUID)= .01
SM(ORTHOPX/LIQUID)= .05	SM(CLINOPX/LIQUID)= .50	SM(SPINEL /LIQUID)= .05	SM(GARNET /LIQUID)= .30
SM(PLAG /LIQUID)= .07	SM(AMPHIB /LIQUID)= .50	EU(OLIVINE/LIQUID)= .01	EU(ORTHOPX/LIQUID)= .05
EU(CLINOPX/LIQUID)= .51	EU(SPINEL /LIQUID)= .03	EU(GARNET /LIQUID)= .50	EU(PLAG /LIQUID)= .34
EU(AMPHIB /LIQUID)= .60	TB(OLIVINE/LIQUID)= .01	TB(ORTHOPX/LIQUID)= .12	TB(CLINOPX/LIQUID)= .31
TB(SPINEL /LIQUID)= .02	TB(GARNET /LIQUID)= 1.70	TB(PLAG /LIQUID)= .05	TB(AMPHIB /LIQUID)= .65
DY(OLIVINE/LIQUID)= .01	DY(ORTHOPX/LIQUID)= .15	DY(CLINOPX/LIQUID)= .21	DY(SPINEL /LIQUID)= .05
DY(GARNET /LIQUID)= 3.17	DY(PLAG /LIQUID)= .06	DY(AMPHIB /LIQUID)= .64	ER(OLIVINE/LIQUID)= .01
ER(ORTHOPX/LIQUID)= .23	ER(CLINOPX/LIQUID)= .65	ER(SPINEL /LIQUID)= .06	ER(GARNET /LIQUID)= 6.56
ER(PLAG /LIQUID)= .03	ER(AMPHIB /LIQUID)= .55	YB(OLIVINE/LIQUID)= .01	YB(ORTHOPX/LIQUID)= .34
YB(CLINOPX/LIQUID)= .62	YB(SPINEL /LIQUID)= .02	YB(GARNET /LIQUID)= 11.50	YB(PLAG /LIQUID)= .03
YB(AMPHIB /LIQUID)= .50	LU(OLIVINE/LIQUID)= .01	LU(ORTHOPX/LIQUID)= .42	LU(CLINOPX/LIQUID)= .56
LU(SPINEL /LIQUID)= .02	LU(GARNET /LIQUID)= 11.90	LU(PLAG /LIQUID)= .06	LU(AMPHIB /LIQUID)= .45

```
                PO=0.0
                PA=0.0
                DO 9500 J=1,M
                X(L,J)=(X(K,J)-(Z(K,J)*FLOAT(MDF)/100.0))/(1.0-(FLOAT(MDF)/100.0))
          C     X HERE, IS THE CALCULATED SOURCE AT THE POINT OF COMPLETE LOSS OF
          C     A PHASE.
                DA=X(L,J)*CK(I,J)+DA
                PO=Y(L,J)*CK(I,J)+PO
                PA=Z(L,J)*CK(I,J)+PA
           9500 CONTINUE
                DO 8500 MF=MFA,MFB,5
                FS=((FLOAT(MF)-FLOAT(MFA))/100.0)/(1.0-(FLOAT(MFA)/100.0))
                P2(MF)=PO+((PA-PO)*FLOAT(MF)/100.0)
                D=(DA-(FS*P2(MF)))/(1-FS)
                CP1=1.0/(FLOAT(MF)/100.0)*C(I)
                CP2=DA*(1-(FLOAT(MFA)/100.0))*(FLOAT(MF)/100.0)
                CP3=D*(FLOAT(MFA)/100.0)*(1-(FLOAT(MF)/100.0))
                CP4=(D*(1-(FLOAT(MF)/100.0)))+(FLOAT(MF)/100.0)
                CA(MF,I)=CP1*((FLOAT(MFA)/100.0)+((CP2-CP3)/CP4))
          C     CA CONTAINS CALCULATED TRACE ELEMENT CONTENTS IN LIQUID.
           8500 CONTINUE
                MF=MFB
                C(I)=CA(MF,I)
           7500 CONTINUE
                DO 7502 MF=MFA,MFB,5
                WRITE(6,61) MF, (CA(MF,I),I=1,N)
           7502 CONTINUE
                GO TO 8501
            201 WRITE(6,63) (CO(I),I=1,N)
             63 FORMAT(1H0,*INITIAL*/1X,*CONC.*,3X,12F9.2)
                IF(KOPT.EQ.0) GO TO 30
                IF (NP.EQ.1) GO TO 30
                DO 501 L=2,NP
                K=L-1
                WRITE(6,502) MGA(K)
            502 FORMAT (1H0,//    ,1X,*CALCULATED SOURCE COMPOSITION AT*,I3,*X
               $PARTIAL MELTING*)
                WRITE(6,52) (X(L,J),MN(J),J=1,M)
            501 CONTINUE
                GO TO 30
          C
          C
          C     CALCULATIONS OF FRACTIONAL CRYSTALLIZATION MODELS BEGINS.
           2000 WRITE(6,2001)
           2001 FORMAT(1H1,////,1X,   *CALCULATION OF TRACE ELEMENT FRACTIONAL CRY
               $STALLIZATION MODELS FOR SURFACE EQUILIBRIUM(SEQ),TOTAL EQUILIBRIUM
               $(TEQ).*)
                WRITE(6,2002)
           2002 FORMAT(1H0,   1X,*WEIGHT PROPORTION OF MINERALS FRACTIONATED*)
                WRITE(6,2003) (X(1,J),MN(J),J=1,M)
           2003 FORMAT(1H ,10(F5.3,A8))
                WRITE(6,55)
                WRITE(6,2004) (NAM(I),I=1,N)
           2004 FORMAT(1H0,*X XSTAL*,4X,12(A4,5X),/)
                DO 9000 MFX=5,95,5
                FX=(100.0-FLOAT(MFX))/100.0
                DO 8000 I=1,N
```

```
                      Dx=0.0
                      DO 7000 J=1,M
                      DX=X(1,J)*CK(I,J)+DX
    175           7000 CONTINUE
                      C(I)=CO(I)*(FX**(DX-1))
                      CT(I)=CO(I)/(FX*(DX*(1-FX)))
                 8000 CONTINUE
                      WRITE(6,5000) MFX,(C(K),K=1,N)
    183           5000 FORMAT(1H ,I3,*(SEQ)*,12F9.2)
                      WRITE(6,5005) (CT(K),K=1,N)
                 5005 FORMAT(1H ,3X,*(TEQ)*,12F9.2)
                 9000 CONTINUE
                      GO TO 201
    185           6000 STOP
                      END
```

SYMBOLIC REFERENCE MAP (R=1)

ENTRY POINTS
4114 PMELT

VARIABLES	SN	TYPE	RELOCATION				
7143	C	REAL	ARRAY	7763	CA	REAL	ARRAY
5541	CK	REAL	ARRAY	7061	CO	REAL	ARRAY
5504	CP1	REAL		5505	CP2	REAL	
5506	CP3	REAL		5507	CP4	REAL	
7653	CT	REAL	ARRAY	5473	D	REAL	
5502	DA	REAL		5512	DX	REAL	
5503	FS	REAL		5511	FX	REAL	
5465	I	INTEGER		5466	J	INTEGER	
5476	K	INTEGER		5464	KOPT	INTEGER	
5477	K1	INTEGER		5470	L	INTEGER	
5463	M	INTEGER		5501	MDF	INTEGER	
5472	MF	INTEGER		5471	MFA	INTEGER	
5500	MFB	INTEGER		5510	MFX	INTEGER	
15653	MGA	INTEGER	ARRAY	5527	MN	INTEGER	ARRAY
5462	N	INTEGER		5513	NAM	INTEGER	ARRAY
5467	NP	INTEGER		7225	P	REAL	ARRAY
5475	PA	REAL		5474	PO	REAL	
7535	P2	REAL	ARRAY	5731	X	REAL	ARRAY
6241	Y	REAL	ARRAY	6551	Z	REAL	ARRAY

FILE NAMES	MODE						
0 INPUT		2043	OUTPUT	0	TAPE5	FMT	2043 TAPE6 FMT

EXTERNALS	TYPE	ARGS
EOF	REAL	1

INLINE FUNCTIONS	TYPE	ARGS	
FLOAT	REAL	1	INTRIN

D. Sample Calculations

VALUES OF DISTRIBUTION COEFFICIENTS

CR(OLIVINE/LIQUID)= .20	CR(ORTHOPX/LIQUID)= 2.00	CR(CLINOPX/LIQUID)= 10.00	CR(SPINEL /LIQUID)= 10.00
CR(GARNET /LIQUID)= 2.00	CR(PLAG /LIQUID)= .01	CR(AMPHIB /LIQUID)= 12.00	NI(OLIVINE/LIQUID)= 12.00
NI(ORTHOPX/LIQUID)= 1.10	NI(CLINOPX/LIQUID)= 2.00	NI(SPINEL /LIQUID)= 5.00	NI(GARNET /LIQUID)= .40
NI(PLAG /LIQUID)= .01	NI(AMPHIB /LIQUID)= 3.00	TI(OLIVINE/LIQUID)= .01	TI(ORTHOPX/LIQUID)= .06
TI(CLINOPX/LIQUID)= .30	TI(SPINEL /LIQUID)= .40	TI(GARNET /LIQUID)= 0.00	TI(PLAG /LIQUID)= .01
TI(AMPHIB /LIQUID)= 0.00	LA(OLIVINE/LIQUID)= .01	LA(ORTHOPX/LIQUID)= .02	LA(CLINOPX/LIQUID)= .12
LA(SPINEL /LIQUID)= .10	LA(GARNET /LIQUID)= .01	LA(PLAG /LIQUID)= .14	LA(AMPHIB /LIQUID)= .16
CE(OLIVINE/LIQUID)= .01	CE(ORTHOPX/LIQUID)= .03	CE(CLINOPX/LIQUID)= .15	CE(SPINEL /LIQUID)= .08
CE(GARNET /LIQUID)= .03	CE(PLAG /LIQUID)= .10	CE(AMPHIB /LIQUID)= .20	SM(OLIVINE/LIQUID)= .01
SM(ORTHOPX/LIQUID)= .05	SM(CLINOPX/LIQUID)= .50	SM(SPINEL /LIQUID)= .05	SM(GARNET /LIQUID)= .30
SM(PLAG /LIQUID)= .07	SM(AMPHIB /LIQUID)= .50	EU(OLIVINE/LIQUID)= .01	EU(ORTHOPX/LIQUID)= .05
EU(CLINOPX/LIQUID)= .51	EU(SPINEL /LIQUID)= .03	EU(GARNET /LIQUID)= .50	EU(PLAG /LIQUID)= .34
EU(AMPHIB /LIQUID)= .60	TB(OLIVINE/LIQUID)= .01	TB(ORTHOPX/LIQUID)= .12	TB(CLINOPX/LIQUID)= .31
TB(SPINEL /LIQUID)= .02	TB(GARNET /LIQUID)= 1.70	TB(PLAG /LIQUID)= .05	TB(AMPHIB /LIQUID)= .65
DY(OLIVINE/LIQUID)= .01	DY(ORTHOPX/LIQUID)= .15	DY(CLINOPX/LIQUID)= .21	DY(SPINEL /LIQUID)= .05
DY(GARNET /LIQUID)= 3.17	DY(PLAG /LIQUID)= .06	DY(AMPHIB /LIQUID)= .64	ER(OLIVINE/LIQUID)= .01
ER(ORTHOPX/LIQUID)= .23	ER(CLINOPX/LIQUID)= .65	ER(SPINEL /LIQUID)= .06	ER(GARNET /LIQUID)= 6.56
ER(PLAG /LIQUID)= .03	ER(AMPHIB /LIQUID)= .55	YB(OLIVINE/LIQUID)= .01	YB(ORTHOPX/LIQUID)= .34
YB(CLINOPX/LIQUID)= .62	YB(SPINEL /LIQUID)= .02	YB(GARNET /LIQUID)= 11.50	YB(PLAG /LIQUID)= .03
YB(AMPHIB /LIQUID)= .50	LU(OLIVINE/LIQUID)= .01	LU(ORTHOPX/LIQUID)= .42	LU(CLINOPX/LIQUID)= .56
LU(SPINEL /LIQUID)= .02	LU(GARNET /LIQUID)= 11.90	LU(PLAG /LIQUID)= .06	LU(AMPHIB /LIQUID)= .45

CALCULATION OF TRACE ELEMENT PARTIAL MELTING MODELS

SOURCE MODAL COMPOSITION
.510 OLIVINE .210 ORTHOPX .230 CLINOPX .050 SPINEL 0.000 GARNET 0.000 PLAG 0.000 AMPHIB

WEIGHT FRACTION OF LIQUID CONTRIBUTED BY EACH PHASE AT SMALL DEGREE OF MELTING IN MELTING INTERVAL 1
.010 OLIVINE .200 ORTHOPX .690 CLINOPX .100 SPINEL 0.000 GARNET 0.000 PLAG 0.000 AMPHIB

WEIGHT FRACTION OF LIQUID CONTRIBUTED BY EACH PHASE AT F= 100% PARTIAL MELTING
.510 OLIVINE .210 ORTHOPX .230 CLINOPX .050 SPINEL 0.000 GARNET 0.000 PLAG 0.000 AMPHIB

CALCULATED CONCENTRATION(PPM) TRACE ELEMENTS IN THE LIQUID

% MELT	CR	NI	TI	LA	CE	SM	EU	TB	DY	ER	YB	LU
5	942.97	286.21	10407.56	4.47	13.38	3.6.	1.44	1.42	9.64	3.45	3.42	.56
10	1059.96	290.25	8227.56	2.94	9.08	3.06	1.20	1.11	7.28	3.09	3.08	.50
15	1197.22	295.46	6779.23	2.18	6.86	2.60	1.02	.91	5.84	2.78	2.78	.45
20	1358.70	301.96	5747.65	1.74	5.50	2.26	.89	.77	4.86	2.52	2.53	.41
25	1548.89	309.91	4975.95	1.44	4.59	1.99	.78	.66	4.[illegible]	2.29	2.31	.38
30	1772.60	319.52	4377.18	1.23	3.93	1.77	.69	.58	3.63	2.09	2.12	.35
35	2034.37	331.07	3899.38	1.07	3.43	1.58	.62	.52	3.21	1.92	1.95	.32
40	2337.23	344.92	3509.23	.95	3.05	1.43	.56	.47	2.88	1.77	1.80	.30
45	2680.58	361.55	3184.94	.85	2.74	1.31	.51	.42	2.61	1.63	1.67	.27
50	3056.77	381.62	2911.21	.77	2.48	1.20	.47	.39	2.38	1.51	1.55	.25
55	3446.79	406.04	2677.16	.70	2.27	1.10	.43	.36	2.19	1.40	1.45	.24
60	3816.79	436.09	2474.82	.65	2.09	1.02	.40	.33	2.02	1.31	1.35	.22
65	4119.16	473.63	2298.24	.60	1.93	.95	.37	.31	1.88	1.22	1.27	.21
70	4302.40	521.52	2142.84	.56	1.80	.88	.35	.28	1.75	1.14	1.19	.20
75	4329.34	584.29	2005.08	.52	1.68	.82	.32	.27	1.64	1.07	1.12	.18
80	4194.13	669.62	1882.16	.49	1.58	.77	.30	.25	1.54	1.01	1.05	.17
85	3925.14	791.65	1771.85	.46	1.48	.73	.29	.24	1.46	.95	.99	.16
90	3571.43	979.53	1672.33	.43	1.40	.68	.27	.22	1.38	.89	.94	.16
95	3183.45	1304.63	1582.12	.41	1.33	.64	.25	.21	1.31	.85	.89	.15
100	2800.00	2000.00	1500.00	.39	1.26	.61	.24	.20	1.24	.80	.84	.14
INITIAL CONC.	2800.00	2000.00	1500.00	.39	1.26	.61	.24	.20	1.24	.80	.84	.14

CALCULATION OF TRACE ELEMENT PARTIAL MELTING MODELS

SOURCE MODAL COMPOSITION
.510 OLIVINE .210 ORTHOPX .230 CLINOPX .050 SPINEL 0.000 GARNET 0.000 PLAG 0.000 AMPHIB

WEIGHT FRACTION OF LIQUID CONTRIBUTED BY EACH PHASE AT SMALL DEGREE OF MELTING IN MELTING INTERVAL 1
.010 OLIVINE .200 ORTHOPX .690 CLINOPX .100 SPINEL 0.000 GARNET 0.000 PLAG 0.000 AMPHIB

WEIGHT FRACTION OF LIQUID CONTRIBUTED BY EACH PHASE AT F= 100% PARTIAL MELTING
.510 OLIVINE .210 ORTHOPX .230 CLINOPX .050 SPINEL 0.000 GARNET 0.000 PLAG 0.000 AMPHIB

CALCULATED CONCENTRATION(PPM) TRACE ELEMENTS IN THE LIQUID

% MELT	CR	NI	TI	LA	CE	SM	EU	TB	DY	ER	YB	LU
5	942.97	286.21	10407.56	4.47	13.38	3.68	1.44	1.42	9.64	3.45	3.42	.56
10	1059.96	290.25	8227.56	2.94	9.08	3.06	1.20	1.11	7.28	3.09	3.08	.50
15	1197.22	295.46	6779.23	2.18	6.86	2.60	1.02	.91	5.84	2.78	2.78	.45
20	1358.70	301.96	5747.65	1.74	5.50	2.26	.89	.77	4.86	2.52	2.53	.41
25	1548.69	309.91	4975.95	1.44	4.59	1.99	.78	.66	4.16	2.29	2.31	.38
30	1772.60	319.52	4377.18	1.23	3.93	1.77	.69	.58	3.63	2.09	2.12	.35
35	2034.37	331.07	3899.30	1.07	3.43	1.58	.62	.52	3.21	1.92	1.95	.32
40	2337.23	344.92	3509.23	.95	3.05	1.43	.56	.47	2.88	1.77	1.80	.30
45	2680.58	361.55	3184.94	.85	2.74	1.31	.51	.42	2.61	1.63	1.67	.27
50	3056.77	381.62	2911.21	.77	2.48	1.20	.47	.39	2.38	1.51	1.55	.25
55	3446.79	406.04	2677.16	.70	2.27	1.10	.43	.36	2.19	1.40	1.45	.24
60	3816.79	436.09	2474.82	.65	2.09	1.02	.40	.33	2.02	1.31	1.35	.22
65	4109.16	473.63	2298.24	.60	1.93	.95	.37	.31	1.88	1.22	1.27	.21
70	4302.40	521.52	2142.84	.56	1.80	.88	.35	.28	1.75	1.14	1.19	.20
75	4329.34	584.29	2005.08	.52	1.68	.82	.32	.27	1.64	1.07	1.12	.18
80	4194.13	669.62	1882.16	.49	1.58	.77	.30	.25	1.54	1.01	1.05	.17
85	3925.14	791.65	1771.85	.46	1.48	.73	.29	.24	1.46	.95	.99	.16
90	3571.43	979.53	1672.33	.43	1.40	.69	.27	.22	1.38	.89	.94	.16
95	3183.45	1304.63	1582.12	.41	1.33	.64	.25	.21	1.31	.85	.89	.15
100	2800.00	2000.00	1500.00	.39	1.26	.61	.24	.20	1.24	.80	.84	.14
INITIAL CONC.	2800.00	2000.00	1500.00	.39	1.26	.61	.24	.20	1.24	.80	.84	.14

CALCULATION OF TRACE ELEMENT PARTIAL MELTING MODELS

SOURCE MODAL COMPOSITION
.650 OLIVINE .190 ORTHOPX .140 CLINOPX .020 SPINEL 0.000 GARNET 0.000 PLAG 0.000 AMPHIB

WEIGHT FRACTION OF LIQUID CONTRIBUTED BY EACH PHASE AT SMALL DEGREE OF MELTING IN MELTING INTERVAL 1
.010 OLIVINE .100 ORTHOPX .800 CLINOPX .090 SPINEL 0.000 GARNET 0.000 PLAG 0.000 AMPHIB

WEIGHT FRACTION OF LIQUID CONTRIBUTED BY EACH PHASE AT F= 100% PARTIAL MELTING
.650 OLIVINE .190 ORTHOPX .140 CLINOPX .020 SPINEL 0.000 GARNET 0.000 PLAG 0.000 AMPHIB

CALCULATED CONCENTRATION(PPM) TRACE ELEMENTS IN THE LIQUID

% MELT	CR	NI	TI	LA	CE	SM	EU	YB	DY	ER	YB	LU
5	1668.04	229.03	10543.42	0.00	8.41	1.63	.59	.45	0.00	0.00	1.64	.31
10	2097.51	231.94	7755.65	0.00	5.38	1.21	.47	.34	0.00	0.00	1.44	.27
15	2730.94	235.86	6097.41	0.00	3.94	.98	.38	.27	0.00	0.00	1.27	.24
20	3734.66	240.87	4998.91	0.00	3.11	.83	.32	.22	0.00	0.00	1.12	.21
25	5509.11	247.13	4218.40	0.00	2.56	.71	.28	.19	0.00	0.00	1.00	.19
30	9307.37	254.81	3635.79	0.00	2.17	.61	.24	.16	0.00	0.00	.90	.17
35	21961.47	264.14	3184.67	0.00	1.88	.54	.21	.14	0.00	0.00	.82	.16
40	*********	275.46	2825.35	0.00	1.66	.48	.19	.13	0.00	0.00	.74	.14
45	-23937.68	289.18	2532.63	0.00	1.48	.43	.17	.11	0.00	0.00	.67	.13
50	-14886.01	305.91	2289.76	0.00	1.34	.39	.15	.10	0.00	0.00	.62	.12
55	-12436.15	326.47	2085.15	0.00	1.22	.35	.14	.09	0.00	0.00	.57	.11
60	-12273.58	352.06	1910.54	0.00	1.12	.32	.13	.09	0.00	0.00	.52	.10
65	-14210.11	384.47	1759.90	0.00	1.03	.30	.12	.08	0.00	0.00	.48	.09
70	-21231.16	426.49	1628.69	0.00	.96	.27	.11	.07	0.00	0.00	.45	.09
75	-85761.19	482.70	1513.46	0.00	.89	.25	.10	.07	0.00	0.00	.42	.08
80	27817.58	561.22	1411.51	0.00	.83	.24	.09	.06	0.00	0.00	.39	.08
85	10446.51	677.87	1320.73	0.00	.78	.22	.09	.06	0.00	0.00	.36	.07
90	5964.15	868.22	1239.42	0.00	.74	.20	.08	.06	0.00	0.00	.34	.07
95	3971.63	1232.20	1166.22	0.00	.70	.19	.07	.05	0.00	0.00	.32	.06
100	2873.00	2200.00	1100.00	0.00	.66	.18	.07	.05	0.00	0.00	.30	.06
INITIAL CONC.	2873.00	2200.00	1100.00	0.00	.66	.18	.07	.05	0.00	0.00	.30	.06

CALCULATION OF TRACE ELEMENT PARTIAL MELTING MODELS

SOURCE MODAL COMPOSITION
.744 OLIVINE .218 ORTHOPX .030 CLINOPX .008 SPINEL 0.000 GARNET 0.000 PLAG 0.000 AMPHIB

WEIGHT FRACTION OF LIQUID CONTRIBUTED BY EACH PHASE AT SMALL DEGREE OF MELTING IN MELTING INTERVAL 1
.050 OLIVINE .400 ORTHOPX .500 CLINOPX .050 SPINEL 0.000 GARNET 0.000 PLAG 0.000 AMPHIB

WEIGHT FRACTION OF LIQUID CONTRIBUTED BY EACH PHASE AT F= 100% PARTIAL MELTING
.744 OLIVINE .218 ORTHOPX .030 CLINOPX .008 SPINEL 0.000 GARNET 0.000 PLAG 0.000 AMPHIB

CALCULATED CONCENTRATION(PPM) TRACE ELEMENTS IN THE LIQUID

% MELT	CR	NI	TI	LA	CE	SM	EU	TB	DY	ER	YB	LU
5	3928.93	221.65	6130.84	9.73	6.80	1.13	.28	.60	0.00	0.00	1.24	.21
10	5746.51	224.47	3916.86	5.57	3.97	.74	.18	.40	0.00	0.00	1.01	.17
15	9703.12	228.26	2862.87	3.90	2.80	.54	.14	.30	0.00	0.00	.84	.15
20	24012.07	233.13	2246.73	2.99	2.16	.42	.11	.24	0.00	0.00	.71	.13
25	-97516.59	239.20	1842.70	2.43	1.75	.35	.09	.20	0.00	0.00	.62	.11
30	-19030.53	246.66	1557.47	2.04	1.48	.29	.07	.17	0.00	0.00	.54	.10
35	-11719.75	255.72	1345.44	1.76	1.27	.25	.06	.15	0.00	0.00	.48	.09
40	-9211.50	266.72	1181.71	1.54	1.12	.22	.06	.13	0.00	0.00	.42	.08
45	-8180.03	280.07	1051.51	1.37	.99	.20	.05	.12	0.00	0.00	.38	.07
50	-7911.84	296.34	945.55	1.24	.90	.18	.04	.10	0.00	0.00	.35	.06
55	-8265.02	316.36	857.66	1.12	.81	.16	.04	.09	0.00	0.00	.31	.06
60	-9429.90	341.30	783.62	1.03	.75	.14	.04	.09	0.00	0.00	.29	.05
65	-12261.72	372.92	720.41	.95	.69	.13	.03	.08	0.00	0.00	.26	.05
70	-21044.40	413.95	665.84	.88	.64	.12	.03	.07	0.00	0.00	.24	.05
75	*********	468.94	618.26	.82	.59	.11	.03	.07	0.00	0.00	.23	.04
80	20329.93	545.93	576.44	.77	.56	.10	.03	.06	0.00	0.00	.21	.04
85	8939.77	660.68	539.39	.72	.52	.10	.02	.06	0.00	0.00	.19	.04
90	5432.55	848.88	506.35	.68	.49	.09	.02	.06	0.00	0.00	.18	.03
95	3761.71	1212.12	476.72	.64	.46	.09	.02	.05	0.00	0.00	.17	.03
100	2800.00	2200.00	450.00	.61	.44	.08	.02	.05	0.00	0.00	.16	.03
INITIAL CONC.	2800.00	2200.00	450.00	.61	.44	.08	.02	.05	0.00	0.00	.16	.03

CALCULATION OF TRACE ELEMENT FRACTIONAL CRYSTALLIZATION MODELS FOR SURFACE EQUILIBRIUM(SEQ),TOTAL EQUILIBRIUM(TEQ).

WEIGHT PROPORTION OF MINERALS FRACTIONATED
.100 OLIVINE .500 ORTHOPX .150 CLINOPX .020 SPINEL 0.000 GARNET .230 PLAG 0.000 AMPHIB

CALCULATED CONCENTRATION(PPM) TRACE ELEMENTS IN-THE LIQUID

% XSTAL	CR	NI	TI	LA	CE	SM	EU	TB	DY	ER	YB	LU
5(SEQ)	677.43	235.65	1467.18	2.10	2.41	2.62	2.50	2.98	3.30	4.89	5.40	5.49
(TEQ)	681.33	236.38	1467.02	2.10	2.41	2.62	2.50	2.98	3.29	4.89	5.40	5.49
10(SEQ)	617.20	221.42	1541.48	2.21	2.54	2.74	2.62	3.13	3.46	5.10	5.61	5.70
(TEQ)	631.28	224.17	1540.78	2.21	2.54	2.74	2.61	3.13	3.45	5.10	5.61	5.69
15(SEQ)	559.33	207.30	1624.12	2.33	2.68	2.89	2.74	3.29	3.63	5.33	5.85	5.93
(TEQ)	588.07	213.16	1622.35	2.33	2.68	2.88	2.74	3.28	3.63	5.32	5.84	5.91
20(SEQ)	503.88	193.32	1716.62	2.46	2.83	3.04	2.88	3.47	3.83	5.59	6.12	6.18
(TEQ)	550.41	203.18	1713.04	2.46	2.83	3.04	2.87	3.46	3.82	5.57	6.09	6.15
25(SEQ)	450.87	179.46	1820.89	2.62	3.01	3.22	3.04	3.67	4.05	5.88	6.41	6.47
(TEQ)	517.27	194.09	1814.47	2.61	3.00	3.21	3.02	3.65	4.04	5.84	6.36	6.41
30(SEQ)	400.35	165.75	1939.38	2.79	3.21	3.42	3.21	3.90	4.31	6.20	6.74	6.78
(TEQ)	487.90	185.78	1928.67	2.78	3.20	3.40	3.18	3.87	4.28	6.13	6.65	6.69
35(SEQ)	352.38	152.18	2075.24	2.99	3.44	3.66	3.41	4.16	4.60	6.57	7.12	7.14
(TEQ)	461.69	178.15	2058.20	2.98	3.42	3.62	3.36	4.12	4.55	6.46	6.98	6.99
40(SEQ)	307.00	138.77	2232.70	3.23	3.71	3.92	3.65	4.47	4.93	6.99	7.55	7.54
(TEQ)	438.15	171.13	2206.39	3.20	3.68	3.86	3.57	4.40	4.85	6.83	7.34	7.32
45(SEQ)	264.28	125.53	2417.46	3.50	4.03	4.24	3.92	4.82	5.32	7.43	8.04	8.01
(TEQ)	416.89	164.63	2377.58	3.46	3.98	4.14	3.80	4.72	5.21	7.23	7.74	7.69
50(SEQ)	224.27	112.48	2637.42	3.83	4.40	4.61	4.23	5.25	5.79	8.06	8.62	8.56
(TEQ)	397.60	158.61	2577.56	3.76	4.33	4.47	4.06	5.09	5.61	7.69	8.18	8.10
55(SEQ)	187.05	99.62	2903.94	4.23	4.86	5.06	4.61	5.76	6.35	8.75	9.30	9.20
(TEQ)	380.02	153.02	2814.27	4.13	4.75	4.85	4.37	5.53	6.09	8.22	8.68	8.55
60(SEQ)	152.71	86.97	3233.89	4.72	5.43	5.61	5.08	6.39	7.04	9.59	10.14	9.98
(TEQ)	363.93	147.81	3098.85	4.57	5.25	5.31	4.72	6.04	6.65	8.82	9.24	9.05
65(SEQ)	121.33	74.57	3653.53	5.35	6.15	6.31	5.67	7.18	7.92	10.64	11.17	10.95
(TEQ)	349.14	142.94	3447.47	5.11	5.88	5.86	5.13	6.66	7.33	9.51	9.88	9.62
70(SEQ)	93.04	62.43	4206.13	6.18	7.11	7.23	6.43	8.23	9.06	12.00	12.50	12.18
(TEQ)	335.51	136.38	3864.46	5.81	6.68	6.53	5.62	7.43	8.17	10.33	10.61	10.26
75(SEQ)	67.97	50.60	4968.56	7.33	8.43	8.49	7.47	9.66	10.64	13.83	14.28	13.81
(TEQ)	322.90	134.10	4448.33	6.72	7.74	7.38	6.22	8.39	9.22	11.29	11.47	11.00
80(SEQ)	46.28	39.13	6092.24	9.03	10.39	10.34	8.96	11.76	12.94	16.45	16.80	16.11
(TEQ)	311.21	130.08	5203.69	7.98	9.18	8.49	6.96	9.64	10.58	12.46	12.47	11.85
85(SEQ)	28.20	28.09	7923.80	11.83	13.60	13.32	11.34	15.15	16.65	20.58	20.72	19.65
(TEQ)	300.33	126.30	6268.05	9.82	11.29	9.98	7.89	11.33	12.40	13.89	13.66	12.84
90(SEQ)	14.03	17.61	11476.99	17.29	19.89	19.05	15.81	21.65	23.77	28.22	27.84	26.01
(TEQ)	290.19	122.73	7879.78	12.75	14.67	12.12	9.12	13.74	15.00	15.70	15.11	14.01
95(SEQ)	4.25	7.92	21621.17	33.10	38.08	35.10	27.88	39.86	43.67	48.40	46.14	41.98
(TEQ)	280.71	119.35	10607.27	18.18	20.92	15.41	10.80	17.44	18.95	18.04	16.90	15.42
INITIAL CONC.	740.00	250.00	1400.00	2.00	2.30	2.50	2.40	2.85	3.15	4.70	5.20	5.30

CALCULATION OF TRACE ELEMENT FRACTIONAL CRYSTALLIZATION MODELS FOR SURFACE EQUILIBRIUM(SEQ),TOTAL EQUILIBRIUM(TEQ).

WEIGHT PROPORTION OF MINERALS FRACTIONATED
.090 OLIVINE .420 ORTHOPX .170 CLINOPX .020 SPINEL 0.000 GARNET .300 PLAG 0.000 AMPHIB

CALCULATED CONCENTRATION(PPM) TRACE ELEMENTS IN THE LIQUID

% XSTAL	CR	NI	TI	LA	CE	SM	EU	TB	DY	ER	YB	LU
5(SEQ)	676.09	237.68	1467.04	2.10	2.41	2.61	2.50	2.98	3.30	4.89	5.40	5.50
(TEQ)	680.12	238.27	1466.88	2.10	2.41	2.61	2.50	2.98	3.30	4.89	5.40	5.49
10(SEQ)	614.69	225.36	1541.18	2.21	2.54	2.74	2.61	3.13	3.46	5.10	5.62	5.71
(TEQ)	629.20	227.58	1540.48	2.20	2.54	2.74	2.61	3.13	3.45	5.10	5.62	5.70
15(SEQ)	555.83	213.02	1623.64	2.32	2.68	2.88	2.73	3.29	3.64	5.34	5.87	5.95
(TEQ)	585.37	217.82	1621.84	2.32	2.67	2.88	2.72	3.28	3.63	5.32	5.85	5.93
20(SEQ)	499.54	200.67	1715.93	2.46	2.83	3.04	2.86	3.47	3.83	5.60	6.14	6.21
(TEQ)	547.26	208.86	1712.29	2.45	2.83	3.03	2.85	3.46	3.82	5.57	6.11	6.18
25(SEQ)	445.88	188.31	1819.95	2.61	3.01	3.21	3.01	3.67	4.06	5.89	6.44	6.50
(TEQ)	513.80	200.60	1813.41	2.60	3.00	3.20	2.99	3.65	4.04	5.84	6.38	6.44
30(SEQ)	394.87	175.94	1938.13	2.78	3.20	3.41	3.18	3.90	4.31	6.21	6.77	6.83
(TEQ)	484.20	192.98	1927.23	2.77	3.19	3.38	3.14	3.87	4.28	6.14	6.69	6.73
35(SEQ)	346.55	163.55	2073.64	2.98	3.43	3.64	3.37	4.16	4.60	6.58	7.16	7.19
(TEQ)	457.82	185.91	2056.30	2.96	3.41	3.60	3.32	4.12	4.56	6.47	7.02	7.05
40(SEQ)	300.99	151.15	2230.65	3.21	3.70	3.90	3.59	4.47	4.94	7.01	7.59	7.61
(TEQ)	434.17	179.34	2203.89	3.18	3.66	3.84	3.51	4.40	4.87	6.84	7.39	7.40
45(SEQ)	258.23	138.74	2414.86	3.48	4.01	4.21	3.85	4.82	5.34	7.50	8.10	8.10
(TEQ)	412.84	173.22	2374.31	3.43	3.95	4.11	3.72	4.72	5.22	7.25	7.80	7.78
50(SEQ)	218.33	126.31	2634.13	3.80	4.38	4.57	4.15	5.25	5.80	8.09	8.69	8.66
(TEQ)	393.51	167.50	2573.29	3.73	4.30	4.43	3.96	5.09	5.63	7.72	8.26	8.21
55(SEQ)	181.36	113.86	2899.77	4.19	4.83	5.01	4.51	5.76	6.37	8.77	9.40	9.34
(TEQ)	375.91	162.15	2808.68	4.08	4.71	4.80	4.24	5.53	6.11	8.25	8.78	8.69
60(SEQ)	147.33	101.38	3228.56	4.67	5.39	5.55	4.94	6.39	7.06	9.62	10.26	10.15
(TEQ)	359.82	157.13	3091.46	4.50	5.20	5.24	4.56	6.04	6.69	8.85	9.37	9.22
65(SEQ)	116.50	88.89	3646.64	5.29	6.10	6.24	5.49	7.18	7.95	10.68	11.33	11.16
(TEQ)	345.04	152.42	3437.57	5.03	5.81	5.76	4.93	6.66	7.38	9.56	10.04	9.83
70(SEQ)	88.81	76.37	4197.02	6.10	7.04	7.14	6.20	8.23	9.10	12.05	12.70	12.45
(TEQ)	331.44	147.97	3870.93	5.69	6.58	6.41	5.36	7.43	8.22	10.38	10.81	10.52
75(SEQ)	64.42	63.81	4956.17	7.22	8.34	8.36	7.16	9.66	10.69	13.89	14.54	14.16
(TEQ)	318.86	143.78	4429.33	6.55	7.59	7.21	5.88	8.39	9.29	11.36	11.72	11.32
80(SEQ)	43.49	51.22	6074.62	8.85	10.26	10.16	8.54	11.76	13.01	16.34	17.15	16.59
(TEQ)	307.21	139.82	5175.98	7.72	8.97	8.25	6.50	9.64	10.68	12.55	12.78	12.25
85(SEQ)	26.20	38.58	7896.79	11.59	13.41	13.05	10.72	15.15	16.77	20.71	21.23	20.35
(TEQ)	296.37	136.07	6225.40	9.41	10.95	9.63	7.28	11.33	12.56	14.01	14.06	13.34
90(SEQ)	12.83	25.88	11429.52	16.88	19.55	18.58	14.76	21.65	23.97	28.44	28.67	27.13
(TEQ)	286.28	132.52	7808.58	12.02	14.06	11.57	8.27	13.74	15.24	15.86	15.63	14.65
95(SEQ)	3.79	13.07	21504.89	32.08	37.23	33.98	25.50	39.86	[illegible].16	48.89	47.94	44.34
(TEQ)	276.85	129.15	10471.60	16.66	19.65	14.50	9.58	17.44	19.36	18.27	17.59	16.24
INITIAL CONC.	740.00	250.00	1400.00	2.00	2.30	2.50	2.40	2.85	3.15	4.70	5.20	5.30

REFERENCES

Andrews, A. J. and Fyfe, W. S. 1976. Metamorphism and massive sulfide generation in oceanic crust. Geoscience Canada, 3, pp. 84-94.

Arth, J. G. 1976. Behavior of trace elements during magmatic processes - a summary of theoretical models and their applications. J. Res. U.S. Geol. Surv., 4, pp. 41-47.

Aumento, F., Mitchell, W. S. and Fratta, M. 1976. Interaction between sea water and oceanic layer two as a function of time and depth-1. Field evidence. Can. Mineral., 14, pp. 264-290.

Bhattacharji, S. 1967. Mechanics of flow differentiation in ultramafic and mafic sills. J. Geol., 75, pp. 101-112.

Bischoff, J. L. and Dickson, F. W. 1975. Seawater-basalt interaction at 200°C and 500 bars: implications for origin of sea-floor heavy metal deposits and regulation of seawater chemistry. Earth Planet. Sci. Lett., 25, pp. 385-397.

Bjornsson, S., Arnorsson, S. and Tómasson, J. 1972. Economic evaluation of Reykjanes thermal brine area, Iceland. Am. Assoc. Petrol. Geol. Bull., 56, pp. 2380-2391.

Blanchard, D. P., Rhodes, J. M., Dungan, M. A., Rodgers, K. V., Donaldson, C. H., Brannon, J. C., Jacobs, J. W. and Gibson, E. K. 1976. The chemistry and petrology of basalts from leg 37 of the Deep Sea Drilling Project. J. Geophys. Res., 81, pp. 4231-4246.

Bonatti, E. 1975. Metallogenesis at oceanic spreading centers. Annu. Rev. Earth Planet. Sci., 3, pp. 1401-1431.

Bonatti, E., Honnerez, J. and Ferrara, G. 1971. Peridotite-gabbro-basalt complex from the equatorial mid-Atlantic ridge. Phil. Trans. Roy. Soc. London, Ser. A 268, pp. 385-402.

Bonatti, E., Honnerez, J., Kirst, P. and Radicati, F. 1975. Metagabbros from the mid-Atlantic ridge at 06°N: contact-hydrothermal-dynamic metamorphism beneath the axial valley. J. Geol., 83, pp. 61-78.

Bonatti, E., Zerbi, M., Kay, R. and Rydell, H. 1976. Metalliferous deposits from the Apennine ophiolites: Mesozoic equivalents of modern deposits from oceanic spreading centers. Geol. Soc. Am. Bull., 87, pp. 83-94.

Bougault, H. and Hekinian, R. 1975. Rift valley in the Atlantic ocean near 36°50'N: petrology and geochemistry of basaltic rocks. Earth Planet. Sci. Lett., 24, pp. 249-261.

Brock, P. W. G. 1974. The sheeted dike layer of the Betts Cove ophiolite complex does not represent spreading. Can. J. Earth Sci., 11, pp. 208-210.

Brown, G. M. 1967. Mineralogy of basaltic rocks. In: The Poldervaart Treatise on Rocks of Basaltic Composition, V. 1, H. H. Hess and A. Poldervaart (eds.). J. Wiley & Sons, pp. 103-162.

Bryan, W. B., Thompson, G., Frey, F. A. and Dickey, J. S. 1976. Inferred geologic settings and differentiation in basalts from the Deep Sea Drilling Project. J. Geophys. Res., 81, pp. 4285-4304.

Burns, R. G. 1970. Mineralogical Applications of Crystal Field Theory. Cambridge University Press. Cambridge. 224 p.

Burns, R. G. and Fyfe, W. S. 1966. Distribution of elements in geological processes. Chem. Geol. 1, pp. 49-56.

Burns, R. G. and Fyfe, W. S. 1967. Trace element distribution rules and their significance. Chem. Geol., 2, pp. 89-104.

Bursnall, J. T. and DeWit, M. J. 1975. Timing and development of the orthotectonic zone in the Appalachian orogen of northwest Newfoundland. Can. J. Earth Sci., 12, pp. 1712-1722.

Byerly, G. R., Melson, W. G. and Vogt, P. R. 1976. Rhyodacites, andesites, ferrobasalts and ocean tholeiites from the Galapagos spreading center. Earth Planet. Sci. Lett., 30, pp. 215-221.

Campbell, I. H. and Nolan, J. 1974. Factors affecting the stability field of Ca-poor pyroxene and the origin of the Ca-poor minimum in Ca-rich pyroxenes from tholeiitic intrusions. Contrib. Mineral. Petrol., 48, pp. 205-219.

Cann, J. R. 1969. Spilites from the Carlsberg ridge, Indian ocean. J. Petrol., 10, pp. 1-19.

Cann, J. R. 1970. Rb, Sr, Y, Zr and Nb in some ocean floor basaltic rocks. Earth Planet. Sci. Lett., 10, pp. 7-11.

Cann, J. R. 1971. Metamorphic rocks from Palmer Ridge. Phil. Trans. Roy. Soc. London, Ser. A, 268, pp. 605-617.

Carter, J. L. 1970. Mineralogy and chemistry of the earth's upper mantle based on the partial fusion-partial crystallization model. Geol. Soc. Am. Bull., 81, pp. 2021-2034.

Christensen, N. I. and Salisbury, M. H. 1975. Structure and constitution of the lower oceanic crust. Reviews of Geophys. and Space Physics, 13, pp. 57-86.

Church, W. R. 1969. Metamorphic rocks of Burlington Peninsula and adjoining areas of Newfoundland and their bearing on continental drift in North America. In: North Atlantic-Geology and Continental Drift, M. Kay (ed.), Am. Assoc. Pet. Geol., Mem. 12, pp. 212-233.

Church, W. R. 1972. Ophiolite: its definition, origin as oceanic crust and mode of emplacement in orogenic belts with special reference to the Appalachians. Can. Dept. Energy, Mines, Resources. Earth Physics Br. Publ. 42, pp. 71-85.

Church, W. R. 1976. Ages of zircons from the Bay of Islands ophiolite complex, western Newfoundland: comment. Geology, 4, pp. 623-624.

Church, W. R. 1977. The ophiolites of southern Quebec: oceanic crust of Betts Cove type. Can. J. Earth Sci., in press.

Church, W. R. and Coish, R. A. 1976. Oceanic versus island arc origin of ophiolites. Earth Planet. Sci. Lett., 31, pp. 8-14.

Church, W. R. and Riccio, L. 1974. The sheeted dyke layer of the Betts Cove ophiolitic complex does not represent spreading: Discussion. Can. J. Earth Sci., 11, pp. 1499-1502.

Church, W. R. and Riccio, L. 1977. Fractionation trends in the Bay of Islands ophiolite of Newfoundland: polycyclic cumulate sequences in ophiolites and their classification. Can. J. Earth Sci., in press.

Church, W. R. and Stevens, R. K. 1971. Early Paleozoic ophiolite complexes of Newfoundland as mantle-ocean crust sequences. J. Geophys. Res., 76, pp. 1460-1466.

Clague, D. A. and Bunch, T. E. 1976. Formation of ferro-basalt at East Pacific mid-ocean spreading centers. J. Geophys. Res., 81, pp. 4247-4256.

Coish, R. A. 1977. Ocean floor metamorphism in the Betts Cove ophiolite, Newfoundland. Contrib. Mineral. Petrol., 60, pp. 255-270.

Coleman, R. G. 1967. Low temperature reaction zones and alpine ultramafic rocks of California, Oregon and Washington. U.S. Geol. Surv. Bull. 1247, 49 p.

Cooper, J. R. 1936. Geology of the southern half of the Bay of Islands complex. Newfoundland Dept. Nat. Res., Geol. Sec. Bull. 4, 62 p.

Cronan, D. S. 1976. Basal metalliferous sediments from the eastern Pacific. Geol. Soc.Am. Bull., 87, pp. 928-934.

Dallmeyer, R. D. and Williams, H. 1975. $^{40}Ar/^{39}Ar$ release spectra of hornblende from the Bay of Islands metamorphic aureole, western Newfoundland: their bearing on the timing of ophiolite obduction at the Ordovician continental margin. Can. J. Earth Sci., 12, pp. 1686-1690.

DeGrace, J. R., Kean, B. F., Hsu, E. and Green, T. 1976. Geology of the Nippers Harbour map area (2E/13), Newfoundland. Nfld. Dept. Mines Energy Rpt. 76-3, 73 p.

Dewey, J. F. and Bird, J. M. 1971. Origin and emplacement of the ophiolite suite: Appalachian ophiolites of Newfoundland. J. Geophys. Res., 76, pp. 3170-3206.

Einarson, G. W. 1975. Low rank metamorphism in the Bay of Islands ophiolite complex, western Newfoundland. Geol. Soc. Am. Mtg., north central section, abstr. with prog. 7, p. 752.

Ehlers, E. G. 1972. The Interpretation of Geological Phase Diagrams. W. H. Freeman and Co. San Francisco. 280 p.

Elder, J. W. 1967. Steady free convection in a porous medium heated from below. J. Fluid Mech., 27, pp. 29-48.

Engel, C. G. and Fisher, F. L. 1975. Granitic to ultramafic rock complexes of the Indian ocean ridge system, western Indian ocean. Geol. Soc. Am. Bull., 86, pp. 1553-1578.

Floyd, P. A. and Winchester, J. A. 1975. Magma type and tectonic setting discrimination using immobile elements. Earth Planet. Sci. Lett., 27, pp. 211-218.

Fodor, R. V., Keil, K. and Bunch, T. E. 1975. Contributions to the mineral chemistry of Hawaiian rocks IV: pyroxenes in rocks from Haleakala and west Maui volcanoes, Maui, Hawaii. Contrib. Mineral. Petrol., 50, pp. 173-195.

Frey, F. A., Bryan, W. B. and Thompson, G. 1974. Atlantic ocean floor: geochemistry and petrology of basalts from Legs 2 and 3 of the Deep Sea Drilling Project. J. Geophys. Res., 79, pp. 5507-5532.

Miyashiro, A. 1975b. Origin of the Troodos and other ophiolites: a reply to Hynes. Earth Planet. Sci. Lett., 25, pp. 217-222.

Miyashiro, A. 1975c. Origin of the Troodos and other ophiolites: a reply to Moores. Earth Planet. Sci. Lett., 25, pp. 227-235.

Miyashiro, A. and Shido, F. 1975. Tholeiitic and calc-alkaline series in relation to the behaviours of titanium, vanadium, chromium and nickel. Am. J. Sci., 275, pp. 265-277.

Miyashiro, A., Shido, F. and Ewing, M. 1971. Metamorphism in the mid-Atlantic ridge near 24° and 30°N. Phil. Trans. Roy. Soc. London, Ser. A268, pp. 589-603.

Montigny, R., Bougault, H., Bottinga, Y. and Allegre, C. J. 1973. Trace element geochemistry and genesis of the Pindos ophiolite suite. Geochim. Cosmo. Acta, 37, pp. 2135-2147.

Moores, E. M. 1975. Discussion of "Origin of Troodos and other ophiolites: a reply to Hynes", by A. Miyashiro. Earth Planet. Sci. Lett., 25, pp. 223-226.

Moores, E. M. and Jackson, E. D. 1974. Ophiolites and oceanic crust. Nature, 250, pp. 136-139.

Gast, P. W. 1968. Trace element fractionation and the origin of tholeiitic and alkaline magma types. Geochim. Cosmo. Acta, 32, pp. 1057-1085.

Green, D. H. and Ringwood, A. E. 1967. The genesis of basaltic magmas. Contrib. Mineral. Petrol., 15, pp. 103-190.

Greenland, L. P. 1970. An equation for trace element distribution during magmatic crystallization. Am. Mineral., 55, pp. 455-465.

Hajash, A., Jr. 1974. An experimental investigation of high temperature seawater-basalt interactions. Geol. Soc. Am. Ann. Mtg. abstr. with prog. 6, p. 771.

Hajash, A., Jr. 1975. Hydrothermal processes along mid-ocean ridges: an experimental investigation. Contrib. Mineral. Petrol., 53, pp. 205-226.

Harris, P. G. 1957. Zone refining and the origin of potassic basalts. Geochim. Cosmo. Acta, 12, pp. 195-208.

Hart, R. A. 1973. A model for the chemical exchange in the basalt-seawater system of oceanic layer 2. Can. J. Earth Sci., 10, pp. 799-815.

Hart, S. R. 1969. K, Rb, Cs contents and K/Rb, K/Cs ratios of fresh and altered submarine basalts. Earth Planet. Sci. Lett., 6, pp. 295-303.

Hart, S. R., Erlank, A. J. and Kable, E. J. D. 1974. Sea floor alteration: some chemical and Sr isotope effects. Contrib. Mineral. Petrol., 44, pp. 219-230.

Haskin, L. A., Haskin, M. A., Frey, F. A. and Wildeman, T. R. 1968. Relative and absolute abundances of the rare earths. In: Origin and Distribution of the Elements, L. H. Ahrens (ed.), pp. 889-912.

Hekinian, R. and Thompson, G. 1976. Comparative geochemistry of volcanics from rift valleys, transform faults and aseismic ridges. Contrib. Mineral. Petrol., 57, pp. 145-162.

Hertogen, J. and Gijbels, R. 1976. Calculation of trace element fractionation during partial melting. Geochim. Cosmo. Acta, 40, pp. 313-322.

Hill, R. and Roeder, P. L. 1974. The crystallization of spinel from basaltic liquids as a function of oxygen fugacity. J. Geol., 82, pp. 709-729.

Honnerez, J. and Kirst, P. 1975. Petrology of rodingites from the equatorial mid-Atlantic fracture zones and their geotectonic significance. Contrib. Mineral. Petrol., 49, pp. 237-257.

Hynes, A. 1975. Comment on "The Troodos ophiolitic complex was probably formed in an island arc", by A. Miyashiro. Earth Planet. Sci. Lett., 25, pp. 213-216.

Irvine, T. N. 1974. Simple and multiple oxides in magmatic rock systems. Carnegie Inst. Wash. Ybk. 73, pp. 300-316.

Irvine, T. N. 1975. Crystallization sequences in the Muskox intrusion and other layered intrusions-II. Origin of chromitite layers and similar deposits of other magmatic ores. Geochim. Cosmo. Acta, 39, pp. 991-1020.

Jackson, E. D., Green II, H. W. and Moores, E. M. 1975. The Vourinos ophiolite, Greece: cyclic units of lineated cumulates overlying harzburgite tectonite. Geol. Soc. Am. Bull., 86, pp. 390-398.

Jenner, G. A. 1977. Geochemistry of the volcanic and sedimentary rocks in the Snooks Arm Group, Newfoundland. Unpubl. Msc. thesis, Univ. of Western Ontario, 142 p.

Kay, R., Hubbard, N. J. and Gast, P. W. 1970. Chemical characteristics and origin of oceanic ridge volcanic rocks. J. Geophys. Res., 75, pp. 1585-1613.

Kay, R. W. and Senechal, R. G. 1976. The rare earth geochemistry of the Troodos ophiolite complex. J. Geophys. Res., 81, pp. 964-970.

Keen, M. J. 1975. The oceanic crust. Geoscience Canada, 2, pp. 36-43.

Kennedy, M. J. 1971. Structure and stratigraphy of the Fleurs-de-Lys area, Burlington Peninsula, Newfoundland. Geol. Assoc. Can., 24, pp. 59-71.

Kennedy, M. J. 1975. Repetitive orogeny in the northeastern Appalachians: New plate models based upon Newfoundland examples. Tectonophysics, 28, pp. 39-87.

Kennedy, M. J. 1976. Southeastern margin of the northeastern Appalachians: late Precambrian orogeny on a continental margin. Geol. Soc. Am. Bull., 87, pp. 1317-1325.

Kushiro, I. 1960. Si-Al relationships in clinopyroxenes from igneous rocks. Am. J. Sci., 258, pp. 548-554.

LaBas, M. J. 1962. The role of aluminum in igneous clinopyroxenes with relation to their parentage. Am. J. Sci., 260, pp. 267-288.

Liou, J. G. 1973. Synthesis and stability relations of epidote, $Ca_2Al_2FeSi_3O_{12}(OH)$. J. Petrol., 14, pp. 381-413.

Lister, C. R. B. 1972. On the thermal balance of a mid-ocean ridge. Geophys. J. R. Astr. Soc., 26, pp. 515-535.

Lister, C. R. B. 1974. On the penetration of water into hot rock. Geophys. J. R. Astr. Soc., 39, pp. 465-509.

Lister, C. R. B. 1977. Qualitative models of spreading center processes, including hydrothermal penetration. Tectonophysics, 37, pp. 203-218.

Lofgren, G. 1974. An experimental study of plagioclase morphology: isothermal crystallization. Am. J. Sci., 274, pp. 243-273.

Lowell, R. P. 1975. Circulation in fractures, hot springs and convective heat transport on mid-ocean ridge crests. Geophys. J. R. Astr. Soc., 40, pp. 351-365.

Magaritz, M. and Taylor, H. P., Jr. 1976. Oxygen, hydrogen and carbon isotope studies of the Franciscan formation, Coast Ranges, California. Geochim. Cosmo. Acta., 40, pp. 215-234.

Mattinson, J. W. 1975. Early Paleozoic ophiolite complexes of Newfoundland: isotopic ages of zircons. Geology, 3, pp. 181-183.

Mattinson, J. M. 1976. Ages of zircons from the Bay of Islands ophiolite complex, western Newfoundland. Geology, 4, pp. 393-394.

Melson, W. G. and Thompson, G. 1971. Petrology of a transform fault zone and adjacent ridge segment. Phil. Trans. Roy. Soc. London, 268 A, pp. 423-441.

Menzies, M. 1973. Mineralogy and partial melt textures within an ultramafic-mafic body, Greece. Contrib. Mineral. Petrol., 42, pp. 273-285.

Menzies, M. 1976a. Rare earth geochemistry of fused ophiolitic and alpine lherzolites-I. Othris, Lanzo and Troodos. Geochim. Cosmo. Acta, 40, pp. 645-656.

Menzies, M. A. 1976b. Rifting of a Tethyan continent-rare earth evidence of an accreting plate margin. Earth Planet. Sci. Lett., 28, pp. 427-438.

Miyashiro, A. 1973. The Troodos ophiolitic complex was probably formed in an island arc. Earth Planet. Sci. Lett., 19, pp. 218-224.

Miyashiro, A. 1974. Volcanic rock series in island arcs and active continental margins. Am. J. Sci., 274, pp. 321-355.

Miyashiro, A. 1975a. Classification, characteristics and origin of ophiolites. J. Geol., 83, pp. 249-281.

Miyashiro, A. 1975b. Origin of the Troodos and other ophiolites: a reply to Hynes. Earth Planet. Sci. Lett., 25, pp. 217-222.

Miyashiro, A. 1975c. Origin of the Troodos and other ophiolites: a reply to Moores. Earth Planet. Sci. Lett., 25, pp. 227-235.

Miyashiro, A. and Shido, F. 1975. Tholeiitic and calc-alkaline series in relation to the behaviours of titanium, vanadium, chromium and nickel. Am. J. Sci., 275, pp. 265-277.

Miyashiro, A., Shido, F. and Ewing, M. 1971. Metamorphism in the mid-Atlantic ridge near 24° and 30°N. Phil. Trans. Roy. Soc. London, Ser. A268, pp. 589-603.

Montigny, R., Bougault, H., Bottinga, Y. and Allegre, C. J. 1973. Trace element geochemistry and genesis of the Pindos ophiolite suite. Geochim. Cosmo. Acta, 37, pp. 2135-2147.

Moores, E. M. 1975. Discussion of "Origin of Troodos and other ophiolites: a reply to Hynes", by A. Miyashiro. Earth Planet. Sci. Lett., 25, pp. 223-226.

Moores, E. M. and Jackson, E. D. 1974. Ophiolites and oceanic crust. Nature, 250, pp. 136-139.

Moores, E. M. and Vine, F. J. 1971. The Troodos massif, Cyprus and other ophiolites as oceanic crust: evaluation and implications. Phil. Trans. Roy. Soc. Lond. 268A, pp. 443-466.

Mottl, M., Corr, R. F. and Holland, H. D. 1974. Chemical exchange between seawater and mid-ocean ridge basalt during hydrothermal alteration: an experimental study. Geol. Soc. Am. Ann. Mtg. abstr. with prog., 6, pp. 879-880.

Muehlenbachs, K. and Clayton, R. N. 1972. Oxygen isotope geochemistry of submarine greenstones. Can. J. Earth Sci., 9, pp. 471-478.

Muehlenbachs, K. and Clayton, R. N. 1975. The interaction of seawater with the oceanic crust: oxygen isotope studies. EOS Trans. Am. Geophys. Union, 56, p. 1074.

Muir, I. D. and Tilley, C. E. 1964. Basalts from the northern part of the rift zone of the mid-Atlantic ridge. J. Petrol., 5, pp. 409-434.

Murray, R. J. 1954. The clinopyroxenes of the Garbh Eilean sill, Shiant Isles. Geol. Mag., 91, pp. 17-31.

Mysen, B. O. 1976. Nickel partitioning between upper mantle crystals and partial melts as a function of pressure, temperature and nickel concentrations. Carnegie Inst. Washington Ybk., 75, pp. 662-668.

Mysen, B. O. and Kushiro, I. 1976. Compositional variation of coexisting phases with degree of melting of peridotite under upper mantle conditions. Carnegie Inst. Washington Ybk., 75, pp. 546-554.

Neale, E. R. W., Kean, B. F. and Upadhyay, H. D. 1975. Post-ophiolite unconformity, Tilt Cove-Betts Cove area, Newfoundland. Can. J. Earth Sci., 12, pp. 880-886.

Norman, R. E. and Strong, D. F. 1975. The geology and geochemistry of ophiolitic rocks exposed at Ming's Bight, Newfoundland. Can. J. Earth Sci., 12, pp. 777-797.

Norrish, K. and Hutton, J. T. 1969. An accurate X-ray spectrographic method for the analysis of a wide range of geological samples. Geochim. Cosmo. Acta, 33, pp. 431-451.

O'Nions, R. K. and Pankhurst, R. J. 1976. Sr isotope and rare earth element geochemistry of DSDP leg 37 basalts. Earth Planet. Sci. Lett., 31, pp. 255-261.

Pearce, J. A. 1975. Basalt geochemistry used to investigate past tectonic environments on Cyprus. Tectonophysics, 25, pp. 41-67.

Pearce, J. A. and Cann, J. R. 1971. Ophiolite origin investigated by discriminant analyses using Ti, Zr and Y. Earth Planet. Sci. Lett., 12, pp. 339-349.

Pearce, J. A. and Cann, J. R. 1973. Tectonic setting of basic volcanic rocks determined using trace element analyses. Earth Planet. Sci. Lett., 19, pp. 290-300.

Peterson, D. W. 1961. Descriptive modal classification of igneous rocks. A.G.I. data sheet 23, Geotimes, 6, pp. 30-36.

Philpotts, J. A., Schnetzler, C. C. and Hart, S. R. 1969. Submarine basalts: some K, Rb, Sr, Ba, rare earth, H_2O and CO_2 data bearing on their alteration, modification by plagioclase and possible source materials. Earth Planet. Sci. Lett., 10, pp. 293-299.

Raith, M. 1976. The Al-Fe(III) epidote miscibility gap in a metamorphic profile through the penninic series of the Tavern Window, Austria. Contrib. Mineral. Petrol. 57, pp. 99-117.

Riccio, L. 1972. The Betts Cove ophiolite, Newfoundland. Unpubl. MSc. thesis, University of Western Ontario, 91 p.

Riccio, L. 1976. Stratigraphy and petrology of western Newfoundland ophiolites. Unpubl. Phd. thesis, Univ. Western Ontario, 264 p.

Ringwood, A. E. 1966. The mineralogy of the mantle. In: Advances in Earth Sciences, P. M. Hurley (ed.), M.I.T. Press, Boston, pp. 287-356.

Ringwood, A. E. 1975. Composition and Petrology of the Earth's Mantle. McGraw-Hill. 618 p.

Roeder, P. L. and Emslie, R. F. 1970. Olivine-liquid equilibrium. Contrib. Mineral. Petrol., 29, pp. 275-289.

Sayles, F. L., Ku, T.-L. and Bowker, P. C. 1975. Chemistry of ferromanganoan sediment of the Bauer Deep. Geol. Soc. Am. Bull., 86, pp. 1423-1431.

Schilling, J.-G. 1975. Rare earth variations across 'normal segments' of the Reykjanes ridge, 60° - 53°N, mid-Atlantic ridge 29°S and East Pacific Rise, 2° - 19°S and evidence on the composition of the underlying low velocity layer. J. Geophys. Res., 80, pp. 1459-1473.

Schilling, J.-G. and Winchester, J. W. 1967. Rare earth fractionation and magmatic processes. In: Mantles of Earth and Terrestrial Planets, S. K. Runcorn (ed.), pp. 267-283.

Schroeter, T. G. 1971. Geology of the Nippers Harbour area, Newfoundland. Unpubl. Msc. thesis, Univ. of Western Ontario. 92 p.

Shaw, D. M. 1970. Trace element fractionation during anatexis. Geochim. Cosmo. Acta., 34, pp. 237-243.

Shido, F., Miyashiro, A. and Ewing, M. 1974. Compositional variations in pillow lavas from the mid-Atlantic ridge. Marine Geol., 16, pp. 177-190.

Shimazu, Y. 1959. A thermodynamical aspect of the earth's interior-physical interpretation of magmatic differentiation process. J. Earth Sci., Nagoya Univ., 7, pp. 1-34.

Sigurdsson, H. and Schilling, J.-G. 1976. Spinels in mid-Atlantic ridge basalts: chemistry and occurrence. Earth Planet. Sci. Lett., 29, pp. 7-20.

Smewing, J. D. and Potts, P. J. 1976. Rare earth abundances in basalts and metabasalts from the Troodos massif, Cyprus. Contrib. Mineral. Petrol., 57, pp. 245-258.

Smewing, J. D., Simonian, K. O. and Gass, I. G. 1975. Metabasalts from the Troodos massif, Cyprus: genetic implication deduced from petrography and trace element geochemistry. Contrib. Mineral. Petrol., 51, pp. 49-64.

Smith, C. H. 1958. Bay of Islands igneous complex, western Newfoundland. Geol. Surv. Can., Mem. 290, 132 p.

Snelgrove, A. K. 1931. Geology and ore deposits of the Betts Cove-Tilt Cove area, Notre Dame Bay, Newfoundland. Can. Min. Met. Bull., 24, pp. 477-519.

Spooner, E. T. C. 1977. Hydrodynamic model for the origin of the ophiolitic cupriferous pyrite ore deposits of Cyprus. I.M.M. London, in press.

Spooner, E. T. C., Beckinsale, R. D., Fyfe, W. S. and Smewing, J. D. 1974. O^{18} enriched ophiolitic metabasic rocks from E. Liguria (Italy), Pindos (Greece) and Troodos (Cyprus). Contrib. Mineral. Petrol., 47, pp. 41-62.

Spooner, E. T. C. and Fyfe, W. S. 1973. Sub sea-floor metamorphism, heat and mass transfer. Contrib. Mineral. Petrol., 42, pp. 287-304.

Stevens, R. K. 1970. Cambro-Ordovician flysch sedimentation and tectonics in west Newfoundland and their possible bearing on a proto-Atlantic ocean. In: Flysch Sedimentology in North America, J. Lajoie (ed.), Geol. Assoc. Can. Spec. paper 7, pp. 155-177.

Stevens, R. K. 1976. Lower Paleozoic evolution of west Newfoundland. Unpubl. Phd. thesis, Univ. of Western Ontario, 268 p.

Tómasson, J. and Kristmonnsdóttir, H. 1972. High temperature alteration minerals and thermal brines, Reykjanes, Iceland. Contrib. Mineral. Petrol., 36, pp. 123-134.

Upadhyay, H. 1973. The Betts Cove ophiolite and related rocks of the Snooks Arm Group, Newfoundland. Unpubl. Phd. thesis, Memorial Univ. Newfoundland, 272 p.

Upadhyay, H., Dewey, J. F. and Neale, E. R. W. 1971. The Betts Cove ophiolite complex, Newfoundland: Appalachian oceanic crust and mantle. Geol. Assoc. Can., 24, pp. 27-34.

Upadhyay, H. D. and Neale, E. R. W. 1976. The Betts Cove - Tilt Cove ophiolite and associated rocks, Newfoundland. Geol. Soc. Am. NE. section, Ann. Mtg., programs with abstr., 8, p. 290.

Upadhyay, H. and Strong, D. F. 1973. Geological setting of the Betts Cove copper deposits, Newfoundland: an example of ophiolite mineralization. Econ. Geol., 68, pp. 161-167.

Wager, L. R. and Brown, G. M. 1968. Layered igneous rocks. Oliver and Boyd, Edinburgh.

Wilkinson, J. F. G. 1956. Clinopyroxenes of alkali olivine-basalt magma. Am. Mineral., 41, pp. 724-743.

Williams, D. L., Von Herzen, R. P., Sclater, J. G. and Anderson, R. N. 1974. The Galapagos spreading centre: lithosphere cooling and hydrothermal circulation. Geophys. J. R. Astr. Soc., 38, pp. 587-608.

Williams, H. 1963. Twillingate map area, Newfoundland. Geol. Surv. Can. paper 63-36.

Williams, H. 1975. Structural succession, nomenclature and interpretation of transported rocks in western Newfoundland. Can. J. Earth Sci., 12, pp. 1874-1894.

Williams, H. and Einarson, G. W. 1976. Discussion of "Prehnite and pumpellyite-bearing mineral assemblages, west side of the Appalachian metamorphic belt, Pennsylvania to Newfoundland" by E-an Zen. J. Petrol., 17, pp. 135-136.

Williams, H., Hibbard, J. P. and Bursnall, J. T. 1977. Geological setting of asbestos-bearing ultramafic rocks along the Baie Verte lineament, Newfoundland. Geol. Surv. Can., paper 77-1A, pp. 351-360.

Williams, H., Kennedy, M. J. and Neale, E. R. W. 1972. The Appalachian structural province. In: Variations in Tectonic Style in Canada, R. A. Price and R. J. W. Douglas (eds.), Geol. Assoc. Can. Spec. paper 11, pp. 181-261.

Williams, H. and Malpas, J. 1972. Sheeted dikes and brecciated dike rocks within transported igneous complexes, Bay of Islands, western Newfoundland. Can. J. Earth Sci., 9, pp. 1216-1229.

Williams, H. and Smyth, W. R. 1973. Metamorphic aureoles beneath ophiolite suites and Alpine peridotites: Tectonic implications with west Newfoundland examples. Am. J. Sci., 273, pp. 594-621.

Williams, H. and Stevens, R. K. 1974. The ancient continental margin of eastern North America. In: The Geology of Continental Margins, C. A. Burk and C. L. Drake (eds.). Springer-Verlag, New York. pp. 781-796.

Winchester, J. A. and Floyd, P. A. 1976. Geochemical magma type discrimination: application to altered and metamorphosed igneous rocks. Earth Planet. Sci. Lett., 28, pp. 459-469.

Wolery, T. J. and Sleep, N. H. 1976. Hydrothermal circulation and geochemical flux at mid-ocean ridges. J. Geol., 84, pp. 249-275.

Wood, D. A., Gibson, I. L. and Thompson, R. N. 1976. Elemental mobility during zeolite facies metamorphism of the Tertiary basalts of eastern Iceland. Contrib. Mineral. Petrol., 55, pp. 241-254.

Wyllie, P. J. 1971. The Dynamic Earth: textbook in geosciences. John Wiley & Sons. 416 p.

Yoder, H. S., Jr. 1976. Generation of Basaltic Magmas. National Academy Sciences, Washington, D.C. 265 p.